

Final

E-200-116

EVALUATION AND DESIGN OF DRAINED LOW-LEVEL
RADIOACTIVE DISPOSAL SITES
FINAL REPORT
PROJECT E25-606, CONTRACT NO. DE-AS07-83ID12449

edited by

Geoffrey G. Eichholz
Project Director

submitted to

U.S. DEPARTMENT OF ENERGY
Idaho Operations Office
Idaho Falls, ID 83401

Program in Nuclear Engineering & Health Physics
Georgia Institute of Technology
Atlanta, GA 30332

December, 1984

CONTENTS

List of Figures	ii
Summary	iv
Project Personnel	vi
Introduction	1
Trench Hydrology	13
Test Bed Construction	21
Materials	26
Laboratory Tests	29
Test Bed Experiments	36
Waste Leaching in Unsaturated Conditions	50
Computer Simulation	51
Flow Model	55
Initial Condition	57
Boundary Conditions	57
Trench Facility Design	59
Calculation of Gravel Reservoir Requirements	61
Conclusions	67
Acknowledgments	68
Bibliography	69
Appendix A	72
1 - Water Characteristics and Hydraulic Conductivity Models	
a - Brooks and Corey	72
b - Haverkamp	74
c - Van Genuchten	75
2 - Equilibrium Sorption Isotherms	
a - Linear Adsorption	77
b - Freundlich Isotherm	78
c - Langmuir Isotherm	79
Appendix B - Model Implementation	80
Table B.1 - Program Variables	82
Table B.2 - Input Data For Flow Equation	86
Table B.3 - Program Listing	87

LIST OF FIGURES

- Figure 1a Closed trench with soil cap, showing cap drainage
- Figure 1b Clay bottom liner (Ref. 1)
- Figure 2 Trench designs for shallow aquifer and arid site (Ref. 2)
- Figure 3 Section along track of migrating radionuclides (Ref. 3)
- Figure 4 Views of two burial sites (from Ref. 3)
- Figure 5 Cross section through concrete vault facility (Ref. 3)
- Figure 6 Profile of encapsulation and cover - Canonsburg site
(Ref.4)
- Figure 7 Sections of typical drained trench (Ref. 2)
- Figure 8 Water Budget for cover system - Canonsburg site (Ref. 4)
- Figure 9 Hydrology of shallow land burial trench (from Ref. 7)
- Figure 10 Soil moisture plots at Maxey Flats at two depths (Ref. 8)
- Figure 11 Soil moisture plots at two depths in a trench cap at Maxey
Flats (Ref. 8)
- Figure 12 Groundwater response to rainfall for one week in February
1983 (Ref. 6)
- Figure 13 Cross section of Test bed trench
- Figure 14 Sketch of test bed elevation
- Figure 15 Views of test bed during construction
- Figure 16 Views of instrumentation on test bed
- Figure 17 Particle size distributions
- Figure 18 Views of laboratory test columns

Figure 19	Electrode calibration - GT Sand
Figure 20	Electrode calibration - SRP #1 soil
Figure 21	Electrode calibration - SRP #2 soil
Figure 22	Drainage curves - Rollo Sand
Figure 23	Resolved drainage curve - Rollo Sand
Figure 24	Moisture Profiles - Rollo Sand
Figure 25	Moisture Profiles for GT Sand at different times
Figure 26	Moisture Profiles for FP Soil at different times
Figure 27	Drainage Curves for GT Sand at different heights
Figure 28	Drainage curves for FP Soil at different heights
Figure 29	Drainage Curves for three soil types
Figure 30	Resolved Drainage Curves for two sands
Figure 31	Calculated Moisture Profiles - Comparable forces
Figure 32	Calculated Moisture Profiles - Suction dominant
Figure 33	Diagram of Migration Model
Figure 33	Diagram of Migration Model
Figure 34	Verification of Flow Model
Figure 35	Repository Concept
Figure 36	Comparative infiltration rates during initial and wet runs (after Ref. 25)

SUMMARY

Low-level waste disposal in shallow trenches has been the subject of much critical assessment in recent years. Historically most trenches have been located in fairly permeable settings and any liquid waste stored has migrated at rates limited mainly by hydraulic effects and the ion exchange capacity of underlying soil minerals. Attempts to minimize such seepage by choosing sites in very impermeable settings lead to overflow and surface runoff, whenever the trench cap is breached by subsidence or erosion.

The work undertaken in the project described in this report was directed to an optimum compromise situation where less reliance is placed on cap permanence, any ground seepage is directed and controlled, and the amount of waste leaching that would occur is minimized by keeping the soil surrounding the waste at all times at only residual moisture levels.

Measurements have been conducted to determine these residual levels for some representative soils, to estimate the impact on waste migration of high unsaturated flow conditions and to generate a conceptual design of a disposal facility which would provide adequate drainage to keep the waste from being exposed to continuous leaching by standing water. An attempt has also been made to quantify the reduced source terms under such periodic, unsaturated flow conditions, but those tests have not been conclusive to date.

Since most disposal sites even in humid regions of the United States are exposed only to intermittent rainfall and as most trench designs incorporate some gravel base for drainage, the results of this project have broader applications in assessing actual migration conditions in shallow trench disposal sites.

Project Personnel
(all parttime)

Geoffrey G. Eichholz, Ph.D.	Project Director
T. Fisher Craft, Ph.D.	Senior Research Scientist
M. Frank Petelka, M.S.H.P.	Graduate Research Assistant
Jooho Whang, M.S.H.P.	Graduate Research Assistant
Fernando N. deSousa, M.S.H.P.	Graduate Research Assistant
Marino C. Kaminski, B.S.	Graduate Research Assistant
Bonny A. Wright, B.S.H.P.	Graduate Research Assistant
Denise D. Hardy, B.S.	Graduate Research Assistant
Martha R. Poston, B.S.H.P.	Graduate Research Assistant
Hobert W. Jones, B.S.	Graduate Research Assistant
Bruce W. Patton, B.S.	Graduate Research Assistant

Some of the work was shared with a parallel project conducted for the Savannah River Laboratory.

INTRODUCTION

Shallow land burial of low-level radioactive wastes has been practiced since the early days of the U.S. atomic energy program. Unfortunately, early programs were only required to meet "maximum permissible concentration" standards for any nuclear facility effluents and very little control was effected on site inventory and waste form. As a consequence, many of those sites contained liquid wastes which seeped into the ground, where they were retained primarily by ion exchange and adsorption processes on mineral surfaces. The appearance of low levels of radioactive materials, especially tritium, in groundwaters offsite drew public attention to disposal conditions that were insufficiently controlled by more recent standards and as a consequence waste disposal of low-level waste was looked on by the public with disfavor as a potential source of hazardous contamination of groundwater. To meet these objections the U.S. Nuclear Regulatory Commission has issued guidelines, under Title 10 Code of Federal Regulations Part 61, that prescribe waste form characteristics and site suitability criteria, but no quantitative performance objectives. The U.S. Environmental Protection Agency, on the other hand, is in the process of specifying effluent concentration levels under Hazardous Waste Regulations (40CFR 122,265) or the Resource Conservation and Recovery Act (RCRA).

In either case, performance assessment depends on a good understanding of the mechanisms that govern mobilization and migration of the waste materials through soil or fractured rock into any accessible aquifer, since groundwater transport is the only feasible pathway, other than deliberate or accidental intrusion, by which the waste materials can return to the accessible environment. Most of the calculational models described in the literature assume, that sooner or later water infiltrates the burial trench, saturates the soil, leaches some of the waste at a rate controlled mainly by solubility considerations, and that the dissolved waste travels with the water, subject to retardation by surface adsorption on surrounding minerals, until an aquifer is reached, through which in due course it may reach the surface, in springs or wells, to enter the food chain.

Control of this process, in 10CFR61 and related documents, is envisaged primarily by four precautions: 1.use of a solid waste form, that, hopefully, is not excessively subject to dissolution; 2.waste deposition well above the water table; 3.use of an impermeable soil formation to minimize water flow towards the aquifer; and 4.installation of a stable impermeable trench cap to inhibit or retard water infiltration into the trench.

These approaches are illustrated in Figures 1 and 2 (Refs. 1 & 2) which illustrate diagrammatically the main elements of such a trench. In Figure 1 additional lining is introduced to contain water in the trench.

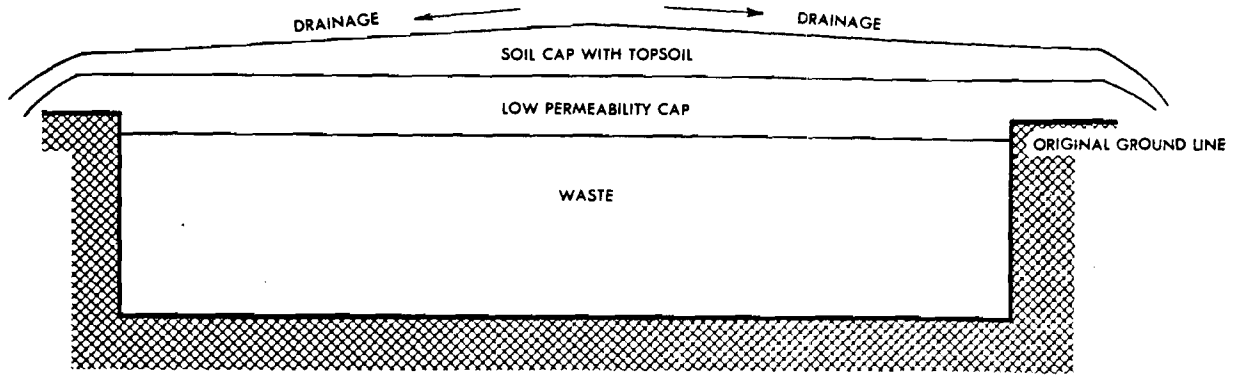
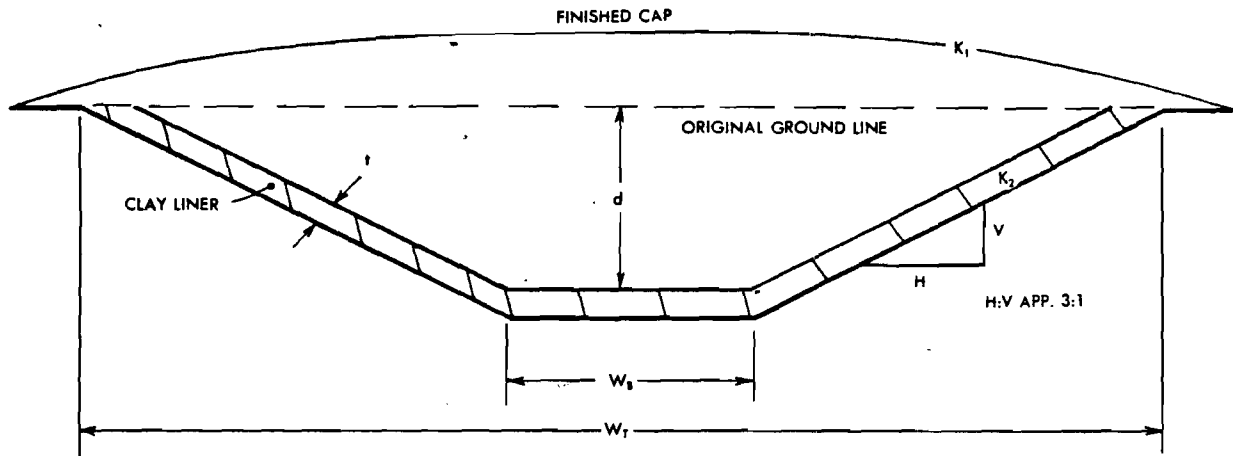
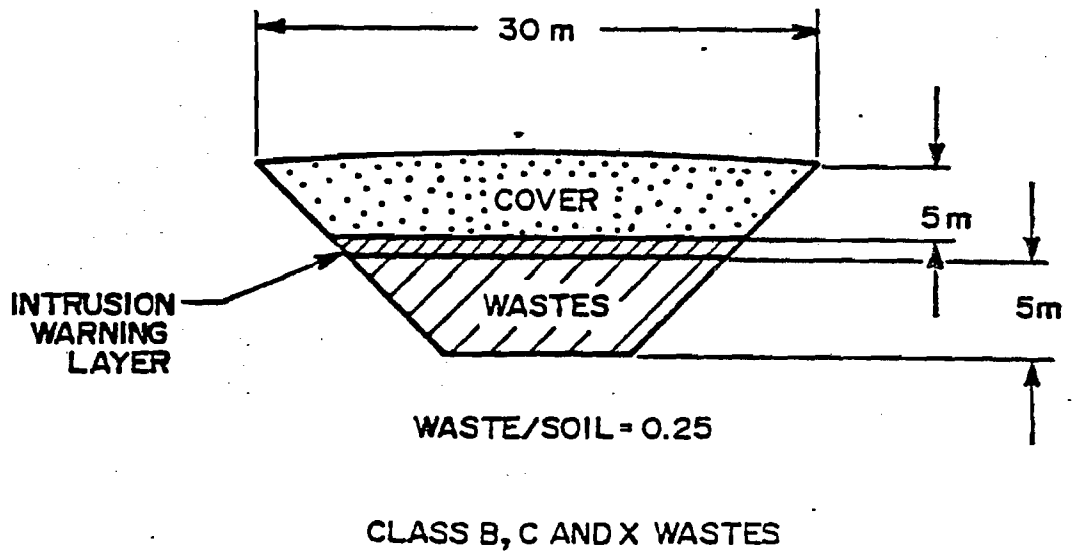
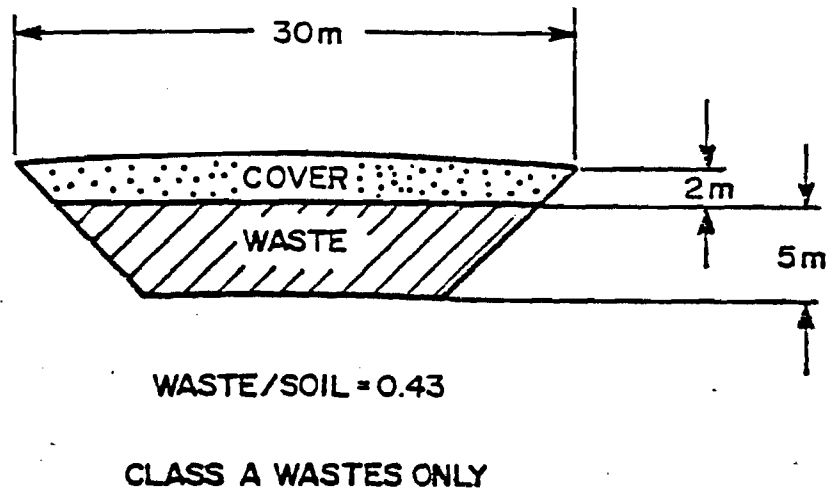


Figure 1a Closed trench with soil cap, showing cap drainage



- H:V APPROXIMATELY 3:1
- W_T = TOTAL WIDTH
- W_B = BOTTOM WIDTH
- K_1 = COEFFICIENT OF PERMEABILITY FOR FINISHED CAP
- K_2 = COEFFICIENT OF PERMEABILITY FOR LINER
- d = DEPTH
- t = THICKNESS
- V = VERTICAL
- H = HORIZONTAL

Figure 1b Clay bottom liner (Ref. 1)



RAE-100210

Figure 2 Trench designs for shallow aquifer and arid site (Ref. 2)

Figure 2 also shows a possible warning layer "to deter intruders". Short of actually concreting the walls or the trench bottom, some seepage ultimately will occur with a plume following the hydraulic gradient in the water table (Fig 3, from Ref.3). Figure 4(Ref.3) illustrates the actual construction of some shallow trenches.

Several problems can arise in this approach. First of all, the trench cap will tend to collapse or erode in time, due to consolidation or compaction of the waste materials and the interstices between them, settling of backfill soil, and the effect of surface water. This means that sooner or later water will enter the trench unless very elaborate cap structures are devised. Figures 5 and 6 give examples of such cap designs, which add enormously to the cost of disposal and are almost equivalent to the surface bunker retrievable storage concept.

The second problem arises from the fact, that with a highly impermeable base formation any infiltrated water in the trench has nowhere to go and sooner or later will fill the trench and overflow. This "bath tub effect" has been observed at some sites and results in surface flow of trench water, instead of downward seepage towards the water table, and an early return to the accessible environment of potentially contaminated water. In addition, the waste would find itself engulfed by standing water so that any leaching effects would be greatly increased. Abatement of the bath tub effect by reliance on even more elaborate cap structures is questionable and expensive, particularly since there is no guarantee that lateral inflow into the trench would not occur. McCray et al. (Ref.5) have reported observations on such interflow.

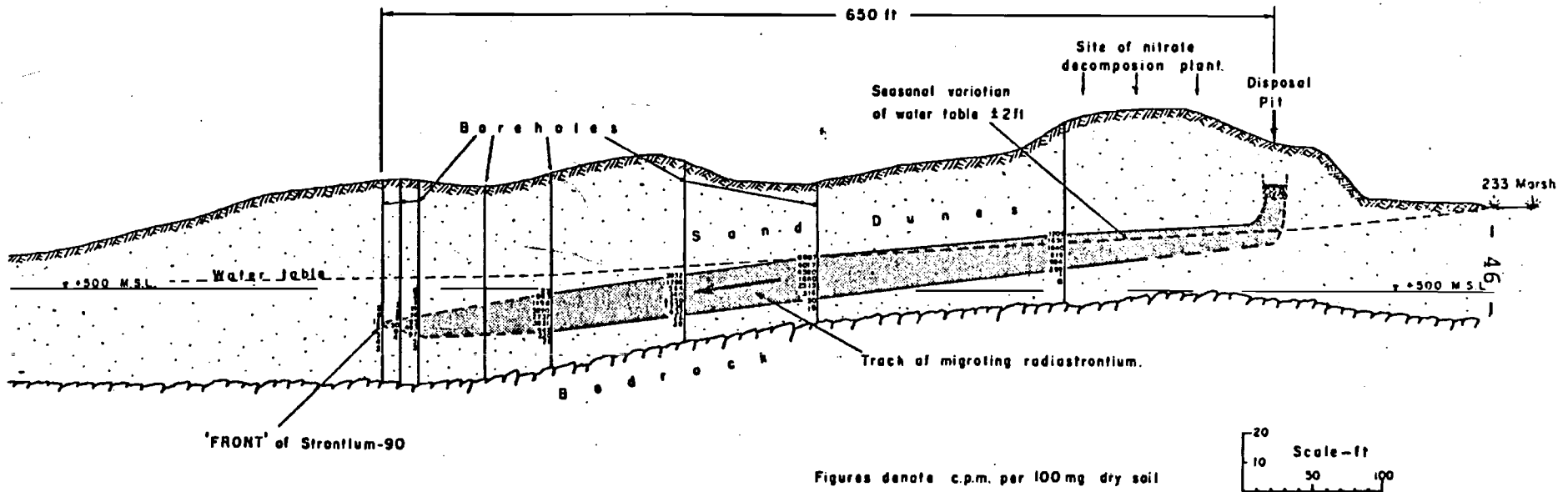
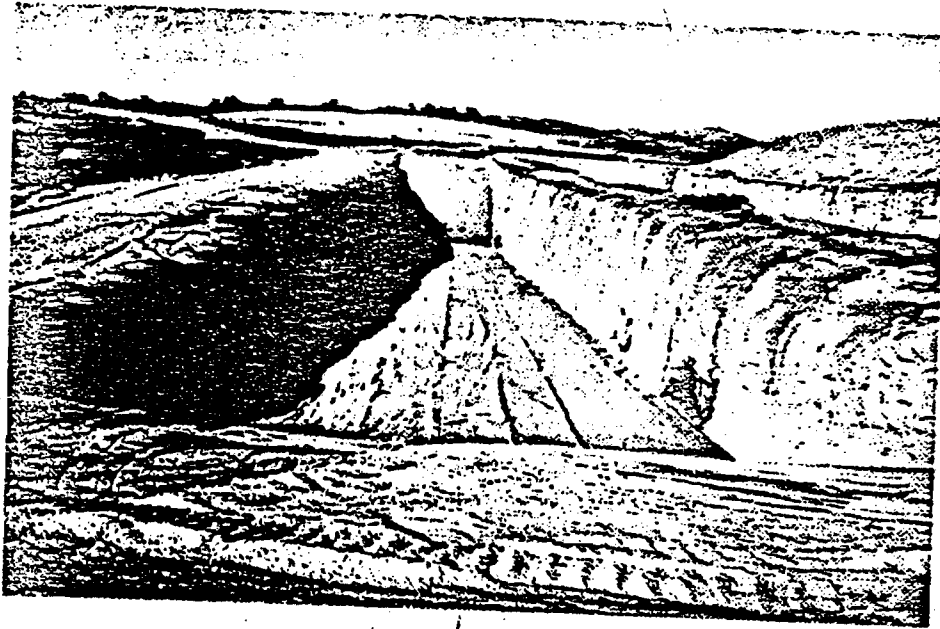
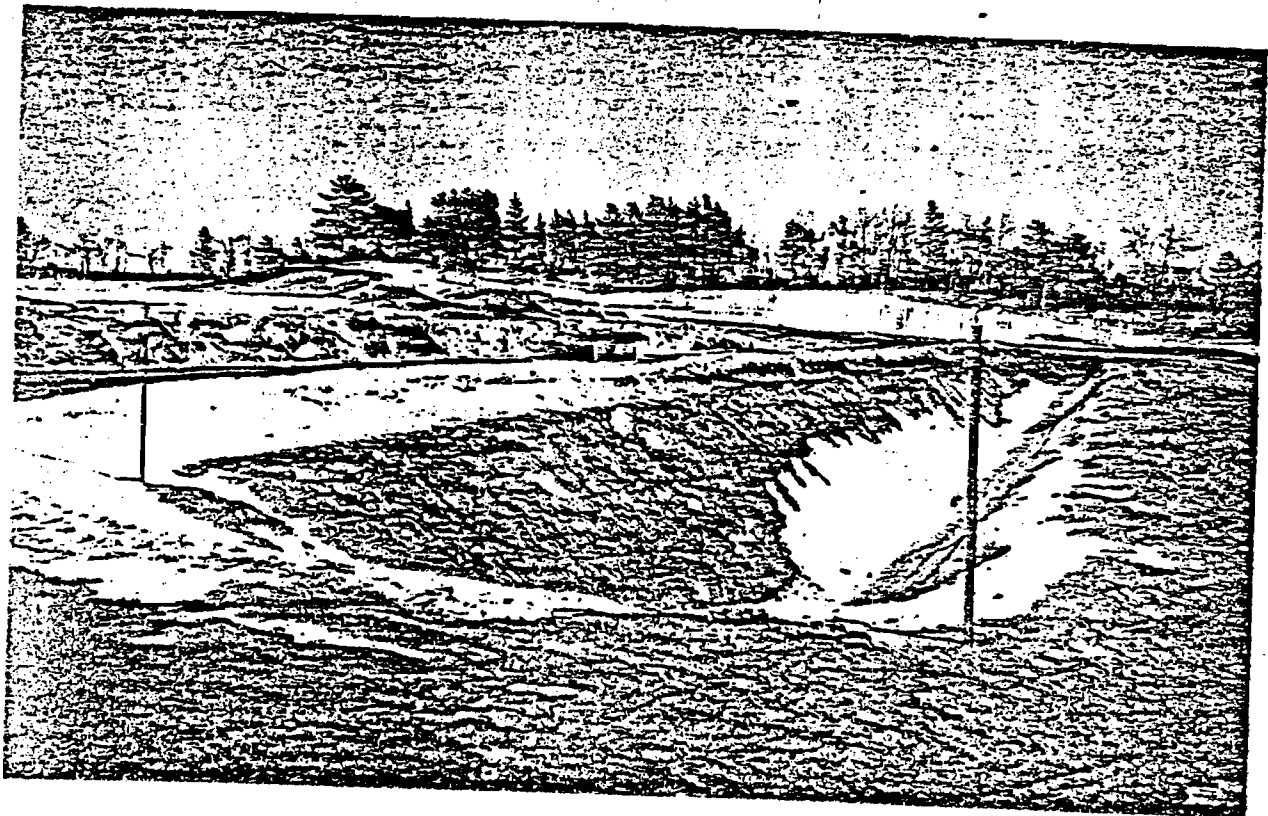


Figure 3 Section along track of migrating radionuclides (Ref 3)



Waste Burial Pit at the Los Alamos Scientific Laboratory (New Mexico, USA) Dug into Tuff (180' x 15 x 8 m Deep). Note Steep Slope and Relatively Clean Cut Walls [11]



A Trench Dug into Sand in Area "C" at CRNL Showing Shallow Sloped Walls

Figure 4 Views of two burial sites (from Ref. 3)

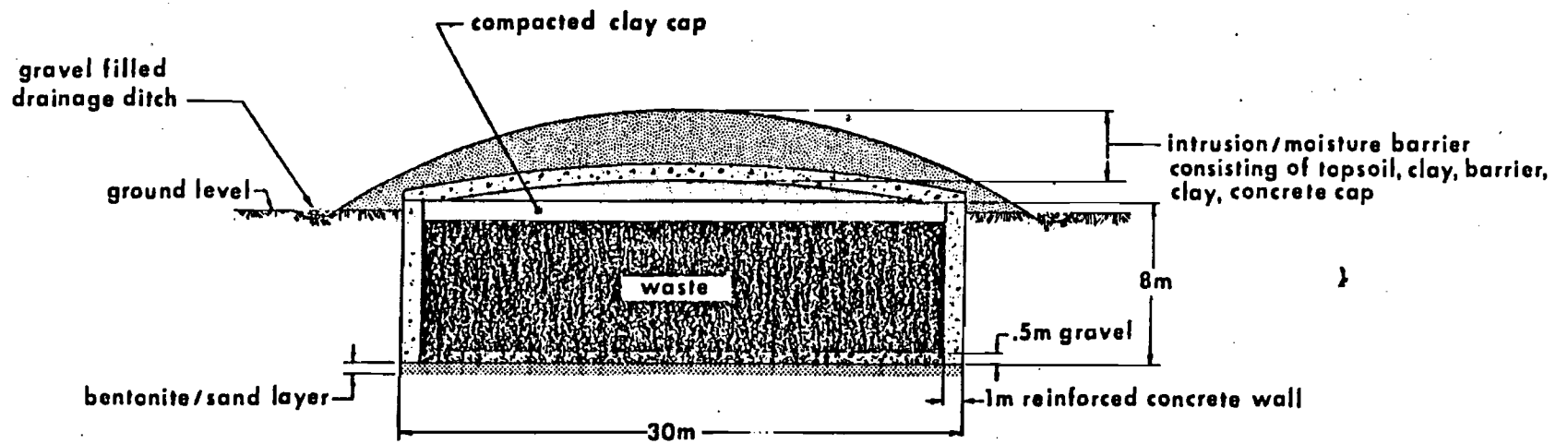


Figure 5 Cross section through concrete vault facility (Ref. 3)

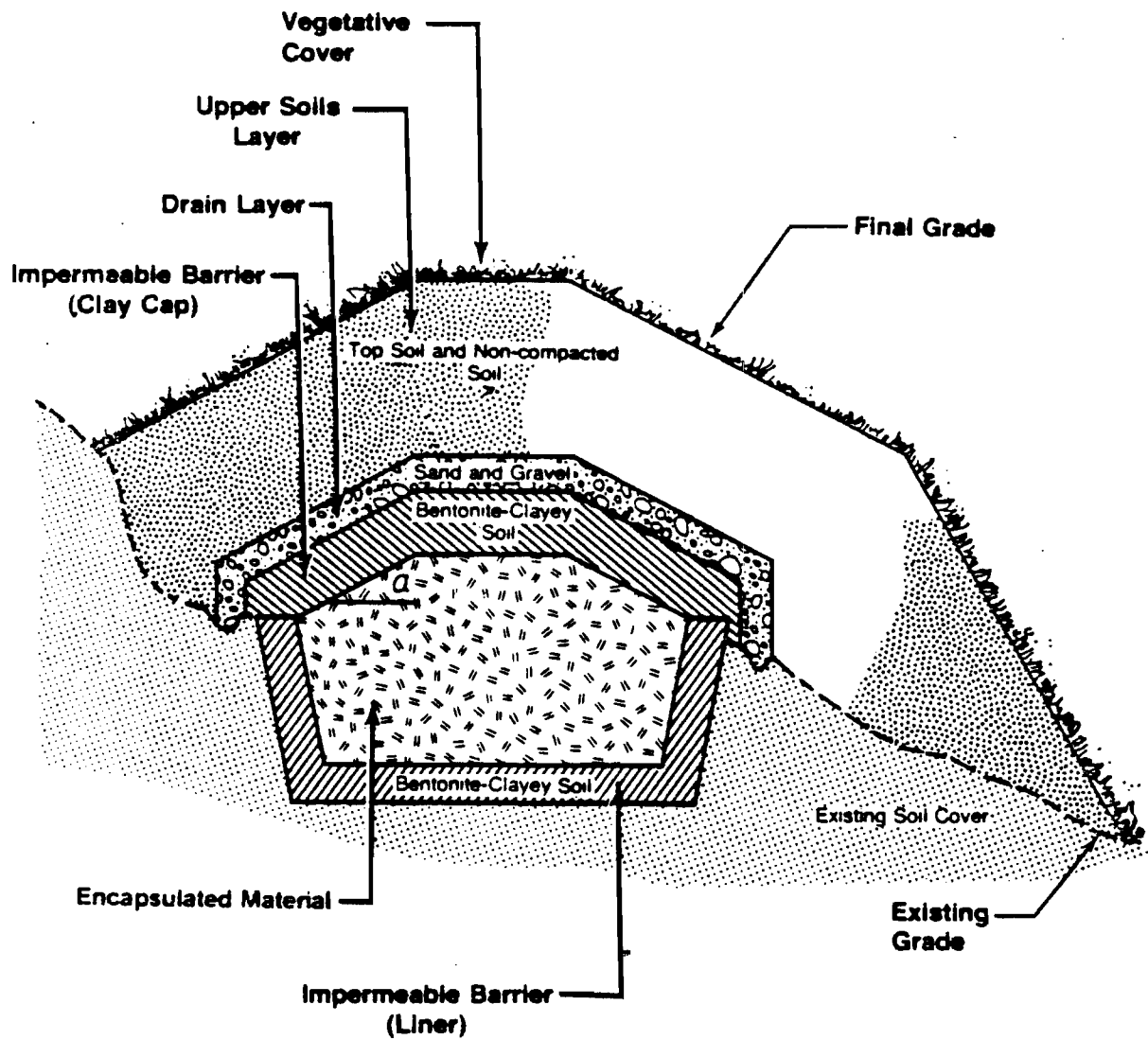


Figure 6 Profile of encapsulation and cover - Canonsburg site (Ref. 4)

a - Slope Angle

An alternative way of dealing with the threat of a bath tub effect is by the installation of drains, combined in some cases by deliberate pumping from the trenches. This approach is illustrated in Figure 7 (Ref. 2), where the pump well is also used for monitoring purposes, and has been proposed for the Central Disposal Facility at Oak Ridge for hazardous wastes (Ref. 6). For the Canonsburg site, Metry et al. (Ref. 4) also propose a near-surface drain to minimize infiltration, see Figure 8.

In the work described in this report this approach has been taken a stage further by allowing the drained-off water to seep into the ground along a predetermined seepage path. This eliminates the need for active pumping which would normally be impractical after closure of the site. By also selecting conditions promoting easy drainage, one also minimizes the amount of moisture in contact with the waste, so that leaching effects may be greatly reduced, resulting in a much smaller source term for any hazard prediction. This project has been concerned with studying the effects of avoiding high water content in the waste area on leach effects and model calculations and with a consideration of conceptual designs for this approach.

A preliminary account of this work was presented at the DOE Participants Meeting in Denver in September, 1984 (Ref. 7).

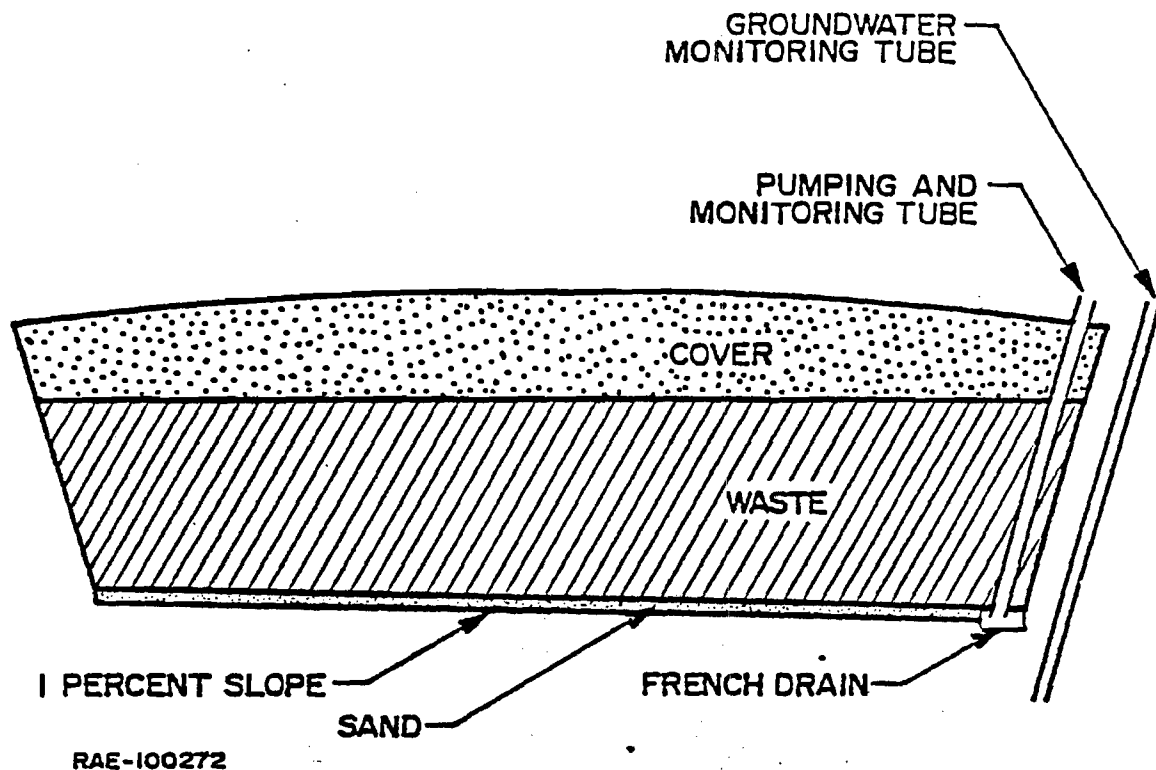


FIGURE 7-a. CROSS SECTION OF TYPICAL TRENCH

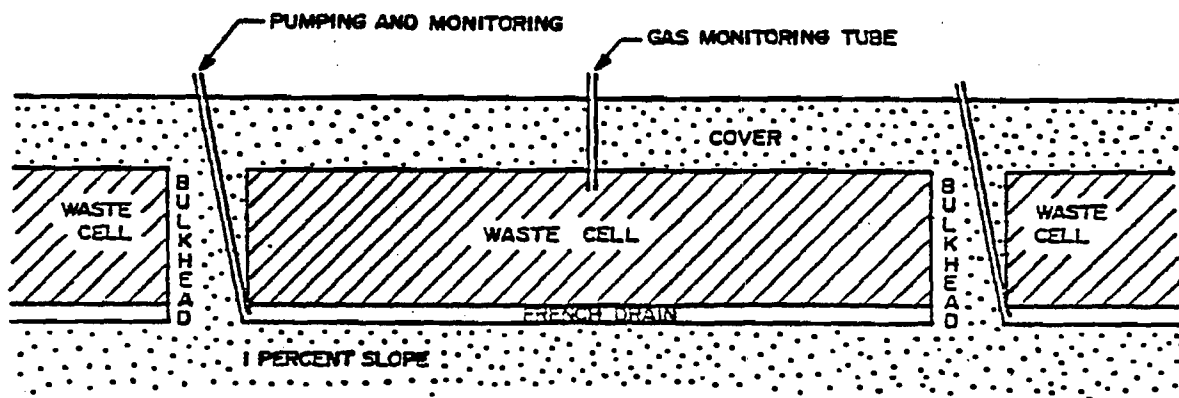


FIGURE 7-b. SECTION OF TYPICAL TRENCH ALONG ITS LONG AXIS

Figure 7 Sections of typical drained trench (Ref. 2)

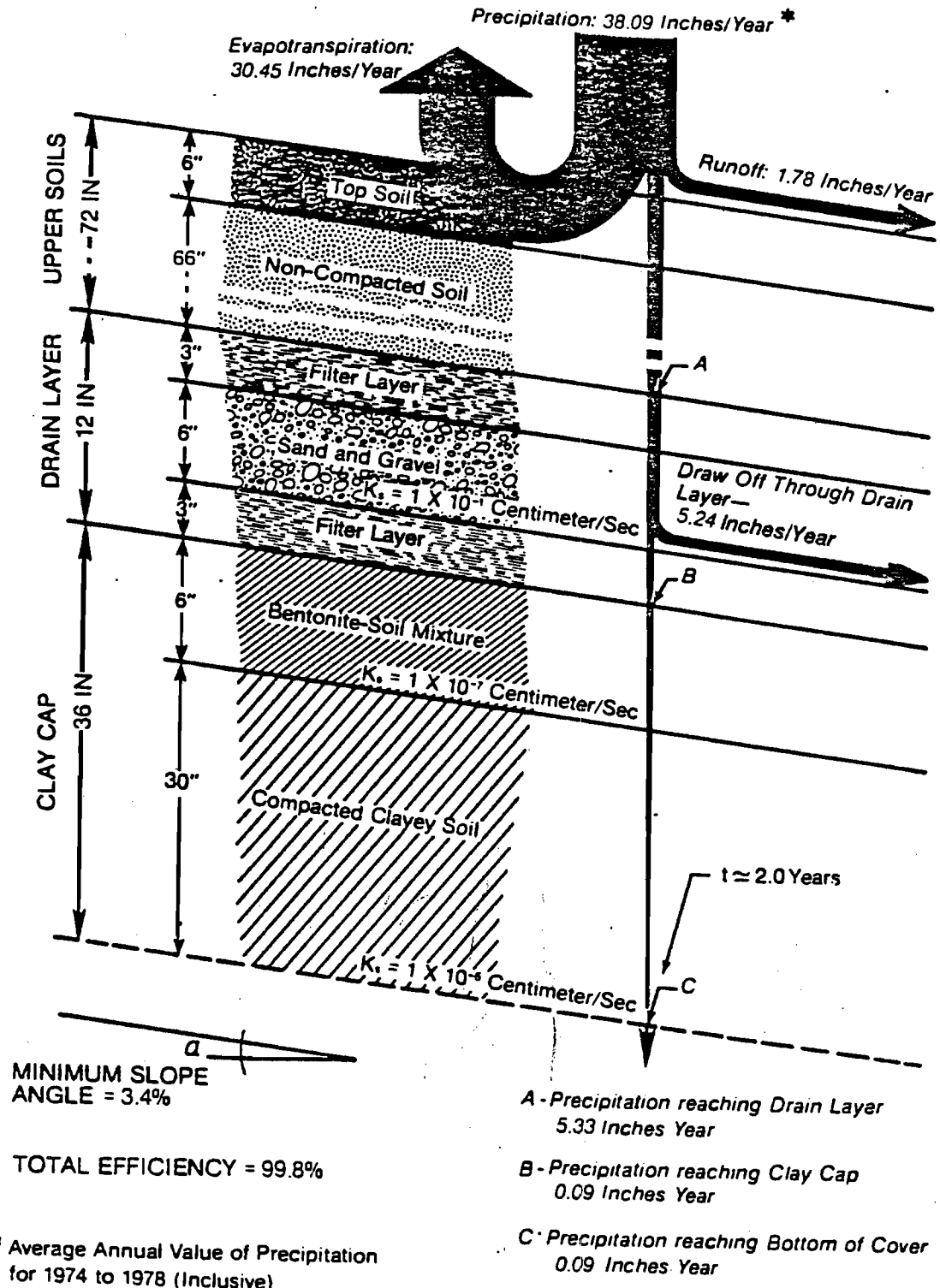


Figure 8 Water budget for cover system -- Canonsburg site (Ref. 4)

TRENCH HYDROLOGY

The hydrology of a burial trench is shown diagrammatically in Figure 9. A very high proportion of precipitated water is returned to the atmosphere by evaporation and evapotranspiration and only 20-25% or less will actually infiltrate the trench itself. Once there, water movement is subject to a balance of gravitational and capillary forces, though for fairly permeable backfill surrounding waste packages it is reasonable to assume a slow, but steady net downward flow. As this flow passes the buried wastes it is usually assumed that some leaching will occur, i.e. decontamination of buried waste material by the passing flow of water and dissolution of some radioactive materials, that may then remain in solution or adsorb on some fine suspended particulates that may be present. Self-retention within the backfill soil presumably occurs, but is rarely included in any assessment model.

Although 10CFR61 assumes location of the trench in an impermeable medium, any impact assessment ordinarily takes the finite permeability of the surrounding soil for granted and accepts it as the normal pathway for the dissolved waste ions or complexes (9,10). Innumerable measurements have been reported on the resultant flow through such soil and on retardation effects on the migration of any dissolved ions due to sorption-desorption effects on any mineral surfaces in contact with the water flow (11-15). These processes are generally considered part of the engineered barriers of the system, but invariably are assumed to be subject to saturated flow.

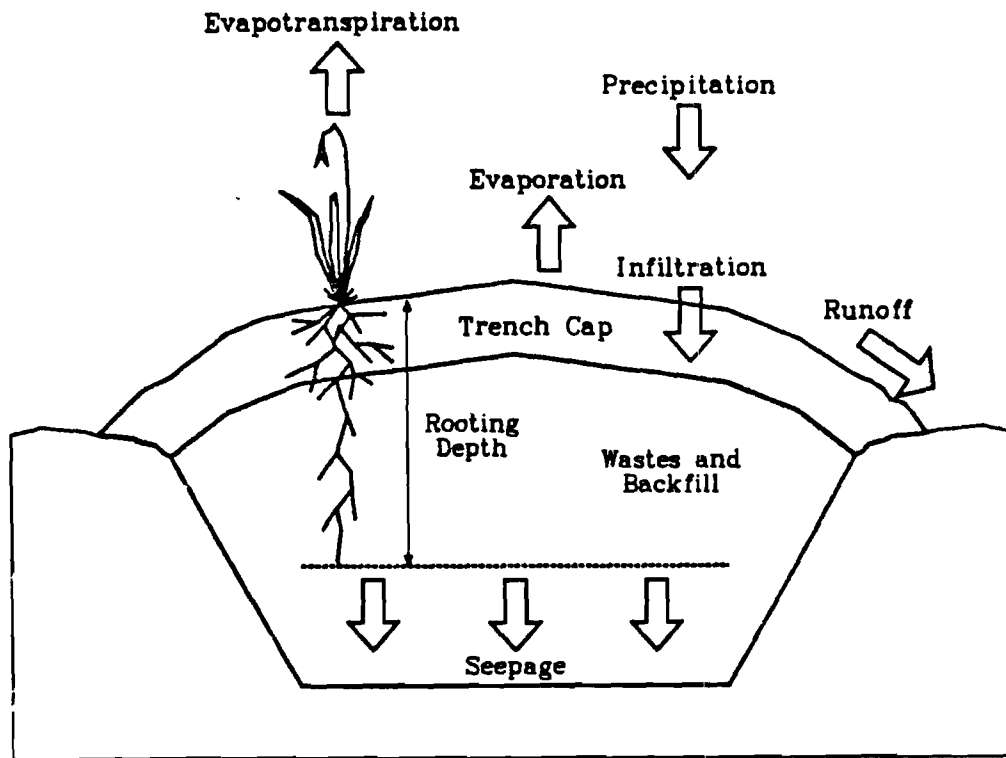


Figure 9 Hydrology of shallow land burial trench(from Ref. 7)

Actually, most soil systems will not be saturated unless the soil is unusually retentive or the water is allowed to back up, as in the bathtub situation (16). For arid sites in the Western U.S., soil saturation would be rare; this has been studied by the Los Alamos group (17-19). Figures 10 and 11 show variations in moisture profiles at Maxey Flats observed near the surface (0.9m) and at depth (2.4m). Strong seasonal variations are evident near the surface; a smooth curve exists at depth. In both cases moisture levels were well below saturation most of the time, though in the trench cap significant water retention occurred because of suction effects from its lower surface. Observations by Davis et al. (Fig. 12) also show that variations in the level of the water table following rainfall depend on rapid infiltration flow and only slow drainage rates (21). Thus, even in the "humid zone" of the Eastern United States unsaturated moisture conditions may prevail for much of the time, between heavy showers, as occur in the South, or during periods when the surface is frozen or snow-covered in the North. If the backfill and surrounding soils are fairly permeable, this implies that the waste may find itself in moderately dry surroundings much of the time and the time-averaged leach rate may be substantially different from that assumed for "conservative", saturated conditions. The present study was directed to investigate the benefits of reducing the ambient moisture levels around the waste as much as possible by accepting a periodic mode of infiltration and removing the major cause of water back up.

Migration of dissolved wastes under unsaturated conditions is a fairly complex process. In a clay-rich soil not all of the water present

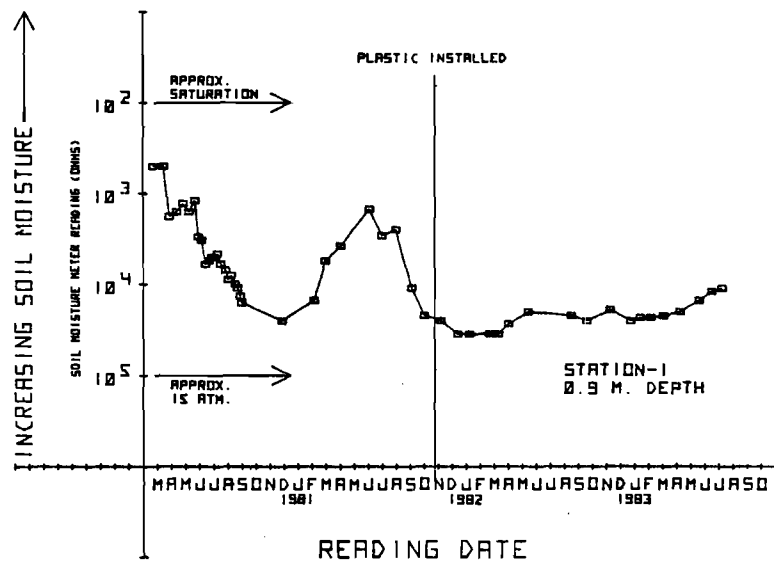
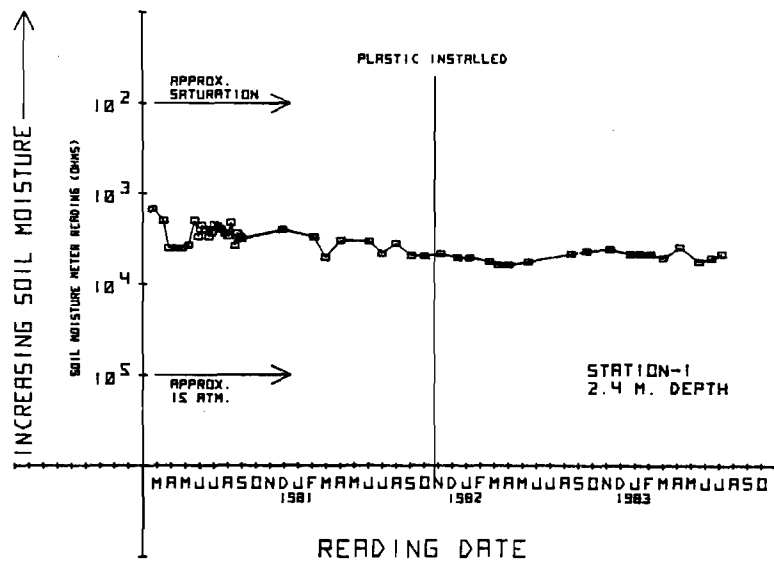


Figure 10 Soil moisture plots at Maxey Flats at two depths (Ref. 8)

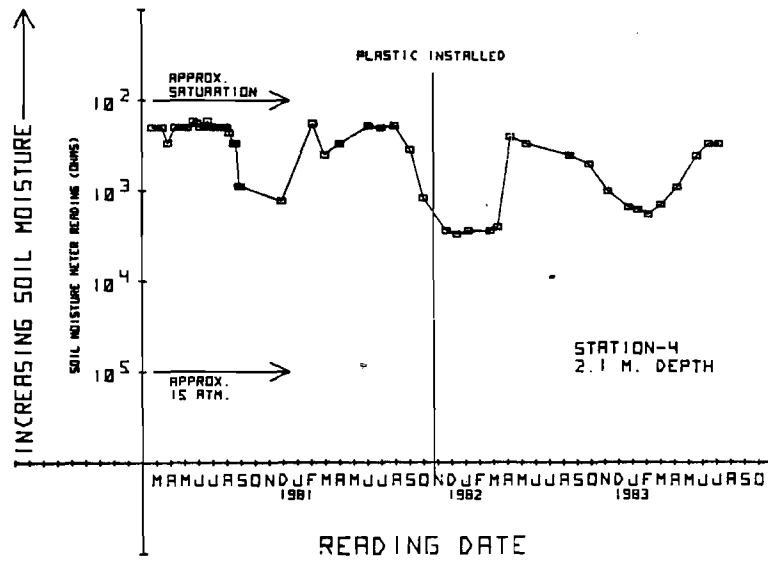
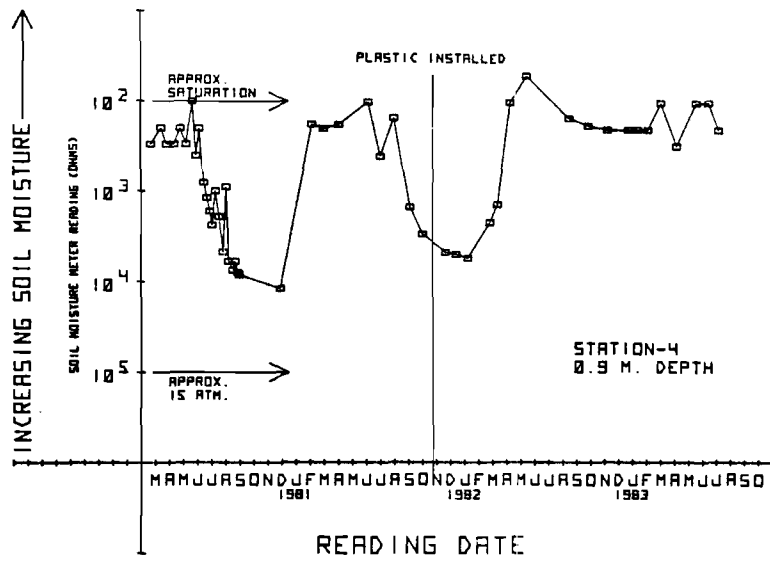


Figure 11 Soil moisture plots at two depths in a trench cap at Maxey Flats (Ref. 8)

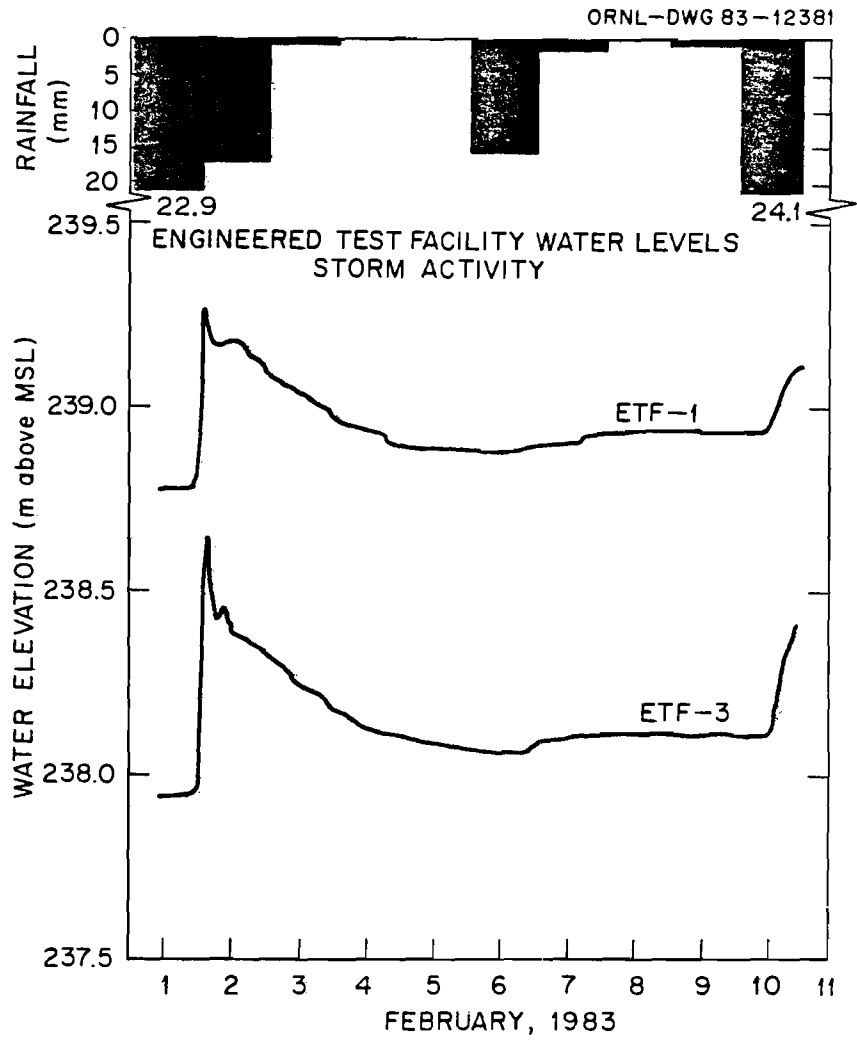


Figure 12 Groundwater response to rainfall for one week in February 1983

(Ref. 6)

in the soil is mobile, but may be bound in the clay structure. The mobile water may move slowly and would not fill all of the pores (22). As a result the volumetric flow rate for a given percent saturation value would not be proportional to the water content. As moisture content decreases the capillary force begins to predominate. This has two consequences:

1. Except in highly permeable, coarse materials, like coarse sand, the moisture level will reach a finite minimum residual moisture concentration, which depends on the hydraulic conductivity of the soil and, typically, its clay content, and which will be retained indefinitely at depths below those affected by evapotranspiration.
2. Above any major structural interface, a moist column will be retained by suction forces that may have a higher moisture content than the drained volume above. This leads to an effect of water flow around cavities, such as waste materials, reducing effectively the amount of water available for leaching. It also imposes a need to allow a soil layer above any built-in drain before emplacing wastes.

All of these effects have been studied in this project to the extent that they affect disposal trench design. The work undertaken in this project consisted of four main tasks:

- a) Construction of a test bed to study the response of a soil column to steady or periodic infiltration under unsaturated flow conditions;
- b) Development of a simple computer model to permit generalization of the data obtained;

- c) Study of waste leaching conditions when exposed to unsaturated flow;
and
- d) Conceptual design of a shallow waste burial facility to minimize immersion of the waste material by the provision of drains and directing the off flow.

Various subsidiary tasks, such as characterization of soils, calibration of moisture probes, and code development benefited from parallel work going on under the sponsorship of the Savannah River Laboratory, EI Du Pont de Nemours & Co.

TEST BED CONSTRUCTION

One of the prime objectives of this investigation was the measurement and demonstration of flow and drainage conditions of representative soil columns under unsaturated conditions. Tests were also conducted on laboratory scale columns, but from the start it was considered essential to conduct field scale tests to minimize wall effects and drain interface effects.

The test bed was intended to be readily drained and to be accessible from one side to measure moisture profiles during the course of a run. It had to be easy to dismantle, capable of being layered if necessary, and subject to various methods of introducing water flow.

A site was chosen on a natural slope behind the Frank Neely Nuclear Research Center and the Electronics Research Building on the Georgia Tech Campus. Figure 13 is a sketch cross section of the trench. The bed itself consisted of a wooden box, 6ft high, 2 ft. x 2ft. in cross section which was installed in the trench cut whose walls had been lined with plastic sheet and braced. Figure 14 shows the major dimensions in plan. Figure 15 presents two stages in the construction of the trench and the installation of the test box. Some major problems were encountered in the construction and installation of the drain pan, which underwent several modifications. Similarly, experience led to various improvements in revetment of the trench walls and the sloping of the drainage bed at the bottom of the trench. The assistance of the Georgia Tech Physical Plant Department in cutting the trench and supplying gravel and other materials is gratefully acknowledged.

The front panel is removable for loading and unloading. Figure 16a shows a series of tensiometers that were installed to measure moisture profiles. The tensiometers were Soiltest Inc., Model 120; great care had to be taken in their installation to remove any residual air bubbles. It was found that the tensiometers were insufficiently responsive at low moisture concentrations and, for that reason, most later tests relied on electrical conductivity probes. Figure 16b shows the contact panel and meter for these probes on top of the test bed.

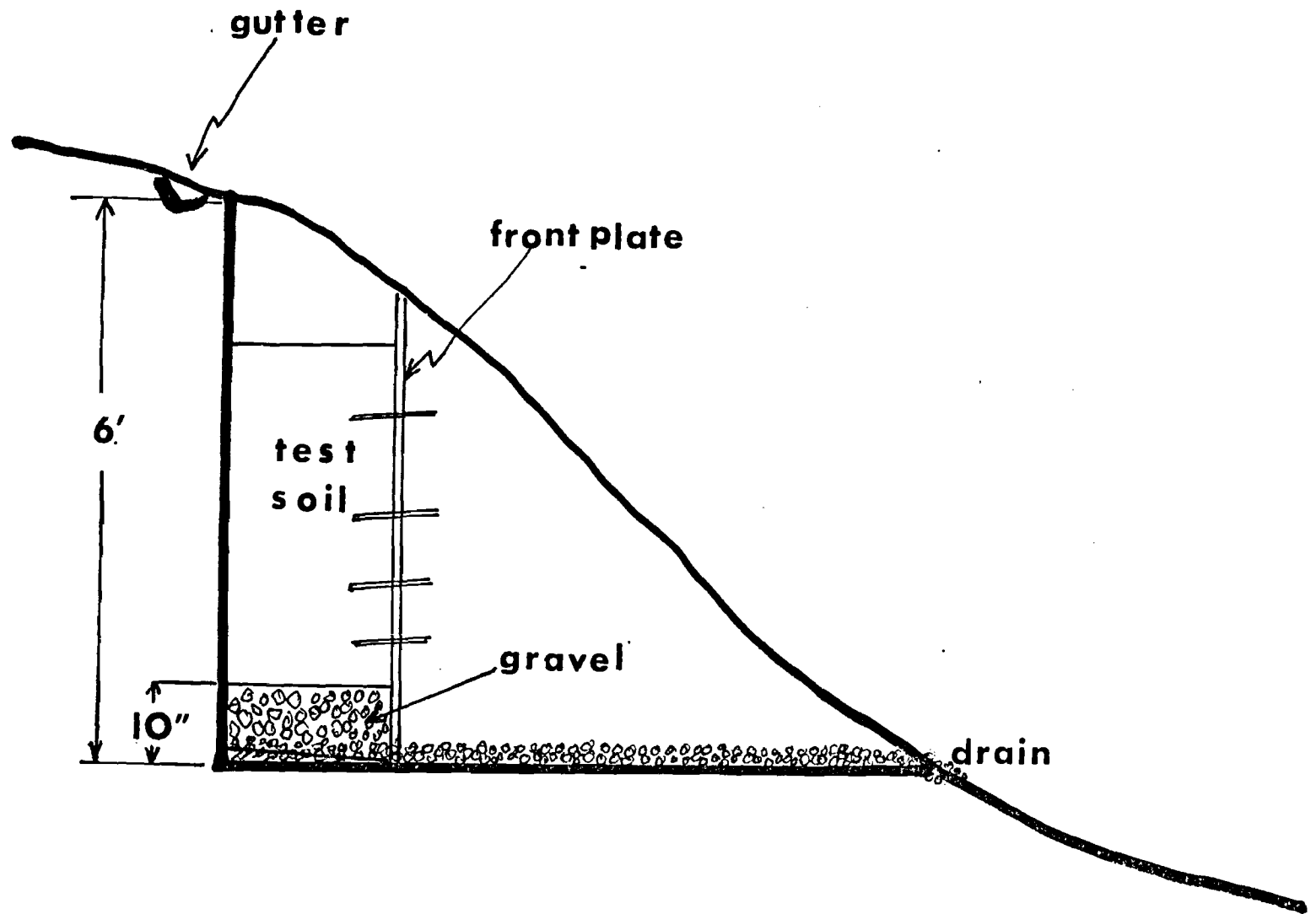


Figure 13 Cross section of Test bed trench

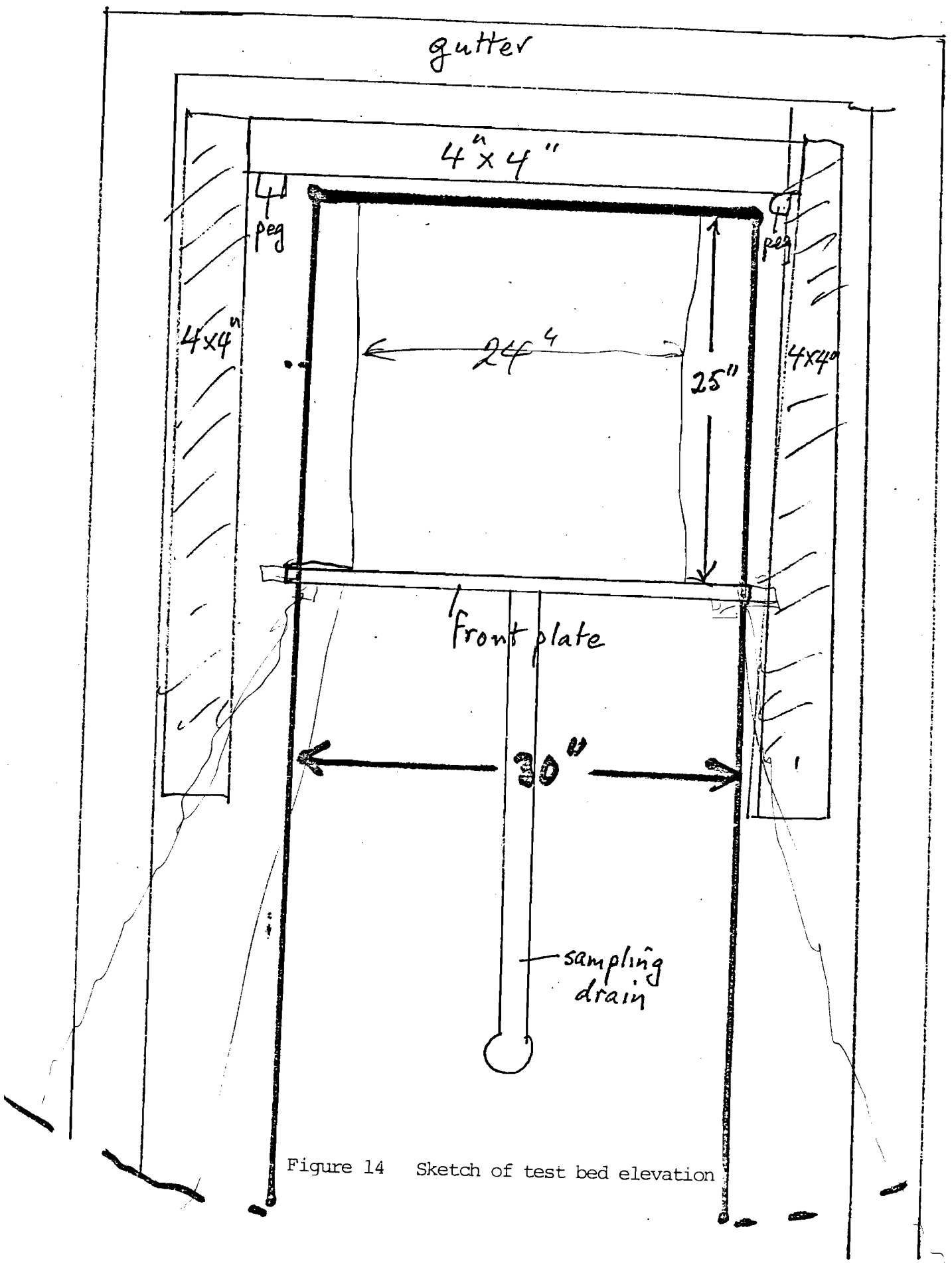


Figure 14 Sketch of test bed elevation

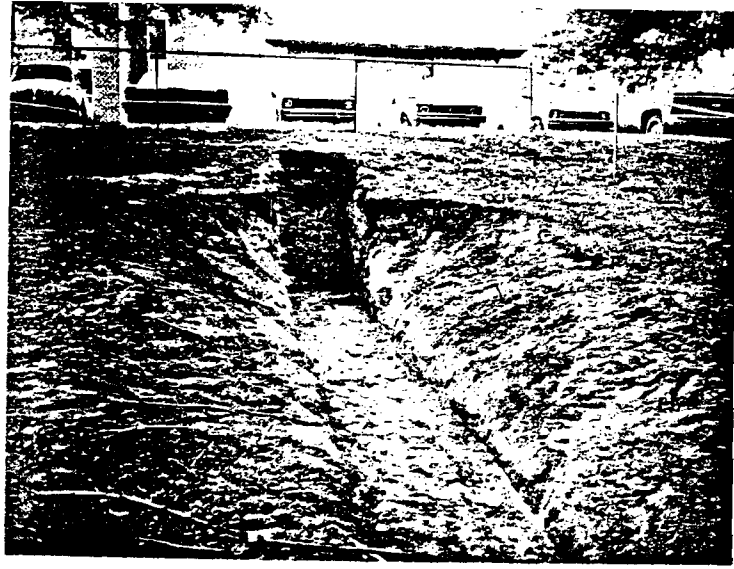


Figure 15 Views of test bed during construction

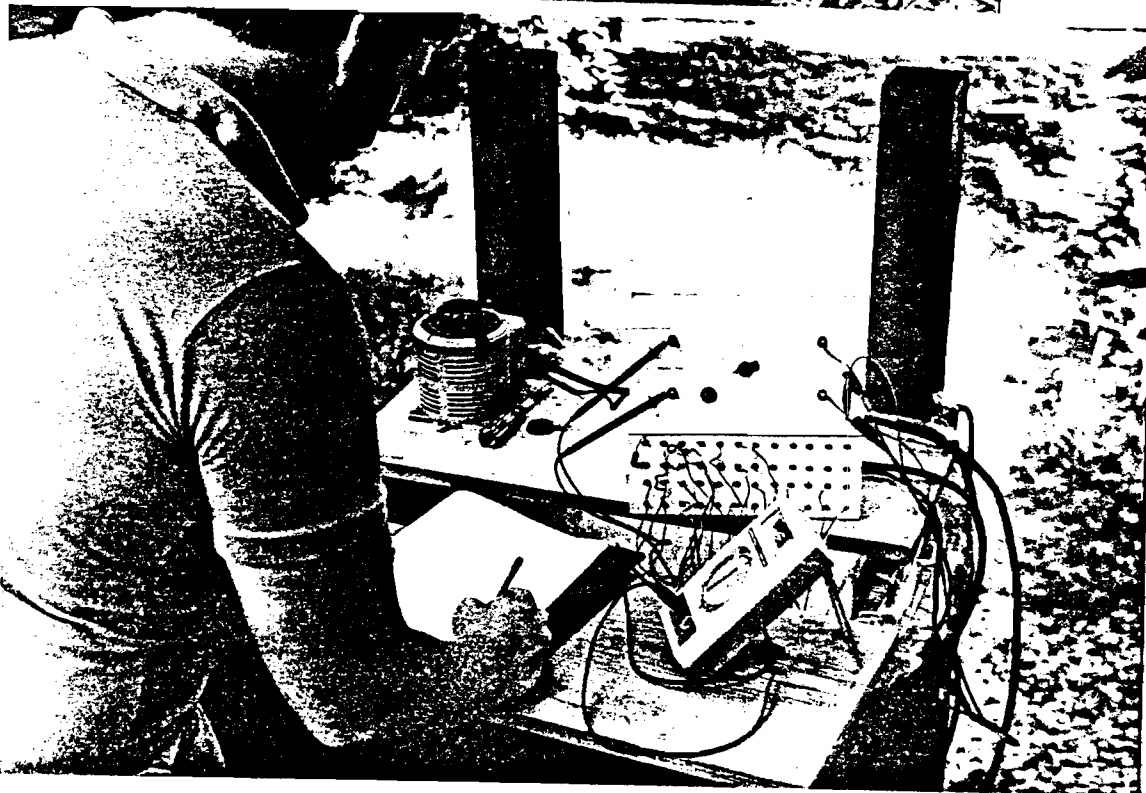


Figure 16 Views of instrumentation on test bed

MATERIALS

Test work was done with two types of sand, referred to as Rollo Sand and GT Sand, two types of fairly clayey soils, SRP No. 1 and No. 2, and a synthetic mixture, FP soil. Table 1 lists the basic properties and composition of these soils.

TABLE 1 - SOIL PROPERTIES

SOIL TYPE	BULK DENSITY (g/cm ³)	POROSITY	SAND FRACTION (%)	SILT FRACTION (%)	CLAY FRACTION (%)	SATURATED HYDRAULIC CONDUCTIVITY (cm/day)
Rollo Sand	1.4.0	0.472	98.9	1.1	0.0	-
G.T. Sand	1.38	0.479	97.4	2.6	0.0	2000
SRP #1	1.24	0.32	62.0	9.0	29.0	30
SRP #2	1.20	0.547	56.0	4.0	40.0	60
FP Soil	1.42	0.466	73.4	15.5	11.4	-

Particle size analyses were conducted and the distribution curves of the four soils under study were determined. The results are shown in Table 2; Figure 17 shows the distribution curve of three of the soils.

Table 2 - PARTICLE SIZE DISTRIBUTION - G. T. SAND

DIAMETER (μ m)	% PASSING (%)	DIAMETER (μ m)	% PASSING (%)
1410.0	90.7	23.0	1.5
1000.0	80.7	13.0	1.5
707.0	65.8	9.3	0.7
500.0	46.6	6.6	0.7
250.0	10.4	5.0	0.7
105.0	2.9	3.5	0.0
75.0	2.6	2.7	0.0
36.0	1.5	1.3	0.0

TABLE 3 - PARTICLE SIZE DISTRIBUTION - ROLLO SAND

DIAMETER (μm)	% PASSING (%)	DIAMETER (μm)	% PASSING (%)
1410.0	86.0	36.4	1.2
1000.0	51.3	23.0	1.2
707.0	12.8	13.3	1.2
500.0	4.5	9.4	1.2
250.0	1.3	6.7	0.6
105.0	1.1	4.7	0.6
75.0	1.1	3.4	0.0

TABLE 4 - PARTICLE SIZE DISTRIBUTION - SRP #1

DIAMETER (μm)	% PASSING (%)	DIAMETER (μm)	% PASSING (%)
1410.0	97.1	7.6	30.4
1000.0	94.5	5.4	29.7
500.0	80.4	3.8	29.7
250.0	61.0	2.7	29.0
75.0	34.8	2.0	28.3
63.0	34.2	1.1	27.7
29.0	33.1	1.0	27.0
18.4	32.4	0.8	26.3
10.7	31.7	0.7	25.6

TABLE 5 - PARTICLE SIZE DISTRIBUTION - SRP #2

DIAMETER (μm)	% PASSING (%)	DIAMETER (μm)	% PASSING (%)
1410.0	97.1	16.5	42.3
1000.0	94.6	9.6	41.6
500.0	84.2	6.9	40.9
250.0	62.1	4.9	40.3
75.0	43.3	2.4	39.6
63.0	43.1	1.0	38.9
25.8	43.0		

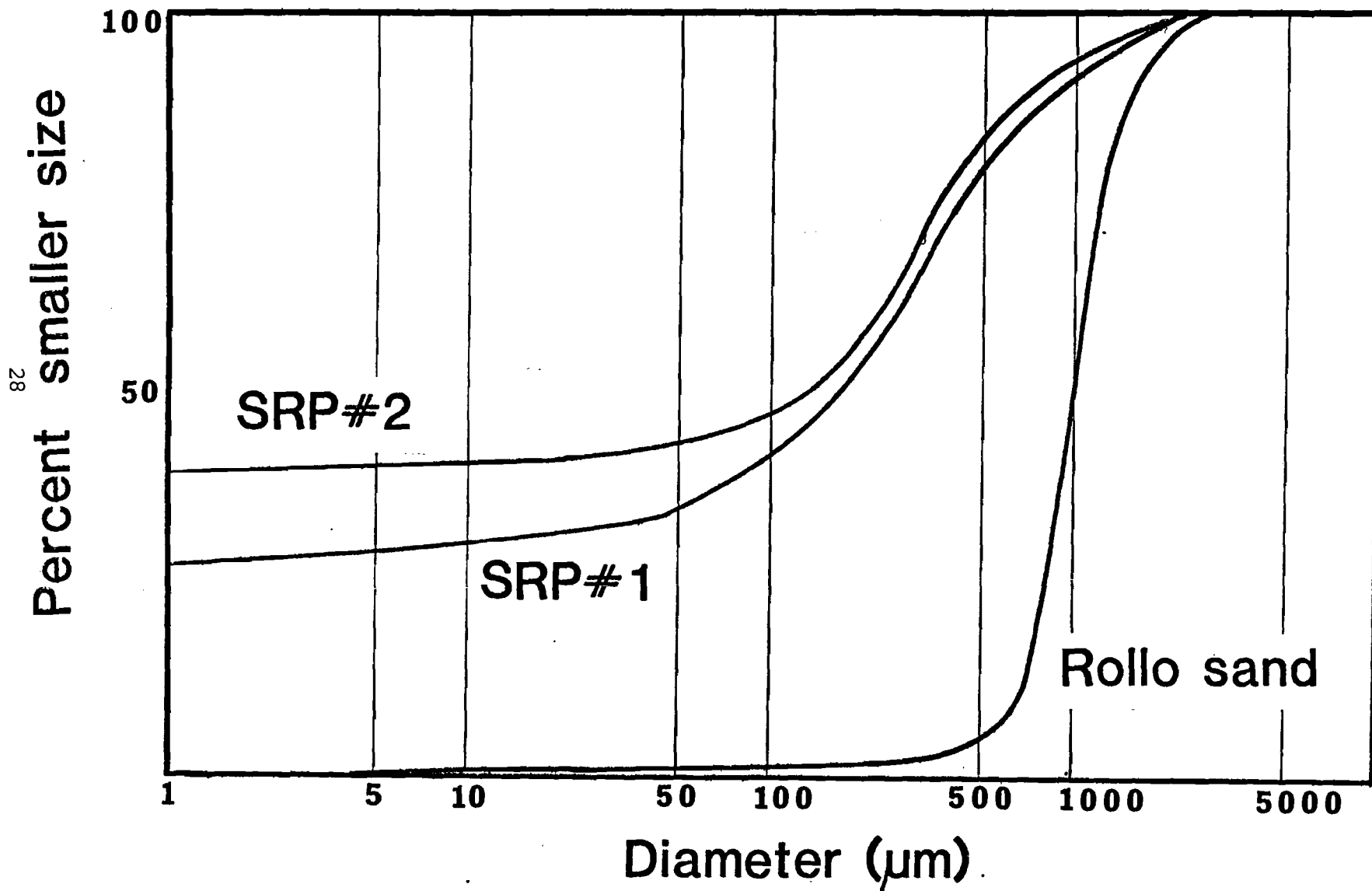


Figure 17 Particle size distributions

LABORATORY TESTS

Bench-scale tests were conducted to evaluate the basic properties of the soils, to measure residual moisture levels and to calibrate the conductivity probes for use in the test bed. Column tests were conducted in three sizes of tubes, which are shown in Figure 18. The short tubes, top right were employed mainly to obtain residual moisture contents, though care had to be taken to allow for the suction layer above the bottom screens. The other columns had built-in electrodes and were calibrated by direct weight-loss moisture determinations. The larger columns, Fig 18c, have been used for hydraulic conductivity measurements and for radiotracer tests.

Figures 19-21 present electrode calibration curves, plotting electric resistance between adjoining electrodes versus percent saturation, for GT sand and the two SRP soil samples. For consistent results, care had to be taken to ensure even packing and the column had to be presaturated to remove any remaining air. The calibrations for the various columns were consistent, but in practice the electrodes had to be recalibrated for the large test bed.

Since the purpose of the project was to minimize soil water content surrounding the waste material, it was important to measure how low a moisture content could be obtained by draining. Due to capillarity effects all soils will retain a minimum moisture content once water has infiltrated, with the amount retained dependent on pore size, surface watability and clay content.

Table 6 shows the results of a series of tests on sized sand columns. As expected, the finer sizes (large mesh number) retain more water in their smaller pores. Table 7 compares the residual water content for two sands and two SRP soils, whose size distribution was shown in Figure 17. Again, as expected, the SRP soils with their high clay content and fine size components show relatively high residual water values.

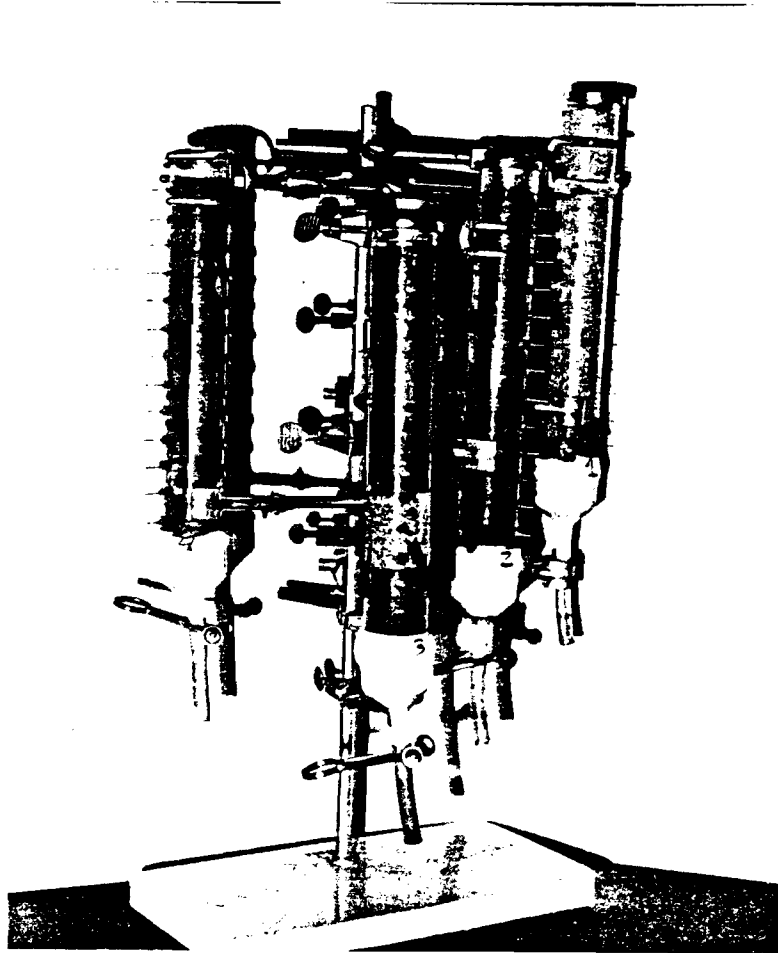
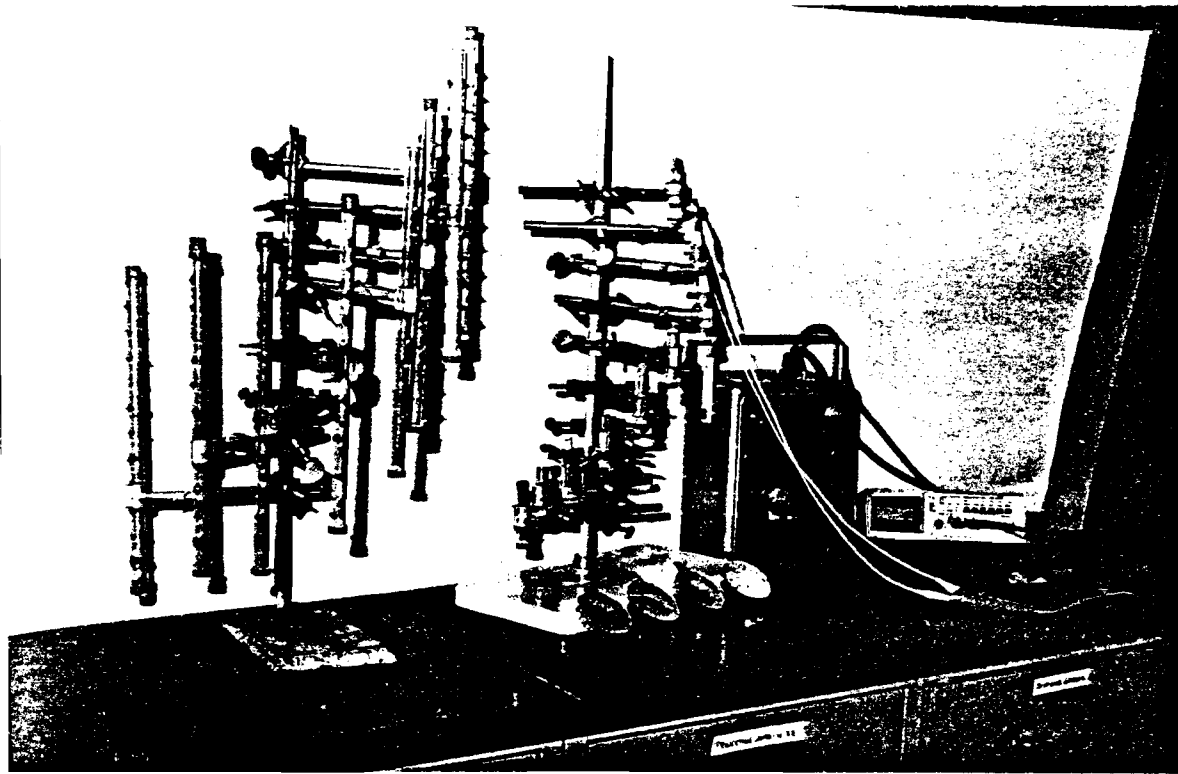


Figure 18 Views of laboratory test columns

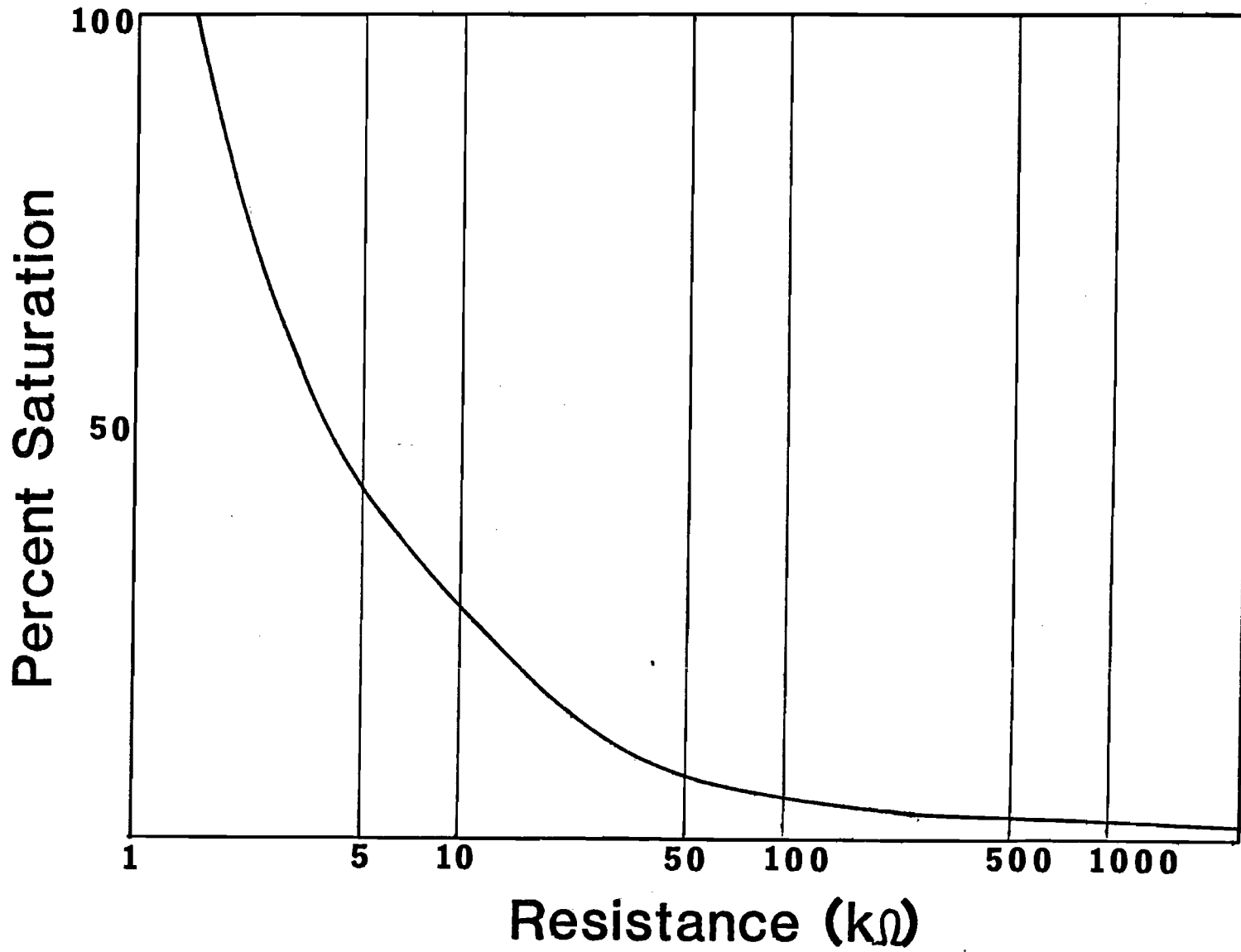


Figure 19 Electrode calibration - GF Sand

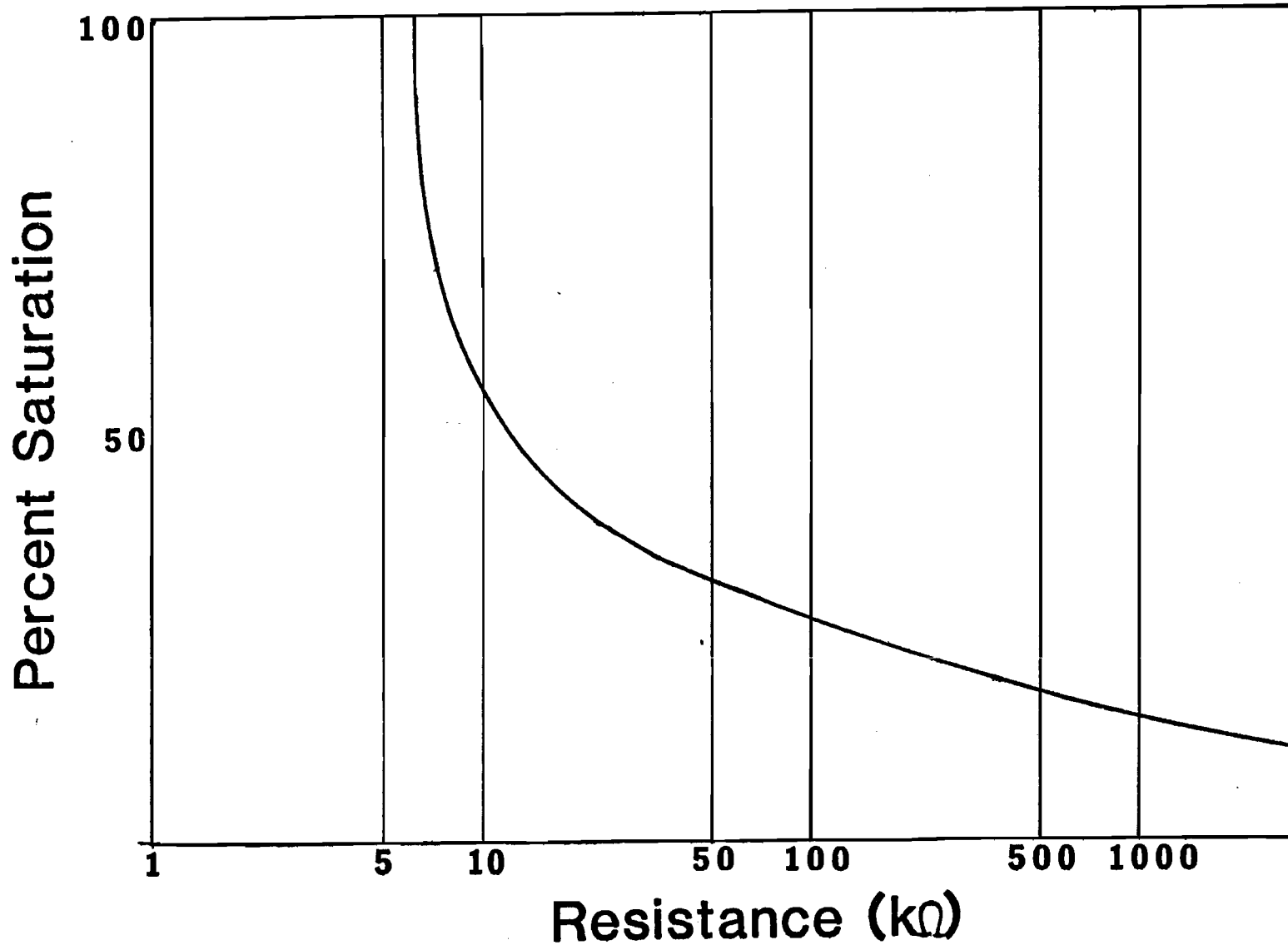


Figure 20 Electrode calibration - SRP # 1 soil

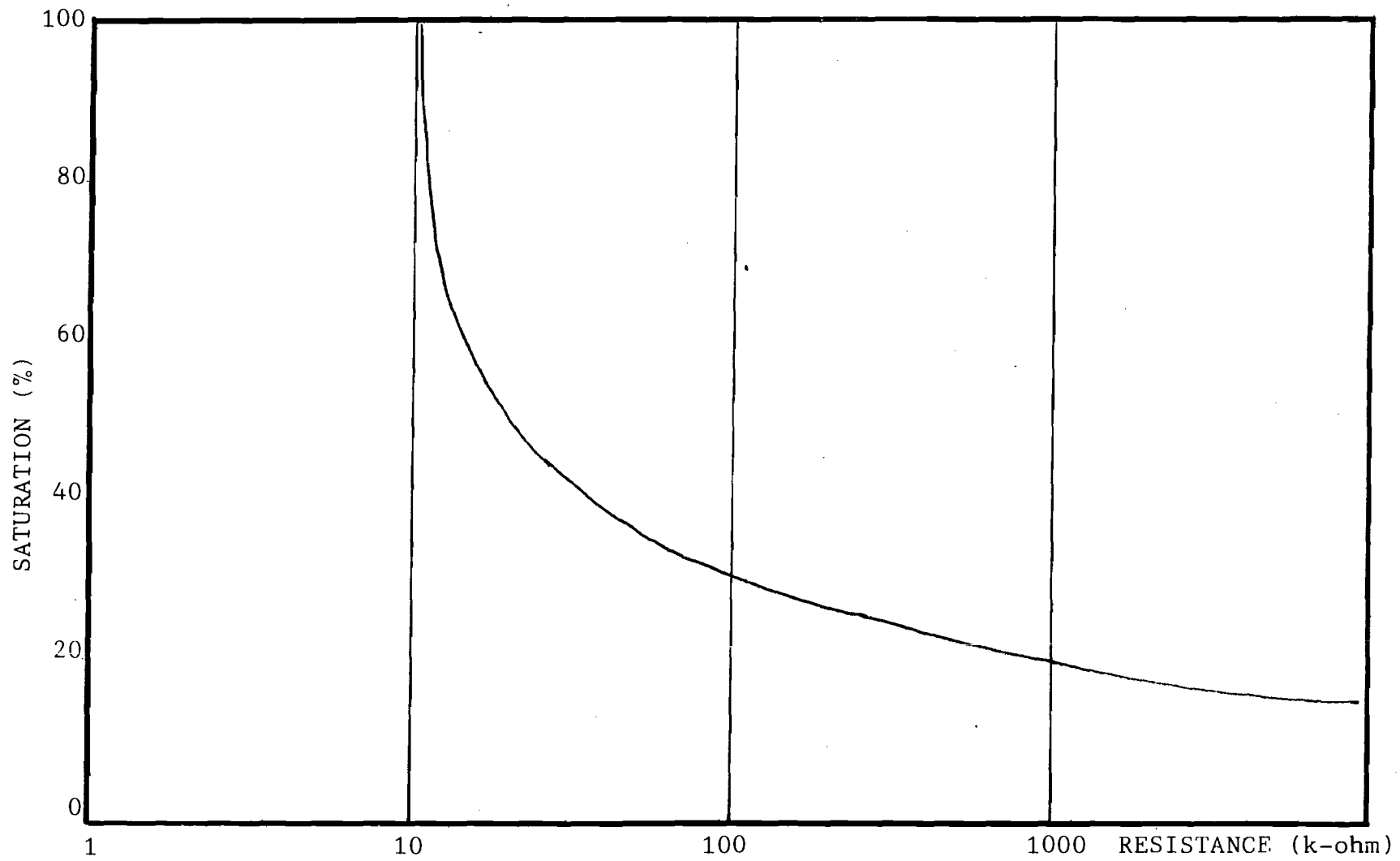


Figure 21 Electrode calibration - SRP # 2 soil

TABLE 6 - RESIDUAL WATER CONTENT FOR SIZED SAND SAMPLES

MESH SIZE	RESIDUAL WATER CONTENT (%)
14-16	0.05
16-20	0.16
25-30	0.18
30-55	0.25
40-50	0.33
50-60	0.61

TABLE 7 - RESIDUAL WATER CONTENT

SOIL TYPE	RESIDUAL WATER CONTENT
Rollo Sand	0.89%
G. T. Sand	1.59
SRP #1	10.51
SRP #2	17.37

One of the consequences of the capillarity effect, also, is the retention of moisture due to surface tension at any major interface. This applies particularly whenever a dense soil layer lies above a cavity, such as a waste volume or a gravel bed. If the interface is sloped, this effect can lead to substantial lateral waste movement. Table 8 records measurements of the wet layers at the open bottom ends of the columns. For the SRP soils this retained wet layer was substantial and even after 30 days there was some continued water loss.

Similar observations have been carried out on the test bed for Rollo sand, GT sand and FP soil. The observed minimum wet base layers were found to be 15cm high for the GT sand and about 30cm for the FP soil.

TABLE 8 - RESIDUAL WET LAYERS AT OPEN ENDS (30 DAYS)

MATERIAL	3CM COLUMN	1.2 CM COLUMN
Rollo Sand	2cm	2cm
G. T. Sand	8	2
SRP #1	14	2
SRP #2	16	2

TEST BED EXPERIMENTS

Use of the test bed had to be planned carefully, if only because the amount of material needed to fill it represented about two cubic yards or about half a ton of soil material, which had to be carefully screened and prepared. Since the tensiometers proved to be insufficiently responsive to rapid changes, most moisture profiles were obtained with the use of electric conductivity probes, which had to be carefully installed and calibrated. An early problem with a floating electric ground potential was overcome by careful grounding of the measuring unit.

The principal purpose of the test bed experiments has been the collection of data of drainage rates, residual moisture, bed support performance and response to cyclic infiltration. At this time work on the latter effect is only beginning and no definite results can be reported.

Among the most interesting results are a succession of drainage curves of which Fig. 22 is a representative sample. It shows moisture measurements at three levels in the box, 19, 94 and 144 cm. from the top, following saturation loading, in Rollo sand. Drainage is very rapid in this medium and at the 144 cm. level a distinct knee appears demarking the transition from the gravitational regime to the tension regime. Fig. 23 shows the resolution of that curve into two exponential rates from which the appropriate rate constants can be derived. These constants in turn can be inserted into the flow model to determine the time variation in the water content following a step increase in water inflow.

Another type of observation represents the moisture profile for a given water content in the column. Fig. 24 shows a typical profile observed in the test bed. These results have been correlated with calculations of an unsaturated flow model for a cylindrical system. This program can generate moisture contours that are critically dependent on the relative magnitude of the gravitational and the tension drainage coefficients.

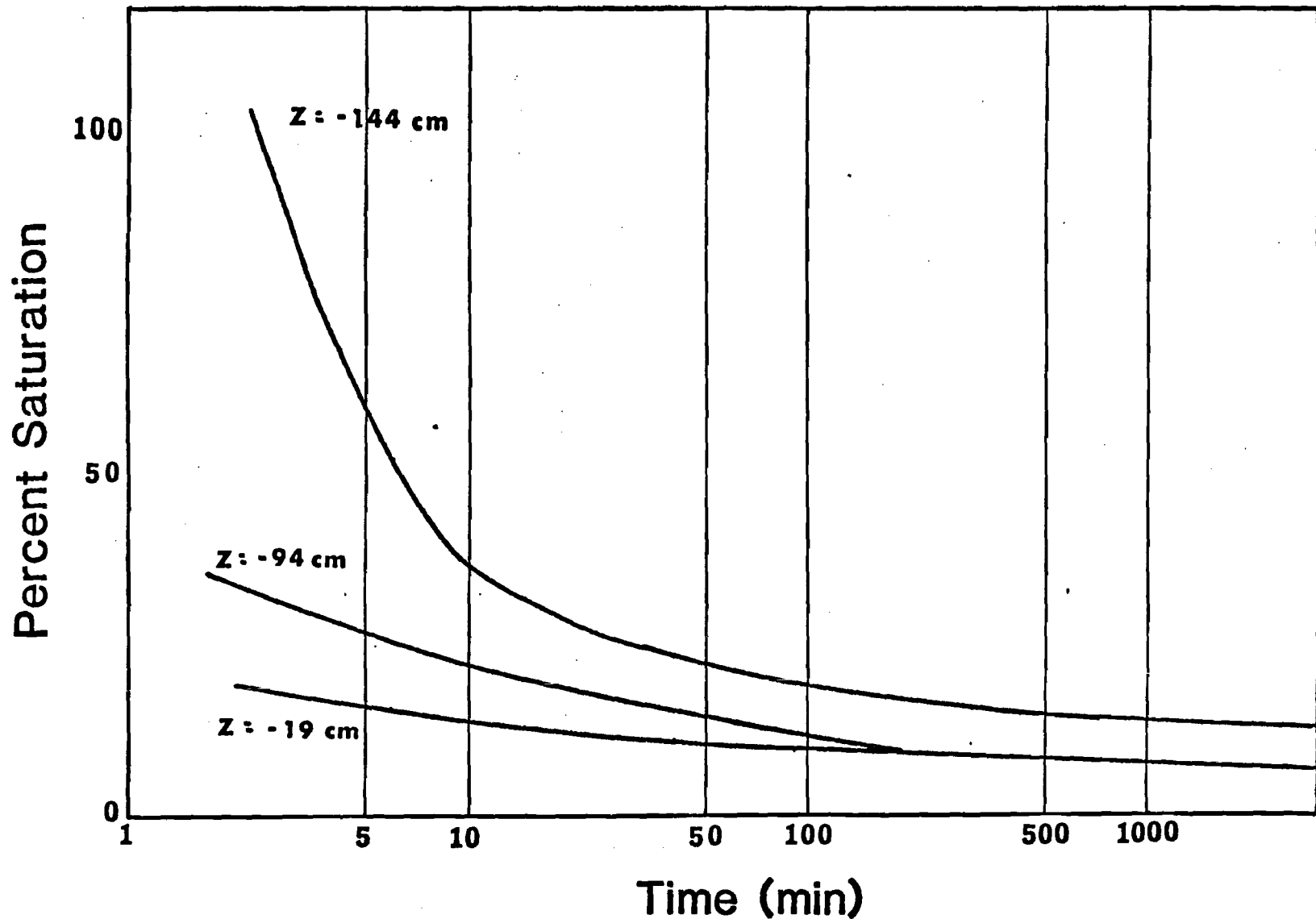


Figure 22 Drainage curves - Rollo Sand

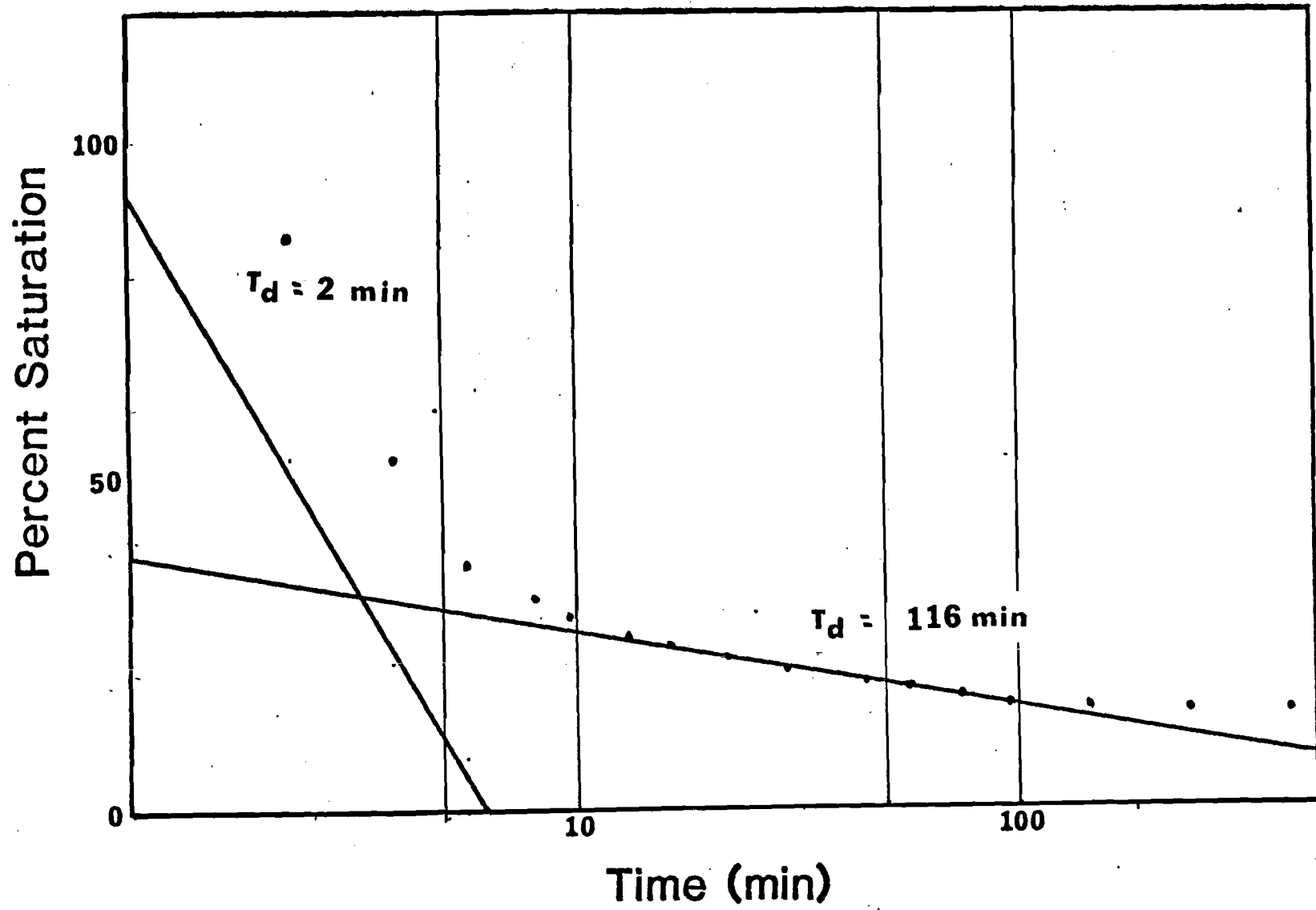


Figure 23 Resolved drainage curve - Rollo Sand

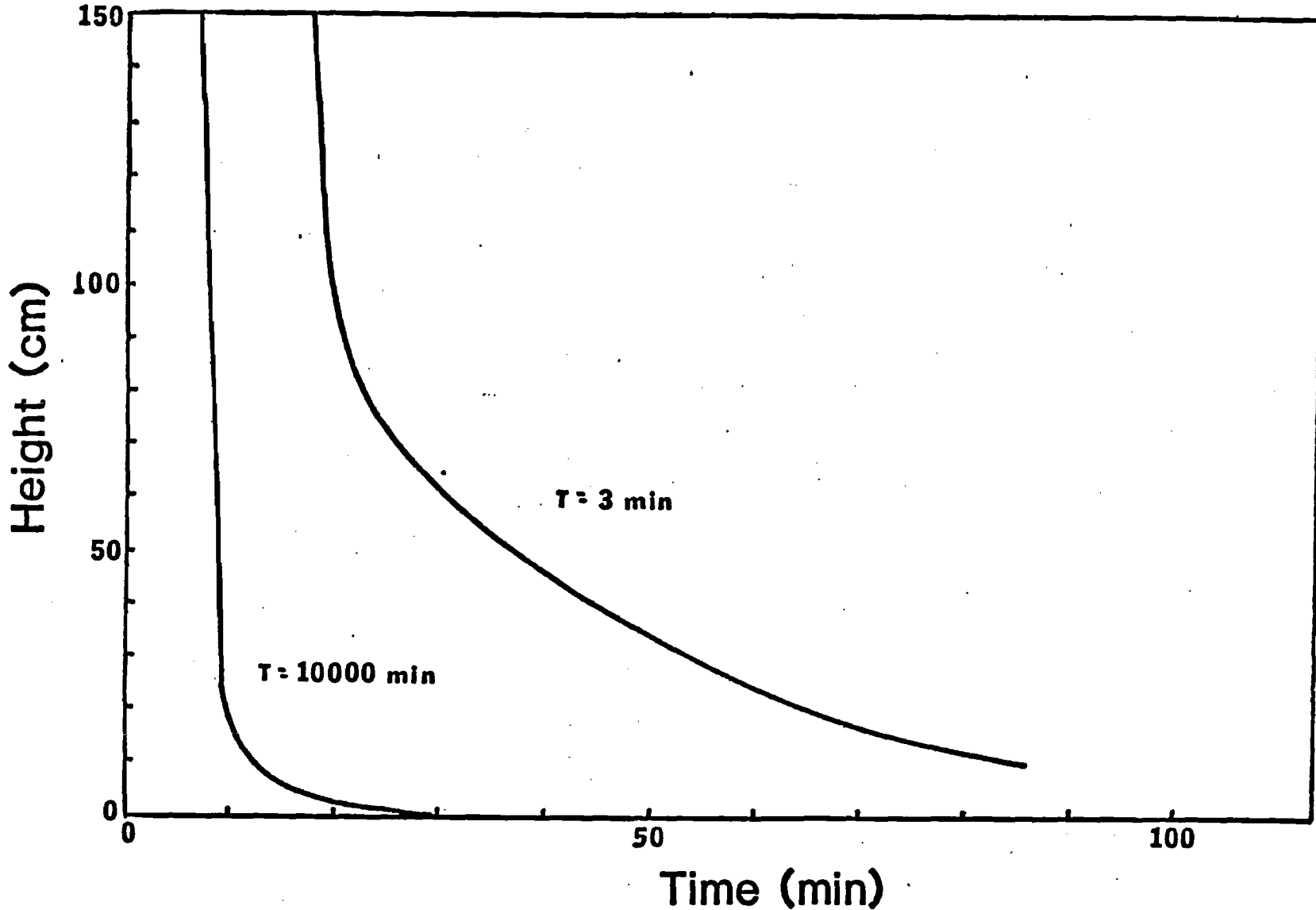


Figure 24 Moisture Profiles - Rollo Sand

Figure 25 shows the moisture profile for GT SAND plotted against the height above the drain. The curve on the right shows the profile at one minute after drainage begins. The middle curve describes the profile after 30 minutes of drainage. The curve on the left shows the moisture profile after 8800 minutes of drainage (about 6 days). The moisture content is seen to be uniform at a height greater than 20 cm above the drain. There is an interface between the soil at residual moisture content (11% of saturation) and the more saturated (75%) soil directly above the drain. Groups of electrodes were placed at 10 cm intervals inside the lysimeter. We cannot determine the exact location of the interface; it lies between 10 cm and 20 cm above the drain. Figure 25 clearly shows that in an unsaturated soil areas of higher saturation can be generated by changes in the soil properties.

Figure 26 is the moisture profile for FP SOIL. The curves compare the moisture profiles at two different times. The curves show the interface between the wet soil and the soil at residual moisture content occurring at a height of between 30 cm and 40 cm. The residual water content of the FP SOIL is estimated to be approximately 30 percent of saturation.

Figure 27 are the drainage curves for GT SAND at different heights above the drain. The lower curve describes the percent saturation as a function of time for the top of the soil column, 50 cm above the drain and 10 cm below the soil surface. This curve illustrates the initial rapid drainage of the soil followed by a slower decline to the residual moisture content. The upper curve reveals the moisture content at the bottom of the lysimeter, 10 cm above the drain. The graph shows a long plateau where the moisture content at the bottom is nearly constant while the upper portions of the column are draining. It is thought that the infiltration into this zone from above occurs at the same rate as the drainage into the gravel, thereby keeping the moisture content constant. As the upper region approaches the residual moisture content, the downward flow of water slows and the lower area begins to drain.

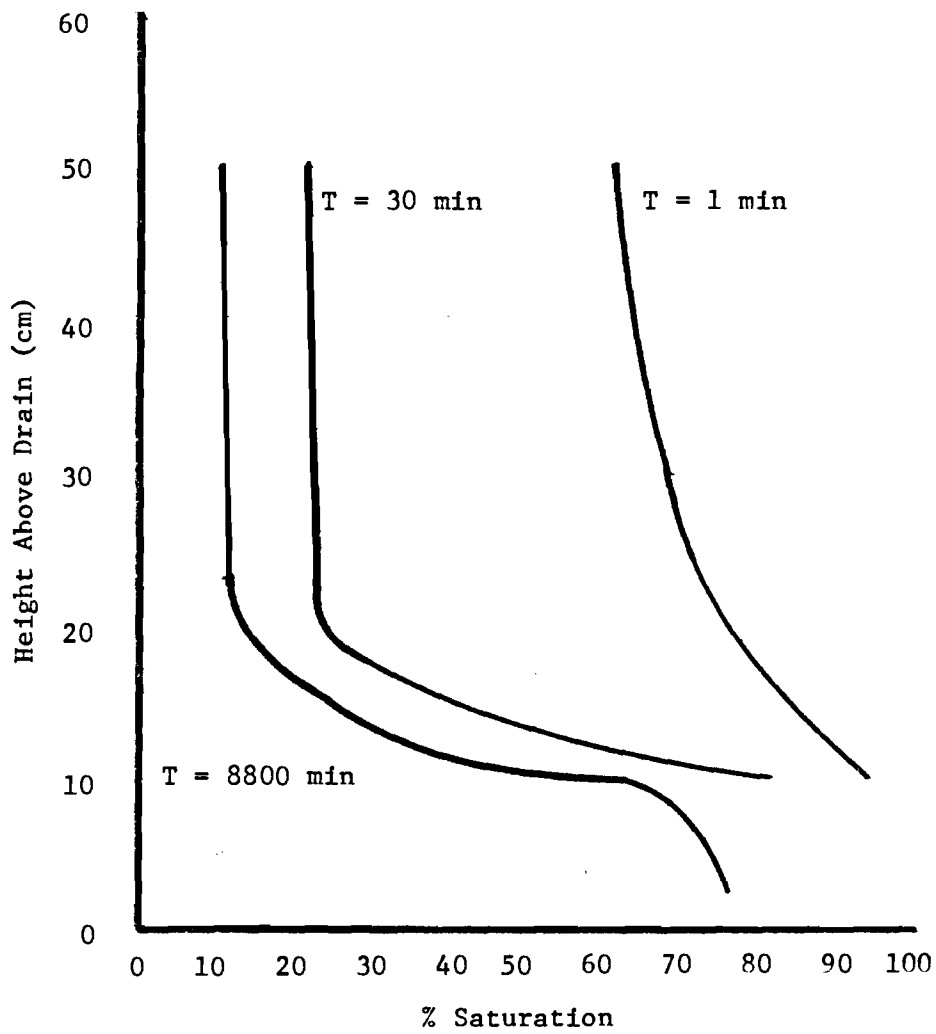


Figure 25 Moisture Profiles for GF Sand at different times

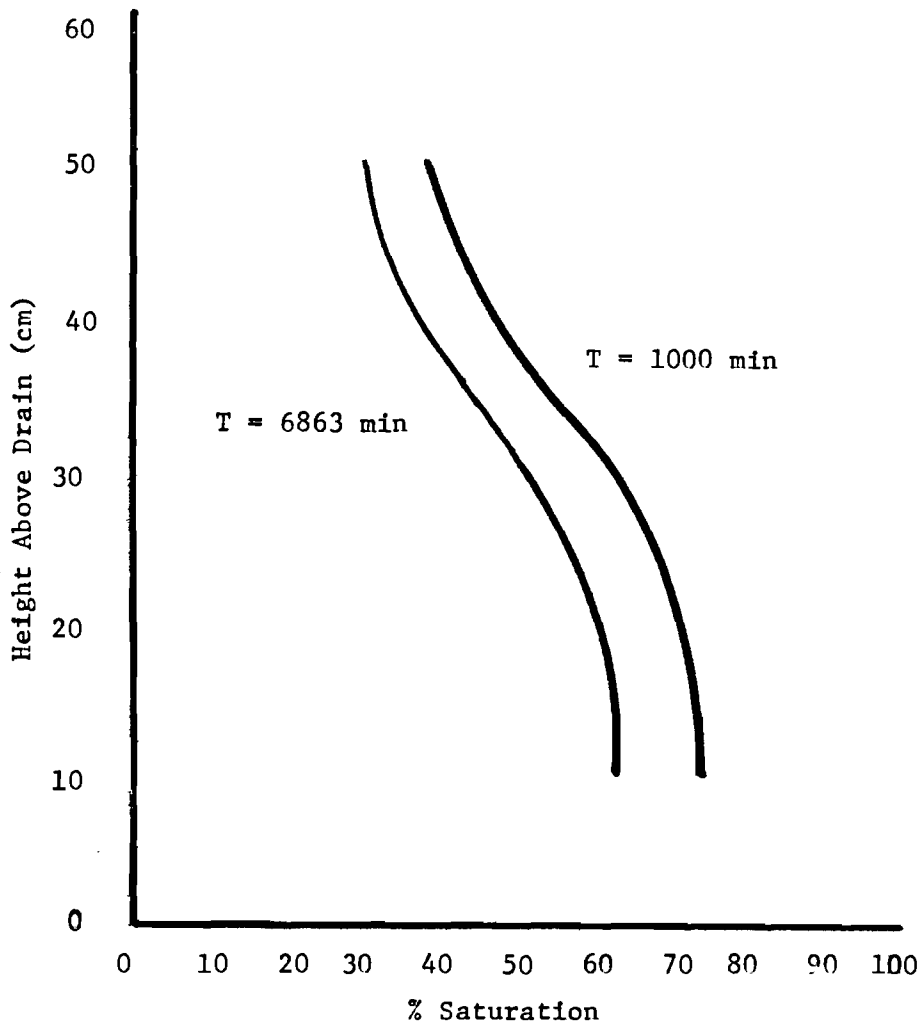


Figure 26 Moisture Profiles for FP Soil at different times

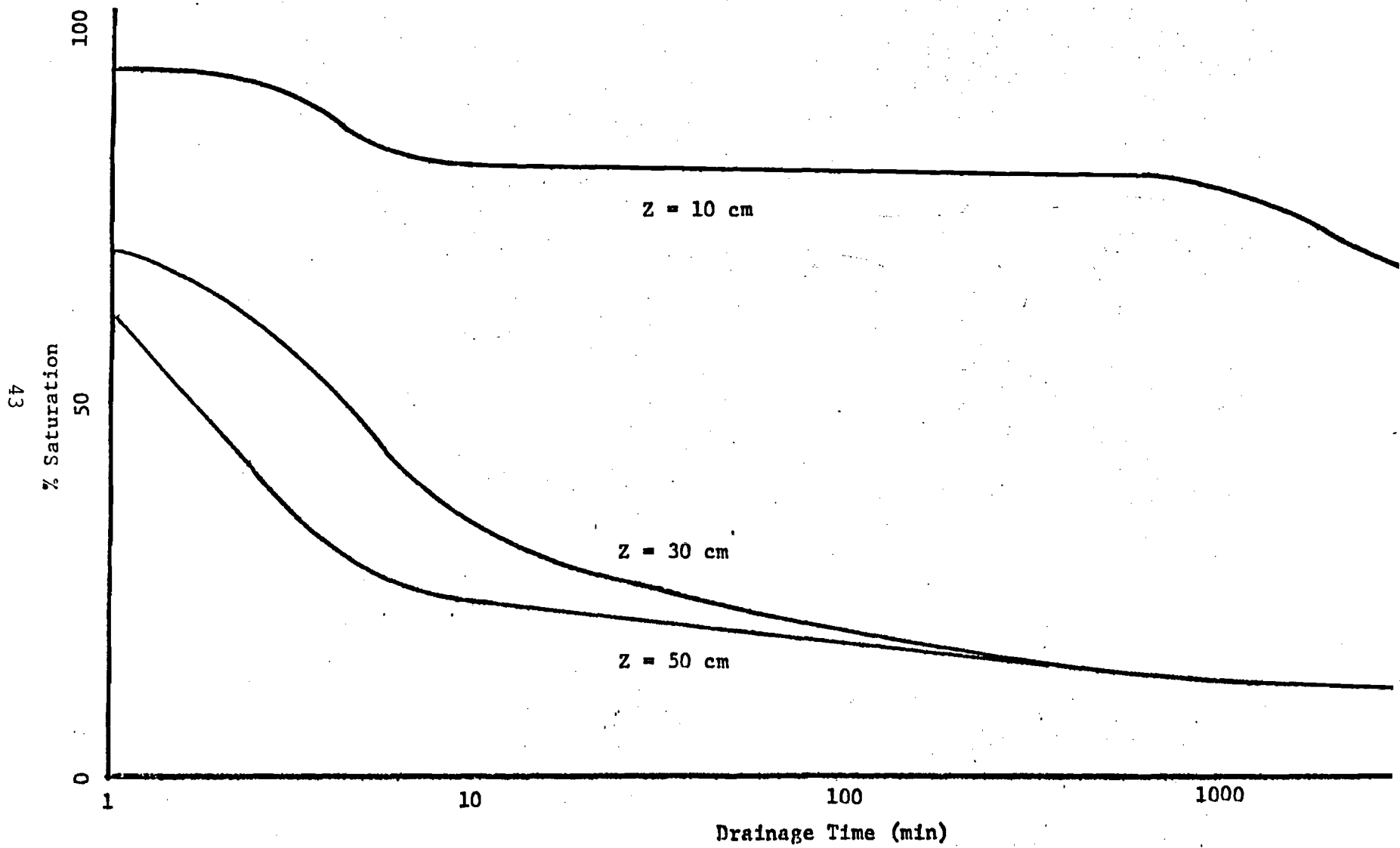


Figure 27 Drainage Curves for GT Sand at different heights

It can be seen from the figure that the drainage from a high percent saturation to a low percent saturation occurs very rapidly in GT SAND. It takes 10 minutes to go from 70 percent of saturation to 30%. The soil returns to its residual moisture content within 1440 minutes (24 hours). If precipitation occurs less than daily, the soil will drain between infiltrations.

Figure 28 are the drainage curves for FP SOIL at different heights above the drain. The curves are of the same general type as the GT SAND drainage curves. The dotted region between 10 and 150 minutes indicates that the system had not reached equilibrium before the start of the drainage test.

Water was ponded over the soil surface for one hour prior to the start. The $Z = 10$ cm curve clearly shows the rise from residual moisture content to about 64% of saturation. The residual moisture content of the FP SOIL is about 30% of saturation. This value is reached in approximately 4000 minutes (3 days).

Figure 29 is a comparison of the drainage curves for the three soils. The two sands have similar curves. There is an initial region of rapid drainage followed by a couple of hours of slower drainage. The sands have attained residual moisture content in less than five hours. Rollo Sand and GT SAND have residual moisture contents of 12 and 10 percent of saturation respectively. The FP SOIL, with its significant clay fraction, requires an order of magnitude more time to reach its residual moisture content. The measurements used in Figure 26 were taken 10 cm below the surface.

Figure 30 shows the drainage curves for Rollo Sand and GT Sand resolved into their component parts. The curves are percent of saturation plotted against log time. Both sands show a two-part drainage curve. The initial portion is presumably the gravity drainage of the larger pores and is significant for the first 10 minutes. The second component continues to drain for several hours until residual moisture content is reached. Rollo

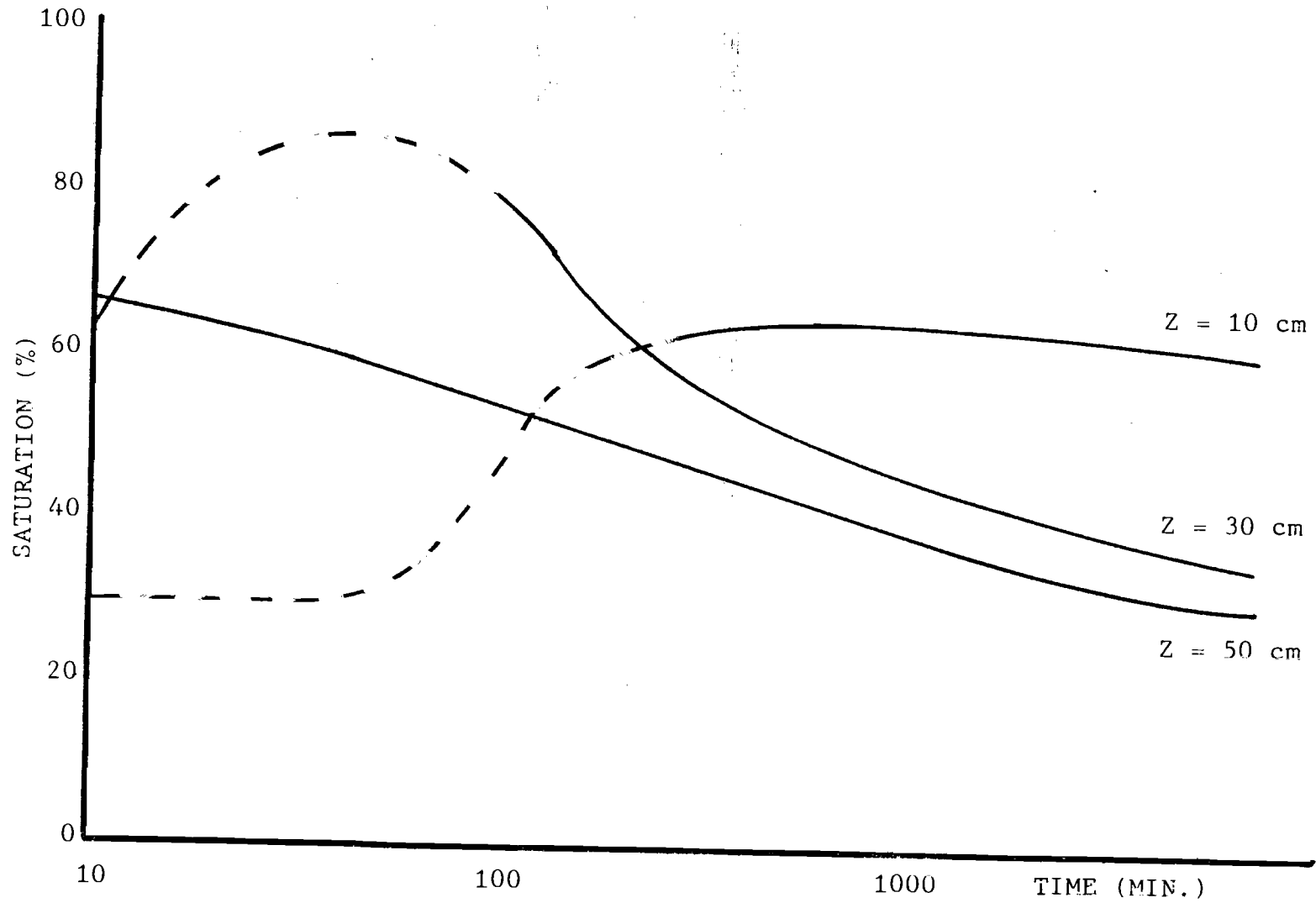


Figure 28 Drainage curves for FP Soil at different times

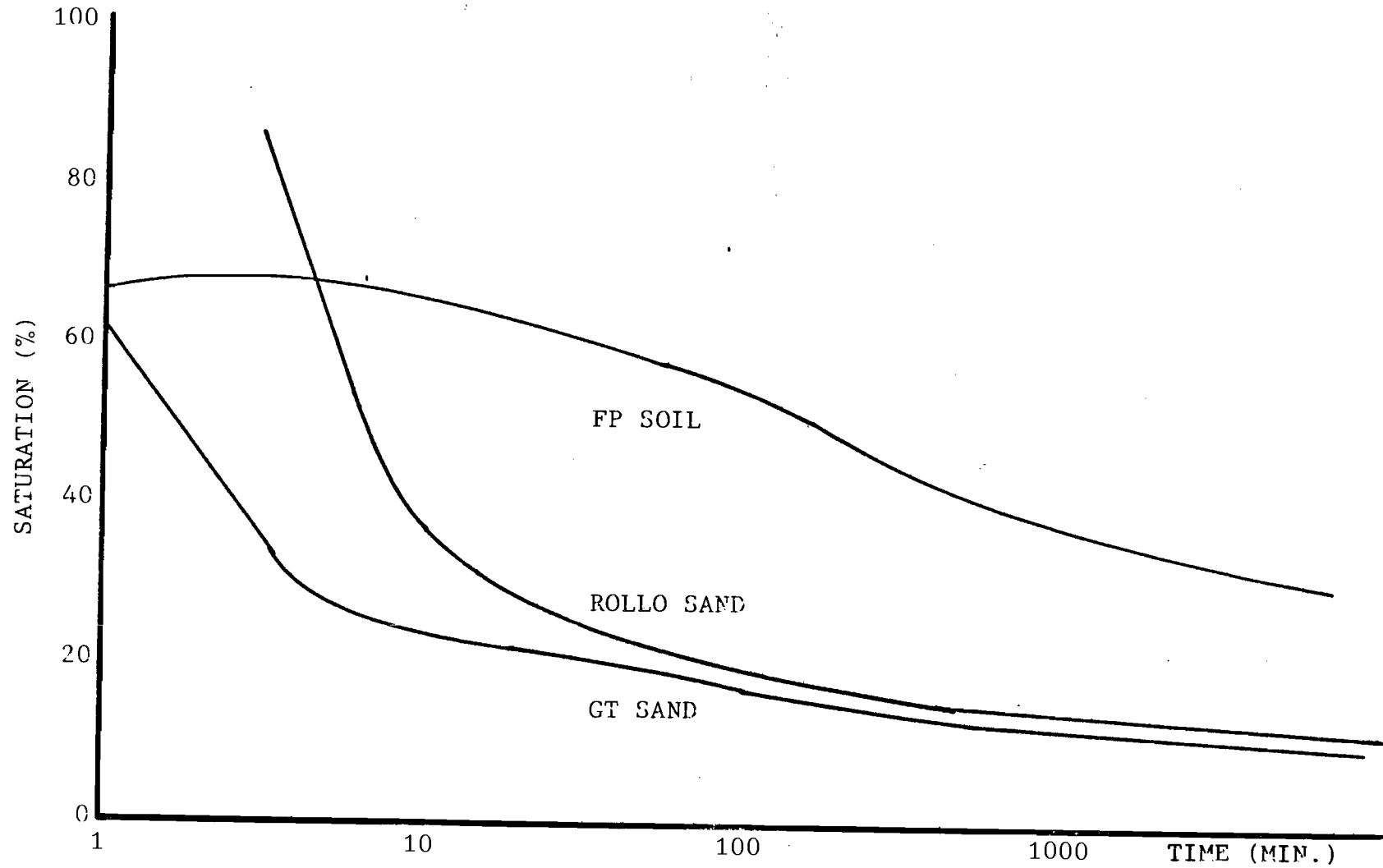


Figure 29 Drainage Curves for three soil types

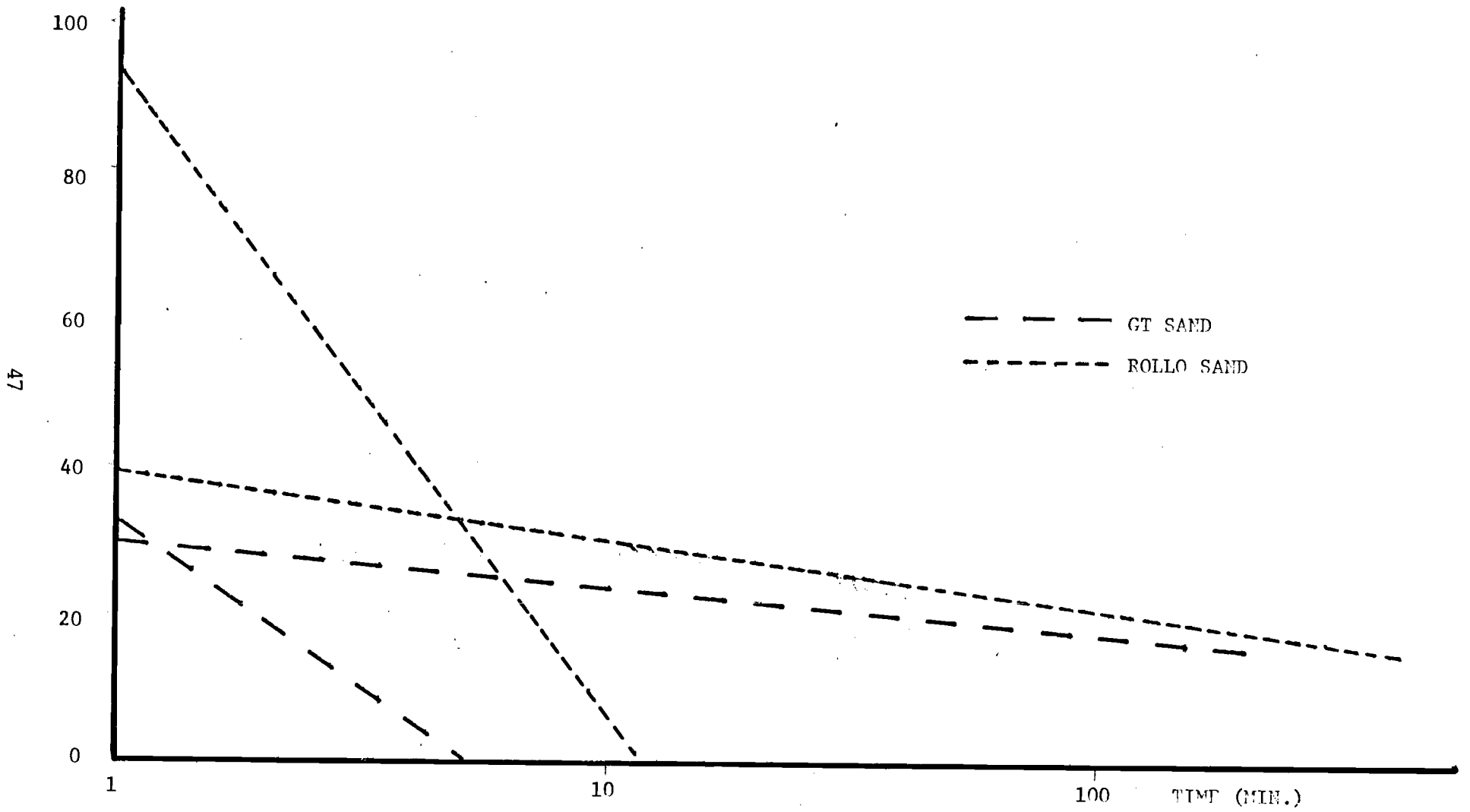


Figure 30 Resolved Drainage Curves for two sands

Sand is shown to drain faster, which is to be expected, due to its large, uniform sized particles. It is interesting to note that the time of drainage is a function of the percent saturation. The drainage equation can be expressed as:

$$T = C e^{-(k s)}$$

where T is the drainage time, C is an empirical constant, k is the drainage constant and s is the percent saturation.

Rollo Sand was found to have drainage constants of 0.247 s^{-1} and 0.0266 s^{-1} for the rapid and slow drainage respectively. GT Sand has k's of 0.384 s^{-1} . The initial drainage rates are only significant in the first five to ten minutes. It must be remembered that these values are calculated for the top 10 cm of the soil column. The curves become more complex with depth due to the variable infiltration of moisture from above.

A drainage curve resolution was not done for the FP Soil. The soil had not achieved its equilibrium conditions due to a insufficient initial infiltration time. The experiment is being repeated using a much longer infiltration time.

Calibration fo the electrodes was done in the field by taking a soil sample from between each electrode pair. The water content was determined gravimetrically. The bulk density and porosity were also determined under field conditions.

An important feature of a well-drained bed is the retained moisture at the bottom of the column. In the test bed, the sand layers were supported by a mesh screen that was placed on top of the coarse gravel bed which provided the drainage path. In sand, ordinarily, little moisture should be retained due to surface tension effects at the lower surface. However, it was found that the wire mesh supported a film of water of sufficient strength to maintain significant moisture in the sandbed up to a height of

about 14 cm. Proper choice of the supporting material is obviously important to minimize this effect, while yet retaining the bed material sufficiently to avoid clogging of the gravel layer. In practice it is felt that a graded gravel layer can supply enough support for the soil and may be preferable to a screen or open-mesh liner material.

Since the usefulness of the drainage layer could be impaired by silting over a long period, qualitative observations were maintained on silt infiltration into the gravel bed. It was found that a little fine silt material was washed into the gravel in the early stages of the test, but later, with the readily mobile material removed from the bottom soil layer, no further silt movement seemed to occur.

WASTE LEACHING IN UNSATURATED CONDITIONS

One of the principal objectives of this work is the reduction in the source term from water attack on the waste material by reduction of the quantity of water in contact with the waste and the time available for migration processes. For vitrified waste, Pescatore and Machiels (23) have argued that for slow flow rates the diffusion rate of waste ions to the surface layer becomes the rate-determining step. Most waste depository models assume that water flow is continuous, saturated and that the leach rate is proportional to flow rate at a constant solubility. Under unsaturated flow conditions or cyclic flow conditions, it is not at all clear if leaching occurs in a constant fashion and whether it is necessarily proportional to volumetric flow rate. Test work is under way with simulated waste to study these processes, but the results are inconclusive so far, partly because of slow leaching rates and partly because of the need to employ equilibrated water for reasonable simulation, whose composition is, to some extent, affected by the nature of the simulated waste itself. Similar considerations affect the leachability and migration rates of other waste trench simulations, such as the SRP lysimeter tests (15), where flow also is unsaturated much of the time.

The test work conducted in the laboratory has been of two types, recirculating water through simulated waste material and once-through flow tests. The simulated waste consisted on ion exchange resins labeled with Cs-137 or Tc-99m. This material was chosen, because it was felt that other waste forms either would be too insoluble to result in statistically valid desorption or would be too inhomogeneous for comparison. The recirculated tests suffered from constant change in pH due to the effect of the waste resin and those tests were not pursued. Once-through flow tests with equilibrated water were more controllable, but have resulted in too low a level of desorption to be usable so far; these tests are continuing and it is hoped to place them on a more productive basis.

In the meantime, for calculational purposes it is assumed that the leach rate is proportional to the time-integrated volumetric flow. That is a problematic assumption, because of the diffusion rate and concentration-gradient dependence of the leach process which makes it improbable that the leach source term is proportional to water volume under pulsed conditions. However, for the moment that assumption seems the best available.

COMPUTER SIMULATION

To evaluate the effects of unsaturated flow under time-dependent conditions, a one-dimensional computer program has been developed. This program can describe pulse flow conditions in the test bed and the movement of the moisture profile. Details of the program are presented in Appendix A.

The results depend, of course, on the relative magnitude of the pressure head (gravitational force) and the suction head (capillarity). Figures 31 and 32 illustrates two cases where their relative magnitudes vary.

The general features of computer model for this facility are shown in Figure 33. On the left are the physical processes involved, on the right the various rate processes that determine waste migration from the source.

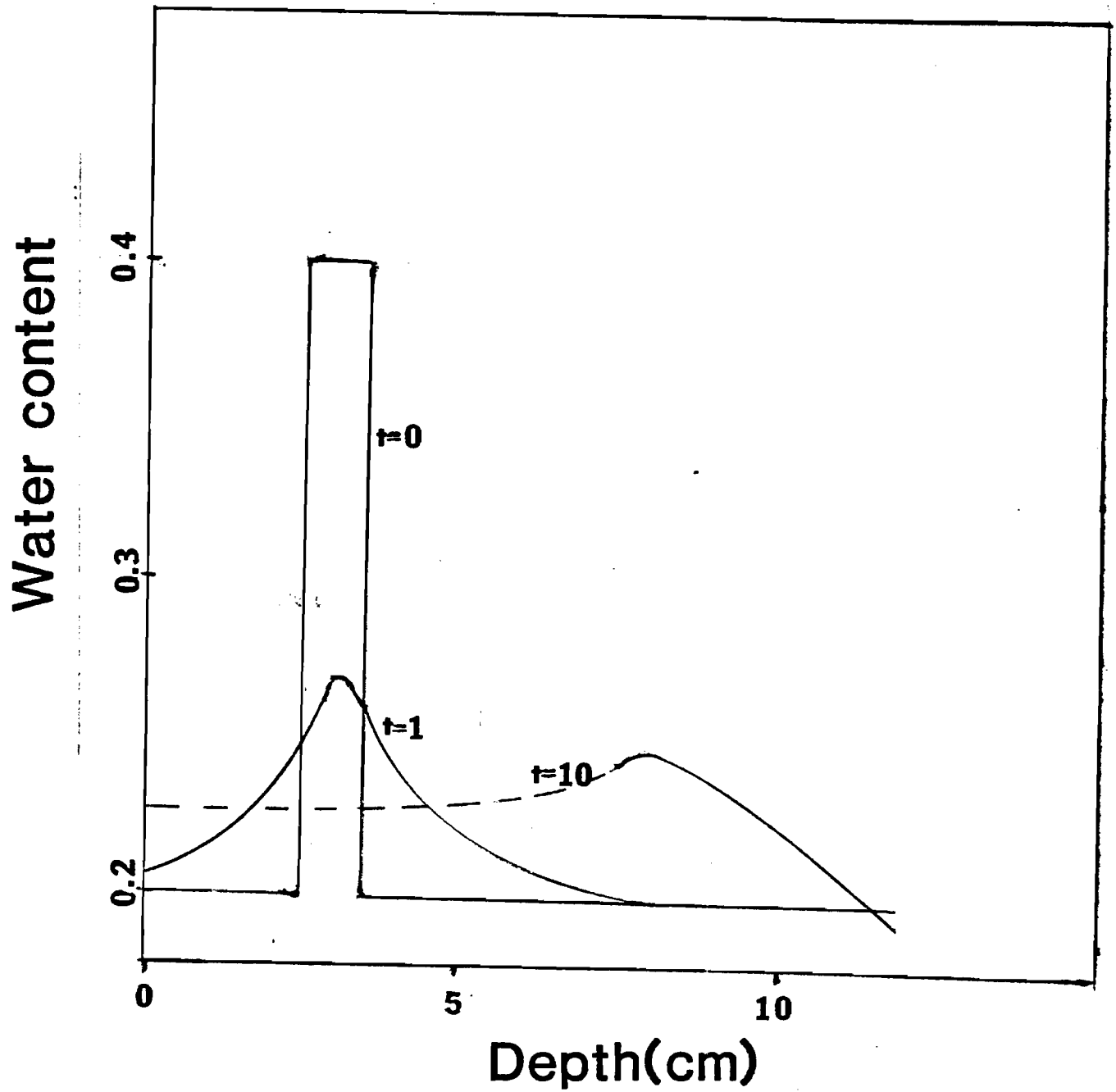


Figure 31 Calculated Moisture Profiles - Comparable forces

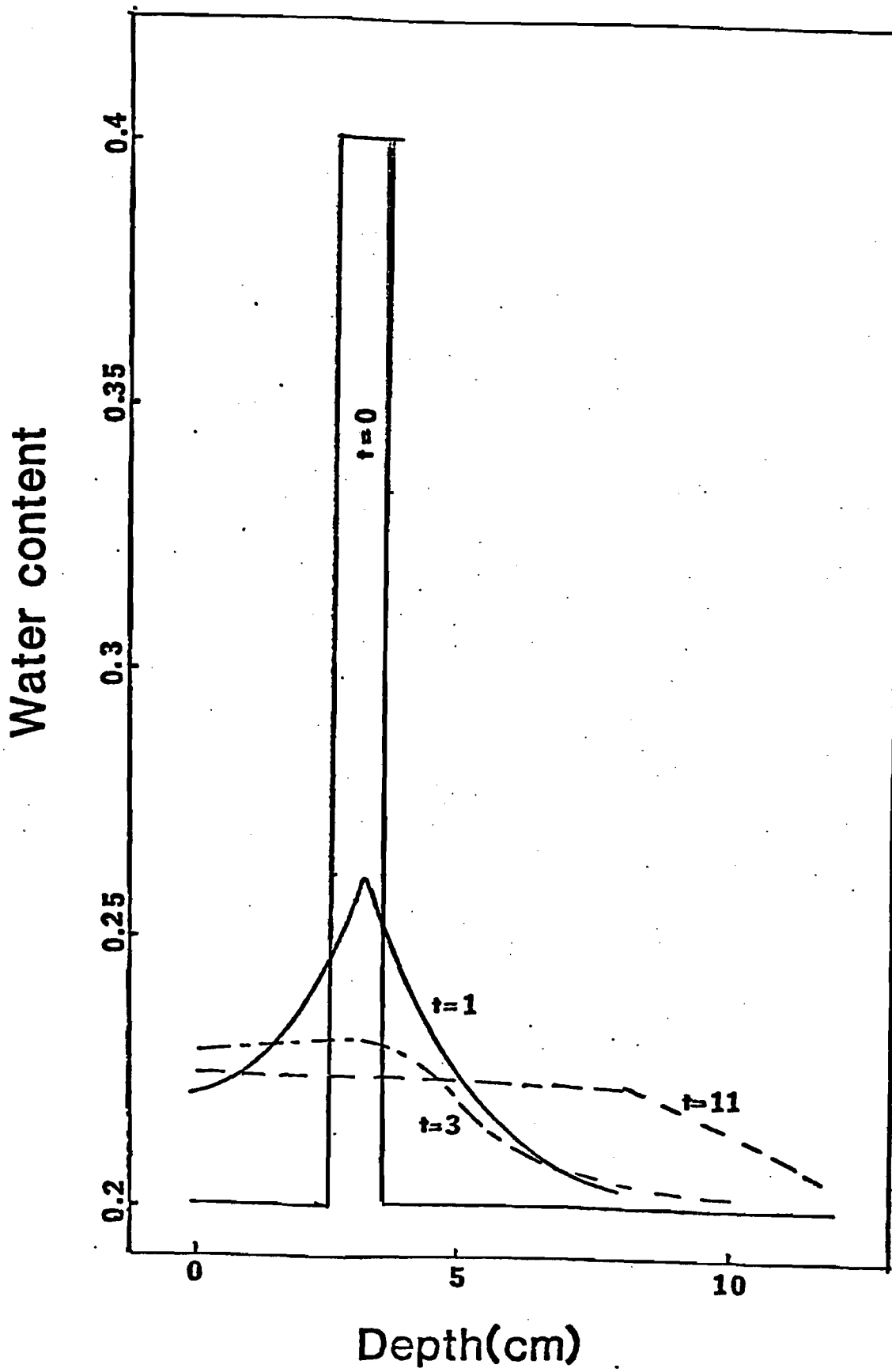


Figure 32 Calculated Moisture Profiles - Suction dominant

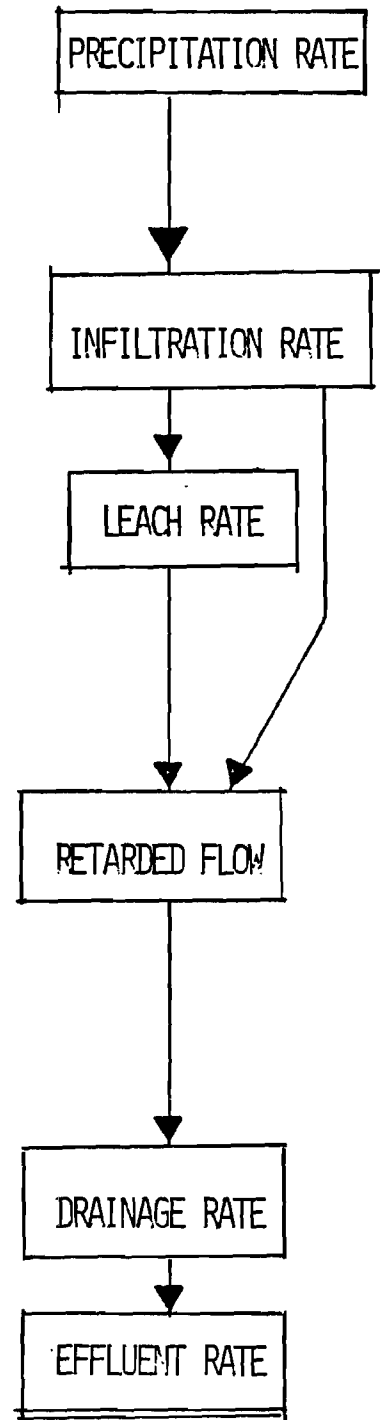
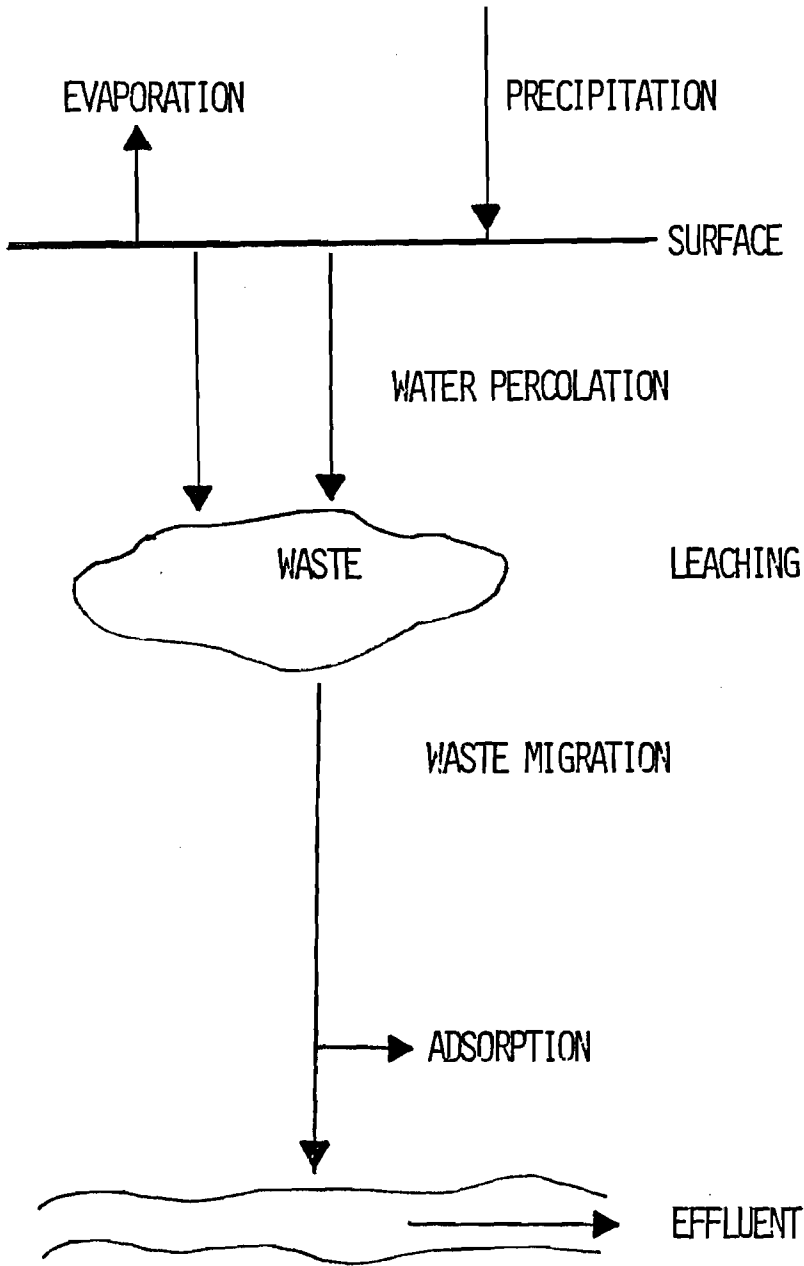


Figure 33 Diagram of Migration Model

Details of the model development go beyond the scope of this report and will be available shortly in extended form (de Sousa, Ph.D Thesis, 1985). The program description is attached in Appendix A - C. The model is based on a finite element technique which was used to solve the one-dimensional unsaturated flow and transport equations. Boundary conditions include provision for a Neumann variable flux condition, so as to represent a seepage boundary, as well as a Dirichlet constant boundary condition.

In order to use the water flow and transport model to simulate a shallow land burial site performance, it is necessary to determine how well can the model simulate the unsaturated regime present in the soils. Since the transport model uses the results obtained with the flow model, the latter was the first one to be checked.

Flow model

The first simulation done to check the accuracy of the water flow model corresponded to the situation in which an homogeneous saturated column of soil was submitted to a constant infiltration equal to the saturated hydraulic conductivity of the soil; the boundary condition at the bottom of the column corresponded to a free draining profile. In this situation the column should remain saturated, and the pressure head should not change with time, since the infiltration and the drainage rates are equal; the results obtained, given in Table 9, showed that the model was simulating correctly that situation. This simulation was useful to the extent that it showed the logic of the model was correct and the matrices were being well assembled and solved.

The ability of the model to reproduce unsaturated flow was checked by simulating the situation presented by Van Genuchten (28) based on the experiments done by Warrick (29). This experiment was chosen because it represents one of the most difficult cases to simulate, which is when a dry soil is subjected to a large infiltration rate.

The experiment consisted of an homogeneous soil column, 125 cm long, which was subjected to the following conditions:

TABLE 9 - FLOW MODEL VERIFICATION

TIME= .050 NL= 1 NT= 1			
NNODE	COORDINATE	PRESSURE HEAD	
1	.000	-34.460	
2	1.000	-34.460	
3	2.000	-34.450	
4	3.000	-34.460	
5	4.000	-34.450	
6	5.000	-34.460	
7	6.000	-34.460	
8	7.000	-34.460	
9	8.000	-34.450	
10	9.000	-34.450	
11	10.000	-34.460	
12	11.000	-34.460	
13	12.000	-34.460	
14	13.000	-34.460	

TIME= .125 NL= 1 NT= 2			
NNODE	COORDINATE	PRESSURE HEAD	
1	.000	-34.460	
2	1.000	-34.460	
3	2.000	-34.460	
4	3.000	-34.460	
5	4.000	-34.460	
6	5.000	-34.460	
7	6.000	-34.460	
8	7.000	-34.450	
9	8.000	-34.460	
10	9.000	-34.450	
11	10.000	-34.460	
12	11.000	-34.460	
13	12.000	-34.450	
14	13.000	-34.450	

TIME= .225 NL= 1 NT= 3			
NNODE	COORDINATE	PRESSURE HEAD	
1	.000	-34.460	
2	1.000	-34.460	
3	2.000	-34.460	
4	3.000	-34.450	
5	4.000	-34.460	
6	5.000	-34.460	
7	6.000	-34.460	
8	7.000	-34.460	
9	8.000	-34.460	
10	9.000	-34.460	
11	10.000	-34.460	
12	11.000	-34.460	
13	12.000	-34.460	
14	13.000	-34.460	

Initial Condition:

$$\theta(x,0) = \begin{cases} 0.15 + 0.0008333 & 0 < x \leq 60 \\ 0.20 & 60 < x < 125 \end{cases} \quad (1)$$

Boundary Conditions:

$$h(0,t) = -14.495 \quad (2)$$

$$h(125,t) = -159.19 \quad (3)$$

The water content - hydraulic conductivity and the water content - pressure head relations are given by:

$$\theta(h) = \begin{cases} 0.6829 - 0.09524 e_{\eta} |h| & h \leq -29.484 \\ 0.4531 - 0.02732 e_{\eta} |h| & -29.484 < h \leq -14.495 \end{cases} \quad (4)$$

$$k(h) = \begin{cases} 19.34 \times 10^5 |h|^{-3.4095} & h \leq -29.484 \\ 516.8 |h|^{-0.97814} & -29.484 < h \leq -14.495 \end{cases} \quad (5)$$

The flow model is written in terms of pressure head and so the initial pressure head distribution is given by substituting eq.1 in eq.4; the boundary condition at the surface (eq.2) implies that the soil is maintained saturated at the top of the column at all times.

The results obtained by using linear finite elements (LFE) and mass lumped linear finite elements (MLFE) are shown in Figure 34. It is seen that in both cases a reasonable simulation is obtained; more accurate results can be obtained if the spatial and time intervals are decreased at the expense of a larger computational time. Another important aspect is that the LFE simulation presents some oscillations at the early stages, and that they decreased as the time increased. These oscillations can be decreased by again decreasing the spatial and time increments. It is then seen that the flow model generates accurate results when used to simulate unsaturated water flow.

The transport model is now being checked, and the same situations used for the flow model will be used to determine if it can be used to simulate the movement of radionuclides through unsaturated soils.

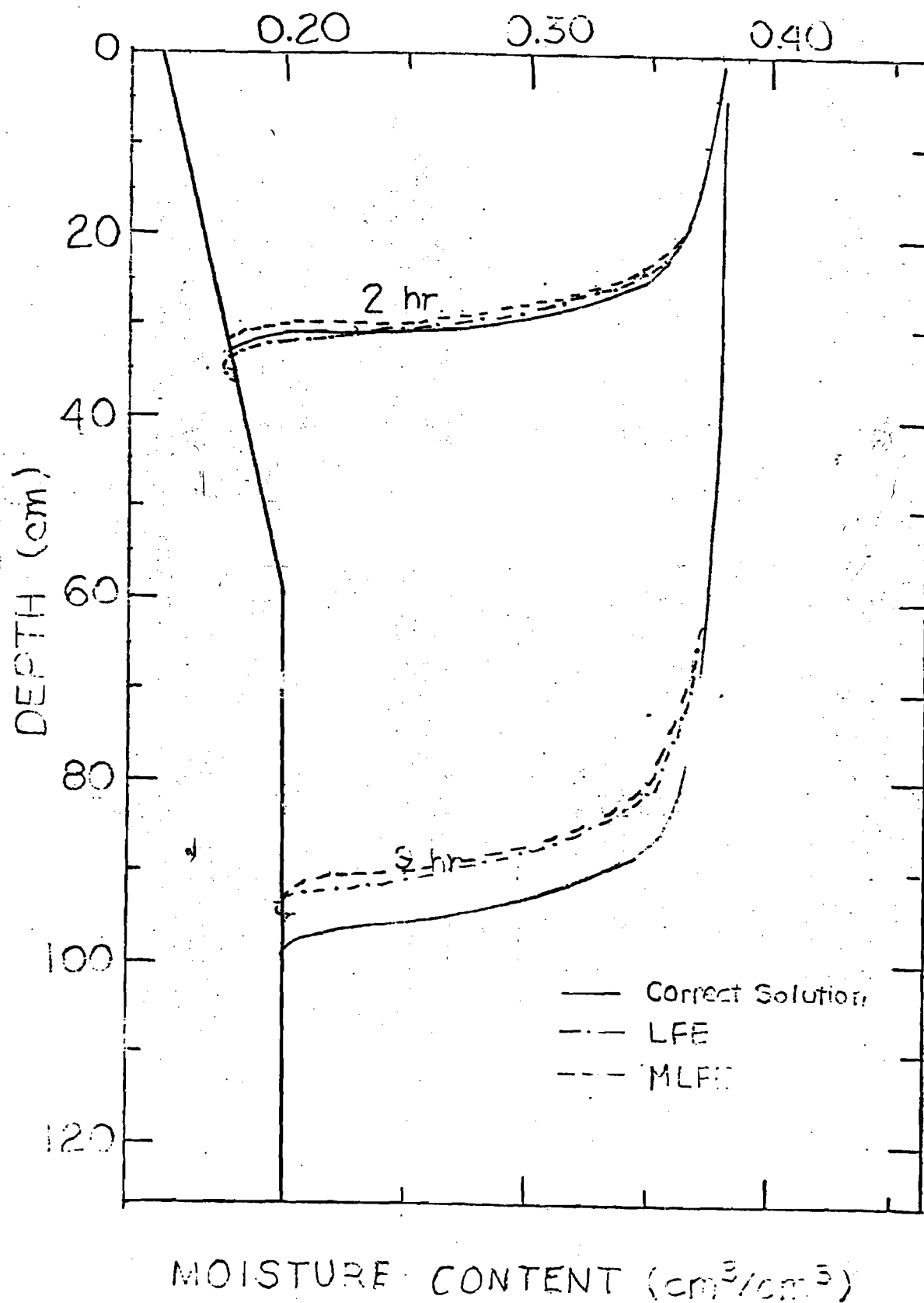


Figure 34 Verification of Flow Model

TRENCH FACILITY DESIGN

The work described above has provided some guides for the design of a facility that is specifically intended to minimize waste leaching by facilitating drainage through the backfill, thus preventing any standing water in the waste volume regardless of the condition of the cap. Since it has been shown that soils with a high clay content retain a substantial amount of moisture at all times, it is evident that a fairly permeable sandy loam would be preferred for the backfill material.

As Table 8 has shown, even for fairly sandy soil there will be a wet layer of up to 12cm above any gravel base; hence waste emplacement should be on top of a soil layer of at least a foot. This will also facilitate waste placement and protect the gravel layer against the action of tracked vehicles in the trench.

Figure 35 is a generalized diagram of the trench design envisaged. (A mesh separator is shown between backfill and gravel bed, but present experience indicates that it is probably unnecessary). The main feature of importance is the gravel bed, which is common to most waste trenches, but assumes a central role in the present design. Given a reasonably permeable backfill soil, it is assumed that following a rainfall most of the infiltrated water will percolate rapidly through the backfill to reach the gravel bed, which must have enough capacity to store this water over a long enough period to permit slow, orderly seepage into the ground without backing up.

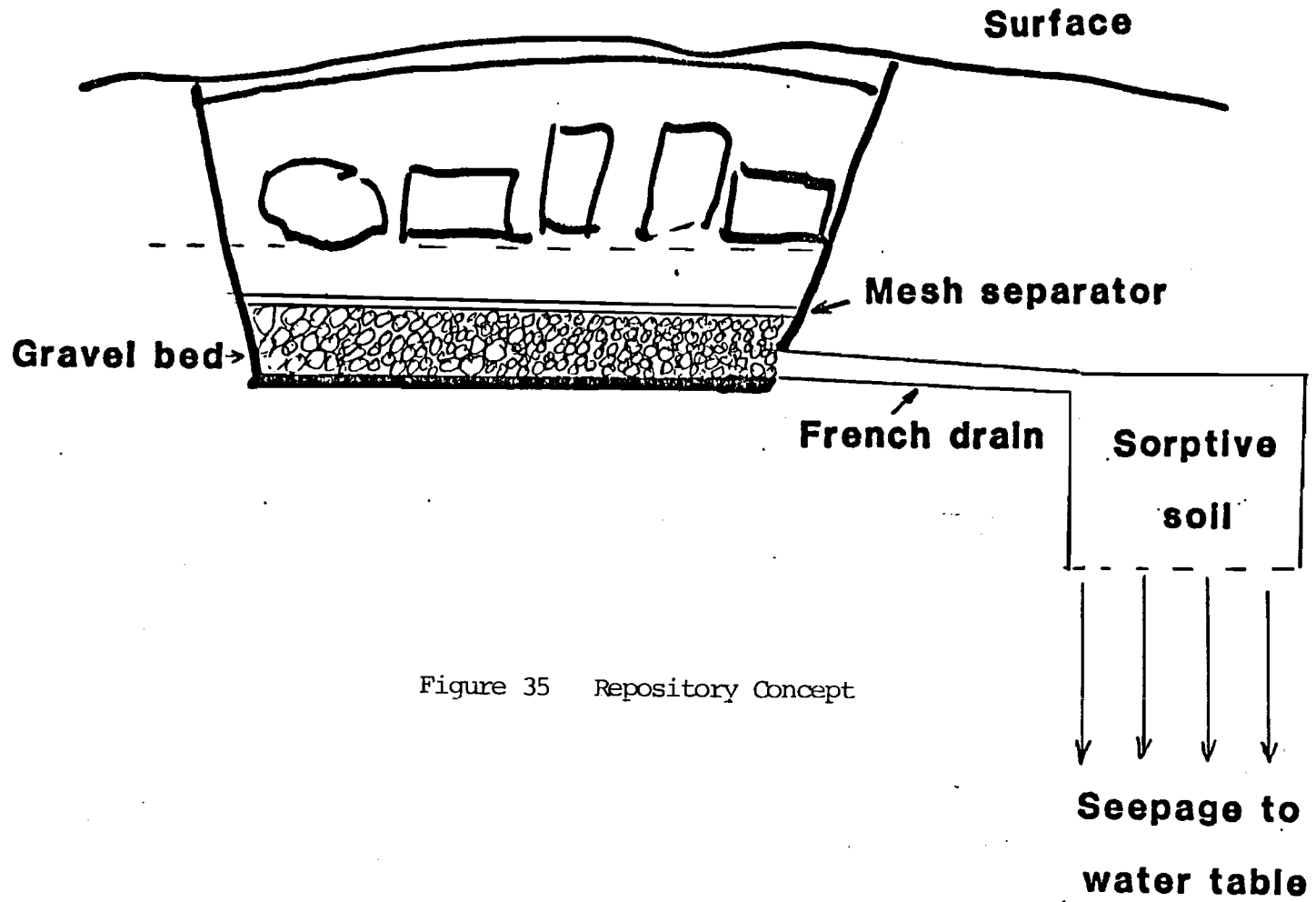


Figure 35 Repository Concept

Calculation of Gravel Reservoir Requirements

The quantity of water that must be accommodated in a near-surface burial site is dependent on three major factors. These are the amount of precipitation, the rate of infiltration of water into the soil, and the rate of movement of the water within the soil. The latter two factors are interrelated, as the limiting factor may be either the rate of passage through the air-soil interface or the rate at which water percolates away from the interface, leaving room for additional water to enter the soil.

The maximum rate at which water can enter the soil under given conditions is called the infiltration capacity. The actual infiltration rate equals the infiltration capacity only when the intensity of rainfall equals or exceeds the infiltration capacity. The infiltration capacity is at its maximum when the soil is dry, but decreases rapidly at the beginning of a storm and approaches a low, constant rate as the soil becomes saturated. The permeability of the subsoil becomes the ultimate limiting factor.

Soil type, moisture content, organic matter, vegetative cover, and other factors affect infiltration, but a decrease in rate with time is generally observed. This is shown in Fig. 36, where infiltration rate is plotted against time for two typical soil types. The difference between plots for dry (initial) conditions and wet condition demonstrates the large influence of existing moisture content of the soil.

For purposes of calculation, it is assumed that the soil of the burial site is similar to Houston black loam in its infiltration capacity. The scenario for the maximum volume of water would be to commence with dry soil. This allows a high rate of infiltration at the very start, but within 30 minutes this has fallen by approximately an order of magnitude with additional significant rate decrease in the subsequent hour. It is estimated that during the first three hours of rainfall of intensity sufficient to keep the soil surface covered, the total infiltration will be one inch. After three hours the rate for any continuing rainfall period is 0.05 in/hr, (0.125 cm/hr), the equilibrium flow rate.

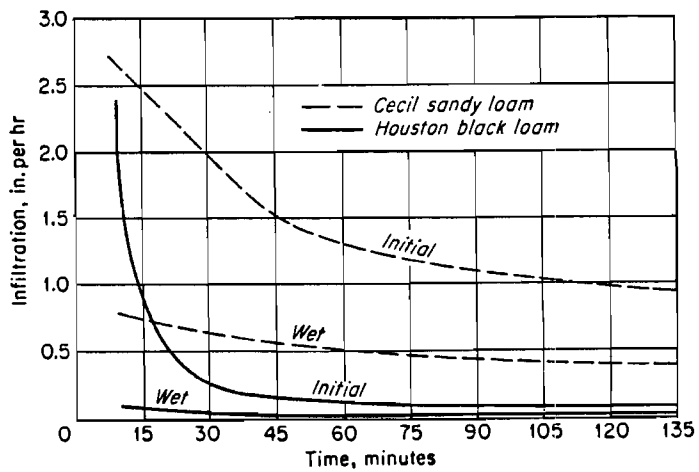


Figure 36 Comparative infiltration rates during initial and wet runs
(after Ref. 25)

The total inflow of water into the burial site during a given episode, therefore, depends on the length of time that the surface to the ground is wet enough to supply 0.05 in. of water per hour. No records of periods of continuous rainfall in the southeast have been located, and the Atlanta Weather Bureau is of the opinion that no such records have been kept. In reviewing the rainfall records for the Atlanta area, it was found that maxima are tabulated for one, two, and seven-day periods. It is considered unlikely that rain would occur continuously for more than a few days, based on seven-day records of 9 inches (10 year return), 10 inches (25 year return) and 12 inches (100 year return). It is therefore concluded that the maximum quantity of rainfall will be 9.25 inches, (~23cm) obtained from the sum of one inch in three hours plus 0.05 in/hr. for 165 additional hours. It is further noted that the return period for this maximum is greater than 10 years, and is more likely to exceed 25 years.

This is based on the assumption of a week during which the rain falls steadily and virtually no surface run-off occurs, a set of circumstances that clearly would not occur very often. The quantity of infiltrated water would also be reduced by evapotranspiration, estimated at 0.25 inch per day. On this basis, the total quantity of water to be considered is reduced to 7.5 inches (18.75cm).

The passage of water from the surface of the ground to the junction with the water table is envisioned as follows: After penetration of the air-ground interface, water proceeds downward at a slow rate determined by the characteristics of the compacted fill soil. It then enters the zone where waste materials have been placed. It is highly unlikely that the waste containers could ever be placed in a very tight configuration and cracks, crevices, and void spaces would be plentiful. Also, any back-filled soil that works into the main volume of waste is not likely to be very well compacted, so the entire waste zone will be conducive to the rapid percolation of water.

The rate of movement of water into the underlying and surrounding undisturbed soil will be lower than the rate of movement through the waste, so a storage volume beneath the waste will be required to prevent water from standing in the waste zone. It is estimated that infiltration will proceed twice as fast through the backfill as through the undisturbed lower strata, so for a steady input of 7.5 inches of water in a week, an accumulation of 2.25 inches (5.6cm) of water can be calculated.

The storage volume under the waste can best be provided by a layer of a highly porous nature. A granular material such as small gravel or coarse sand would be appropriate, but the interstices must be small enough to prevent significant invasion of fines with subsequent clogging. AASHTO number 89 stone would be an appropriate choice, as it would provide a very permeable zone and would not require the placement of a number of layers of different sized media. If compacted to a reasonable density, the void volume of 89 stone is in the 20-25% range. It would therefore require a theoretical depth of 11.25 inches to hold 2.25 inches of water. Such precision is not warranted and specification of one foot (30cm) of this material will assure a very conservative volume.

Placement of a foot of small gravel such as 89 stone under the disposal trenches is a reasonable measure which should provide long-term assurance that the layer would retain its capacity even with a limited amount of siltation from the lower reaches of the backfill.

It may occur that site considerations will make it desirable to increase the size of the drainage area or to move it completely from under the burial area. This can be accomplished by drain lines leading from the layer of emplaced gravel to another drain field. Clay pipes are satisfactory for this type of service as they are resistant to chemical deterioration, can be installed without any particular difficulty, and should remain trouble-free for a very long period of time. They are susceptible to breakage, however, and could be destroyed by the heavy equipment used to place and compact the waste materials.

While the installation of drain lines entirely across the bottom of the excavation within the gravel layer would provide very rapid discharge from the gravel, this is not mandatory. If the lines extend into the gravel a limited distance, the desired result will be obtained because of the very high rate of transmission of water by the gravel layer. From the practical view, it could be advisable to delay installation of the drain tile and its limited adjacent gravel area until the balance of the trench was already filled and compacted.

More than one line should be installed so that the system could operate in a fairly normal manner, even if some of the pipes were broken or became clogged with silt or roots. In the areas where exfiltration is intended, the pipes would be laid with open joints in ditches with a layer of gravel. Tight pipe joints would be used in any zone where dispersion of the water was not wanted.

The area of the extended drain field will be governed by the relative permeability of the subsoil in relation to the permeability of the soil cap covering the waste. In the situation of a remote drain field of the same area as that of the burial excavation, if the soil permeability is less than half of that of the cap, the potential maximum accumulation of water will be more than the 2.25 inches calculated above. This increase can be offset by a deeper gravel layer or a larger drain field, but the volume of the drain lines themselves may be large enough to be significant. In any event, the effect of pipe volume should be considered.

A downward slope of the drain lines is needed, but it does not have to be a very large slope. The usual design of a drain field involves parallel pipe lines fed by a header, but the long-term reliability of the system can be increased by the addition of extra connections at intervals between the parallel lines. This will provide a grid so that in the event of a stoppage, flow to most points can be provided from the other direction.

No unusual requirements are placed on the subsequent seepage path to the aquifer. A fairly clayey soil and a reasonable distance to the water table are desirable and the orientation of the drain field can be chosen to optimize the final water flow direction in this respect. Since the source term is expected to be lower, the retention capacity of the seepage path also need not be as high as for the saturated flow condition and a wider area can be drawn into service, subject mainly to cost and land use limitations.

CONCLUSIONS

The drained trench approach has been, incorrectly, described as a "controlled release" procedure, which would not be in accordance with 10CFR61 regulations. It would be more appropriate to say that it is a more realistic evaluation of what happens in a burial trench and is a preferable approach to a setting that invites bathtub conditions that would lead to uncontrolled release and a very rapid return of contaminants to the biosphere. The drained trench approach is expected to reduce waste leaching significantly, though additional work is required to determine just how much. By eliminating standing water in the trench, frost and subsidence effects should be reduced. The backfill material would normally be more permeable than the undisturbed soil, resulting in lower residual moisture levels, but in some locations it may be desirable to mix some sand or sandy loam into the backfill.

The extra cost of providing a foot-deep layer of gravel or 89 stone is not significantly higher than the base preparation currently practiced in preparing disposal trenches. The more extensive drain field would entail additional costs compared with current procedures; on the other hand, much of this added cost would be recovered by the lesser need for very rigid and elaborate cap designs that are proposed by some at present (26).

The work has shown the importance of taking unsaturated flow conditions into account in designing a facility and assessing its impact. Although it is easier and "conservative" to model saturated flow, it is evident that the calculated impacts may be orders of magnitude too high and give an unrealistic impression of the radiological consequences of trench construction (27). It is still important to bury predominantly solid waste, but in a carefully chosen medium, proper drainage would be expected to provide better insurance in the long run against excessive leaching and release, than reliance on trench cap performance.

ACKNOWLEDGMENTS

We are indebted to Mr. Ed Johnson of the Georgia Highway Department for providing some gravel for this project and to Mr. Jerry A. Connor of the Georgia Tech Physical Plant Department for arranging the trench excavation and supplying sand and other materials.

BIBLIOGRAPHY

1. J.S. Baldwin et al., Procedures and Technology for Shallow Land Burial. Rept. DOE/LLW - 13 Td, National Low-level Radioactive Waste Management Program, Idaho Falls, ID, 1983
2. Rogers & Associates Engineering Corp., A Handbook For Low-level Radioactive Waste Disposal Facilities. Rept. NP-2488LD, Electric Power Research Institute, Palo Alto, CA, 1982
3. M.A. Feraday. A Prospectus for the Development of Shallow Land Burial Disposal Concepts for the CRNL Site. Rept. TR-307, Chalk River Environmental Authority, Chalk River, Ont., 1983
4. A.A. Metry, D.R. Phoenix and A.L. Lenthe, In-site Stabilization of a Low-level Radioactive Site - a case history. Roy Weston Inc., West Chester, PA, 1982
5. J.G. McCray, E.A. Nowatzki and G.M. Thompson, Performance of Shallow Land Burial Trench Caps - Assessment of the soil arch and soil beam concept. Proc. 5th Annual Participants Information Meeting, LLWMP, CONF-8308106, p. 167, 1983
6. F. Homan. Design of the Central Waste Disposal Facility at Oak Ridge National Laboratory (unpublished), 1984
7. G.G. Eichholz, F.N. deSousa, M.F. Petelka and J. Whang. Evaluation and Design of Drained Low-level Disposal Sites. Proc. 6th Annual Participants Information Meeting, Denver, 1984
8. B. Yaron, G. Dagan and J. Goldshmid (eds). Pollutants in Porous Media. Springer Verlag, Berlin, 1984
9. Licensing Requirements for Land Disposal of Radioactive Waste. Final Environmental Impact Statement on 10CFR61. Rept. NUREG - 0945, U.S. Nuclear Regulatory Commission, Washington, D.C. 1982
10. Management of Commercially Generated Radioactive Waste. Final Environmental Impact Statement. Rept. DOE/EIS-0046F, U.S. Dept. of Energy, Wasington, D.C. 1980
11. G.D. DeBuchananne. Geohydraulic Considerations in the Management of Radioactive Waste. Nuclear Technology 24, 356-361 (1974)
12. R.J. Serne and J.F. Relyea. The Status of Radionuclide Sorption-Desorption Studies Performed by the WRIT Program; in The Technology of High-Level Nuclear Waste Disposal, Vol. 1, U.S. Dept. of Energy, 1981

13. L.L. Ames and D. Rai. Radionuclide Interactions with Soil and Rock Media. Rept. EPA 520/6-78-007, U.S. Environmental Protection Agency, Las Vegas, NV, 1978
14. National Low-Level Radioactive Management Program. Managing Low-Level Radioactive Wastes: A Proposed Approach. Rept. DOE/LLW-9, EG&G Idaho, 1983
15. D.G. Jacobs, J.S. Epler and R.R. Rose. Identification of Technical Problems Encountered in the Shallow Land Burial of Low-Level Radioactive Wastes. Rept. ORNL/SUB-80/13619/1, Oak Ridge National Lab, 1980
16. J. Bear, D. Zaslavsky and S. Irmay, Physical Principles of Water Percolation and Seepage. UNESCO, Paris, 1968
17. G.L. DePoorter, W.V. Abeele, B.W. Burton, T.E. Hakonson and B.A. Perkins. Shallow Land Burial Technology Development - Arid. Proc. 4th Annual Participants Information Meeting - DOE - LLWMP, Rept. ORNL/NFW-82/18, 539-566, 1982
18. W.V. Abeele, G.L. DePoorter, T.E. Hakonson and T.W. Nyhan. Shallow Land Burial Technology - Arid. Proc. 5th Annual Participants Information Meeting, LLWMP, CONF-8308106, p. 140, 1983.
19. T.N. Nyhan, W.V. Abeele, G.L. De Poorter, T.E. Hakonson, B.A. Perkins and G.R. Foster. Field Studies of Erosion Control Technologies for Arid Shallow Land Burial Sites at Los Alamos. Proc. 5th Annual Participants Information Meeting, LLWMP, CONF-8308106, p. 193, 1983
20. R.K. Schulz. Study of Unsaturated Zone Hydrology at Maxey Flats. Proc. 5th Annual Participants Information Meeting, LLWMP, CONF-8308106, p. 674, 1983
21. E.C. Davis, B.P. Spalding and S.Y. Lee. Shallow Land Burial Technology - Humid. Proc. 5th Annual Participants Information Meeting, LLWMP, CONF-8308106, p. 121, 1983
22. H.D. Foth and L.M. Turk. Fundamentals of Soil Science, 5th edition. John Wiley & Sons, New York, 1972
23. C. Pescatore and A.J. Machiels. Effects of Water Flow Rates on Leaching; in Geochemical Behavior of Disposed Radioactive Waste, G.S. Barney, J.D. Navratil and W.W. Schulz eds., American Chemical Society, Washington, D.C. 1984
24. S.B. Oblath, J.A. Stone and J.R. Wiley. Special Wasteform Lysimeter Program at the Savannah River Laboratory. Proc. 5th Annual Participants Information Meeting - DOE - LLWMP. CONF-8308106, 441-448, EG&G Idaho, 1983

25. G. R. Free, G. M. Browning, and G. W. Musgrave. Relative Infiltration and Related Physical Characteristics of Certain Soils, U.S. Dept. Agr. Tech. Bull. 729, 1940.
26. L.G. Mezga. The Role of Trench Caps in the Shallow Land Burial of Low-level Wastes. Rept. ORNL-TM-9156, Oak Ridge National Lab., 1984.
27. C. N. Ostrowski, T. J. Nicholson, D. D. Evans and D. H. Alexander, Disposal of High-level Wastes in the Unsaturated Zone: Technical Considerations. Rept. NUREG-1046, U.S. Nuclear Regulatory Commission, Washington, D.C. 1984.
28. M.T. Van Genuchten. Mass Transport in Saturated - Unsaturated Media: One-dimensional Solutions. Reserch Rept. 78-WR-11 Water Resources Program, Princeton Univ., Princeton, NJ, 1978.
29. A.W. Warrick, T.W. Biggar and D.R. Nielsen. Simultaneous Solute and Water Transfer for an Unsaturated Soil. Water Resources Res. 7, 1216-1225, (1971).

APPENDIX A

Water Characteristics, Hydraulic Conductivity and Sorption Models

by F. N. Carneiro de Sousa

What makes the unsaturated flow equation difficult to solve is the fact that the pressure head and the hydraulic conductivity are both a function of the water content; these relations can be incorporated in the model in table form or by means of analytical expressions. In this study the available data for each soil type was fitted to three different analytical relations, which were called Brooks and Corey, Haverkamp, and Van Genuchten models.

The solution of the transport equation needs also a relation to represent the sorption process. The model was developed in such a way that any equilibrium sorption model can be used, and the three most used ones are described in this section. Some alterations have to be done if a kinetic sorption model is to be used.

1. - Water characteristics and Hydraulic Conductivity Models

a - Brooks and Corey

Brooks and Corey (1964) suggested the following relation to represent the soil-water characteristics

$$\frac{\theta - \theta_r}{n - \theta_r} = \left(\frac{\psi_e}{\psi} \right)^\lambda \quad (\text{A.1})$$

where θ is the volumetric water content, n is the porosity, θ_r is the residual water content, ψ is the soil suction, ψ_e is the air-entry value, and λ is the pore-size distribution index.

The associated hydraulic conductivity is given by

$$K = K_s \left(\frac{\theta - \theta_r}{n - \theta_r} \right)^{\frac{2 + 3\lambda}{\lambda}} \quad (\text{A.2})$$

where K is the unsaturated hydraulic conductivity and K_s is the saturated one. This equation was obtained by Brooks and Corey with the use of the Burdine theory (see Van Genuchten model). If the Mualem theory is used the equation becomes

$$K = K_s \left(\frac{\theta - \theta_r}{n - \theta_r} \right)^{\frac{4 + 5\lambda}{\lambda}} \quad (\text{A.3})$$

This set of equations is one of the most used to describe the hydraulic properties of the soil.

b - Haverkamp

Haverkamp (Haverkamp et al., 1977) proposed the following relation for the soil-water characteristics based on laboratory infiltration experiments:

$$\theta = \frac{\alpha (n - \theta_r)}{\alpha + |h|^\beta} + \theta_r \quad (\text{A.4})$$

where n is the porosity, θ_r is the residual water content, h is the pressure head, and α and β are empirical constants.

As is discussed by McKeon (McKeon et al., 1983), this relation provides for the proper behavior of the soil-water characteristics, since as h approaches zero, the water content approaches saturation, and as h assumes large negative values, the water content approaches the residual value.

The associated hydraulic conductivity relation is given by

$$K = K_s \left(\frac{A}{A + |h|^\beta} \right) \quad (\text{A.5})$$

where K_s is the saturated hydraulic conductivity and A and β are empirical constants.

Van Genuchten (1978) presents a relation for the soil-water characteristics which is a development of the Haverkamp relation; it is given by

$$\theta = (n - \theta_r) \left(\frac{1}{1 + |\alpha h|^\beta} \right)^\lambda + \theta_r \quad (\text{A.6})$$

where α and β are empirical constants and $\lambda = 1 - 1/\beta$. This equation provides the same limits and smoothness as those obtained with the Haverkamp model.

The hydraulic conductivity/water content relation presented by Van Genuchten (1980) is an integral form of the Childs and Collis-George (1950) equation, which is an attempt to calculate the unsaturated hydraulic conductivity using a pore-size distribution obtained from the soil-water characteristics curve. Several investigators modified the equation, and Mualem (1976) presented a simple analytical model given by

$$K_r(\theta) = \frac{\left\{ S_e^\beta \sum_{i=1}^m \frac{2(n-i)+1}{\psi_i^2} \right\}}{\left\{ \sum_{i=1}^m \frac{2(m-i)+1}{\psi_i^2} \right\}} \quad (\text{A.7})$$

where m represents the total number of intervals into which the water content is divided (water characteristics curve), n is the number of intervals up to a prescribed value of θ , β is a constant related to the pore-size distribution, $S_e = (\theta - \theta_r) / (n - \theta_r)$, and $K_r = K/K_s$. If $\beta = 0$, Collis-George equation is obtained; if $\beta = 4/3$, it becomes Millington and Quirk (1959) equation; if $\beta = 1$ Kunze (Kunze et al., 1968) is obtained. Mualem (1976) presented an alternative formulation given by

$$K_r = (S_e)^{1/2} \left[\frac{\int_0^{S_e} \frac{dS_e}{dh}}{\int_0^1 \frac{dS_e}{dh}} \right]^2 \quad (\text{A.8})$$

A similar equation is given by Burdine (1958)

$$K_r = S_e^2 \left[\frac{\int_0^{S_e} \frac{1}{h^2} dx}{\int_0^1 \frac{1}{h^2} dx} \right] \quad (\text{A.9})$$

The equation presented by Van Genuchten (1980) is an integral form of the Millington and Quirk equation, and is given by

$$K = K_s S_e^{1/2} \left[1 - (1 - S_e^{1/\lambda})^\lambda \right]^2 \quad (\text{A.10})$$

where $S_e = (\theta - \theta_r) / (n - \theta_r)$, and λ and β and α (from eq. A. 6) are empirical constants obtained from the shape of the water characteristics curve. The advantage of this model is the ability to fit data in the near saturation range.

2-Equilibrium Sorption Isotherms

a-Linear Adsorption

The linear adsorption isotherm is the most common relation used to simulate the sorption of radionuclides by the soil particles. It is given by

$$S = K_d C \quad (\text{A.11})$$

where S is the amount of solution absorbed by the soil matrix, C is the concentration of solute in the soil solution and K_d is the distribution coefficient. The velocity of the tracer (V_t) is related to the water velocity (V_e) by

$$V_t = V_w / R \quad (\text{A.12})$$

where R is the retardation factor which is given by

$$R = 1 + \frac{\rho K_d}{\theta} \quad (\text{A.13})$$

where ρ is the bulk density.

The disadvantage of this relation is that it assumes equilibrium conditions, and it does not describe a maximum quantity of adsorption. On the other hand, its use makes the transport equation linear, facilitating the numerical simulation. A similar relation is presented by Lapidus and Amundson (1952),

$$S = K_1 C + K_2 \quad (\text{A.14})$$

where K_1 and K_2 are constants.

b - Freundlich Isotherm

The Freundlich (1926) isotherm is given by

$$S = K C^n \quad (\text{A.15})$$

where S is the amount of solute adsorbed per unit weight of soil, C is the equilibrium solute solution concentration, and K and n are constants. If n is equal to zero, it becomes the linear isotherm. The disadvantages are that equilibrium conditions are assumed, it does not specify a maximum quantity of adsorption, and its use makes the transport equation non-linear, which implies in an iterative solution.

c-Langmuir Isotherm

The Langmuir isotherm (1918) was originally developed to describe the adsorption of gas molecules onto the surface of solids; it was later extended to represent the adsorption of aqueous solutes onto solid sorbates. It is given by

$$S = \frac{K b C}{1 + K C} \quad (\text{A.16})$$

where S is the amount of solute adsorbed for unit mass of solid, C is the equilibrium solute concentration, K is a constant related to the energy of adsorption, and b is the maximum amount which can be adsorbed by the solid. It becomes the linear isotherm as C approaches zero. The disadvantage is that it assumes equilibrium conditions, and the transport equation becomes non-linear when it is used.

Other equilibrium sorption isotherms as well as kinetic sorption models are given by Travier and Etnier (1981).

APPENDIX B

MODEL IMPLEMENTATION

In this appendix a description is given of the one-dimensional unsaturated flow and transport mode. The program consists of a main program and 12 subroutines. The main program is responsible for the organization of the program, basically, it performs the scheme shown in Fig. B.1.

Subroutine INPU1 is used to initialize the values of all variables needed for the solution of the water flow equation; it defines the geometry and the initial and boundary conditions of the case under study; it also introduces the physical and chemical properties of the soils. Subroutine INPU2 is used to introduce the values of the variables needed to obtain the solution of the transport equation; it includes the initial and boundary conditions as well as the soil properties that were not already introduced by INPU1.

Subroutine SET performs a coordinate transformation; it changes the global coordinates of the nodes of each element to a local coordinate system, which simplifies the evaluation of the element matrices.

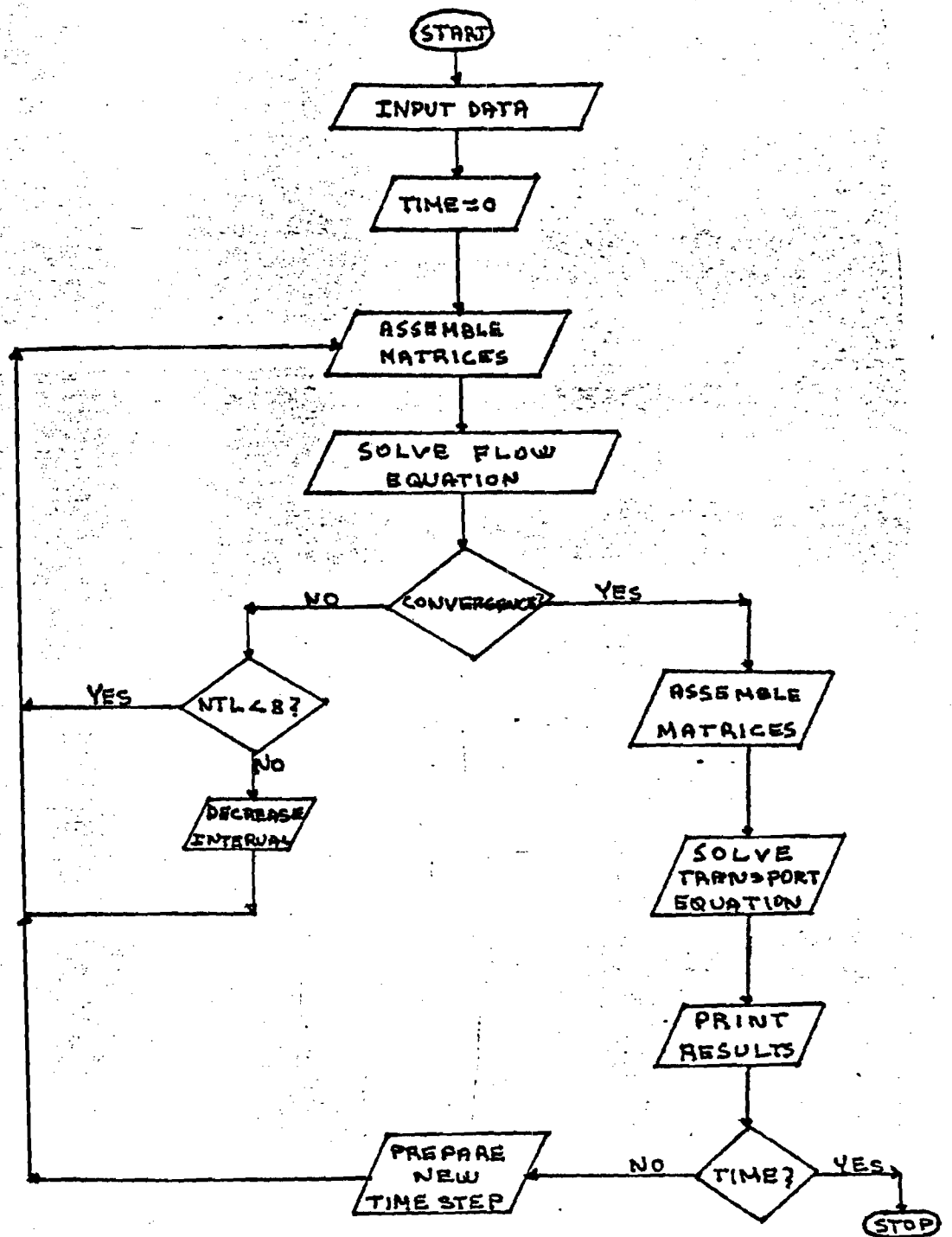


Figure B-1 Model Flow Diagram

Subroutine ELEM generates the local element matrices by calculating each coefficient of the matrices necessary to solve the matrix flow equation. Subroutine ELEM 1 does the same calculations for the transport equation. The soil properties needed for the evaluation of the matrix coefficients are calculated in subroutine HCWC, which is called by subroutine ELEM.

Once the global matrices are assembled, a set of partial differential equations is obtained; these equations are solved by applying a finite difference scheme, and this is done in subroutine CALC1. This subroutine is also responsible for the introduction of the boundary conditions. The output of this subroutine is a system of ordinary equations which is solved by subroutine SOLVE. The method used to solve these equations is the Thomas algorithm, which is a special form of the Gaussian elimination method.

When the solution is obtained for the flow equation, the convergence criteria is checked by subroutine ERROR. If convergence is not attained, the iterative process continues; if convergence is attained, the variables needed for the solution of the transport equation are evaluated by subroutine PROP and the transport equation is then solved. Subroutine OUT presents the values of the hydraulic head, water content, and solute concentration at each time interval.

Table B.1 presents the major variables used in the numerical implementation of the program; Table B2 presents the input cards needed to solve the flow equation, and Table B.3 presents the listing of the actual program.

TABLE B.1 - PROGRAM VARIABLES

AG(30.3)	- Global matrix
AI(3)	- Residual Water Content of each soil
AL1	- Distance between the two last nodes of the soil column.
ALF(3)	- Compressibility of the soil
BI(3)	- Value of α in eq. A.4 and A.5, and value of ψ_a in eq. A.1
BUD(3)	- Bulk density of the soils.
CI(3)	- Pore-size distribution index.
CL	- Value of the constant concentration at the last node of the column when a constant boundary condition is used.
CO(20)	- Variable concentration at the top of the column when a variable boundary condition is used.
CON(30)	- Concentration at time $t + \Delta t$.
CONI(30)	- Initial concentration profile.
COO	- Constant concentration at surface when a constant boundary condition is used.
DEV(30)	- Value of $\partial h / \partial t$ at each node.
DEVO(30)	- Value of $\partial \theta / \partial t$ at each node.
DI(3)	- Value of A in EQ. A.5
DICO(30)	- Distribution coefficient of each soil
DIFU(3)	- Diffusion coefficient of each soil
DISP(3)	- Dispersivity of each soil.
EI(3)	- Value of β in eq. A.5
ERR1	- Value of ϵ_1 in eq. VII. 31.
ERR2	- Value of ϵ_2 in eq. VII.31.
FLUX(30)	- Value of the water flux at each node.
GAM(3)	- Zero-order rate constant of each soil.

TABLE B.1 cont.

- HC1 - Hydraulic conductivity of the first node
- HCL - Hydraulic conductivity of the last node.
- HCOS(3) - Saturated hydraulic conductivity of each soil.
- HEDI1 - Value of the pressure head at first node of each element at time
- HEDI2 - Value of the pressure head at second node of each element at time
- HEDIL(30) - Value of the pressure head at each node at time t .
- HEDIN(30) - Value of the pressure head at each node at time $t + \frac{1}{2} \Delta t$.
- HEDIX(30) - Value of the pressure head at each node at time $t + \Delta t$.
- HEDO - Value of the initial pressure head if it is constant through the soil column.
- HL - constant pressure head at the last node if a constant boundary condition is used.
- HO - Constant pressure head at surface if a constant boundary condition is used.
- I1 - Determines which sorption model is used. .
= 1 Linear adsorption isotherm.
- I2 - Determines which soil-water characteristics model is used.
= 1 Brooks and Corey
= 2 Van Genuchten
= 3 Haverkamp
- I3 - Determines which hydraulic conductivity model is used.
= 1 Brooks and Corey
= 2 Van Genuchten
= 3 Haverkamp
- I4 - If it is equal to one $Q_0(I) = \text{constant}$.
- ICON(30,2) - Relates each node number to its element.
- IE - Constant used to indicate if convergence is attained.
- IK - Constant used to indicate which soil type applies to each element.
- IKK - Constant used to indicate which value of the constant flux at surface is being used

TABLE B.1 cont.

ISA	- Constant used to indicate if the initial concentration is constant over the whole soil profile.
ISP	= 1 equally spaced nodes.
ISS	= 1 Constant initial pressure head.
IST	= 1 Homogeneous soil
ISU	= 1 Transport model is used
ISX	= 1 Mass lumping is used.
JI(3)	- Contains the node number at which each soil type ends.
K1	= 1 Constant concentration at surface.
K2	= 1 Constant flux of concentration at surface at each specified time.
K3	= 1 Free draining profile.
K4	= 1 Constant concentration at last node.
K21	= 1 Constant flux of concentration at surface.
KB1	= 1 Constant flux at surface.
KB2	= 1 Constant flux at last node.
KB3	= 1 Constant pressure head at surface.
KB4	= 1 Constant pressure head at last node.
KB5	= 1 Variable flux at last node.
NELEM	- Number of elements used.
NEWN(2)	- Contains the nodes numbers for each element.
NL	- Number of iterations at each time step.
NNODE	- Number of nodes.
NST	- Maximum number of iterations allowed at each time step.
NT	- Counts number of time steps.
NTM	- Maximum number of time steps allowed.

TABLE B.1 cont.

PF(30)	- Global matrix.
PORO(3)	- Porosity of each soil type.
QL	- Constant flux at last node.
QO(20)	- Values of constant flux at different times at surface.
SCAP1	- Soil water capacity of first node of an element.
SCAP2	- Soil water capacity at second node of an element.
SS(3)	- Specific storage of each soil.
TETIX(30)	- Water content at each node at time .
TETOX(30)	- Water content at each node at time t.
TI	- Time since start of simulation.
TIM	- Value of the time interval at time t.
TIMAX	- Maximum time interval allowed.
TIME	- Total time of simulation.
TIMEX(20)	- Time at which constant flux ends at the surface.
TIMIN	- Minimum time interval allowed.
TIVAL	- Time interval at time t+ t
TORT(3)	- Tortuosity factor of each soil.
XL	- Length of the soil profile.
XLAM	- Decay rate fo the radionuclide under study.
XMG(30,3)	- Global matrix.
W	= 0 explicit algorithm is used. = 1/2 Crank-Nicholson algorithm is used. = 1 Implicit algorithm is used.
Z(30)	- global coordinates of the nodes.

TABLE B.2 - INPUT DATA FOR FLOW EQUATION

CARDS	COLUMNS	FORMAT	VARIABLE	
1	1-8	F8.3	XL	
	9-16	F8.3	TIME	
	17-24	F8.5	TTIVAL	
	25-32	F8.3	TIMAX	
	33-40	F8.5	TIMIN	
	41-48	F8.3		
	49-53	I5	NELEM	
	54-58	I5	NTM	
	59-63	I5	NST	
2	1	I5	ISP	
3	1	I5	ISS	
4	1	F8.3	HEDO	
5	1	I5	IST	
6-8	1-8	F8.3	AI(3)	
	9-16	F8.3	BI(3)	
	17-24	F8.3	CI(3)	
	25-32	F8.3	DI(3)	
	33-40	F8.3	DI(3)	
	41-48	F8.3	HCOS(3)	
	49-56	F8.3	PORO(3)	
	57-64	E8.3	SS(3)	
	65-69	I5	JI(3)	
	9	1-5	I5	ISU
6-13		F8.3	ERR1	
14-21		F8.3	ERR2	
22-26		I5	I1	
27-31		I5	I2	
32-36		I5	I3	
36-40		I5	I4	
10		1-5	I5	KB1
		6-10	I5	KB2
		11-18	F8.3	QL
	19-23	I5	KB3	
	24-28	I5	KB4	
	29-35	F8.3	HO	
	36-42	F8.3	HL	
	43-47	I5	KB5	
11	1	F8.3	QOO	
12	1	I5	ISX	

TABLE B.3 - PROGRAM LISTING

```

PROGRAM OEDIT(IN,OUT,TAPES=IN,TAPE6=OUT)
DIMENSION Z(30),ICON(30,2),HEDIN(30),AI(3),BI(3),CI(3),DI(3),
1 EI(3),HCOS(3),PORO(3),SS(3),TIMEX(20),QO(20),XSG(30,3),
2 XMG(30,3),XPG(30),ZE(2),NEWN(2),JI(3),XM(2,2),XS(2,2),
3 XP(2),TMG(30,3),FPG(30,3),HEDIX(30),HEDIL(30),PF(30),
4 TETIX(30),HEDIS(30),HEDIP(30)
*
----READ INPUT VALUES----
REWIND 6
CALL INPU1(XL,TIME,TIVAL,TIMAX,TIMIN,NELEM,W,NNODE,Z,HEDIN,
1 AI,BI,CI,DI,EI,HCOS,PORO,SS,ISU,I1,I2,I3,ERR1,ERR2,KB1,KB2,
2 KB3,KB4,KB5,QO,QL,HO,HL,ISX,TIMEX,NTM,NST,JI,ICON)
*
----DETERMINE IF TRANSPORT EQUATION IS USED----
*
IF(ISU.LT.1)GO TO 2
*
CALL INPU2(
*
2 CONTINUE
NL=1
NT=1
NNN=1
DO 3 I=1,NNODE
HEDIP(I)=HEDIN(I)
HEDIS(I)=HEDIN(I)
3 HEDIL(I)=HEDIN(I)
TIM=TIVAL
IKK=1
IK=1
TI=0
TI=TI+TIVAL
6 DO 10 I=1,NNODE
DO 10 J=1,3
XSG(I,J)=0
XMG(I,J)=0
10 XPG(I)=0
*
----DETERMINE LOCAL MATRICES----
DO 20 I=1,NELEM
HEDI1=HEDIN(I)
HEDI2=HEDIN(I+1)
DO 15 J=1,2
15 NEWN(J)=ICON(I,J)
*
WRITE(6,1102)NEWN
*1102 FORMAT(/2I5,'NEW NODE')
CALL SET(NEWN,ZE,Z,NELEM,ISP,XL)
CALL ELEM(HEDI1,HEDI2,PORO,SS,ISX,I2,I3,HCOS,AI,BI,CI,DI,EI,
1 JI,NEWN,IK,ZE,XM,XS,XP,NNODE,HC1,HCL,AL1)
*
----ASSEMBLE GLOBAL MATRICES----
20 CALL ASSEM(NEWN,XM,XMG,XS,XSG,XP,XPG)
*
----INTRODUCE BOUNDARY CONDITIONS----
CALL CALC1(TIVAL,HEDIS,XMG,XSG,XPG,NNODE,W,KB1,KB2,KB3,KB4,
3 KB5,QO,QL,HO,HL,TIMEX,TI,HC1,HCL,AL1,IKK,TMG)
CALL SOLVE(TMG,XPG,HEDIX,FPG,NNODE)
*
----CHECK FOR CONVERGENCE----
CALL ERROR(HEDIX,HEDIL,IE,ERR1,ERR2,NNODE)
*
WRITE(6,111)(HEDIX(I),HEDIL(I),I=1,NNODE)
*
111 FORMAT(3X,F8.3,3X,F8.3)
IF(NNN.GT.100)GO TO 21
TI=TIVAL
21 IF(IE.EQ.0)GO TO 50
IF(NL.LE.NST)GO TO 25
TI=TI-.5*TIVAL
TIVAL=0.5*TIVAL
IF(TIVAL.LT.TIMIN)GO TO 100
DO 22 I=1,NNODE
HEDIN(I)=HEDIS(I)+(TIVAL/(2*TIM))*(HEDIS(I)-HEDIP(I))

```

```

22   HEDIL(I)=HEDIN(I)
      NL=1
      GO TO 6
25   DO 30 I=1,NNODE
HEDIN(I)=0.5*(HEDIX(I)+HEDIS(I))
30   HEDIL(I)=HEDIX(I)
      NL=NL+1
      GO TO 6
*   ----CONVERGENCE IS ATTAINED----
50   IF(NNN.GT.1)GO TO 55
      TI=TIVAL
55   DO 57 I=1,NNODE
      H=ABS(HEDIX(I))
      HH=29.484
      IF(H.GT.HH)GO TO 56
      TETIX(I)=.4531-.02732*LOG(H)
      GO TO 57
56   TETIX(I)=.6829-.09524*LOG(H)
57   CONTINUE
      CALL OUT(TI,Z,HEDIX,NT,NL,NNODE,TETIX)
      NNN=NNN+1
      DO 60 I=1,NNODE
      HEDIN(I)=HEDIX(I)+(TIVAL/(2*TIM))*(HEDIX(I)-HEDIS(I))
      HEDIP(I)=HEDIS(I)
      HEDIS(I)=HEDIX(I)
60   HEDIL(I)=HEDIN(I)
      IF(NL.GT.3)GO TO 70
      TIVAL=1.5*TIVAL
      IF(TIVAL.LE.TIMAX)GO TO 70
      TIVAL=TIMAX
70   NT=NT+1
      TI=TI+TIVAL
      IF(TI.GT.TIME)GO TO 100
      IF(NT.GT.NTM)GO TO 100
      NL=1
      TIM=TIVAL
      GO TO 6
100  WRITE(6,1001)TI,NT
1001 FORMAT(3X,"PROGRAM TERMINATED WITH TI=",1X,F8.5,2X,"AND NT=",
1     2X,I5)
      STOP
      END
      SUBROUTINE INPU1(XL,TIME,TIVAL,TIMAX,TIMIN,NELEM,W,NNODE,Z,
1     HEDIN,AI,BI,CI,DI,EI,HCOB,PORO,SS,ISU,I1,I2,I3,ERR1,ERR2,
2     KB1,KB2,KB3,KB4,KB5,QQ,QL,HO,HL,ISX,TIMEX,NTM,NST,JI,ICON)
      DIMENSION Z(30),HCOB(3),PORO(3),SS(3),TIMEX(20),QQ(20),JI(3),
1     ICON(30,2),HEDIN(30),AI(3),BI(3),CI(3),DI(3),EI(3)
      WRITE(6,1000)
      READ(5,1010)XL,TIME,TIVAL,TIMAX,TIMIN,W,NELEM,NTM,NST
      WRITE(6,1020)XL,TIME,TIVAL,TIMAX,TIMIN,W,NELEM,NTM,NST
      NNODE=NELEM+1
*   ----DETERMINE GLOBAL COORDINATES OF THE NODES----
      READ(5,1030)ISP
      DO 1 I=1,NNODE
1     Z(I)=0
      IF(ISP.LT.1)GO TO 5
      DO 2 I=1,NNODE
          Z(I)=(I-1)*X/NELEM
2     WRITE(6,1040)I,Z(I)
      GO TO 10
      DO 7 I=1,NNODE
          READ(5,1050)Z(I)
7     WRITE(6,1040)I,Z(I)

```

```

12 DO 12 J=1,2
* ICON(I,J)=I+J-1
----OBTAIN INITIAL PRESSURE HEADS----
READ(5,1030)ISS
IF(ISS.LT.1)GO TO 17
READ(5,1050)HEDO
WRITE(6,1070)HEDO
* DO 15 I=1,NNODE
DO 15 I=1,12
XX=.15+.000833*(I-1)*5/1
XXX=(.6829-XX)/.09524
HEDIN(I)=-EXP(XXX)
15 WRITE(6,1040)I,HEDIN(I)
DO 14 I=13,26
HEDIN(I)=HEDO
16 WRITE(6,1040)I,HEDIN(I)
* 15 HEDIN(I)=HEDO
GO TO 20
17 DO 18 I=1,NNODE
READ(5,1050)HEDIN(I)
18 WRITE(6,1040)I,HEDIN(I)
20 READ(5,1030)IST
IF(IST.LT.1)GO TO 25
READ(5,1090)AII,BII,CII,DII,EII,HCOSI,POROI,SSI,JII
WRITE(6,1100)AII,BII,CII,DII,EII,HCOSI,POROI,SSI,JII
DO 22 I=1,3
AI(I)=AII
BI(I)=BII
CI(I)=CII
DI(I)=DII
EI(I)=EII
HCOS(I)=HCOSI
PORO(I)=POROI
JI(I)=JII
22 SS(I)=SSI
GO TO 30
25 DO 28 I=1,3
READ(5,1090)AI(I),BI(I),CI(I),DI(I),EI(I),HCOS(I),PORO(I),
1 SS(I),JI(I)
28 WRITE(6,1100)AI(I),BI(I),CI(I),DI(I),EI(I),HCOS(I),PORO(I),
1 SS(I),JI(I)
30 CONTINUE
* ----DETERMINE IF TRANSPORT MODEL IS USED----
* READ(5,1105)ISU,ERR1,ERR2,I1,I2,I3,I4
----OBTAIN BOUNDARY CONDITIONS----
READ(5,1110)KB1,KB2,QL,KB3,KB4,HO,HL,KB5
IF(KB3.LT.1)GO TO 31
HEDIN(1)=HO
31 IF(KB4.LT.1)GO TO 315
HEDIN(NNODE)=HL
HEDIN(NNODE)=HL
IF(I4.LT.1)GO TO 32
315 READ(5,1050)QOO
DO 316 I=1,20
316 TIMEX(I)=TIME
GO(I)=Q.
GO(I)=Q.
TIMEX(1)=TIME/2.
GO(2)=QOO
TIMEX(2)=TIME
GO TO 40
32 DO 35 I=1,20

```

```

      READ(5,1120)TIMEX(I),QO(I)
35  WRITE(4,1130)TIMEX(I),QO(I)
*   ----DETERMINE IF MASS LUMPING IS USED----
40  READ(5,1030)ISX
*   ----
1000 FORMAT(/,7X,"UNSATURATED FLOW AND TRANSPORT",/)
1010 FORMAT(2F8.3,F8.5,F8.3,F8.5,F8.3,3I5)
1020 FORMAT(3X,"XL=",F8.3,3X,"TIME=",F8.3,3X,"TIVAL=",E8.3,3X,
1  "TIMAX=",F8.3,/,3X,"TIMIN=",E8.3,3X,"W=",F8.3,3X,"NELEM=",
2  I5,3X,"NTM=",I5,3X,"NST=",I5)
1030 FORMAT(I5)
1040 FORMAT(4X,I4,6X,F8.3)
1050 FORMAT(F8.3)
1070 FORMAT(/,4X,"HEDO=",F8.3)
1090 FORMAT(7F8.3,E8.3,I5)

1100 FORMAT(3X,7(3X,F8.3),3X,E8.3,3X,I5)
1105 FORMAT(I5,2F8.3,4I5)
1110 FORMAT(2I5,F8.3,2I5,2F8.3,I5)
1120 FORMAT(2F8.3)
1130 FORMAT(3X,F8.3,3X,F8.3)
      RETURN
      END
      SUBROUTINE SET(NEWN,ZE,Z,NELEM,ISP,XL)
      DIMENSION Z(30),ZE(2),NEWN(2)
      IF(ISP.LT.1)GO TO 1
      ZE(1)=0
      ZE(2)=XL/NELEM
      GO TO 5
1  J=NEWN(1)
      JJ=NEWN(2)
      ZE(1)=0
      ZE(2)=Z(JJ)-Z(J)
5  RETURN
      END
      SUBROUTINE ELEM(HEDI1,HEDI2,PORO,SS,ISX,I2,I3,HCOS,AI,BI,
1  CI,DI,EI,JI,NEWN,IK,ZE,XM,XS,XP,MNODE,HC1,HCL,AL1)
      DIMENSION PORO(3),SS(3),HCOS(3),AI(3),BI(3),CI(3),DI(3),
1  EI(3),JI(3),NEWN(2),ZE(2),XM(2,2),XS(2,2),XP(2)
      IAS=NEWN(1)
      IASS=JI(IK)
      IF(IAS.LT.IASS)GO TO 5
      IK=IK+1
5  AL=ZE(2)-ZE(1)
      CALL HCOV(HCO1,HCO2,TETI1,TETI2,SCAP1,SCAP2,HEDI1,HEDI2,
1  I2,I3,IK,PORO,HCOS,AI,BI,CI,DI,EI,IAS)
      IF(ISX.EQ.1)GO TO 10
      XM(1,1)=(AL/12)*(3*(TETI1*SS(1K)/PORO(1K)+SCAP1)+(TETI2*SS(1K)
1  /PORO(1K)+SCAP2))
      XM(1,2)=(AL/12)*(TETI1*SS(1K)/PORO(1K)+SCAP1+TETI2*SS(1K)/
1  PORO(1K)+SCAP2)
      XM(2,1)=XM(1,2)
      XM(2,2)=(AL/12)*(3*(TETI2*SS(1K)/PORO(1K)+SCAP2)+(TETI1*SS(1K)
1  /PORO(1K)+SCAP1))
      GO TO 15
10  XM(1,1)=(AL/6)*(2*(TETI1*SS(1K)/PORO(1K)+SCAP1)+(TETI2*SS(1K)
1  /PORO(1K)+SCAP2))
      XM(1,2)=0
      XM(2,1)=0
      XM(2,2)=(AL/6)*(2*(TETI2*SS(1K)/PORO(1K)+SCAP2)+(TETI1*SS(1K)
1  /PORO(1K)+SCAP1))
15  XS(1,1)=(1/(2*AL))*(HCO1+HCO2)
      XS(1,2)=-XS(1,1)

```

```

XS(2,1)=XS(1,2)
XS(2,2)=XS(1,1)
XP(1)=0.5*(HCO1-HCO2)
XP(2)=XP(1)
IF(IAS.GT.1)GO TO 30
HC1=HCO1
* 30 DO 22 I=1,2
* DO 22 J=1,2
* 22 WRITE(6,112)XM(I,J),XS(I,J),XP(I)
*112 FORMAT(3X,3(E9.3,3X))
* WRITE(6,111)HC1
*111 FORMAT(/,3X,"HC1 =",F8.3)
30 IASL=NEWN(2)
IF(IASL.LT.NNODE)GO TO 40
AL1=AL
HCL=HCO2
40 RETURN
END
SUBROUTINE HCWC(HCO1,HCO2,TETI1,TETI2,SCAP1,SCAP2,HEDI1,
1 HEDI2,I2,I3,IK,PORO,HCOS,AI,BI,CI,DI,EI,IAS)
DIMENSION PORO(3),HCOS(3),AI(3),BI(3),CI(3),DI(3),EI(3)
* 1 TETIX(30)
* ----DETERMINE WHICH WATER CONTENT MODEL APPLIES----
* ----BROOKS AND COREY MODEL----
HEDI1=ABS(HEDI1)
HEDI2=ABS(HEDI2)
IF(I2.GT.1)GO TO 10
XP=CI(IK)
TETI1=AI(IK)+((PORO(IK)-AI(IK))*(BI(IK)/HEDI1)**XP)
TETI2=AI(IK)+((PORO(IK)-AI(IK))*(BI(IK)/HEDI2)**XP)
XPPP=1/XP
XPP=(XP+1)/XP
SCAP1=(XP/(BI(IK)*(PORO(IK)-AI(IK))**XPPP*(TETI1-AI(IK))**XPP))
SCAP2=(XP/(BI(IK)*(PORO(IK)-AI(IK))**XPPP*(TETI2-AI(IK))**XPP))
GO TO 50
* ----VAN GENUCHTEN MODEL----
10 IF(I2.GT.2)GO TO 20
XP=CI(IK)
XPP=1-1/XP
XP1=XP-1
XPP1=XPP+1
TETI1=(PORO(IK)-AI(IK))*((1/(1+(BI(IK)*HEDI1)**XP))**XPP)+AI(IK)
TETI2=(PORO(IK)-AI(IK))*((1/(1+(BI(IK)*HEDI2)**XP))**XPP)+AI(IK)
SCAP1=XPP*(PORO(IK)-AI(IK))*((1/(1+(BI(IK)*HEDI1)**XP))**XPP1)*
1 XP*(BI(IK)**XP)*(HEDI1**XP1)
SCAP2=XPP*(PORO(IK)-AI(IK))*((1/(1+(BI(IK)*HEDI2)**XP))**XPP1)*
1 XP*(BI(IK)**XP)*(HEDI2**XP1)
GO TO 50
* ----HAVERKAMP MODEL----
20 IF(I2.GT.3)GO TO 30
XP=CI(IK)
XPP=XP-1
TETI1=BI(IK)*(PORO(IK)-AI(IK))/(BI(IK)+HEDI1**XP)+AI(IK)
TETI2=BI(IK)*(PORO(IK)-AI(IK))/(BI(IK)+HEDI2**XP)+AI(IK)
SCAP1=BI(IK)*XP*(PORO(IK)-AI(IK))*(1/(BI(IK)+HEDI1**XP)**2)*
1 HEDI1**XPP
SCAP2=XP*BI(IK)*(PORO(IK)-AI(IK))*(1/(BI(IK)+HEDI2**XP)**2)*
1 HEDI2**XPP
----DETERMINE WHICH HYDRAULIC CONDUCTIVITY MODEL APPLIES----
----WARRICK MODEL----
30 IF(I2.GT.4)GO TO 50
XP=-29.484
XPP=-14.495

```

```

IF(HEDI1.GT.XP)GO TO 32
TETI1=.6829-.09524*LOG(HEDI1)
HCO1=1934000/(HEDI1)**3.4095
SCAP1=-.09524/HEDI1
GO TO 34
32 TETI1=.4531-.02732*LOG(HEDI1)
HCO1=516.8/(HEDI1)**0.97814
SCAP1=-.02732/HEDI1
34 IF(HEDI2.GT.XP)GO TO 36
TETI2=.6829-.09524*LOG(HEDI2)
HCO2=1934000/(HEDI2)**3.4095
SCAP2=-.09524/HEDI2
GO TO 100
36 TETI2=.4531-.02732*LOG(HEDI2)
HCO2=516.8/(HEDI2)**.97814
SCAP2=-.02732/HEDI2
GO TO 100
* ----BROOKS AND COREY MODEL----
50 IF(I3.GT.1)GO TO 60
XP=(2+3*CI(IK))/CI(IK)
HCO1=HCOS(IK)*((TETI1-AI(IK))/(PORO(IK)-AI(IK)))**XP
HCO2=HCOS(IK)*((TETI2-AI(IK))/(PORO(IK)-AI(IK)))**XP
GO TO 100
* ----VAN GENUCHTEN MODEL----
60 IF(I3.GT.2)GO TO 70
XP=1-1/CI(IK)
XPP=1/XP
HCO1=HCOS(IK)*((TETI1-AI(IK))/(PORO(IK)-AI(IK)))**0.5*(1-(1-((
1 TETI1-AI(IK))/(PORO(IK)-AI(IK)))**XPP)**XP)**2
HCO2=HCOS(IK)*((TETI2-AI(IK))/(PORO(IK)-AI(IK)))**0.5*(1-(1-((
1 TETI2-AI(IK))/(PORO(IK)-AI(IK)))**XPP)**XP)**2
GO TO 100
* ----HAVERKAMP MODEL----
70 IF(I3.GT.3)GO TO 100
XP=EI(IK)
HCO1=HCOS(IK)*(DI(IK)/(DI(IK)+HEDI1**XP))
HCO2=HCOS(IK)*(DI(IK)/(DI(IK)+HEDI2**XP))
100 IF(HEDI1.LE.0)GO TO 150
TETI1=PORO(IK)
SCAP1=0
HCO1=HCOS(IK)
150 IF(HEDI2.LE.0)GO TO 200
TETI2=PORO(IK)
SCAP2=0
HCO2=HCOS(IK)
* 200 TETIX(IAS)=TETI1
* IF(IAS.LT.25)GO TO 205
* IAS=IAS+1
* TETIX(IAS)=TETI2
* 205 WRITE(6,101)TETI1,TETI2,HCO1,HCO2,SCAP1,SCAP2
*101 FORMAT(3X,6(E9.3,2X))
200 RETURN
END
SUBROUTINE ASSEM(NEWN,XM,XMG,XS,XSG,XR,XPG)
DIMENSION NEWN(2),XM(2,2),XMG(30,3),XS(2,2),XSG(30,3),
XR(2),XPG(30)
NROW=2
DO 11 I=1,2
DO 10 J=1,2
11 NEWN(I)
10 NEWN(J)
RETURN
END

```

```

      XMG(II, KK)=XMG(II, KK)+XM(I, J)
10     XSG(II, KK)=XSG(II, KK)+XS(I, J)
11     XPG(II)=XPG(II)+XP(I)
* 10   WRITE(6, 15) (XMG(II, KK), XSG(II, KK), XPG(II), I=1, NNODE)
* 15   FORMAT(3X, 3(E8.3, 3X))
      RETURN
      END
SUBROUTINE CALC1(TIVAL, HEDIS, XMG, XSG, XPG, NNODE, W, KB1, KB2, KB3,
1     KB4, KB5, Q0, QL, HQ, HL, TIMEX, TI, HCL, HCL, AL1, IKK, TMG)
1     DIMENSION HEDIS(30), XMG(30, 3), XSG(30, 3), XPG(30), TMG(30, 3),
1     FPG(30, 3), TIMEX(20), Q0(20)
      DO 1 I=1, NNODE
      DO 1 J=1, 3
      TMG(I, J)=0
1     FPG(I, J)=0
*     ----DETERMINE IF NEUMANN VARIABLE FLUX APPLIES----
      IF(KB5.LT.1)GO TO 5
      AAL=HCL/AL1
      GO TO 7
5     AAL=0
7     DO 10 I=1, NNODE
      DO 10 J=1, 3
      TMG(I, J)=XMG(I, J)/TIVAL+W*XSG(I, J)
10     FPG(I, J)=XMG(I, J)/TIVAL+(W-1)*XSG(I, J)
      TMG(NNODE, 1)=TMG(NNODE, 1)-W*AAL
      TMG(NNODE, 2)=TMG(NNODE, 2)+W*AAL
      FPG(NNODE, 1)=FPG(NNODE, 1)-(W-1)*AAL
      FPG(NNODE, 2)=FPG(NNODE, 2)+(W-1)*AAL
      DO 15 I=1, NNODE
      DO 15 J=1, 3
15     XMG(I, J)=0
      DO 20 J=2, 3
      L=J-1
20     XMG(I, 1)=XMG(I, 1)+FPG(I, J)*HEDIS(L)
      TI=NNODE-1
      DO 25 I=2, TI
      DO 25 J=1, 3
      K=I+J-2
25     XMG(I, 1)=XMG(I, 1)+FPG(I, J)*HEDIS(K)
      DO 30 J=1, 2
      L=NNODE-2+J
30     XMG(NNODE, 1)=XMG(NNODE, 1)+FPG(NNODE, J)*HEDIS(L)
*     ----DETERMINE IF CONSTANT FLUX APPLIES----
      TTT=TIMEX(IKK)
      IF(TI.LT.TTT)GO TO 35
      IKK=IKK+1
35     Q01=Q0(IKK)-HCL
      Q02=HCL-QL
      IF(KB1.EQ.1)GO TO 40
      Q0(IKK)=0
40     IF(KB2.EQ.1)GO TO 45
      QL=Q0
45     XPG(1)=XPG(1)+XMG(1, 1)+Q01
      L=NNODE-1
      DO 50 I=2, L
      XPG(I)=XPG(I)+XMG(I, 1)
      XPG(NNODE)=XPG(NNODE)+XMG(NNODE, 1)+Q02
*     ----DETERMINE IF CONSTANT HYDRAULIC HEAD APPLIES----
      IF(KB3.LT.1)GO TO 60
      TMG(1, 2)=1
      TMG(1, 3)=0
      XPG(2)=XPG(2)-HQ+TMG(2, 1)
      Q0(1)=HQ

```

```

60      TMG(2,1)=0
      IF(KB4.LT.1)GO TO 70
      NN=NNODE-1
      XPG(NNODE)=HL
      XPG(NN)=XPG(NN)-HL*TMG(NN,3)
      TMG(NNODE,1)=0
      TMG(NNODE,2)=1
      TMG(NN,3)=0
70      CONTINUE
      DO 100 I=1,NNODE
      DO 100 J=1,3
      * 100      WRITE(6,110)FPG(I,J),TMG(I,J),XPG(I)
      * 110      FORMAT(3X,3(E9.3,3X))
      RETURN
      END
      SUBROUTINE SOLVE(TM, XPG, HEDIX, FPG, NNODE)
      DIMENSION TM(30,3), XPG(30), HEDIX(30), FPG(30,3)
      DO 5 I=1,NNODE
      DO 5 J=1,3
      FPG(I,J)=0
      FPG(I,1)=TM(1,2)
      FPG(I,2)=TM(1,3)/FPG(I,1)
      FPG(I,3)=XPG(I)/FPG(I,1)
      DO 10 I=2,NNODE
      II=I-1
      FPG(I,1)=TM(I,2)-TM(I,1)*FPG(II,2)
      FPG(I,2)=TM(I,3)/FPG(I,1)
      FPG(I,3)=(XPG(I)-TM(I,1)*FPG(II,3))/FPG(I,1)
10      HEDIX(NNODE)=FPG(NNODE,3)
      NI=NNODE-1
      DO 20 I=1,NI
      II=NNODE-I
      III=II+1
      HEDIX(II)=FPG(II,3)-FPG(II,2)*HEDIX(III)
20      DO 50 I=1,NNODE
      DO 50 J=1,3
      * 50      WRITE(6,110)FPG(I,J),HEDIX(I)
      * 110      FORMAT(3X,2(E9.3,3X))
      RETURN
      END
      SUBROUTINE ERROR(HEDIX, HEDIL, IE, ERR1, ERR2, NNODE)
      DIMENSION HEDIX(30), HEDIL(30)
      DO 5 I=1,NNODE
      TTT=ABS(HEDIX(I)-HEDIL(I))
      TTTT=ERR2*HEDIX(I)
      TT=ERR1+ABS(TTTT)
      IF(TTT.GT.TT)GO TO 10
      CONTINUE
      IE=0
      GO TO 15
      IE=1
10      RETURN
15      END
      SUBROUTINE OUT(TI-Z, HEDIX, NY, NL, NNODE, TETIX)
      DIMENSION Z(30), HEDIX(30), TETIX(30)
      DO 11 I=1,NNODE
      H=-HEDIX(I)
      HH=29.484
      WRITE(6,111)
      FORMAT("00")
      IF(H.GT.HH)GO TO 1
      TETIX(I)=.4531-.02732*LN(H)
      GO TO 11

```

* 6 TETIX(I)=.6829-.09524*LOG(H)
 * 11 CONTINUE

WRITE(6,20)TI,NL,NT

WRITE(6,150)

WRITE(6,200)(I,Z(I),HEDIX(I),TETIX(I),I=1,NNODE)

FORMAT(/,10X,"TIME= ",1X,F8.5,4X,"NL= ",15,4X,"NT= ",15)

FORMAT(/,4X,"NNODE",8X,"COORDINATE",7X,"PRESSURE HEAD",

7X,"WATER CONTENT")

FORMAT(4X,14,9X,F8.3,10X,F8.3,10X,F8.3)

RETURN

END

```

OR--
125.      .40      .0100      .1      .00001      1.0      25      015      10
1
1
-159.19
1.
.0      .00.      0.      0.      0.      00.      .4
0      .50      .001      0      4      1      0      00.
0      0      0.      1      1      -14.495      -159.19      0
0.00
00
  
```

UNSATURATED FLOW AND TRANSPORT

XL= 125.000 TIME= .400 TIVAL=.100E-01 TIMAX= .100
 TIMIN=.100E-04 W= 1.000 NELEM= 25 NTM= 15 NST= 10

- 1 .000
- 2 5.000
- 3 10.000
- 4 15.000
- 5 20.000
- 6 25.000
- 7 30.000
- 8 35.000
- 9 40.000
- 10 45.000
- 11 50.000
- 12 55.000
- 13 60.000
- 14 65.000
- 15 70.000
- 16 75.000
- 17 80.000
- 18 85.000
- 19 90.000
- 20 95.000
- 21 100.000
- 22 105.000
- 23 110.000
- 24 115.000
- 25 120.000
- 26 125.000

```

-159.190
1 -269.169
2 -257.671
3 -244.426
4 -236.074
5 -225.972
6 -216.303
  
```

EVALUATION AND DESIGN OF DRAINED LOW-LEVEL
RADIOACTIVE DISPOSAL SITES

FINAL REPORT

PROJECT E25-645, CONTRACT NO. DE-AS07-83ID12449

edited by

Geoffrey G. Eichholz
Project Director

submitted to

U.S. DEPARTMENT OF ENERGY
Idaho Operations Office
Idaho Falls, ID 83401

Program in Nuclear Engineering & Health Physics
Georgia Institute of Technology
Atlanta, GA 30332

December, 1984

Revised April, 1985

CONTENTS

List of Figures	ii
Summary	iv
Project Personnel	vi
Introduction	1
Trench Hydrology	13
Test Bed Construction	21
Materials	26
Laboratory Tests	29
Test Bed Experiments	36
Waste Leaching Under Unsaturated Conditions	50
Computer Simulation	51
Flow Model	55
Initial Condition	57
Boundary Conditions	57
Trench Facility Design	59
Calculation of Gravel Reservoir Requirements	59
Conclusions	67
Acknowledgments	70
Bibliography	71
Appendix A	74
1 - Water Characteristics and Hydraulic Conductivity Models	
a - Brooks and Corey	74
b - Haverkamp	76
c - Van Genuchten	77
2 - Equilibrium Sorption Isotherms	
a - Linear Adsorption	79
b - Freundlich Isotherm	80
c - Langmuir Isotherm	81
Appendix B - Model Implementation	82
Table B.1 - Program Variables	85
Table B.2 - Input Data For Flow Equation	89
Table B.3 - Program Listing	90

LIST OF FIGURES

Figure 1	Trench configurations	3
Figure 2	Trench designs for shallow aquifer and arid site (Ref. 2)	4
Figure 3	Section along track of migrating radionuclides (Ref. 3)	6
Figure 4	Views of two burial sites (from Ref. 3)	7
Figure 5	Cross section through concrete vault facility (Ref. 3)	8
Figure 6	Profile of encapsulation and cover - Canonsburg site (Ref.4)	9
Figure 7	Sections of typical drained trench (Ref. 2)	11
Figure 8	Water budget for cover system - Canonsburg site (Ref. 4)	12
Figure 9	Hydrology of shallow land burial trench (from Ref. 7)	14
Figure 10	Soil moisture plots at Maxey Flats at two depths (Ref. 8)	16
Figure 11	Soil moisture plots at two depths in a trench cap at Maxey Flats (Ref. 8)	17
Figure 12	Groundwater response to rainfall for one week in February 1983 (Ref. 6)	18
Figure 13	Cross section of test bed trench	22
Figure 14	Sketch of test bed elevation	23
Figure 15	Views of test bed during construction	24
Figure 16	Views of instrumentation on test bed	25
Figure 17	Particle size distributions	28
Figure 18	Views of laboratory test columns	30

Figure 19	Electrode calibration - GT Sand	31
Figure 20	Electrode calibration - SRP #1 soil	32
Figure 21	Electrode calibration - SRP #2 soil	33
Figure 22	Drainage curves - Rollo Sand	37
Figure 23	Resolved drainage curve - Rollo Sand	38
Figure 24	Moisture Profiles - Rollo Sand	39
Figure 25	Moisture Profiles for GT Sand at different times	41
Figure 26	Moisture Profiles for FP Soil at different times	42
Figure 27	Drainage Curves for GT Sand at different heights	43
Figure 28	Drainage curves for FP Soil at different heights	45
Figure 29	Drainage Curves for three soil types	46
Figure 30	Resolved Drainage Curves for two sands	47
Figure 31	Calculated Moisture Profiles - Comparable forces	52
Figure 32	Calculated Moisture Profiles - Suction dominant	53
Figure 33	Diagram of Migration Model	54
Figure 34	Verification of Flow Model	58
Figure 35	Repository Concept	60
Figure 36	Comparative infiltration rates during initial and wet runs (after Ref. 25)	63
Figure 37	Model Flow Diagram	83

SUMMARY

Low-level waste disposal in shallow trenches has been the subject of much critical assessment in recent years. Historically most trenches have been located in fairly permeable settings and any liquid waste stored has migrated at rates limited mainly by hydraulic effects and the ion exchange capacity of underlying soil minerals. Attempts to minimize such seepage by choosing sites in very impermeable settings lead to overflow and surface runoff, whenever the trench cap is breached by subsidence or erosion.

The work undertaken in the project described in this report was directed to an optimum compromise situation where less reliance is placed on cap permanence, any ground seepage is directed and controlled, and the amount of waste leaching that would occur is minimized by keeping the soil surrounding the waste at only residual moisture levels at all times .

Measurements have been conducted to determine these residual levels for some representative soils, to estimate the impact on waste migration of mainly unsaturated flow conditions, and to generate a conceptual design of a disposal facility which would provide adequate drainage to keep the waste from being exposed to continuous leaching by standing water. An attempt has also been made to quantify the reduced source terms under such periodic, unsaturated flow conditions, but those tests have not been conclusive to date.

It was found that with adequate drainage, in most locations, moisture concentrations around the waste material will rarely rise appreciably above the residual level, thus reducing the waste leach rate substantially, compared with that calculated for saturated conditions.

It is evident that for relatively permeable or loosely-packed backfill the installation of a drainage layer may substantially reduce the environmental impact from dissolved waste materials. For low-permeability, clay-rich soils in tight compression, the reduction in ambient moisture levels around the waste may not be sufficient to justify the added cost and complexity of installing the drainage system. However, for most other situations, the resultant minimization of the source term may result in substantial projected dose reductions. None of the technology involved is novel as such nor does it call for unusual skills.

For low-permeability soils the waste should be placed about 30 cm (1 ft.) above the saturated layer formed by suction forces immediately above the gravel layer.

Since most disposal sites, even in humid regions of the United States, are exposed only to intermittent rainfall and as most trench designs incorporate some gravel base for drainage, the results of this project have broader applications in assessing actual migration conditions in shallow trench disposal sites. Similar considerations may also apply to disposal of hazardous wastes.

PROJECT PERSONNEL
(all part time)

Geoffrey G. Eichholz, Ph.D.	Project Director
T. Fisher Craft, Ph.D.	Senior Research Scientist
M. Frank Petelka, M.S.H.P.	Graduate Research Assistant
Joocho Whang, M.S.H.P.	Graduate Research Assistant
Fernando N. deSousa, M.S.H.P.	Graduate Research Assistant
Marino C. Kaminski, B.S.	Graduate Research Assistant
Bonny A. Wright, B.S.H.P.	Graduate Research Assistant
Denise D. Hardy, B.S.	Graduate Research Assistant
Martha R. Poston, B.S.H.P.	Graduate Research Assistant
Hobert W. Jones, B.S.	Graduate Research Assistant
Bruce W. Patton, B.S.	Graduate Research Assistant

Some of the work was shared with a parallel project conducted for the Savannah River Laboratory.

INTRODUCTION

Shallow land burial of low-level radioactive wastes has been practiced since the early days of the U.S. Atomic energy program. Unfortunately, early disposal sites were only required to meet "maximum permissible concentration" standards for any nuclear facility effluents and very little control was exerted on site inventory and waste form. As a consequence, many of those sites contained liquid wastes which seeped into the ground, where they were retained primarily by ion exchange and adsorption processes on mineral surfaces to the extent possible. The appearance of low levels of radioactive materials, especially tritium, in groundwaters offsite drew public attention to disposal conditions that were insufficiently controlled by more recent standards and as a consequence waste disposal of low-level waste was looked on by the public with some disfavor as a potential source of contamination of groundwater. To meet these objections the U.S. Nuclear Regulatory Commission has issued guidelines, under Title 10 Code of Federal Regulations Part 61, that prescribe waste form characteristics and site suitability criteria. Performance objectives are stated in terms of annual dose limits to the general public via all environmental pathways. The U.S. Environmental Protection Agency, also, is in the process of specifying effluent concentration levels, under Hazardous Waste Regulations (40CFR 122,265) or the Resource Conservation and Recovery Act (RCRA), that again must meet specific calculated population dose values. Both types of objectives must be met by selection of appropriate waste forms, source term control by reducing water flow, and control of effluent movement by appropriate site geology.

In either case, performance assessment depends on a good understanding of the mechanisms that govern mobilization and migration of the waste materials through soil or fractured rock into any significant aquifer, since groundwater transport is the only feasible pathway, other than deliberate or accidental intrusion, by which the waste materials can return to the accessible environment. Most of the calculational models described in the literature assume that sooner or later water infiltrates the burial trench, saturates the soil, leaches some of the waste at a rate controlled mainly by solubility considerations, and that the dissolved waste travels with the water, subject to retardation by surface adsorption on surrounding minerals, until an aquifer is reached, through which in due course it may reach the surface, in springs or wells, to enter the food chain.

Control of this process, in 10CFR61 and related documents, is envisaged primarily by four precautions: 1. use of a solid waste form, that, hopefully, is not excessively subject to dissolution; 2. waste emplacement preferably well above the water table; 3. use of an impermeable soil formation to minimize water flow towards the aquifer; and 4. installation of a stable impermeable trench cap to inhibit or retard water infiltration into the trench.

These approaches are illustrated in Figures 1 and 2 (Refs. 1 & 2) which illustrate diagrammatically the main elements of such a trench. In Figure 1 additional lining is introduced to contain water in the trench.

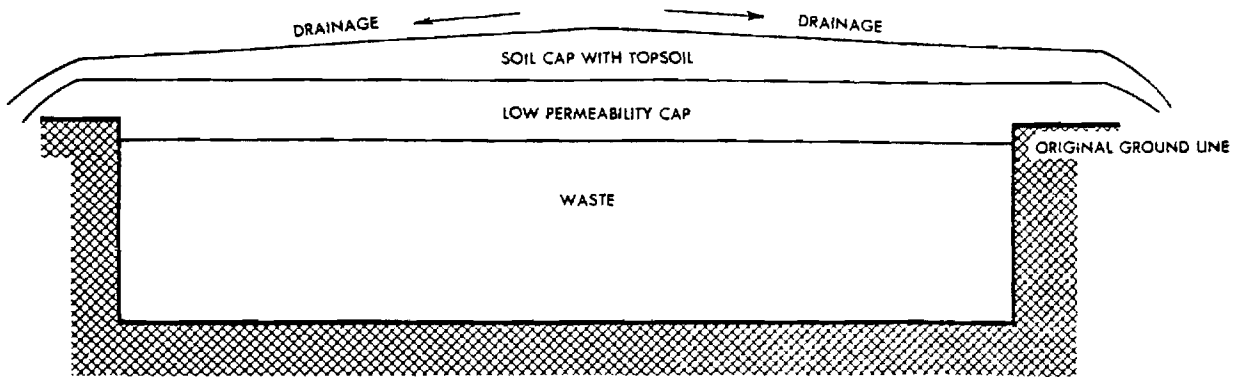
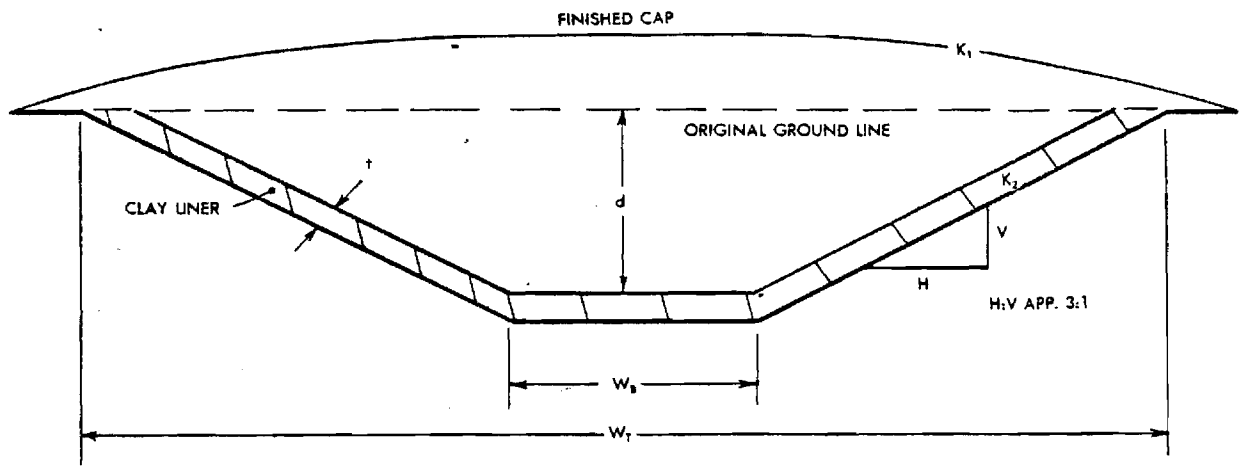


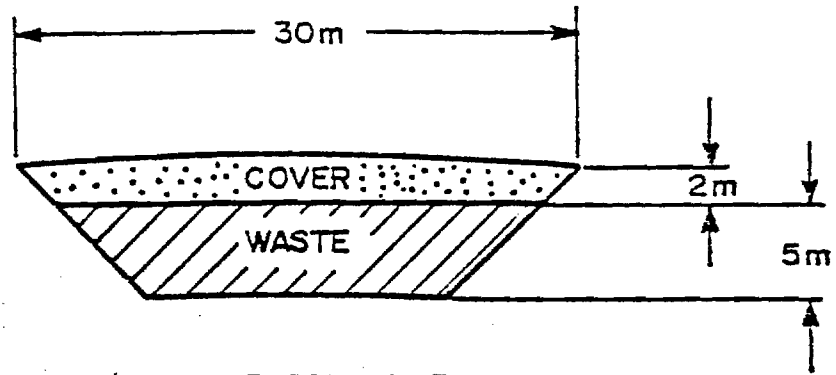
Figure 1a Closed trench with soil cap, showing cap drainage



H:V APPROXIMATELY 3:1
 W_T = TOTAL WIDTH
 W_B = BOTTOM WIDTH
 K_1 = COEFFICIENT OF PERMEABILITY FOR FINISHED CAP
 K_2 = COEFFICIENT OF PERMEABILITY FOR LINER
 d = DEPTH
 t = THICKNESS
 V = VERTICAL
 H = HORIZONTAL

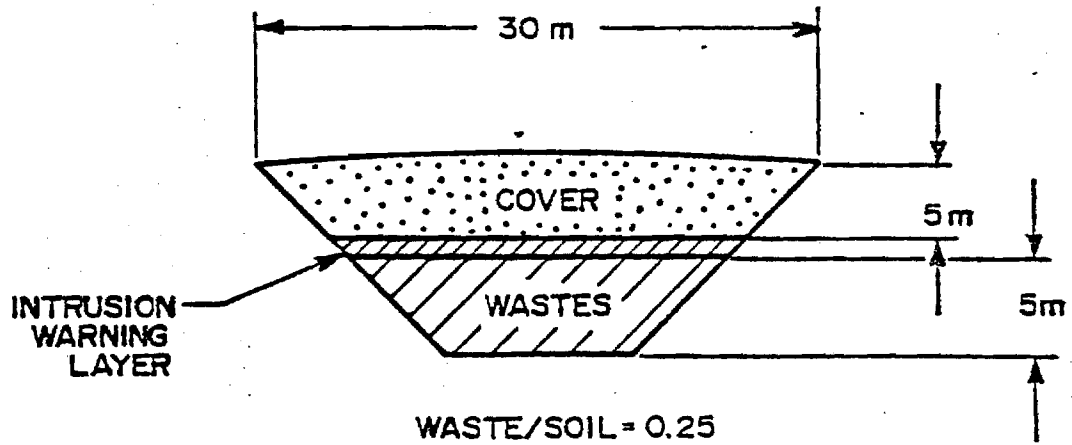
Figure 1b Clay bottom liner (Ref. 1)

Fig. 1 Trench Configurations



WASTE/SOIL = 0.43

CLASS A WASTES ONLY



WASTE/SOIL = 0.25

CLASS B, C AND X WASTES

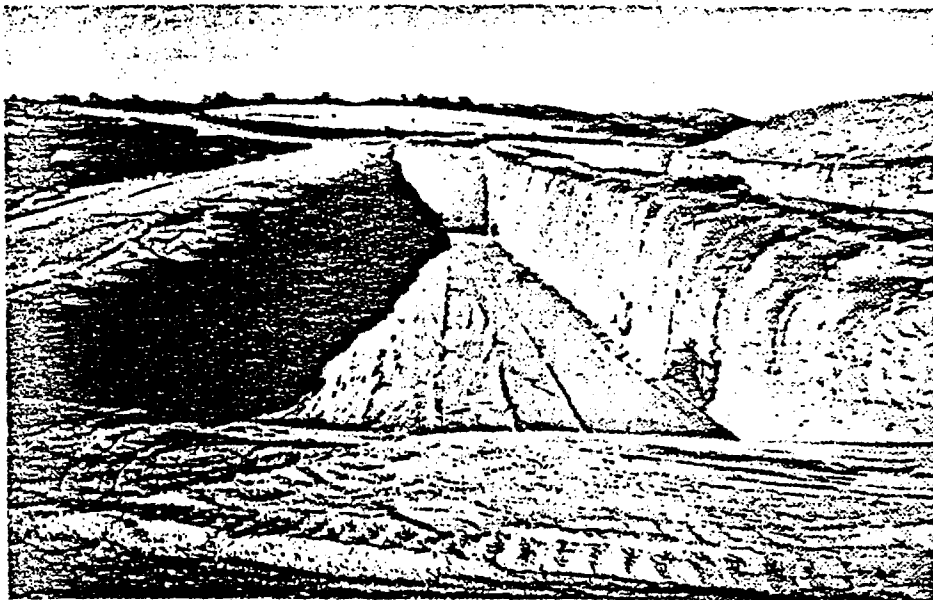
RAE-100210

Figure 2 Trench designs for shallow aquifer and arid site (Ref. 2)

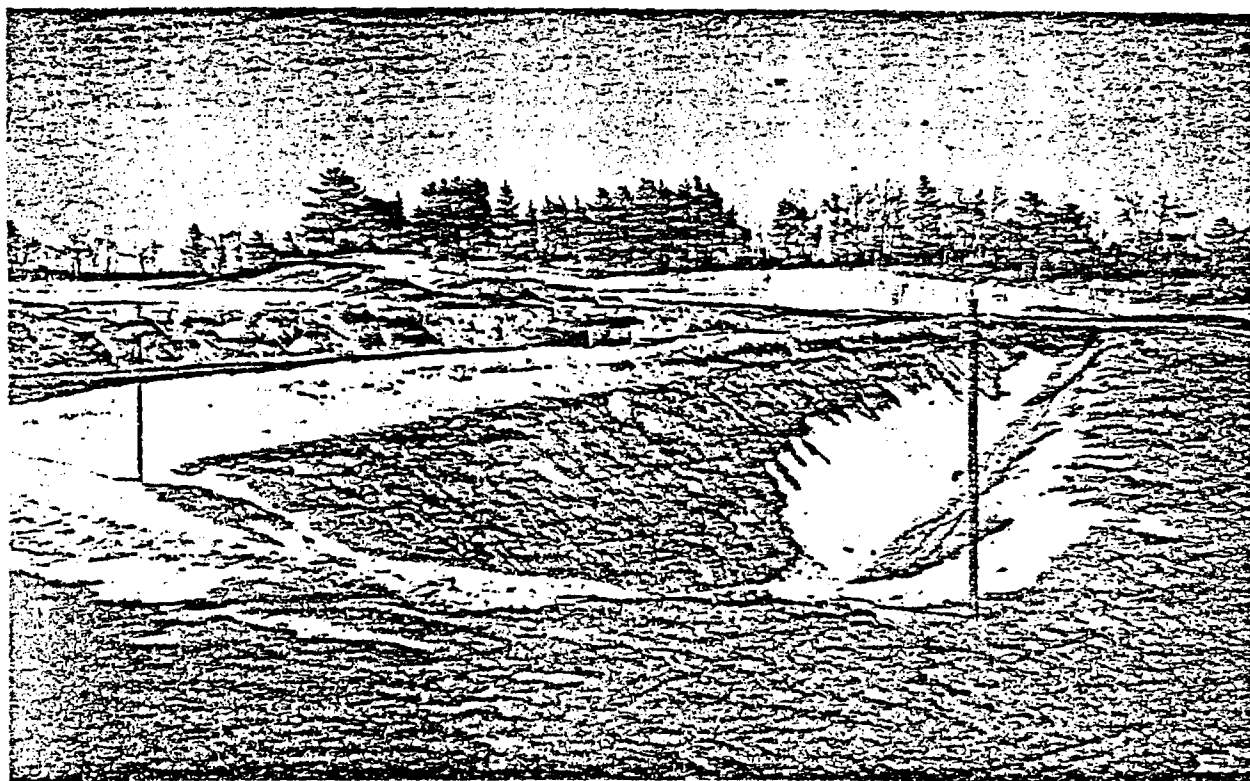
Figure 2 also shows a possible warning layer "to deter intruders". Short of actually concreting the walls or the trench bottom, some seepage ultimately will occur with a plume following the hydraulic gradient in the water table (Fig 3, from Ref.3). Figure 4 (Ref.3) illustrates the actual construction of some shallow trenches.

Several problems can arise in this approach. First of all, the trench cap will tend to collapse or erode in time, due to consolidation or compaction of the waste materials and the interstices between them, settling of backfill soil, and the effect of surface water. This means that sooner or later water will enter the trench unless very elaborate cap structures are devised. Figures 5 and 6 give examples of such cap designs, which add enormously to the cost of disposal and are almost equivalent to the surface-bunker retrievable-storage concept.

The second problem arises from the fact, that with a highly impermeable base formation any infiltrated water in the trench has nowhere to go and sooner or later will fill the trench and overflow. This "bath tub effect" has been observed at some sites and results in surface flow of trench water, instead of downward seepage towards the water table, and an early return to the accessible environment of potentially contaminated water. In addition, the waste would find itself engulfed by standing water so that any leaching effects would be greatly increased. Abatement of the bath tub effect by reliance on even more elaborate cap structures is questionable and expensive, particularly since there is no guarantee that lateral inflow into the trench would not occur. McCray et al. (Ref.5) have reported observations on such interflow.



Waste Burial Pit at the Los Alamos Scientific Laboratory (New Mexico, USA) Dug into Tuff (180' x 15 x 8 m Deep). Note Steep Slope and Relatively Clean Cut Walls [11]



A Trench Dug into Sand in Area "C" at CRNL Showing Shallow Sloped Walls

Figure 4 Views of two burial sites (from Ref. 3)

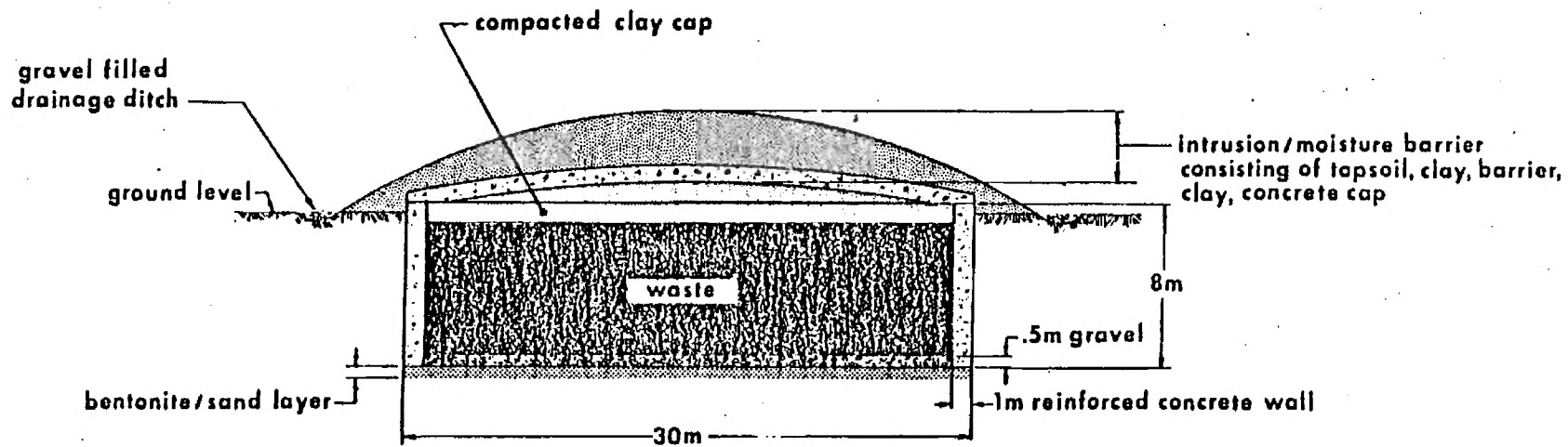


Figure 5 Cross section through concrete vault facility (Ref. 3)

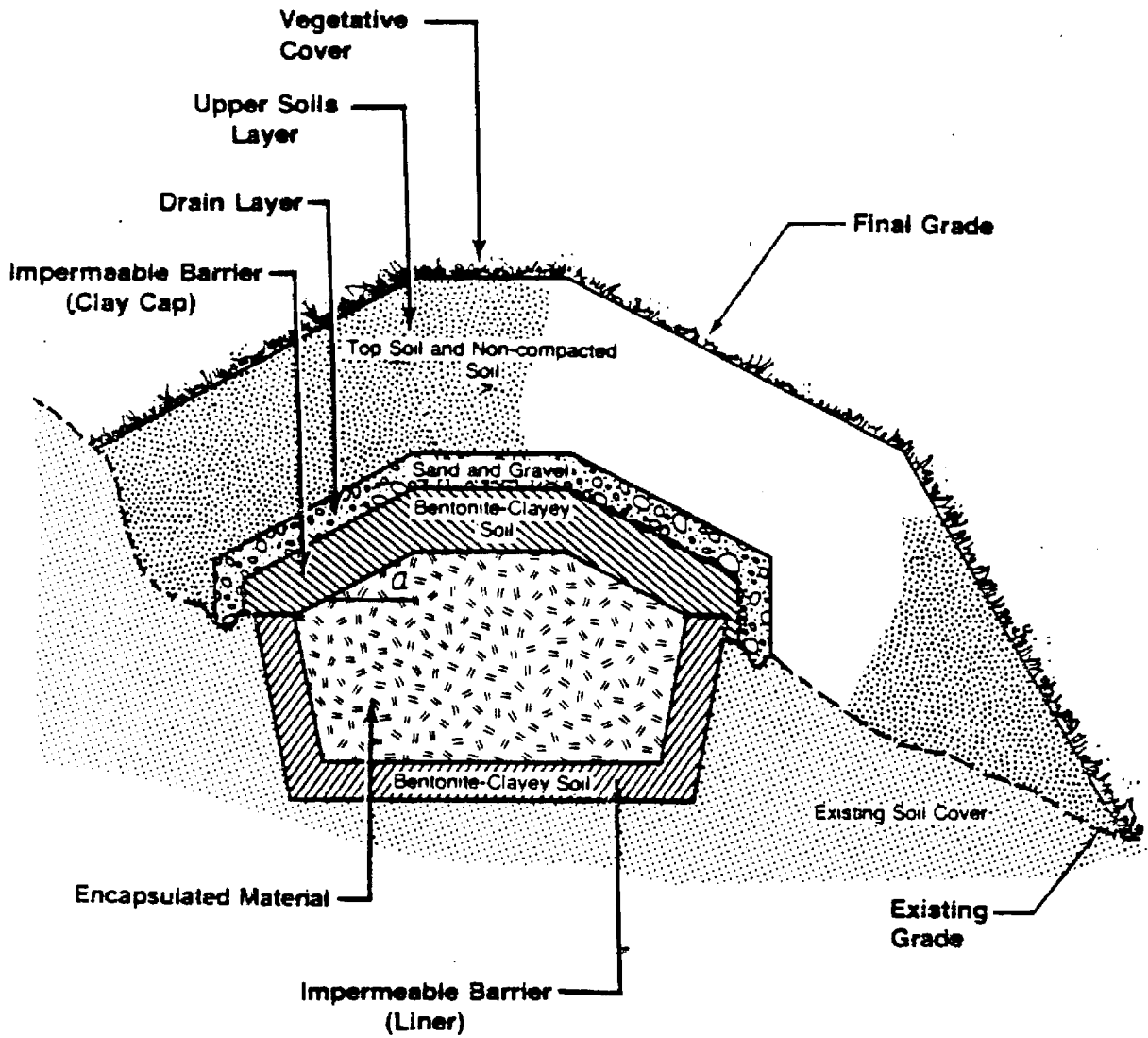


Figure 6 Profile of encapsulation and cover - Canonsburg site (Ref. 4)

α - Slope Angle

An alternative way of dealing with the threat of a bath tub effect is by the installation of drains, combined in some cases by deliberate pumping from the trenches. This approach is illustrated in Figure 7 (Ref. 2), where the pump well is also used for monitoring purposes, and has been proposed for the Central Disposal Facility at Oak Ridge for hazardous wastes (Ref. 6). For the Canonsburg site, Metry et al. (Ref. 4) also propose a near-surface drain to minimize infiltration, see Figure 8.

In the work described in this report this approach has been taken a stage further by allowing the drained-off water to seep into the ground along a predetermined seepage path. This eliminates the need for active pumping which would normally be impractical after closure of the site. By also selecting conditions promoting easy drainage, one also minimizes the amount of moisture in contact with the waste, so that leaching effects may be greatly reduced, resulting in a much smaller source term for any hazard prediction. This project has been concerned with studying the effects of avoiding high water content in the waste area on leach effects and model calculations and with a consideration of conceptual designs for this approach.

A preliminary account of this work was presented at the DOE Participants Meeting in Denver in September, 1984 (Ref. 7).

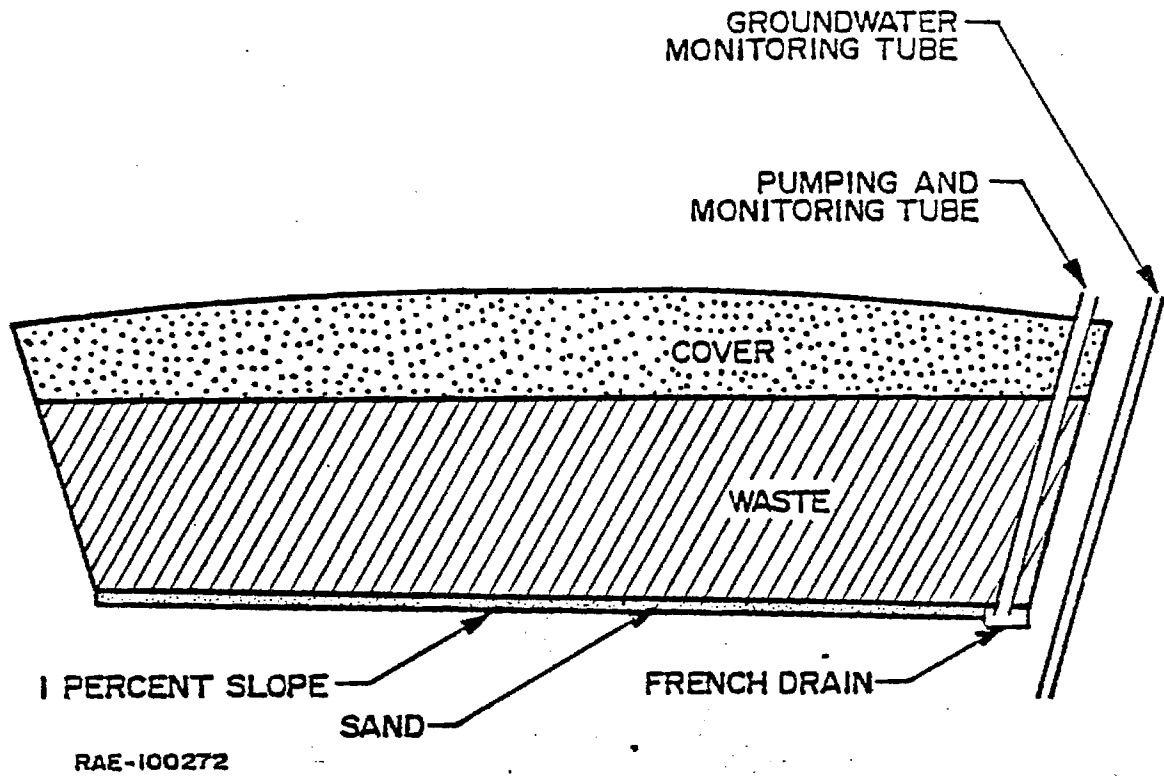


FIGURE 7-a. CROSS SECTION OF TYPICAL TRENCH

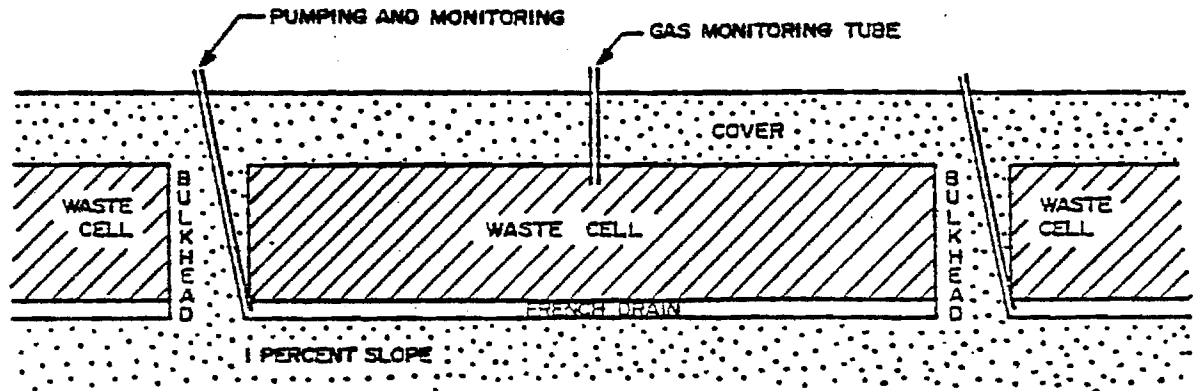


FIGURE 7-b. SECTION OF TYPICAL TRENCH ALONG ITS LONG AXIS

Figure 7 Sections of typical drained trench (Ref. 2)

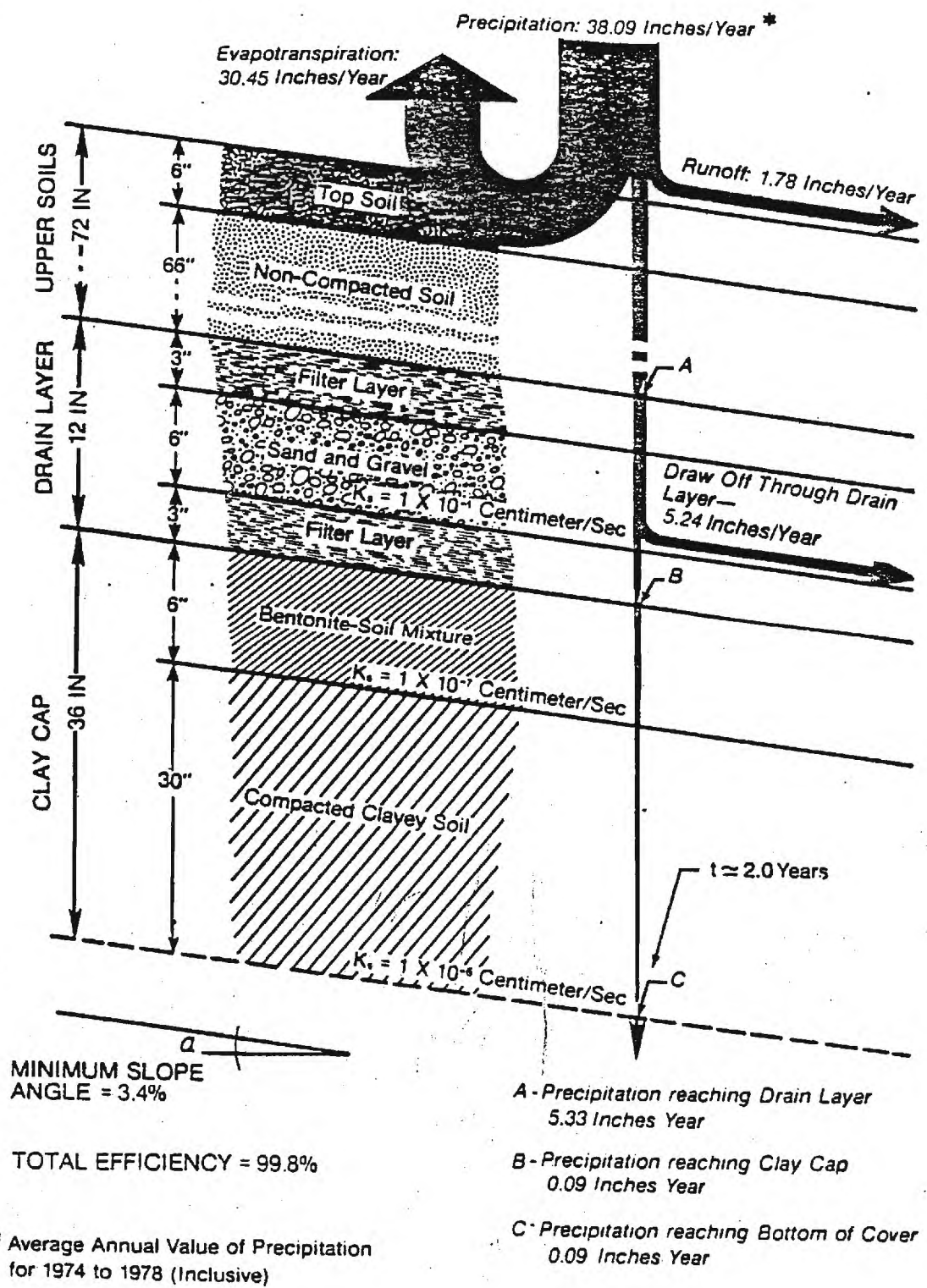


Figure 8 Water budget for cover system - Canonsburg site (Ref. 4)

TRENCH HYDROLOGY

The hydrology of a burial trench is shown diagrammatically in Figure 9. A very high proportion of precipitated water is returned to the atmosphere by evaporation and evapotranspiration and typically only 20-25% or less will actually infiltrate the trench itself. Once there, water movement is subject to a balance of gravitational and capillary forces, though for fairly permeable backfill surrounding waste packages it is reasonable to assume a slow, but steady net downward flow. As this flow passes the buried wastes it is usually assumed that some leaching i.e. decontamination of buried waste material by the passing flow of water, will occur and dissolution of some radioactive materials, that may then remain in solution or adsorb on any fine suspended particulates that may be present. Self-retention within the backfill soil presumably occurs, but is rarely included in any assessment model.

Although 10CFR61 assumes location of the trench in an impermeable medium, any impact assessment ordinarily takes the finite permeability of the surrounding soil for granted and accepts it as the normal pathway for the dissolved waste ions or complexes (9,10). Innumerable measurements have been reported on the resultant flow through such soil and on retardation effects on the migration of any dissolved ions due to sorption-desorption effects on any mineral surfaces in contact with the water flow (11-15). These processes are generally considered part of the engineered barriers of the system, but invariably are assumed to be subject to saturated flow.

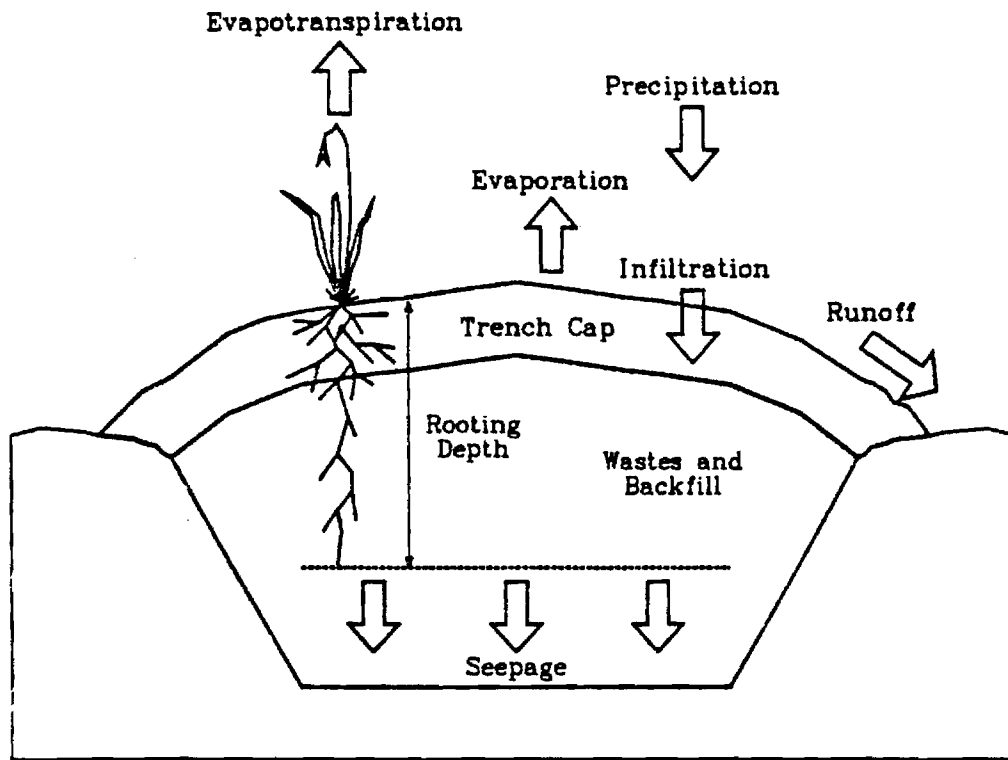


Figure 9 Hydrology of shallow land burial trench(from Ref. 7)

Actually, most soil systems will not be saturated unless the soil is unusually retentive or the water is allowed to back up, as in the bathtub situation (16). For arid sites in the Western U.S., soil saturation would be rare; this has been studied by the Los Alamos group (17-19). Figures 10 and 11 show variations in moisture profiles at Maxey Flats observed near the surface (0.9m) and at depth (2.4m). Strong seasonal variations are evident near the surface; a smooth curve exists at depth. In both cases moisture levels were well below saturation most of the time, though in the trench cap significant water retention occurred because of suction effects from its lower surface. Observations by Davis et al. (Fig. 12) also show that variations in the level of the water table following rainfall depend on rapid infiltration flow and only slow drainage rates (21). Thus, even in the "humid zone" of the Eastern United States unsaturated moisture conditions may prevail for much of the time, between heavy showers, as occur in the South, or during periods when the surface is frozen or snow-covered in the North. If the backfill and surrounding soils are fairly permeable, this implies that the waste may find itself in moderately dry surroundings much of the time and the time-averaged leach rate may be substantially different from that assumed for "conservative", saturated conditions. Some infiltrated water may perch on top of drums and packages or form puddles on plastic wrappings, but the volume available for such water is limited and often such water may be subject to syphon action through surrounding soil. In any case, any subsequent water flow will necessarily by-pass such occupied spaces. The present study was directed to investigate the benefits of reducing the ambient moisture levels around the waste as much as possible by accepting a periodic mode of infiltration and removing the major cause of water back-up.

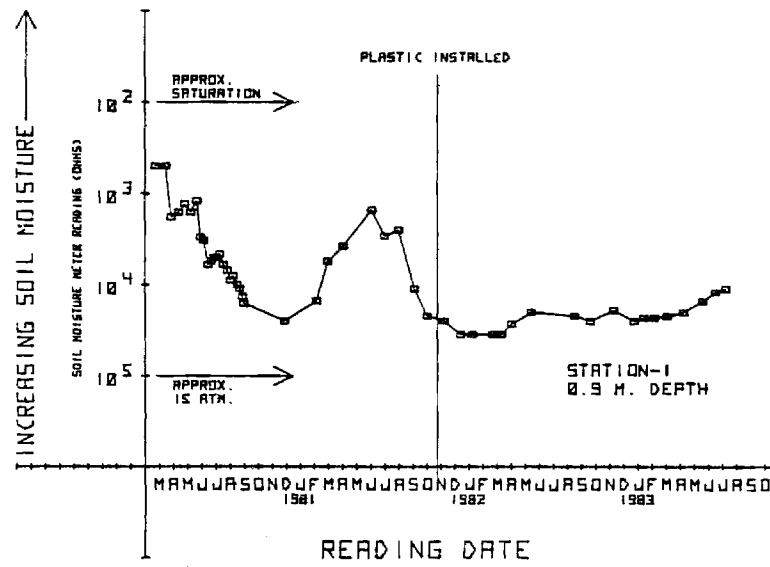
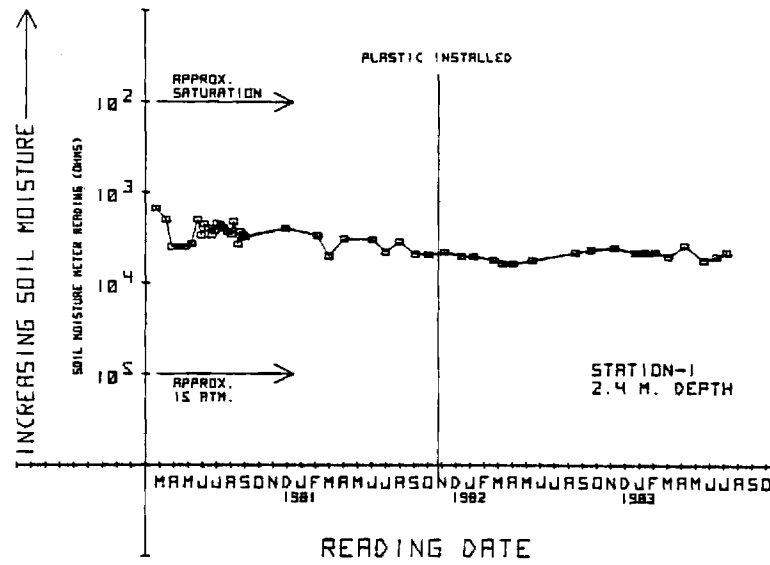


Figure 10 Soil moisture plots at Maxey Flats at two depths (Ref. 8)

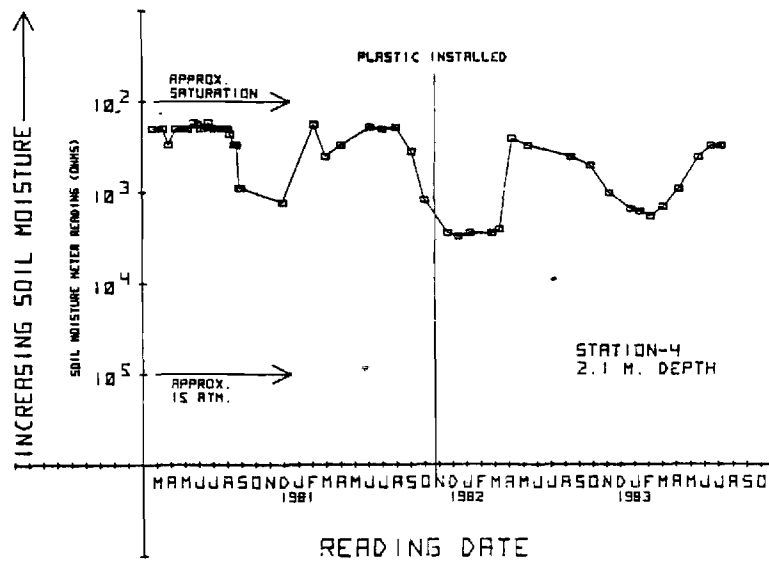
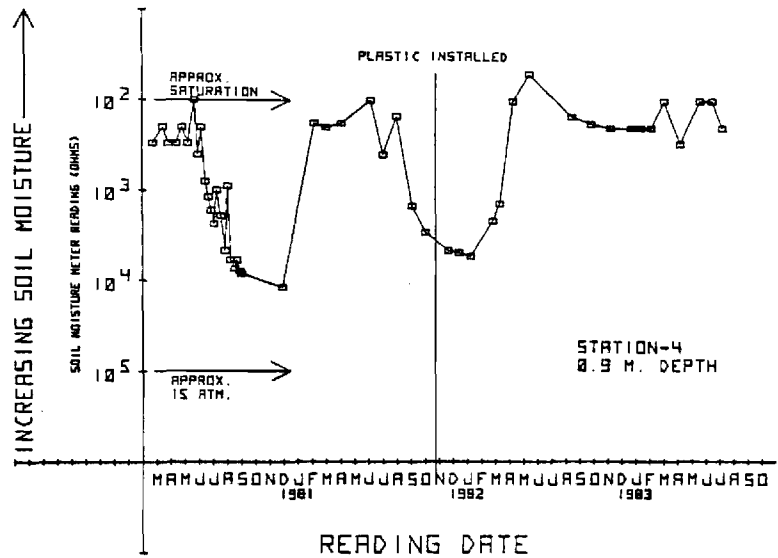


Figure 11 Soil moisture plots at two depths in a trench cap at Maxey Flats (Ref. 8)

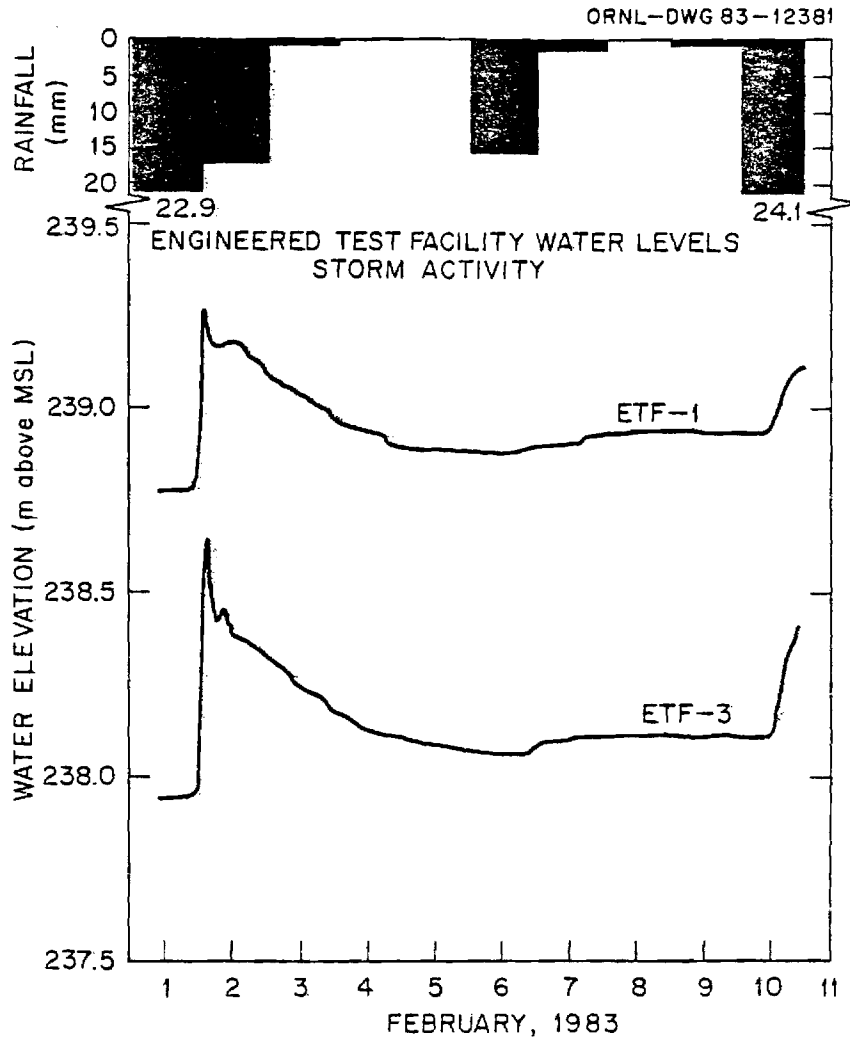


Figure 12 Groundwater response to rainfall for one week in February 1983

(Ref. 6)

Migration of dissolved wastes under unsaturated conditions is a fairly complex process. In a clay-rich soil not all of the water present in the soil is mobile, but may be bound in the clay structure. The mobile water may move slowly and would not fill all of the pores (22). As a result the volumetric flow rate for a given percent saturation value would not be proportional to the water content. As moisture content decreases the capillary force begins to predominate. This has two consequences:

1. Except in highly permeable, coarse materials, like coarse sand, the moisture level will reach a finite minimum residual moisture concentration, which depends on the hydraulic conductivity of the soil and, typically, its clay content, and which will be retained indefinitely at depths below those affected by evapotranspiration.
2. Above any major structural interface, a moist column will be retained by suction forces that may have a higher moisture content than the drained volume above. This leads to an effect of water flow around cavities, such as waste materials, reducing effectively the amount of water available for leaching. It also imposes a need to allow a soil layer above any built-in drain before emplacing wastes.

All of these effects have been studied in this project to the extent that they affect disposal trench design. The work undertaken in this project consisted of four main tasks:

- a) Construction of a test bed to study the response of a soil column to steady or periodic infiltration under unsaturated flow conditions;

- b) Development of a simple computer model to permit generalization of the data obtained;
- c) Study of waste leaching conditions when exposed to unsaturated flow; and
- d) Conceptual design of a shallow waste burial facility to minimize immersion of the waste material by the provision of drains and directing the off flow.

Various subsidiary tasks, such as characterization of soils, calibration of moisture probes, and code development benefited from parallel work going on under the sponsorship of the Savannah River Laboratory, EI Du Pont de Nemours & Co.

TEST BED CONSTRUCTION

One of the prime objectives of this investigation was the measurement and demonstration of flow and drainage conditions of representative soil columns under unsaturated conditions. Tests were also conducted on laboratory scale columns, but from the start it was considered essential to conduct field scale tests to minimize wall effects and drain interface effects.

The test bed was intended to be readily drained and to be accessible from one side to measure moisture profiles during the course of a run. It had to be easy to dismantle, capable of being layered if necessary, and subject to various methods of introducing water flow.

A site was chosen on a natural slope behind the Frank Neely Nuclear Research Center and the Electronics Research Building on the Georgia Tech Campus. Figure 13 is a sketch cross section of the trench. The bed itself consisted of a wooden box, 6ft high, 2 ft. x 2ft. in cross section which was installed in the trench cut whose walls had been lined with plastic sheet and braced. Figure 14 shows the major dimensions in plan. Figure 15 presents two stages in the construction of the trench and the installation of the test box. Some major problems were encountered in the construction and installation of the drain pan, which underwent several modifications. Similarly, experience led to various improvements in revetment of the trench walls and the sloping of the drainage bed at the bottom of the trench. The assistance of the Georgia Tech Physical Plant Department in cutting the trench and supplying gravel and other materials is gratefully acknowledged.

The front panel is removable for loading and unloading. Figure 16a shows a series of tensiometers that were installed to measure moisture profiles. The tensiometers were Soiltest Inc., Model 120; great care had to be taken in their installation to remove any residual air bubbles. It was found that the tensiometers were insufficiently responsive at low moisture concentrations and for that reason most later tests relied on electrical conductivity probes. Figure 16b shows the contact panel and meter for these probes on top of the test bed.

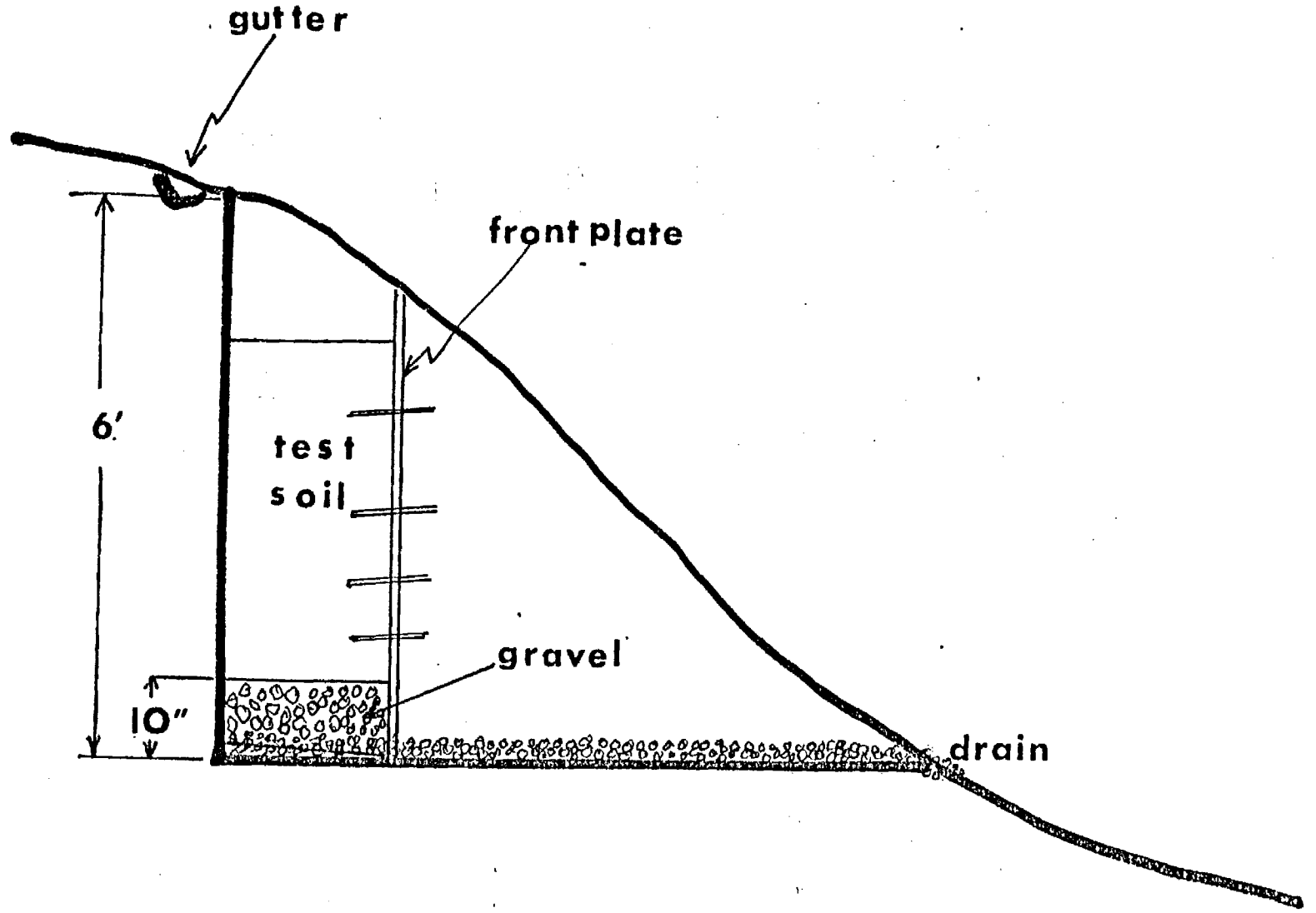


Figure 13 Cross section of Test bed trench

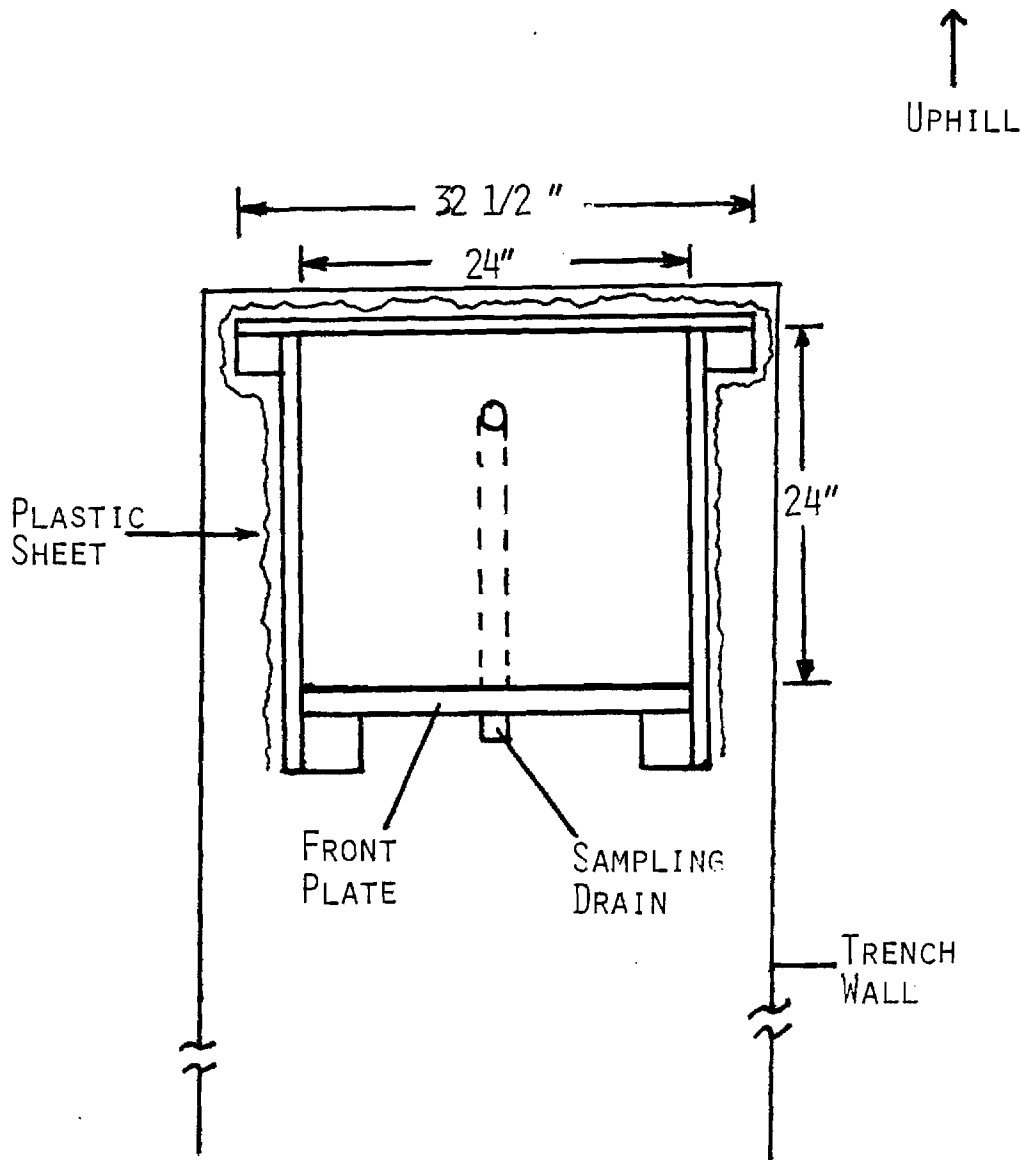


FIGURE 14 SKETCH OF TEST BED PLAN

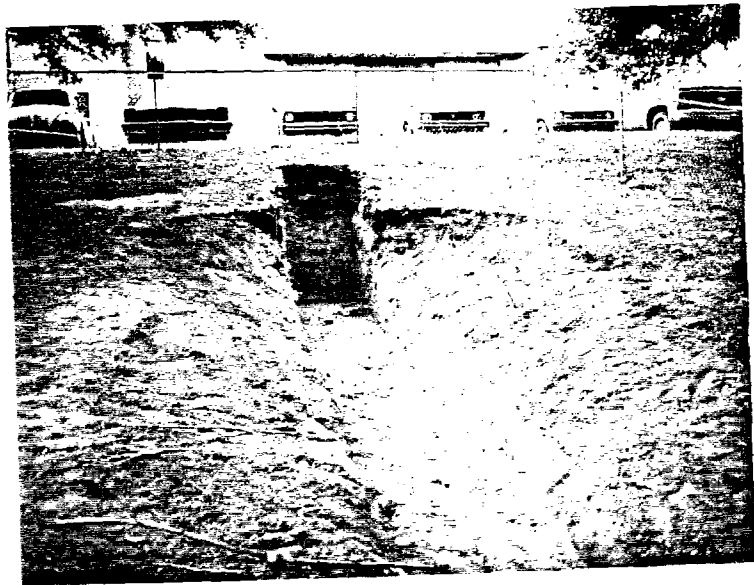


Figure 15 Views of test bed during construction



Figure 16 Views of instrumentation on test bed

MATERIALS

Test work was done with two types of sand, referred to as Rollo Sand and GT Sand, two types of fairly clayey soils, SRP No. 1 and No. 2, and a synthetic mixture, FP soil. These soils were selected to cover a range of soil-moisture conditions and to represent a variety of soils found at different existing sites. Table 1 lists the basic properties and composition of these soils.

TABLE 1 - SOIL PROPERTIES

SOIL TYPE	BULK DENSITY (g/cm ³)	POROSITY	SAND FRACTION (%)	SILT FRACTION (%)	CLAY FRACTION (%)	SATURATED HYDRAULIC CONDUCTIVITY (cm/day)
Rollo Sand	1.4.0	0.472	98.9	1.1	0.0	
G.T. Sand	1.38	0.479	97.4	2.6	0.0	2000
SRP #1	1.24	0.32	62.0	9.0	29.0	30
SRP #2	1.20	0.547	56.0	4.0	40.0	60
FP Soil	1.42	0.466	73.4	15.5	11.4	-

Particle size analyses were conducted and the distribution curves of the four soils under study were determined. The results are shown in Tables 2-5; Figure 17 shows the distribution curves of three of the soils.

Table 2 - PARTICLE SIZE DISTRIBUTION - G. T. SAND

DIAMETER (m)	% PASSING (%)	DIAMETER (m)	% PASSING (%)
1410.0	90.7	23.0	1.5
1000.0	80.7	13.0	1.5
707.0	65.8	9.3	0.7
500.0	46.6	6.6	0.7
250.0	10.4	5.0	0.7
105.0	2.9	3.5	0.0
75.0	2.6	2.7	0.0
36.0	1.5	1.3	0.0

TABLE 3 - PARTICLE SIZE DISTRIBUTION - ROLLO SAND

DIAMETER	% PASSING	DIAMETER	% PASSING
(μm)	(%)	(μm)	(%)
1410.0	86.0	36.4	1.2
1000.0	51.3	23.0	1.2
707.0	12.8	13.3	1.2
500.0	4.5	9.4	1.2
250.0	1.3	6.7	0.6
105.0	1.1	4.7	0.6
75.0	1.1	3.4	0.0

TABLE 4 - PARTICLE SIZE DISTRIBUTION - SRP #1

DIAMETER	% PASSING	DIAMETER	% PASSING
(μm)	(%)	(μm)	(%)
1410.0	97.1	7.6	30.4
1000.0	94.5	5.4	29.7
500.0	80.4	3.8	29.7
250.0	61.0	2.7	29.0
75.0	34.8	2.0	28.3
63.0	34.2	1.1	27.7
29.0	33.1	1.0	27.0
18.4	32.4	0.8	26.3
10.7	31.7	0.7	25.6

TABLE 5 - PARTICLE SIZE DISTRIBUTION - SRP #2

DIAMETER	% PASSING	DIAMETER	% PASSING
(μm)	(%)	(μm)	(%)
1410.0	97.1	16.5	42.3
1000.0	94.6	9.6	41.6
500.0	84.2	6.9	40.9
250.0	62.1	4.9	40.3
75.0	43.3	2.4	39.6
63.0	43.1	1.0	38.9
25.8	43.0		

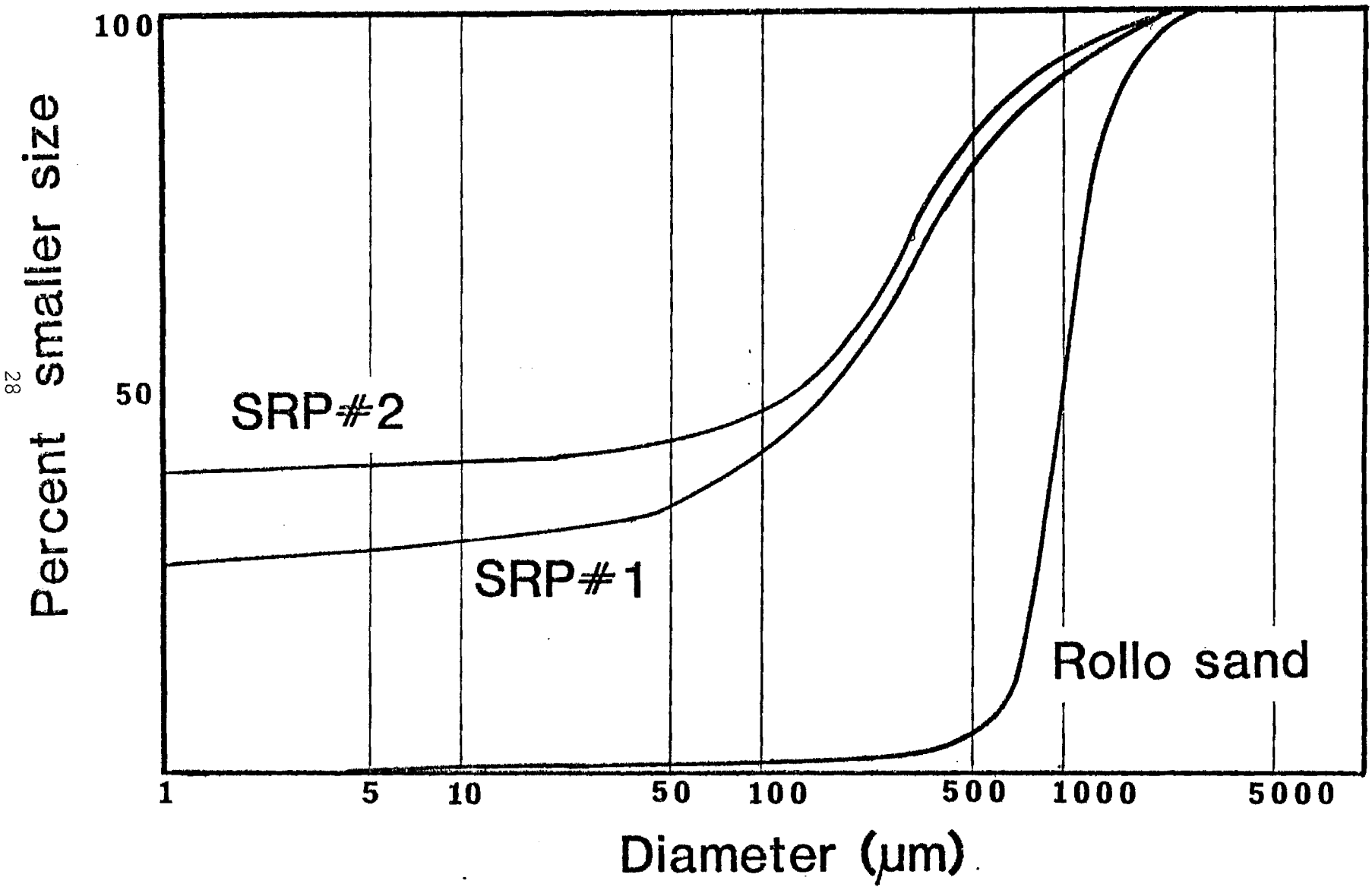


Figure 17 Particle size distributions

LABORATORY TESTS

Bench-scale tests were conducted to evaluate the basic properties of the soils, to measure residual moisture levels and to calibrate the conductivity probes for use in the test bed. Column tests were conducted in three sizes of tubes, which are shown in Figure 18. The short tubes, top right were employed mainly to obtain residual moisture contents, though care had to be taken to allow for the suction layer above the bottom screens. The other columns had built-in electrodes and were calibrated by direct weight-loss moisture determinations. The larger columns, Fig 18c, have been used for hydraulic conductivity measurements and for radiotracer tests.

Figures 19-21 present electrode calibration curves, plotting electric resistance between adjoining electrodes versus percent saturation, for GT sand and the two SRP soil samples. Similar curves have been obtained for the other soil materials. For consistent results, care had to be taken to ensure even packing and the column had to be presaturated to remove any remaining air. The calibrations for the various columns were consistent, but in practice the electrodes had to be recalibrated for the large test bed.

Since the purpose of the project was to minimize soil water content surrounding the waste material, it was important to measure how low a moisture content could be obtained by draining. Due to capillarity effects all soils will retain a minimum moisture content once water has infiltrated, with the amount retained dependent on pore size, surface watability and clay content.

Table 6 shows the results of a series of tests on sized sand columns. As expected, the finer sizes (large mesh number) retain more water in their smaller pores. Table 7 compares the residual water content for two sands and two SRP soils, whose size distribution was shown in Figure 17. Again, as expected, the SRP soils with their high clay content and fine size components show relatively high residual water values.

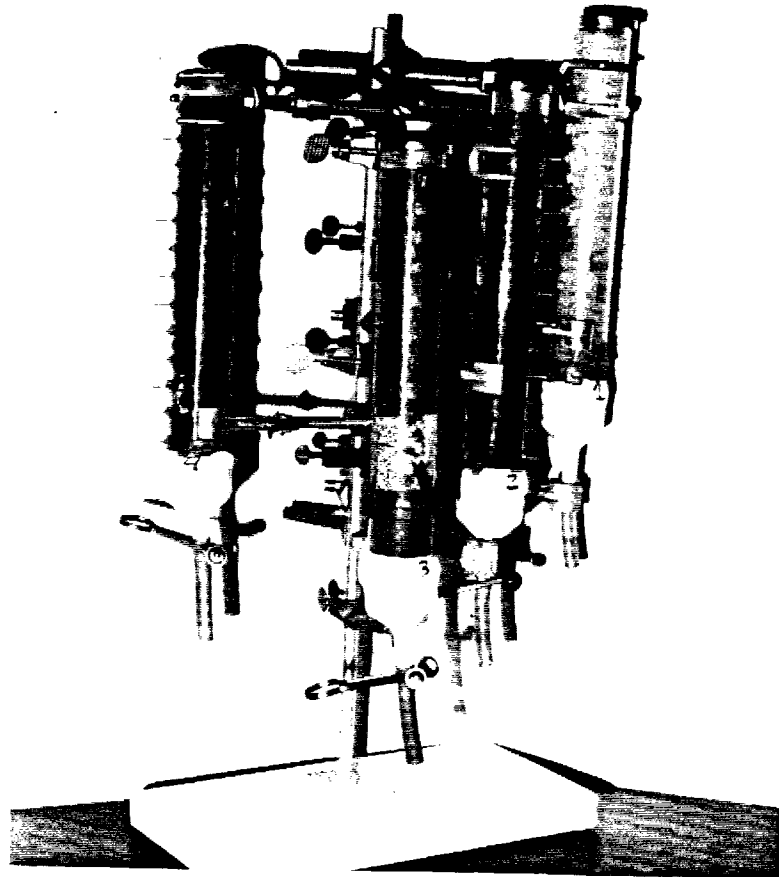
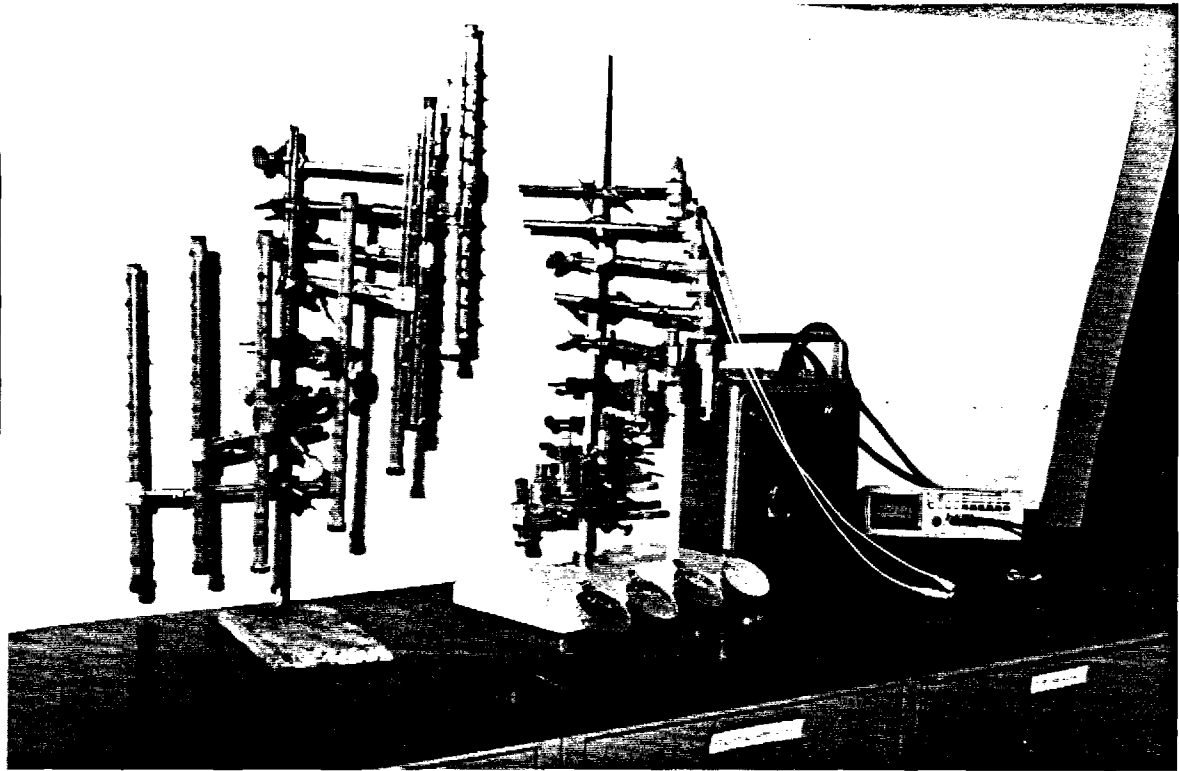


Figure 18 Views of laboratory test columns

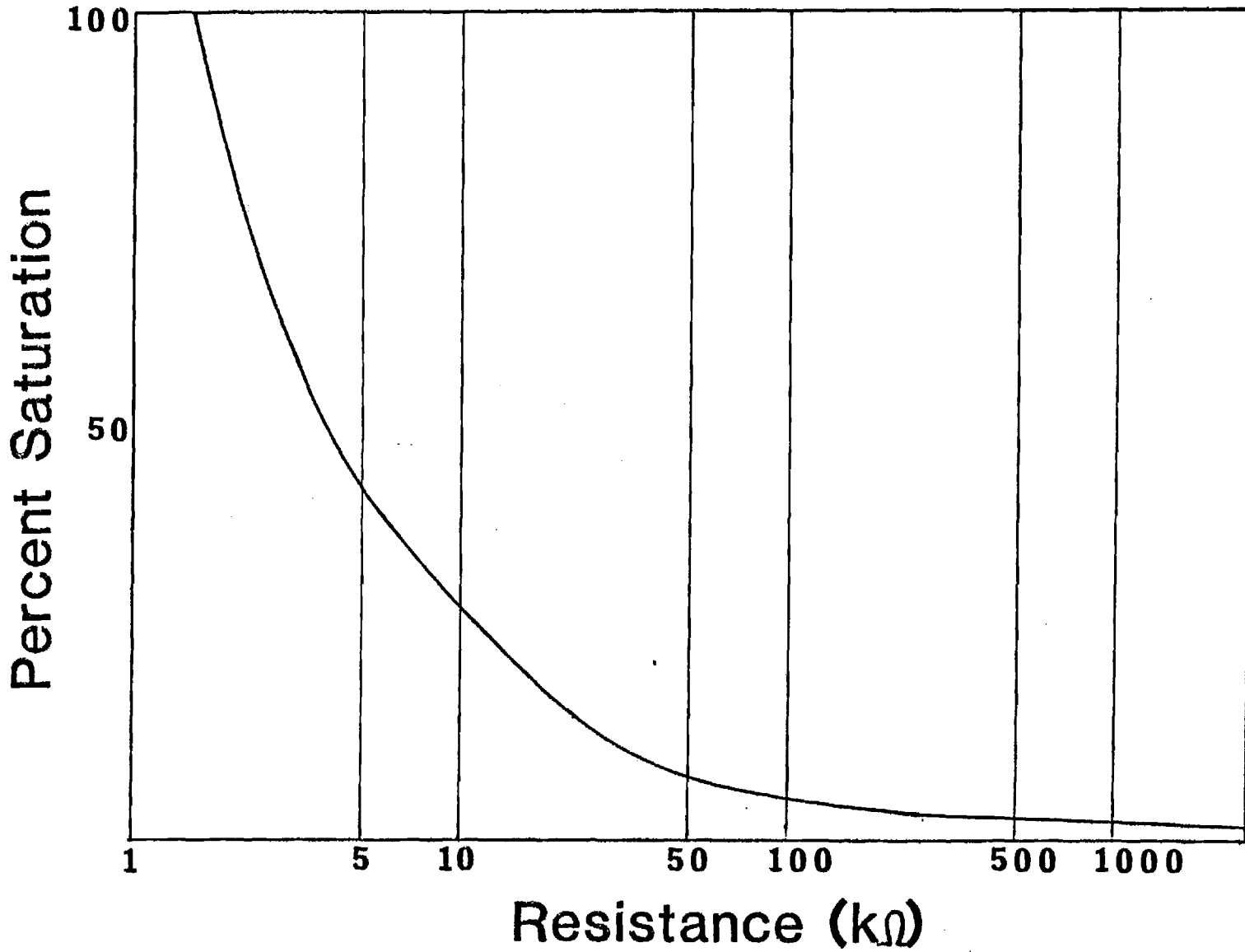


Figure 19 Electrode calibration - GT Sand

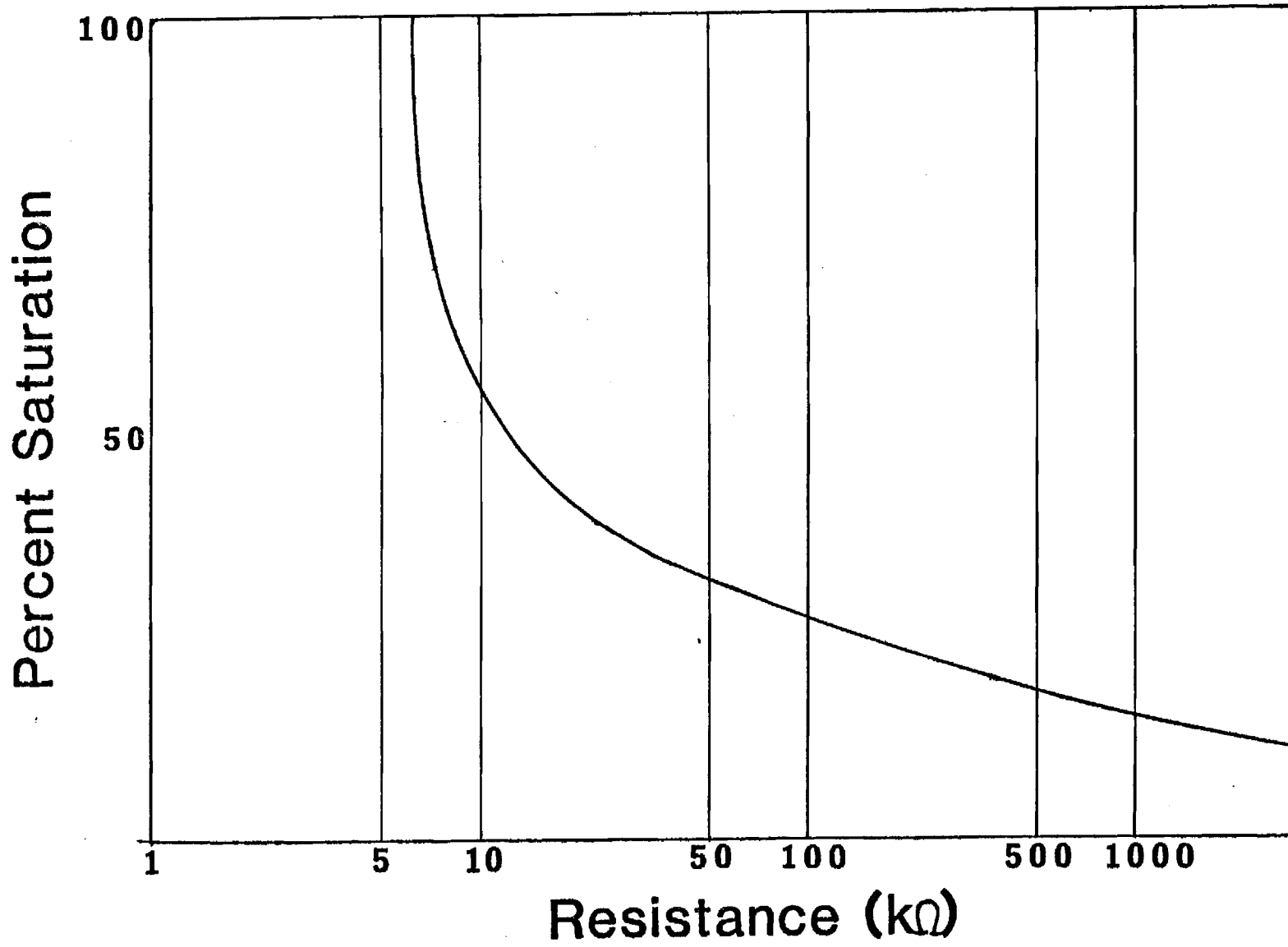


Figure 20 Electrode calibration - SRP # 1 soil

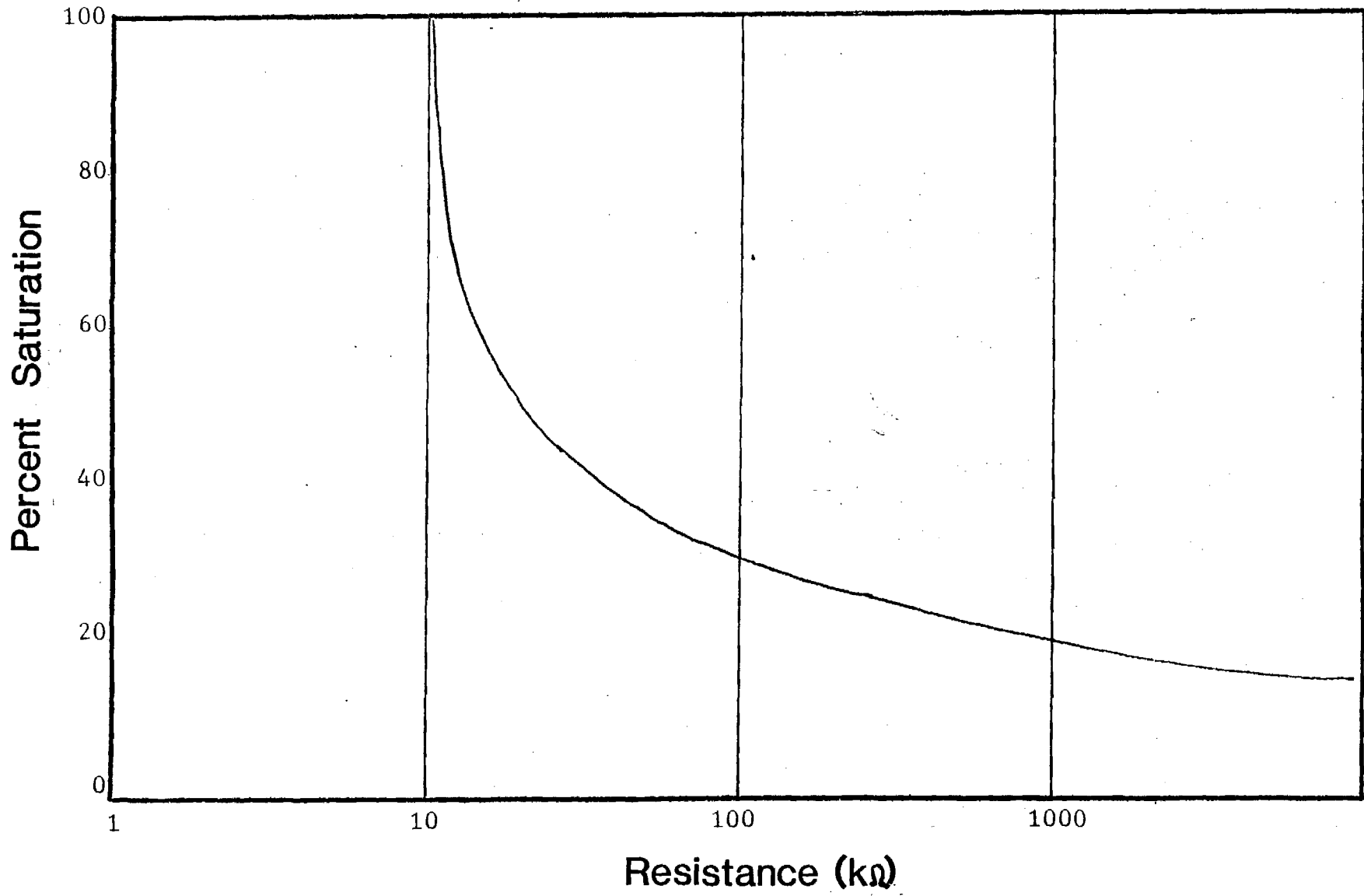


Figure 21 Electrode calibration - SRP # 2 soil

TABLE 6 - RESIDUAL WATER CONTENT FOR SIZED SAND SAMPLES

MESH SIZE	RESIDUAL WATER CONTENT (%)
14-16	0.05
16-20	0.16
25-30	0.18
30-55	0.25
40-50	0.33
50-60	0.61

TABLE 7 - RESIDUAL WATER CONTENT

SOIL TYPE	RESIDUAL WATER CONTENT
Rollo Sand	0.89%
G. T. Sand	1.59
SRP #1	10.51
SRP #2	17.37

One of the consequences of the capillarity effect, also, is the retention of moisture due to surface tension at any major interface. This applies particularly whenever a dense soil layer lies above a cavity, such as a waste volume or a gravel bed. If the interface is sloped, this effect can lead to substantial lateral waste movement. Table 8 records measurements of the wet layers at the open bottom ends of the columns. For the SRP soils this retained wet layer was substantial and even after 30 days there was some continued water loss.

Similar observations have been carried out on the test bed for Rollo sand, GT sand and FP soil. The observed minimum wet base layers were found to be 15cm high for the GT sand and about 30cm for the FP soil.

TABLE 8 - RESIDUAL WET LAYERS AT OPEN ENDS (30 DAYS)

MATERIAL	3CM COLUMN	1.2 CM COLUMN
Rollo Sand	2cm	2cm
G. T. Sand	8	2
SRP #1	14	2
SRP #2	16	2

TEST BED EXPERIMENTS

Use of the test bed had to be planned carefully, if only because the amount of material needed to fill it represented about two cubic yards or about half a ton of soil material, which had to be carefully screened and prepared. Since the tensiometers proved to be insufficiently responsive to rapid changes, most moisture profiles were obtained with the use of electric conductivity probes, which had to be carefully installed and calibrated. An early problem with a floating electric ground potential was overcome by careful grounding of the measuring unit.

The principal purpose of the test bed experiments has been the collection of data on drainage rates, residual moisture, bed support performance and response to cyclic infiltration. At this time, work on the latter effect is continuing and definite results can be reported at this stage only on certain aspects.

Among the most interesting results are a succession of drainage curves of which Fig. 22 is a representative sample. It shows moisture measurements at three levels, z , in the box, 19, 94 and 144 cm. from the top, following saturation loading, in Rollo sand. Drainage is very rapid in this medium and at the 144 cm. level a distinct knee appears demarking the transition from the gravitational regime to the tension regime. Fig. 23 shows the resolution of that curve into two exponential rates from which the appropriate rate constants can be derived. These constants in turn can be inserted into the flow model to determine the time variation in the water content following a step increase in water inflow.

Another type of observation represents the moisture profile for a given water content in the column. Fig. 24 shows a typical profile observed in the test bed. These results have been correlated with calculations of an unsaturated flow model for a cylindrical system. This program can generate moisture contours that are critically dependent on the relative magnitude of the gravitational and the tension drainage coefficients.

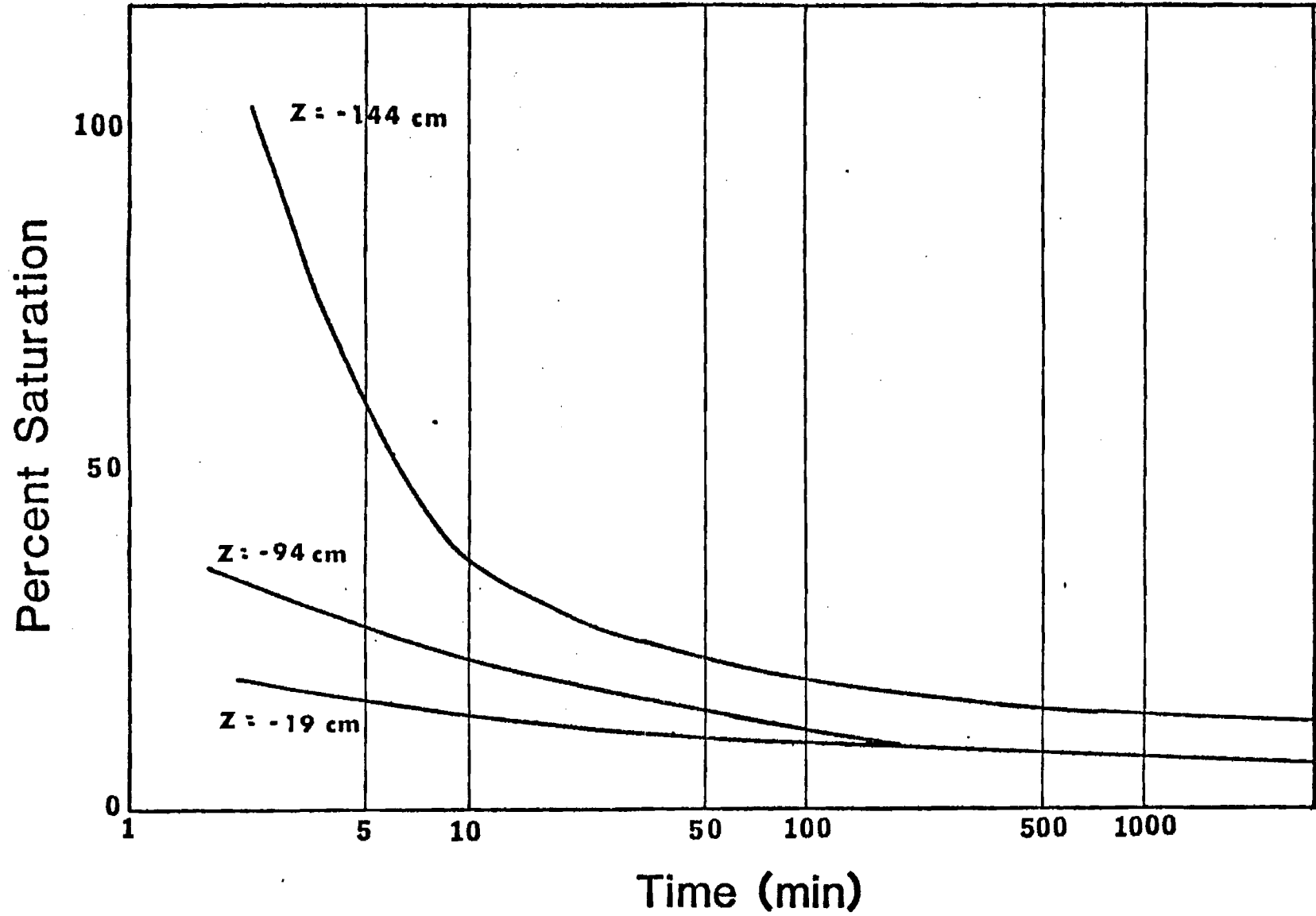


Figure 22 Drainage curves - Rollo Sand

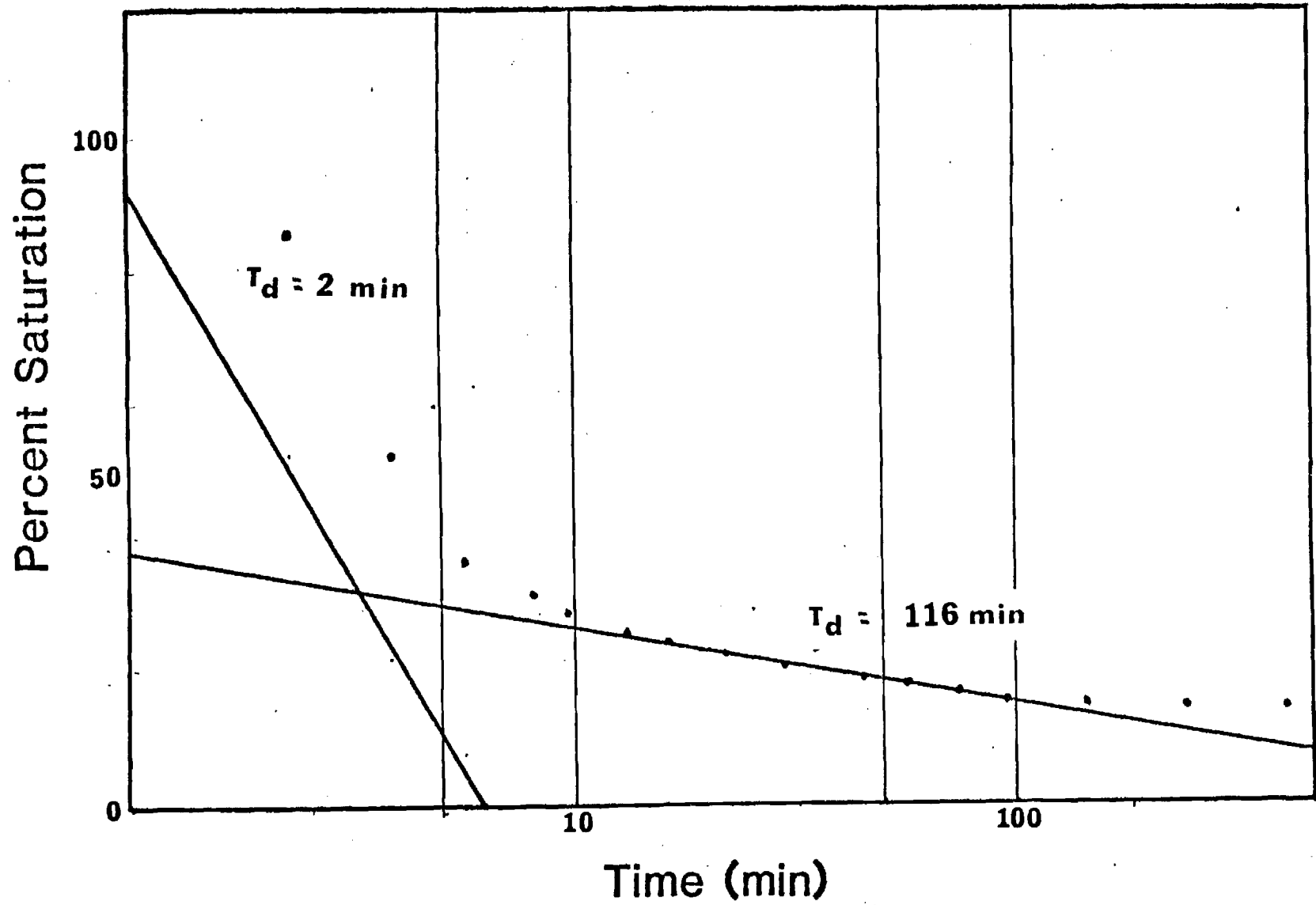


Figure 23 Resolved drainage curve - Rollo Sand

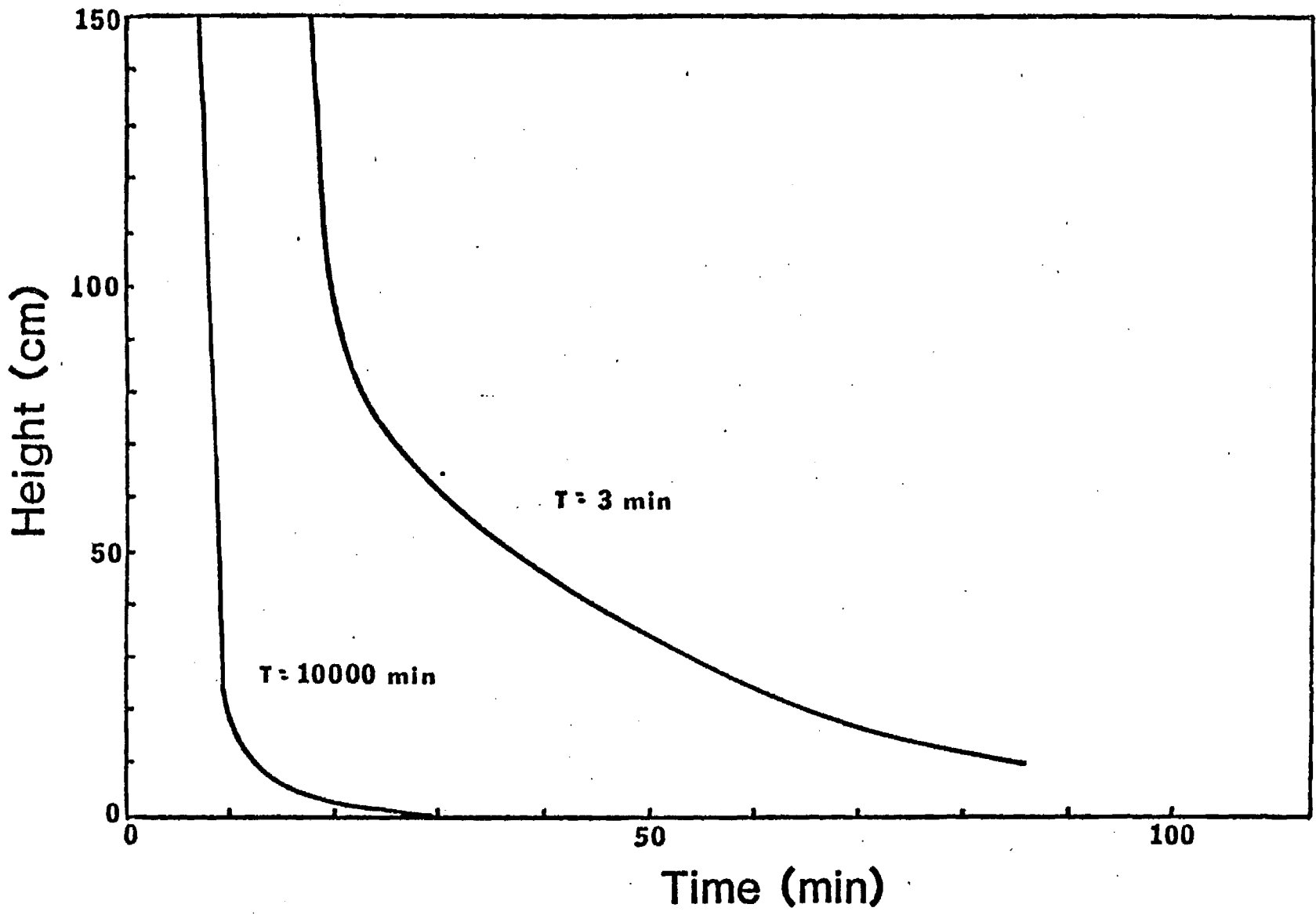


Figure 24 Moisture Profiles - Rollo Sand

Figure 25 shows the moisture profile for GT SAND plotted against the height above the drain. The curve on the right shows the profile at one minute after drainage begins. The middle curve describes the profile after 30 minutes of drainage. The curve on the left shows the moisture profile after 8800 minutes of drainage (about 6 days). The moisture content is seen to be uniform at a height greater than 20 cm above the drain. There is an interface between the soil at residual moisture content (11% of saturation) and the more saturated (75%) soil directly above the drain. Groups of electrodes were placed at 10 cm intervals inside the lysimeter. We cannot determine the exact location of the interface; it lies between 10 cm and 20 cm above the drain. Figure 25 clearly shows that in an unsaturated soil areas of higher saturation can be generated by changes in the soil properties.

Figure 26 is the moisture profile for FP SOIL. The curves compare the moisture profiles at two different times. The curves show the interface between the wet soil and the soil at residual moisture content occurring at a height of between 30 cm and 40 cm. The residual water content of the FP SOIL is estimated to be approximately 30 percent of saturation.

Figure 27 shows the drainage curves for GT SAND at different heights above the drain. The lower curve describes the percent saturation as a function of time for the top of the soil column, 50 cm above the drain and 10 cm below the soil surface. This curve illustrates the initial rapid drainage of the soil followed by a slower decline to the residual moisture content. The upper curve reveals the moisture content at the bottom of the lysimeter, 10 cm above the drain. The graph shows a long plateau where the moisture content at the bottom is nearly constant while the upper portions of the column are draining. It is thought that the infiltration into this zone from above occurs at the same rate as the drainage into the gravel, thereby keeping the moisture content constant. As the upper region approaches the residual moisture content, the downward flow of water slows and the lower area begins to drain.

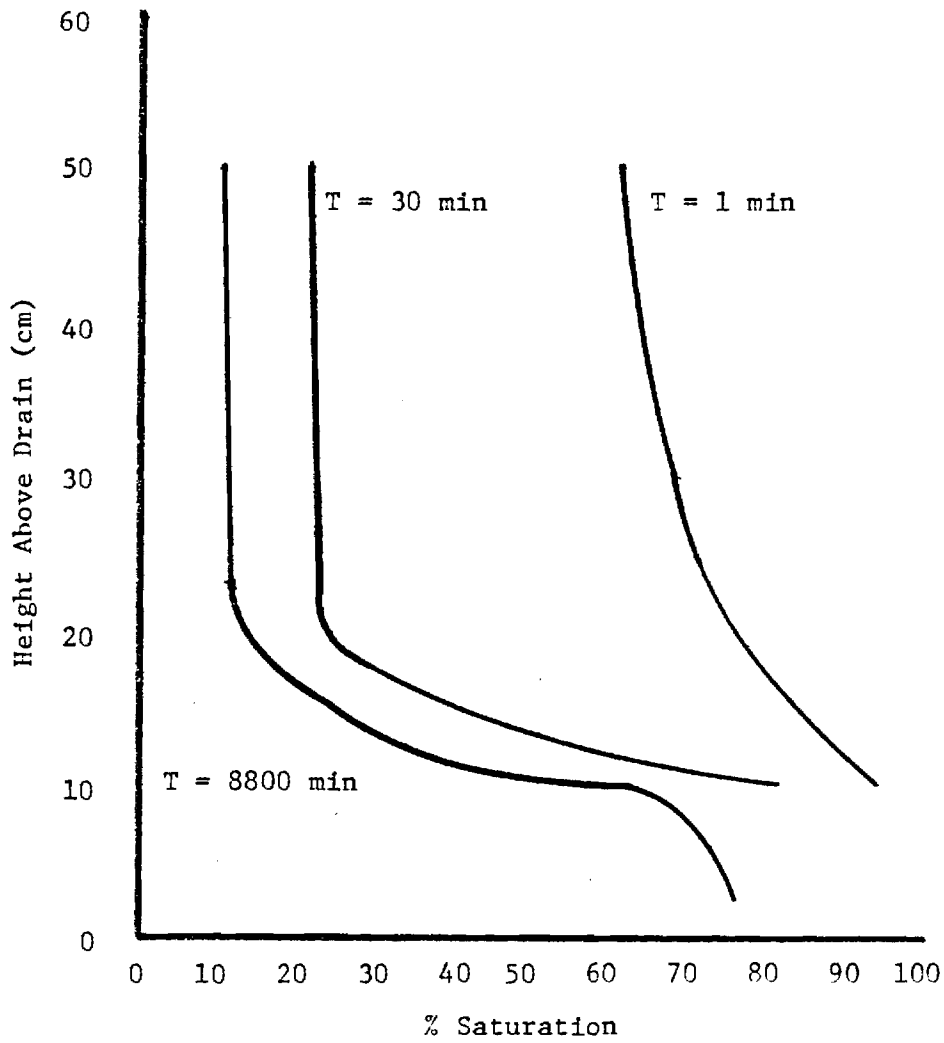


Figure 25 Moisture Profiles for GF Sand at different times

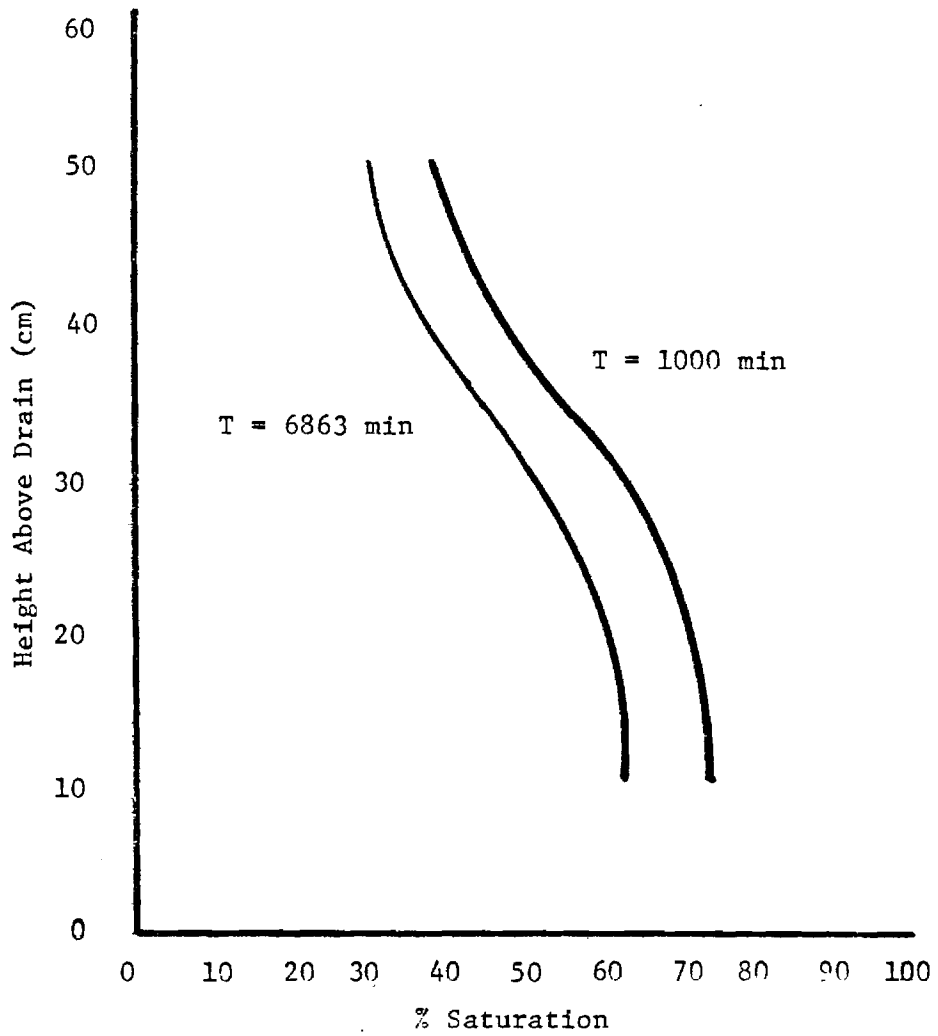


Figure 26 Moisture Profiles for FP Soil at different times

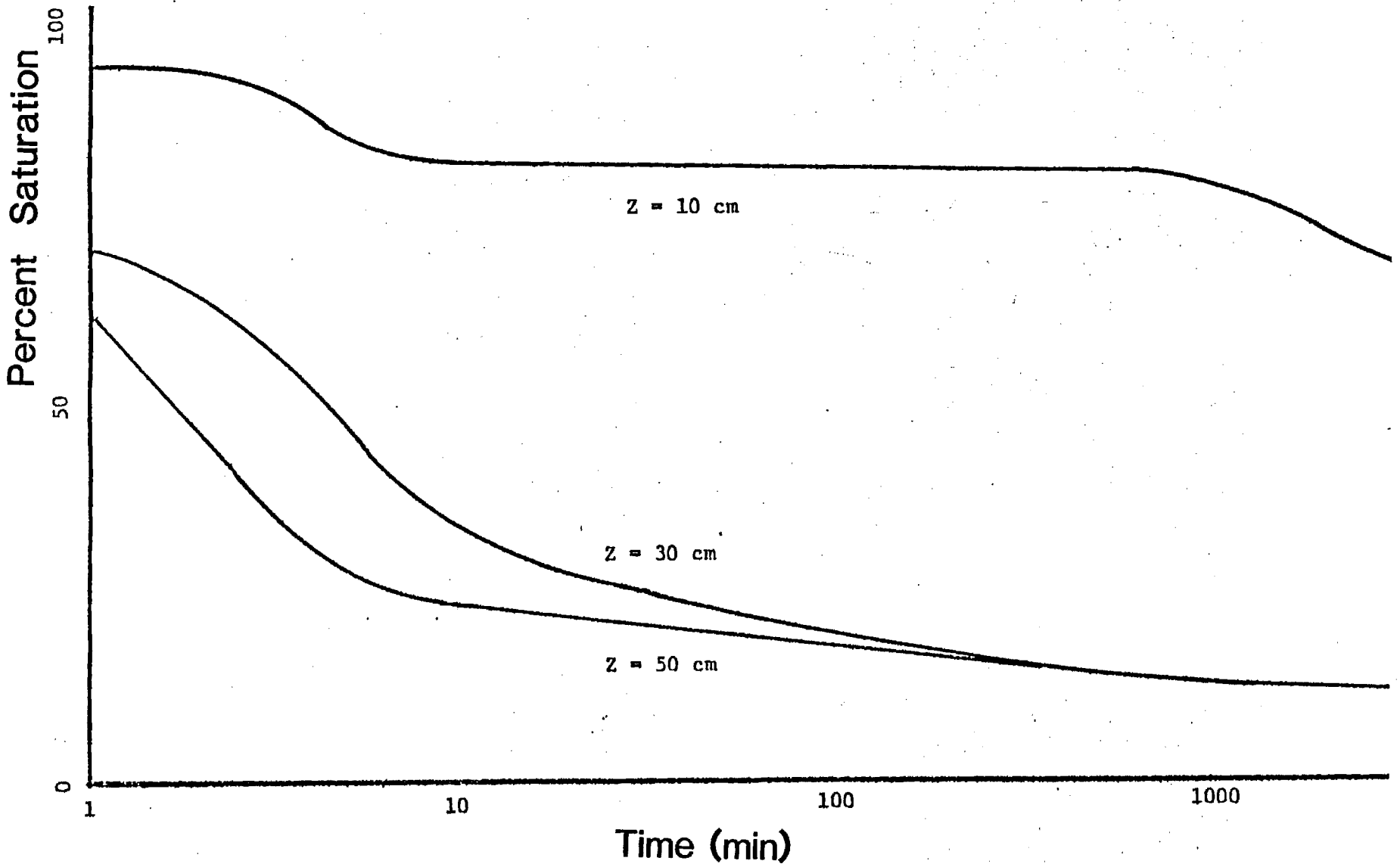


Figure 27 Drainage Curves for GT Sand at different heights

It can be seen from the figure that the drainage from a high percent saturation to a low percent saturation occurs very rapidly in GT SAND. It takes 10 minutes to go from 70 percent of saturation to 30%. The soil returns to its residual moisture content within 1440 minutes (24 hours). If precipitation occurs less than daily, the soil will drain between infiltrations.

Figure 28 shows the drainage curves for FP SOIL at different heights, z , 2, above the drain. The curves are of the same general type as the GT SAND drainage curves. The dotted region between 10 and 150 minutes indicates that the system had not reached equilibrium before the start of the drainage test.

Water was ponded over the soil surface for one hour prior to the start. The $Z = 10$ cm curve clearly shows the rise from residual moisture content to about 64% of saturation. The residual moisture content of the FP SOIL is about 30% of saturation. This value is reached in approximately 4000 minutes (3 days).

Figure 29 is a comparison of the drainage curves for the three soils. The two sands have similar curves. There is an initial region of rapid drainage followed by a couple of hours of slower drainage. The sands have attained residual moisture content in less than five hours. Rollo Sand and GT SAND have residual moisture contents of 12 and 10 percent of saturation respectively. The FP SOIL, with its significant clay fraction, requires an order of magnitude more time to reach its residual moisture content. The measurements used in Figure 26 were taken 10 cm below the surface.

Figure 30 shows the drainage curves for Rollo Sand and GT Sand resolved into their component parts. The curves are percent of saturation plotted against log time. Both sands show a two-part drainage curve. The initial portion is presumably the gravity drainage of the larger pores and is significant for the first 10 minutes. The second component continues to drain for several hours until residual moisture content is reached. Rollo

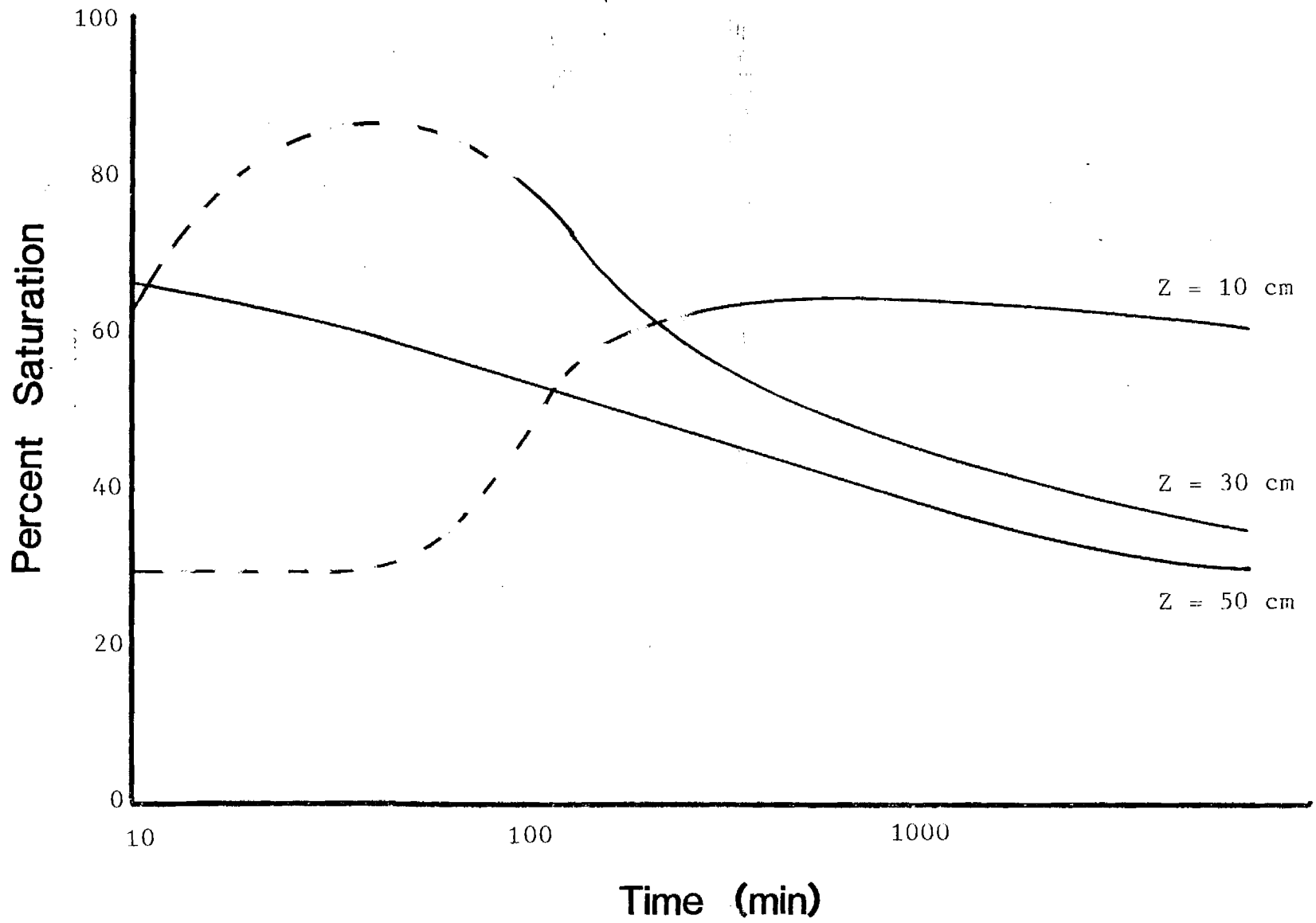


Figure 28 Drainage curves for FP Soil at different elevations in the test bed

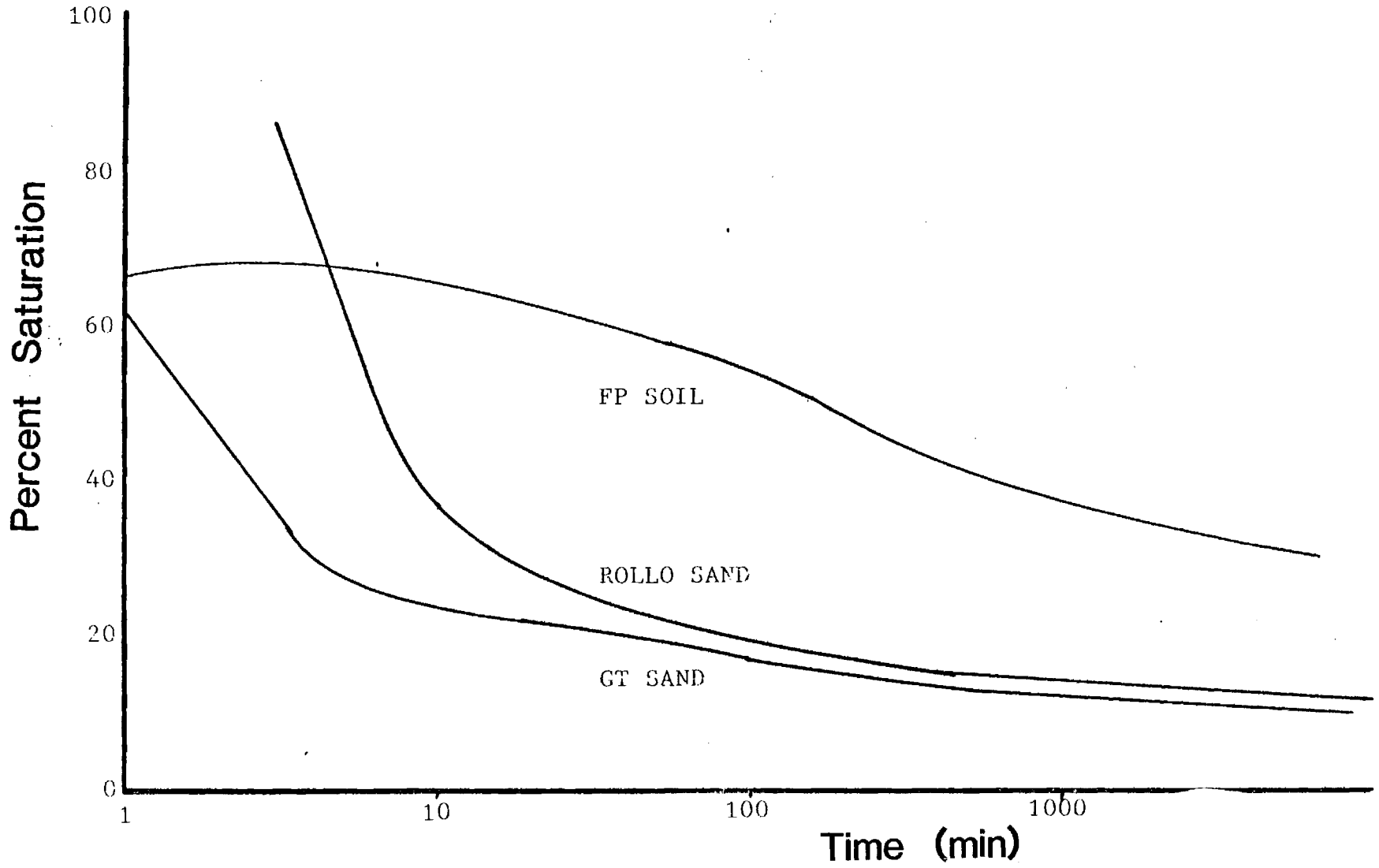


Figure 29 Drainage Curves for three soil types

47

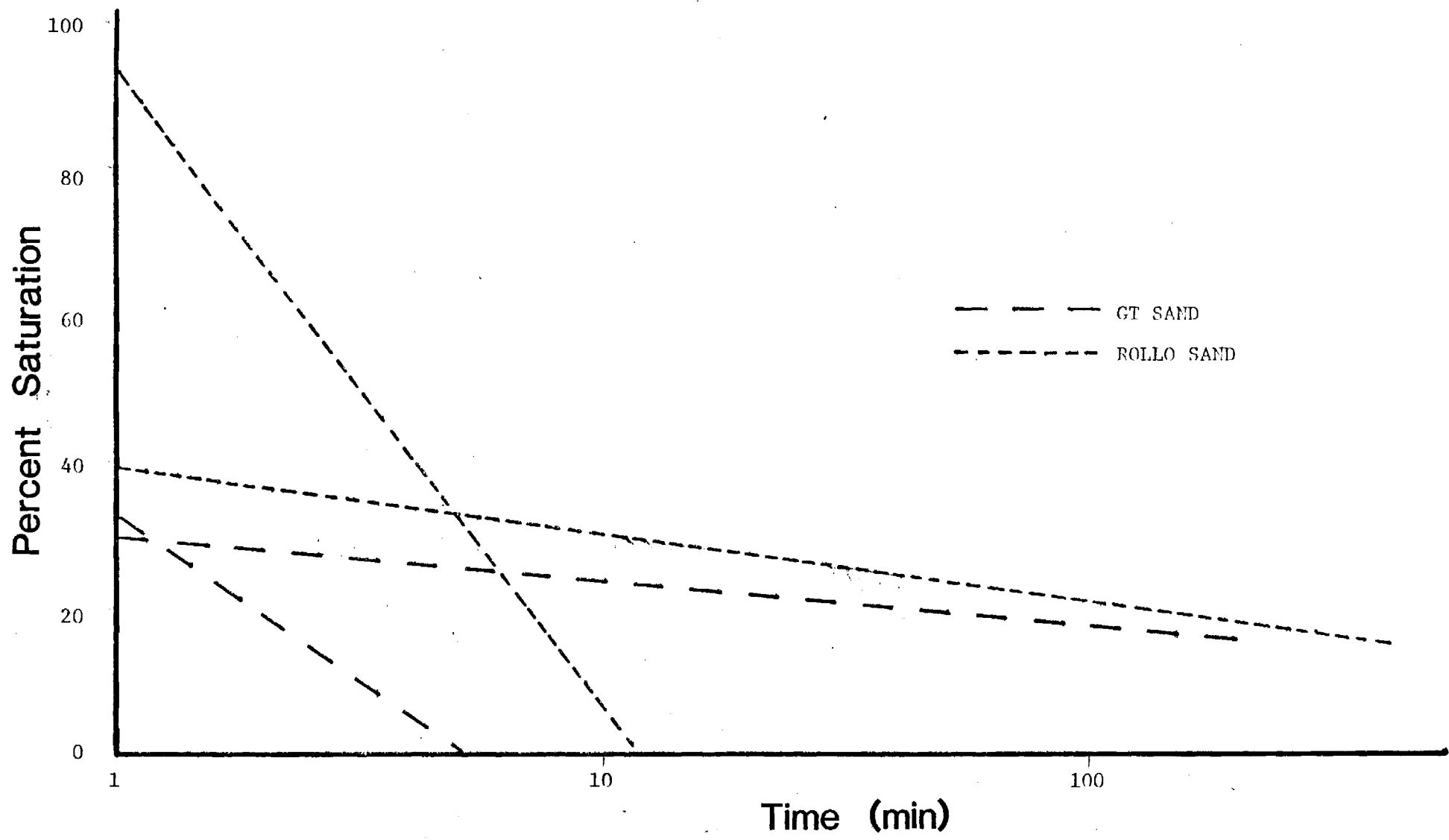


Figure 30 Resolved Drainage Curves for two sands

Sand is shown to drain faster, which is to be expected, due to its large, uniform-sized particles. It is interesting to note that the time of drainage is a function of the percent saturation. The drainage equation can be expressed as:

$$t = C e^{-(k \cdot s)}$$

where t is the drainage time, C is an empirical constant, k is the drainage constant and s is the percent saturation.

Rollo Sand was found to have drainage constants of 0.247 s^{-1} and 0.0266 s^{-1} for the rapid and slow drainage respectively. GT Sand had k 's of 0.384 s^{-1} . The initial drainage rates are only significant in the first five to ten minutes. It must be remembered that these values are calculated for the top 10 cm of the soil column. The curves become more complex with depth due to the variable infiltration of moisture from above.

A drainage curve resolution was not done for the FP Soil. The soil had not achieved its equilibrium conditions due to a insufficient initial infiltration time. The experiment is being repeated using a much longer infiltration time.

Calibration of the electrodes was done in the field by taking a soil sample from between each electrode pair. The water content was determined gravimetrically. The bulk density and porosity were also determined under field conditions.

An important feature of a well-drained bed is the retained moisture at the bottom of the column. In the test bed, the sand layers were supported by a mesh screen that was placed on top of the coarse gravel bed which provided the drainage path. In sand, ordinarily, little moisture should be retained due to surface tension effects at the lower surface. However, it was found that the wire mesh supported a film of water of sufficient strength to maintain significant moisture in the sandbed up to a height of

about 14 cm. Proper choice of the supporting material is obviously important to minimize this effect, while yet retaining the bed material sufficiently to avoid clogging of the gravel layer. In practice it is felt that a graded gravel layer can supply enough support for the soil and may be preferable to a screen or open-mesh liner material.

Since the usefulness of the drainage layer could be impaired by silting over a long period, qualitative observations were maintained on silt infiltration into the gravel bed. It was found that a little fine silt material was washed into the gravel in the early stages of the test, but later, with the readily mobile material removed from the bottom soil layer, no further silt movement seemed to occur.

WASTE LEACHING UNDER UNSATURATED CONDITIONS

One of the principal objectives of this work is the reduction in the source term from water attack on the waste material by reduction of the quantity of water in contact with the waste and of the time available for transfer processes. For vitrified waste, Pescatore and Machiels (23) have argued that for slow flow rates the diffusion rate of waste ions to the surface layer becomes the rate-determining step. Most waste depository models assume that water flow is continuous, saturated and that the leach rate is proportional to flow rate at a constant solubility. Under unsaturated flow conditions or cyclic flow conditions, it is not at all clear if leaching occurs in a constant fashion and whether it is necessarily proportional to volumetric flow rate. Test work has been conducted with simulated waste to study these processes, but the results have been inconclusive so far, partly because of slow leaching rates and partly because of the need to employ equilibrated water for reasonable simulation, whose composition is, to some extent, affected by the nature of the simulated waste itself. Similar considerations affect the leachability and migration rates of other waste trench simulations, such as the SRP lysimeter tests (15), where flow also is unsaturated much of the time.

The test work conducted in the laboratory has been of two types, recirculating water through simulated waste material and once-through flow tests. The simulated waste consisted on ion exchange resins labeled with Cs-137 or Tc-99m. This material was chosen, because it was felt that other waste forms either would be too insoluble to result in statistically valid desorption or would be too inhomogeneous for comparison. The recirculated tests suffered from constant change in pH due to the effect of the waste resin and those tests were not pursued. Once-through flow tests with equilibrated water were more controllable, but have resulted in too low a level of desorption to yield reliable results. For this reason no experimental results on this aspect of the project are reported here in detail. These tests are continuing and it is hoped to place them on a more productive basis.

In the meantime, for calculational purposes it is assumed that the leach rate is proportional to the time-integrated volumetric flow. That is a problematic assumption, because of the diffusion rate and concentration-gradient dependence of the leach process which makes it improbable that the leach source term is proportional to water volume under pulsed conditions. However, for the moment that assumption seems the best available.

COMPUTER SIMULATION

To evaluate the effects of unsaturated flow under time-dependent conditions, a one-dimensional computer program has been developed. This program can describe pulse flow conditions in the test bed and the movement of the moisture profile. Details of the program are presented in Appendix A.

The results depend, of course, on the relative magnitude of the pressure head (gravitational force) and the suction head (capillarity). Figures 31 and 32 illustrates two cases where their relative magnitudes vary.

The general features of computer model for this facility are shown in Figure 33. On the left are the physical processes involved, on the right the various rate processes that determine waste migration from the source.

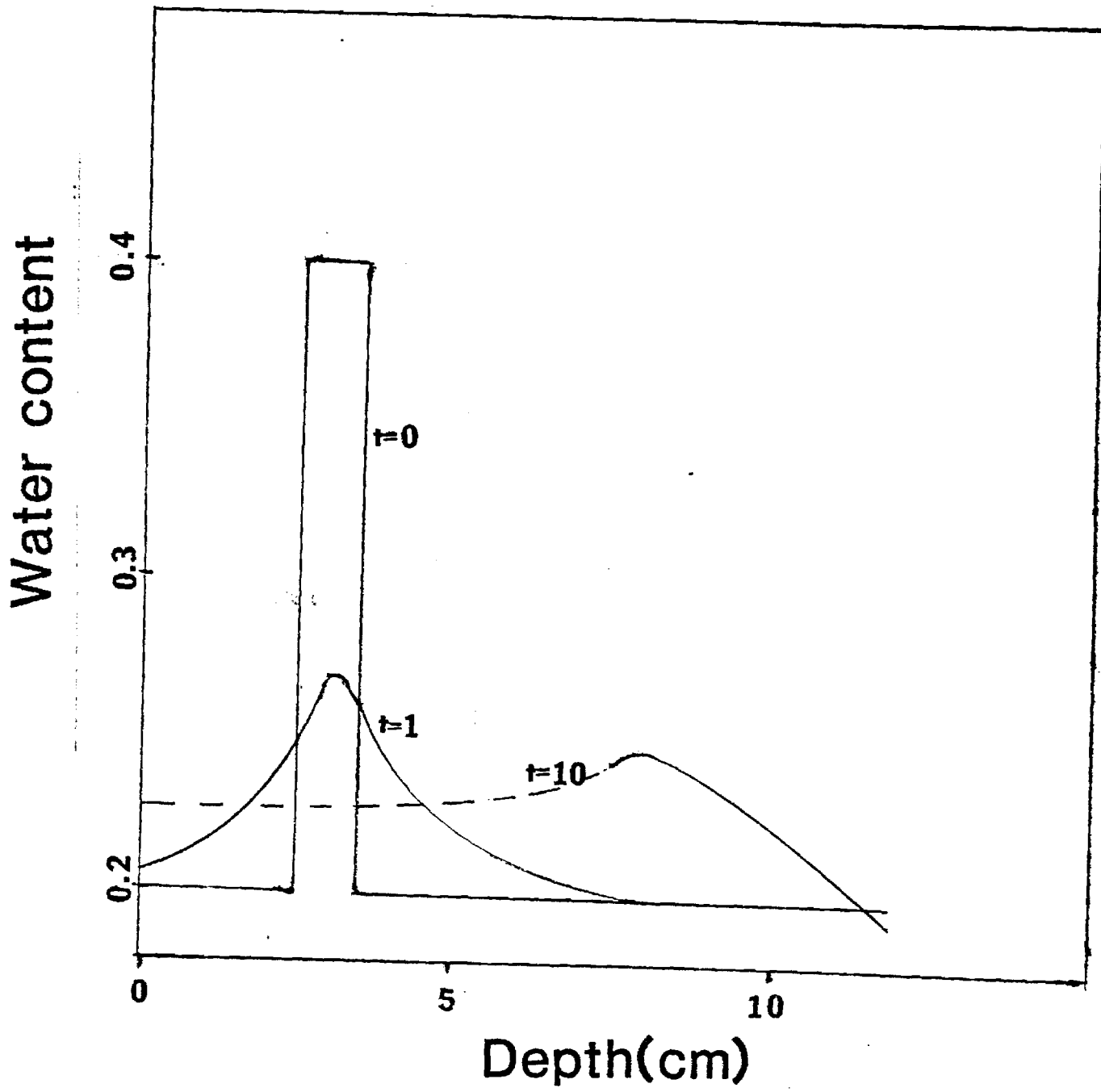


Figure 31 Calculated Moisture Profiles - Comparable forces

Water content

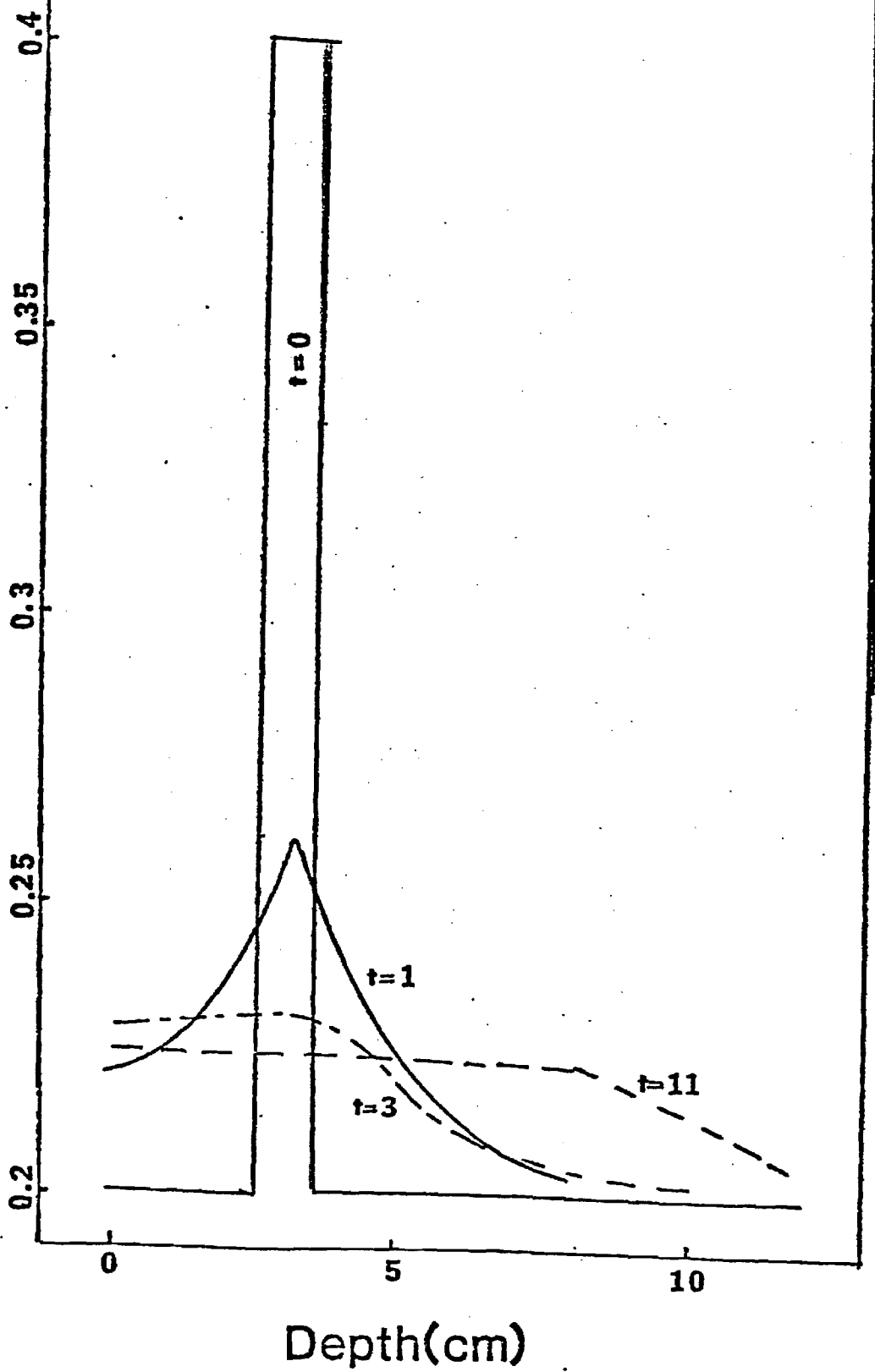


Figure 32 Calculated Moisture Profiles - Suction dominant

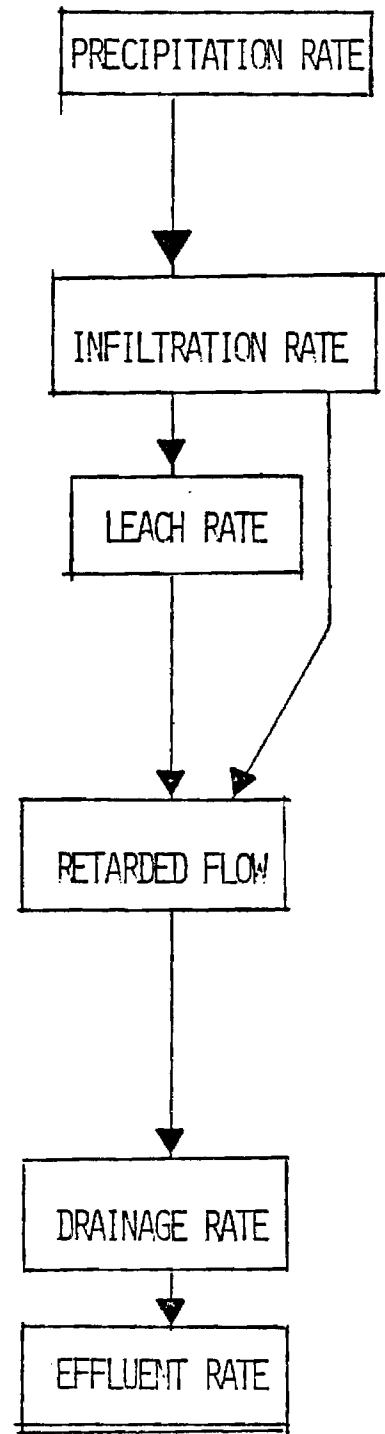
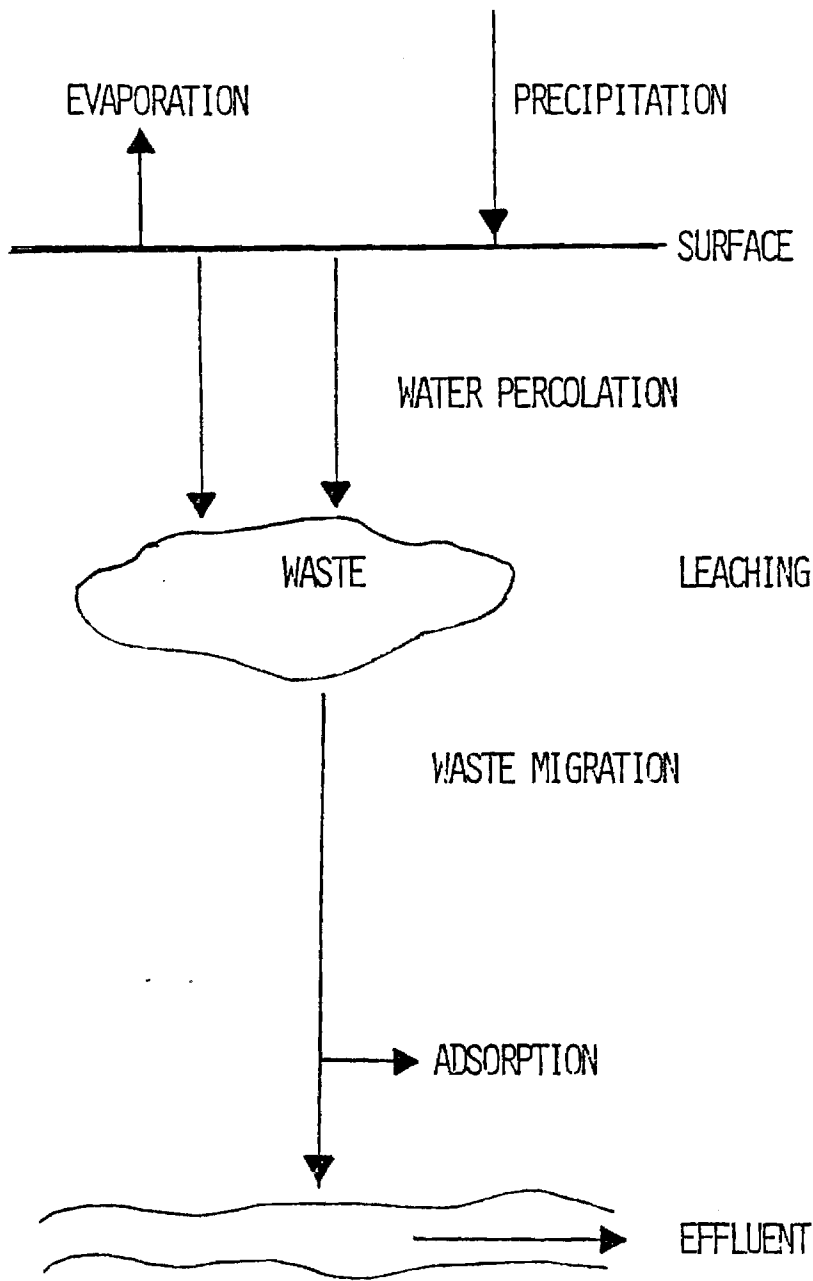


Figure 33 Diagram of Migration Model

Details of the model development go beyond the scope of this report and will be available shortly in extended form (de Sousa, Ph.D Thesis, 1985). The program description is attached in Appendix A - C. The model is based on a finite element technique which was used to solve the one-dimensional unsaturated flow and transport equations. Boundary conditions include provision for a Neumann variable flux condition, so as to represent a seepage boundary, as well as a Dirichlet constant boundary condition.

In order to use the water flow and transport model to simulate a shallow land burial site performance, it is necessary to determine how well the model can simulate the unsaturated regime present in the soils. Since the transport model uses the results obtained with the flow model, the latter was the first one to be checked.

Flow model

The first simulation done to check the accuracy of the water flow model corresponded to the situation in which an homogeneous saturated column of soil was submitted to a constant infiltration equal to the saturated hydraulic conductivity of the soil; the boundary condition at the bottom of the column corresponded to a free draining profile. In this situation the column should remain saturated, and the pressure head should not change with time, since the infiltration and the drainage rates are equal; the results obtained, given in Table 9, showed that the model was simulating that situation correctly. This simulation was useful to the extent that it showed the logic of the model was correct and the matrices were being well assembled and solved.

The ability of the model to reproduce unsaturated flow was checked by simulating the situation presented by Van Genuchten (28) based on the experiments done by Warrick (29). This experiment was chosen because it represents one of the most difficult cases to simulate, which is when a dry soil is subjected to a large infiltration rate.

The experiment consisted of an homogeneous soil column, 125 cm long, which was subjected to the following conditions:

TABLE 9 - FLOW MODEL VERIFICATION

TIME= .050 NL= 1 NT= 1			
NODE	COORDINATE	PRESSURE HEAD	
1	.000	-34.460	
2	1.000	-34.460	
3	2.000	-34.460	
4	3.000	-34.460	
5	4.000	-34.460	
6	5.000	-34.460	
7	6.000	-34.460	
8	7.000	-34.460	
9	8.000	-34.460	
10	9.000	-34.460	
11	10.000	-34.460	
12	11.000	-34.460	
13	12.000	-34.460	
14	13.000	-34.460	

TIME= .125 NL= 1 NT= 2			
NODE	COORDINATE	PRESSURE HEAD	
1	.000	-34.460	
2	1.000	-34.460	
3	2.000	-34.460	
4	3.000	-34.460	
5	4.000	-34.460	
6	5.000	-34.460	
7	6.000	-34.460	
8	7.000	-34.460	
9	8.000	-34.460	
10	9.000	-34.460	
11	10.000	-34.460	
12	11.000	-34.460	
13	12.000	-34.460	
14	13.000	-34.460	

TIME= .225 NL= 1 NT= 3			
NODE	COORDINATE	PRESSURE HEAD	
1	.000	-34.460	
2	1.000	-34.460	
3	2.000	-34.460	
4	3.000	-34.460	
5	4.000	-34.460	
6	5.000	-34.460	
7	6.000	-34.460	
8	7.000	-34.460	
9	8.000	-34.460	
10	9.000	-34.460	
11	10.000	-34.460	
12	11.000	-34.460	
13	12.000	-34.460	
14	13.000	-34.460	

Initial Condition:

$$\theta(x,0) = \begin{cases} 0.15 + 0.0008333 & 0 < x \leq 60 \\ 0.20 & 60 < x < 125 \end{cases} \quad (1)$$

Boundary Conditions:

$$h(0,t) = -14.495 \quad (2)$$

$$h(125,t) = -159.19 \quad (3)$$

The water content - hydraulic conductivity and the water content - pressure head relations are given by:

$$\theta(h) = \begin{cases} 0.6829 - 0.09524 \ln |h| & h \leq -29.484 \\ 0.4531 - 0.02732 \ln |h| & -29.484 < h < -14.495 \end{cases} \quad (4)$$

$$k(h) = \begin{cases} 19.34 \times 10^5 |h|^{-3.4095} & h \leq -29.484 \\ 516.8 |h|^{-0.97814} & -29.484 < h < -14.495 \end{cases} \quad (5)$$

The flow model is written in terms of pressure head and so the initial pressure head distribution is given by substituting eq.1 in eq.4; the boundary condition at the surface (eq. 2) implies that the soil is maintained saturated at the top of the column at all times.

The results obtained by using linear finite elements (LFE) and mass lumped linear finite elements (MLFE) are shown in Figure 34, where they are compared to the numerical solution obtained by Van Genuchten (28). It is seen that in both cases a reasonable simulation is obtained; more accurate results can be obtained if the spatial and time intervals are decreased at the expense of a longer computational time. The LFE simulation presented some oscillations at the early stages, that decreased as the time increased. These oscillations can be minimized by again decreasing the spatial and time increments. Under those conditions the flow model generates accurate results when used to simulate unsaturated water flow.

At the time of writing the transport model was being checked, and it was established, that for the same situations used for the flow model, it can be used to simulate the movement of radionuclides through unsaturated soils.

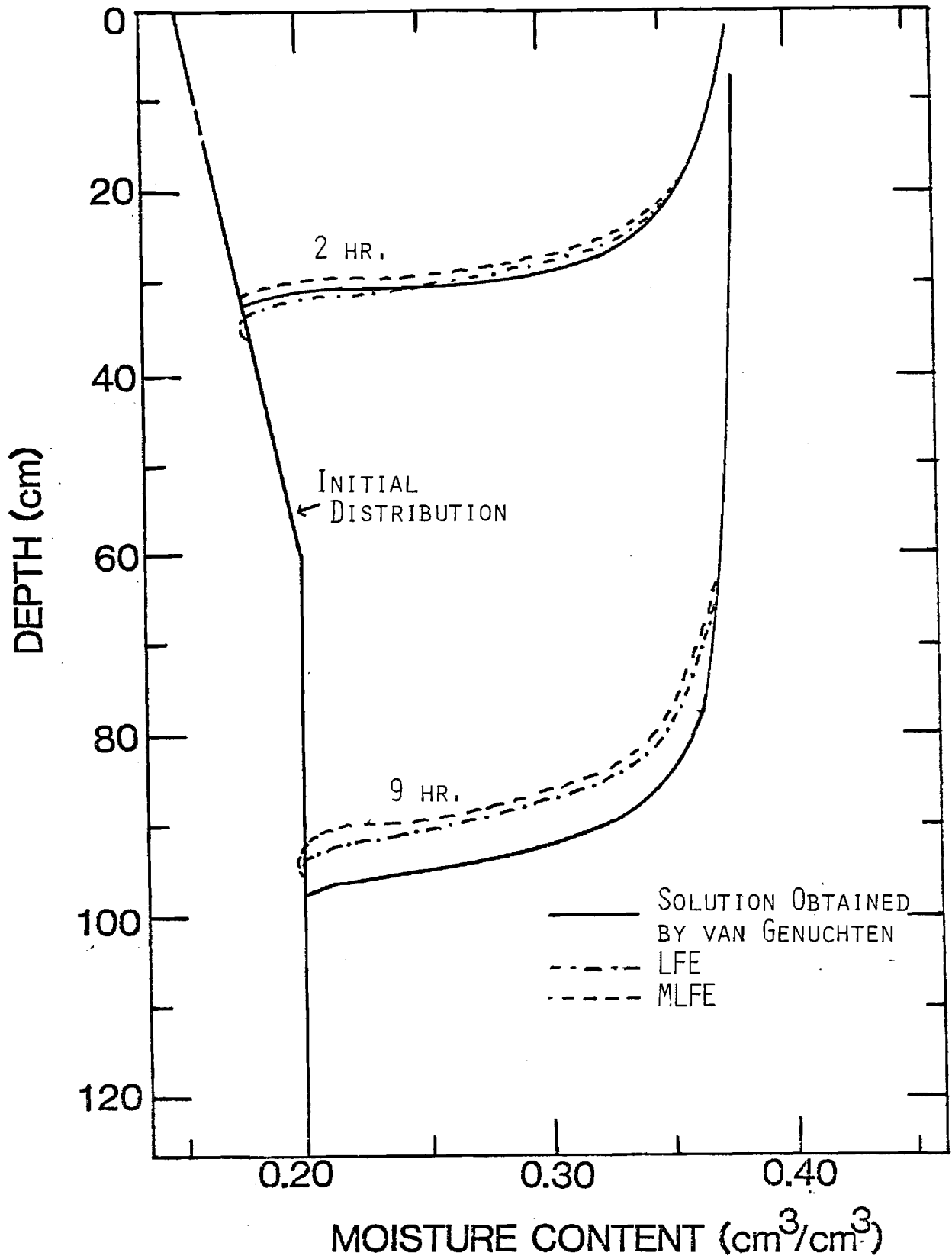


FIGURE 34 VERIFICATION OF FLOW MODEL

TRENCH FACILITY DESIGN

The work described above has provided some guides for the design of a facility that is specifically intended to minimize waste leaching by facilitating drainage through the backfill, thus preventing any standing water in the waste volume regardless of the condition of the cap. Since it has been shown that soils with a high clay content retain a substantial amount of moisture at all times, it is evident that a fairly permeable sandy loam would be preferred for the backfill material.

As Table 8 has shown, even for fairly sandy soil there will be a wet layer of up to 12cm above any gravel base; hence waste emplacement should be on top of a soil layer at least a foot thick. This will also facilitate waste placement and protect the gravel layer against the action of tracked vehicles in the trench.

Figure 35 is a generalized diagram of the trench design envisaged. (A mesh separator between backfill and gravel bed was considered, but present experience indicates that it is probably unnecessary). The main feature of importance is the gravel bed, which is common to most waste trenches, but assumes a central role in the present design. Given a reasonably permeable backfill soil, it is assumed that following a rainfall most of the infiltrated water will percolate rapidly through the backfill to reach the gravel bed, which must have enough capacity to store this water over a long enough period to permit slow, orderly seepage into the ground without backing up. The French drain bed shown would be needed only, if the surrounding soil is so impermeable that backup is still possible or if diversion for seepage to a more desirable, high-exchange capacity, soil is aimed for.

Calculation of Gravel Reservoir Requirements

The quantity of water that must be accommodated in a near-surface burial site is dependent on three major factors. These are the amount of precipitation, the rate of infiltration of water into the soil, and the rate of movement of the water within the soil. The latter two factors are interrelated, as the limiting factor may be either the rate of passage

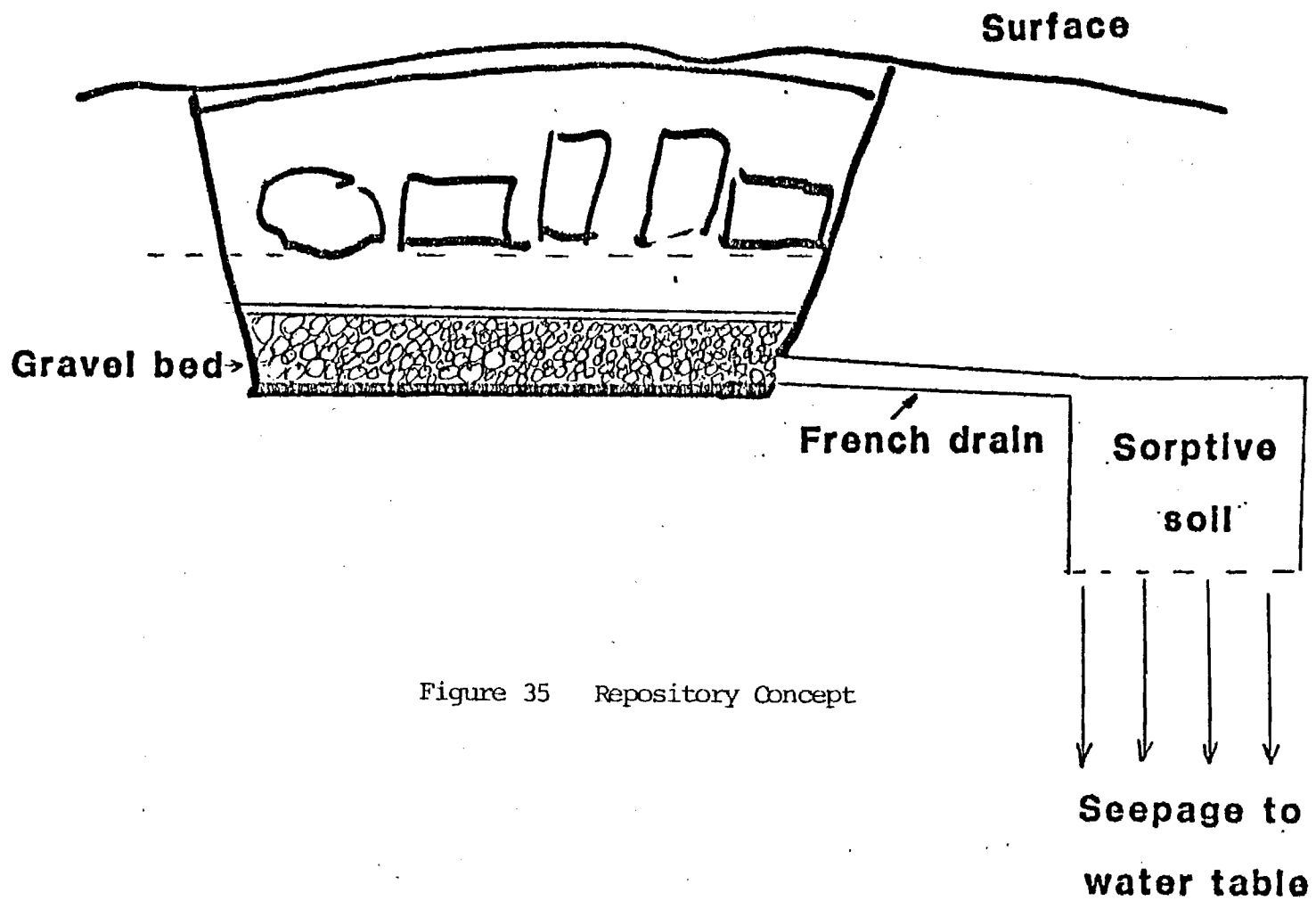


Figure 35 Repository Concept

through the air-soil interface or the rate at which water percolates away from the interface, leaving room for additional water to enter the soil.

Considering the width of a typical disposal trench and the fact that even compacted backfill is likely to be more permeable than most undisturbed soils, seepage from the trench walls may be considered insignificant compared with direct vertical movement. For very impermeable caps lateral flow around the cap edges may have to be considered, but this infiltration component would be otherwise indistinguishable from other infiltrated water as far as moisture retention and waste leaching are concerned. Any flow channeled along the trench wall is unlikely to interact with the waste and will only fractionally increase the reservoir capacity requirements.

The maximum rate at which water can enter the soil under given conditions is called the infiltration capacity. The actual infiltration rate equals the infiltration capacity only when the intensity of rainfall equals or exceeds the infiltration capacity. The infiltration capacity is at its maximum when the soil is dry, but decreases rapidly at the beginning of a storm and approaches a low, constant rate as the soil becomes saturated. The permeability of the subsoil becomes the ultimate limiting factor.

Soil type, moisture content, organic matter, vegetative cover, and other factors affect infiltration, but a decrease in rate with time is generally observed. This is shown in Fig. 36, where infiltration rate is plotted against time for two typical soil types (25). The difference between plots for dry (initial) conditions and wet condition demonstrates the large influence of existing moisture content of the soil.

For purposes of calculation, it was assumed that the soil of the burial site is similar to Houston black loam in its infiltration capacity. The scenario for the maximum volume of water would be to commence with dry soil. This allows a high rate of infiltration at the very start, but within 30 minutes this has fallen by approximately an order of magnitude with additional significant rate decrease in the subsequent hour. It is estimated that during the first three hours of rainfall of intensity

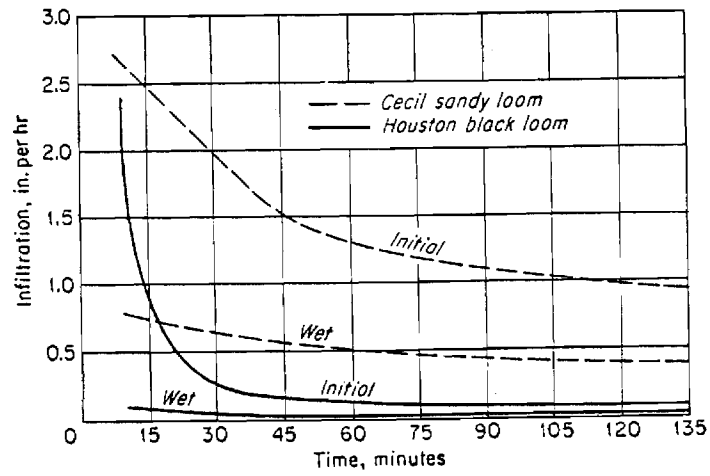


Figure 36 Comparative infiltration rates during initial and wet runs
(after Ref. 25)

sufficient to keep the soil surface covered, the total infiltration will be one inch. After three hours the rate for any continuing rainfall period is 0.05 in/hr, (0.125 cm/hr), the equilibrium flow rate.

The total inflow of water into the burial site during a given episode, therefore, depends on the length of time that the surface of the ground is wet enough to supply 0.05 in. of water per hour. No records of periods of continuous rainfall in the southeast have been located, and the Atlanta Weather Bureau is of the opinion that no such records have been kept. In reviewing the rainfall records for the Atlanta area, it was found that maxima are tabulated for one, two, and seven-day periods. It is considered unlikely that rain would occur continuously for more than a few days, based on seven-day records of 9 inches (10 year return), 10 inches (25 year return) and 12 inches (100 year return). It is therefore concluded that the maximum quantity of rainfall will be 9.25 inches, (23cm) obtained from the sum of one inch in three hours plus 0.05 in/hr. for 165 additional hours. It is further noted that the return period for this maximum is greater than 10 years, and is more likely to exceed 25 years.

This is based on the assumption of a week during which the rain falls steadily and virtually no surface run-off occurs, a set of circumstances that clearly would not occur very often. The quantity of infiltrated water would also be reduced by evapotranspiration, estimated at 0.25 inch per day. On this basis, the total quantity of water to be considered is reduced to 7.5 inches (18.75cm).

The passage of water from the surface of the ground to the junction with the water table is envisioned as follows: After penetration of the air-ground interface, the infiltrating fraction of the water proceeds downward at a slow rate determined by the characteristics of the compacted fill soil. It then enters the zone where waste materials have been placed. It is highly unlikely that the waste containers could ever be placed in a very tight configuration and cracks, crevices, and void spaces would be plentiful. Also, any back-filled soil that subsides into the main volume of waste is not likely to be very well compacted, so the entire waste zone will be conducive to the rapid percolation of water.

The rate of movement of water into the underlying and surrounding undisturbed soil will be lower than the rate of movement through the waste, so a storage volume beneath the waste will be required to prevent water from standing in the waste zone. It is estimated that infiltration will proceed twice as fast through the backfill as through the undisturbed lower strata, so for a steady input of 7.5 inches of water in a week, an accumulation of 2.25 inches (5.6cm) of water can be calculated.

The storage volume under the waste can best be provided by a layer of a highly porous nature. A granular material such as small gravel or coarse sand would be appropriate, but the interstices must be small enough to prevent significant invasion of fines with subsequent clogging. AASHTO number 89 stone would be an appropriate choice, as it would provide a very permeable zone and would not require the placement of a number of layers of different sized media. If compacted to a reasonable density, the void volume of 89 stone is in the 20-25% range. It would therefore require a theoretical depth of 11.25 inches to hold 2.25 inches of water. Such precision is not warranted and specification of one foot (30cm) of this material will assure a very conservative volume.

Placement of a foot of small gravel, such as 89 stone, under the disposal trenches is a reasonable measure which should provide long-term assurance that the layer would retain its capacity even with a limited amount of siltation from the lower reaches of the backfill.

It may occur that site considerations will make it desirable to increase the size of the drainage area or to move it completely from under the burial area. This can be accomplished by drain lines leading from the layer of emplaced gravel to another drain field. Clay pipes are satisfactory for this type of service as they are resistant to chemical deterioration, can be installed without any particular difficulty, and should remain trouble-free for a very long period of time. They are susceptible to breakage, however, and could be destroyed by the heavy equipment used to place and compact the waste materials.

While the installation of drain lines entirely across the bottom of the excavation within the gravel layer would provide very rapid discharge from the gravel, this is not mandatory. If the lines extend into the gravel a limited distance, the desired result will be obtained because of the very high rate of transmission of water by the gravel layer. From the practical view, it could be advisable to delay installation of the drain tile and its limited adjacent gravel area until the balance of the trench was already filled and compacted.

More than one line should be installed so that the system could operate in a fairly normal manner, even if some of the pipes were broken or became clogged with silt or roots. In the areas where exfiltration is intended, the pipes would be laid with open joints in ditches with a layer of gravel. Tight pipe joints would be used in any zone where dispersion of the water was not wanted.

The area of the extended drain field will be governed by the relative permeability of the subsoil in relation to the permeability of the soil cap covering the waste. In the situation of a remote drain field of the same area as that of the burial excavation, if the soil permeability is less than half of that of the cap, the potential maximum accumulation of water will be more than the 2.25 inches calculated above. This increase can be offset by a deeper gravel layer or a larger drain field, but the volume of the drain lines themselves may be large enough to be significant. In any event, the effect of pipe volume should be considered.

A downward slope of the drain lines is needed, but it does not have to be a very large slope. The usual design of a drain field involves parallel pipe lines fed by a header, but the long-term reliability of the system can be increased by the addition of extra connections at intervals between the parallel lines. This will provide a grid so that in the event of a stoppage, flow to most points can be provided from the other direction.

No unusual requirements are placed on the subsequent seepage path to the aquifer. A fairly clayey soil and a reasonable distance to the water table are desirable and the orientation of the drain field can be chosen to optimize the final water flow direction in this respect. Since the source term is expected to be lower, the retention capacity of the seepage path also need not be as high as for the saturated flow condition and a wider area can be drawn into service, subject mainly to cost and land use limitations.

CONCLUSIONS

The work described in this report addresses three issues: a) What are realistic flow conditions in a near-surface disposal trench?; b) How can the water content of the waste layers and the surrounding soil be minimized to permit source reduction?; and c) What modifications in conventional trench design are required to meet this objective?

It has been shown, both by laboratory column tests and with a larger test bed, that sandy or relatively permeable soils will drain fairly rapidly to a low residual moisture level as long as there is a gravel layer below the bed capable of receiving this water. In most parts of the United States rainfall and consequent infiltration into soil, even in the absence of an impermeable cap over the trench, result in a low enough water flow that drainage to unsaturated conditions can occur rapidly in most such cases. In the case of soils with a high clay content, such as the SRP #2 soil, drainage in compacted soil would be much slower, the residual water content may be of the order of 20 - 30% of saturated content, and the standing wet column above the soil-gravel interface may be of the order of a foot (30 cm). In general, such soils should be avoided in designing a drainable trench.

By downgrading the importance of a trench cap, the drained design places fewer limits on trench dimensions, since the gravel layer capacity has to be merely capable of accommodating the infiltrated water flow per unit area. The shaping of trench walls will be governed primarily by slope stability considerations, as in conventional trenches. In most other respects the introduction of the gravel layer at the trench bottom does not change any other trench parameters, other than the recommendation for a buffer soil layer between the gravel layer and the bottom of the waste emplacement. Waste spacing would still be governed primarily by subsidence considerations and ease of backfill. Where the compacted backfill soil is of low permeability, it is recommended to mix some sand into it to improve draining characteristics.

Grading of the backfill would be desirable only near the surface to the extent that a multilayer cap is desired to deflect water infiltration. However, this may be an unnecessary expense as some subsidence may still occur and only a specially constructed, relatively expensive reinforced trench cap would be expected to meet that objective completely over the design life of the facility.

For all but the most impermeable soil types, the extra drain field shown in Fig. 35 would not be needed. Instead, the gravel layer, with its low but freely mobile water layer, will provide a head for slow seepage of water into the underlying ground where, on the way to the water table, any remaining dissolved radionuclides would be subject to soil-sorption retardation effects. Because of the absence of standing water surrounding the waste materials there would be a much lower level of dissolved activity in the water, including probably a lower tritium content.

As expected, the leach tests done under simulated unsaturated flow conditions showed very low leach rates and, though these results cannot be considered conclusive at this stage, it is reasonable to assume that with less average water contact with the waste, the source term will be reduced proportionately. This reduction will then carry through into any calculations of predicted population dose from the facility.

The drained trench approach has been, incorrectly, described as a "controlled release" procedure, which would not be in accordance with 10CFR61 regulations. It would be more appropriate to say that it is a more realistic evaluation of what happens in a burial trench and is a preferable approach to a setting that invites bathtub conditions that would lead to uncontrolled release and a very rapid return of contaminants to the biosphere. The drained-trench approach is expected to reduce waste leaching significantly, though additional work is required to determine just how much. By eliminating standing water in the trench, frost and subsidence effects should be reduced. The backfill material would normally be more permeable than the undisturbed soil, resulting in lower residual moisture levels, but in some locations it may be desirable to mix some sand or sandy loam into the backfill.

The extra cost of providing a foot-deep layer of gravel or 89 stone is not significantly higher than the base preparation currently practiced in preparing disposal trenches. An extensive drain field would entail additional costs compared with current procedures, but would not be needed in most cases; on the other hand, much of this added cost would be recovered by the lesser need for very rigid and elaborate cap designs that are proposed by some at present (26). The principal benefit of this approach lies in the expected reduction in source terms, thus meeting the ALARA criterion.

The work has shown the importance of taking unsaturated flow conditions into account in designing a facility and assessing its impact. Although it is easier and "conservative" to model saturated flow, it is evident that the calculated impacts may be orders of magnitude too high and give an unrealistic impression of the radiological consequences of trench construction (27). It is still important to bury predominantly solid waste, but in a carefully chosen medium proper drainage would be expected to provide better insurance in the long run against excessive leaching and release, than reliance on trench cap performance.

ACKNOWLEDGMENTS

We are indebted to Mr. Ed Johnson of the Georgia Highway Department for providing some gravel for this project and to Mr. Jerry A Connor of the Georgia Tech Physical Plant Department for arranging the trench excavation and supplying sand and other materials.

BIBLIOGRAPHY

1. J.S. Baldwin et al., Procedures and Technology for Shallow Land Burial. Rept. DOE/LLW - 13 Td, National Low-level Radioactive Waste Management Program, Idaho Falls, ID, 1983
2. Rogers & Associates Engineering Corp., A Handbook For Low-level Radioactive Waste Disposal Facilities. Rept. NP-2488LD, Electric Power Research Institute, Palo Alto, CA, 1982
3. M.A. Feraday. A Prospectus for the Development of Shallow Land Burial Disposal Concepts for the CRNL Site. Rept. TR-307, Chalk River Environmental Authority, Chalk River, Ont., 1983
4. A.A. Metry, D.R. Phoenix and A.L. Lenthe, In-site Stabilization of a Low-level Radioactive Site - a case history. Roy Weston Inc., West Chester, PA, 1982
5. J.G. McCray, E.A. Nowatzki and G.M. Thompson, Performance of Shallow Land Burial Trench Caps - Assessment of the soil arch and soil beam concept. Proc. 5th Annual Participants Information Meeting, LLWMP, CONF-8308106, p. 167, 1983
6. F. Homan. Design of the Central Waste Disposal Facility at Oak Ridge National Laboratory (unpublished), 1984
7. G.G. Eichholz, F.N. deSousa, M.F. Petelka and J. Whang. Evaluation and Design of Drained Low-level Disposal Sites. Proc. 6th Annual Participants Information Meeting, Denver, 1984
8. B. Yaron, G. Dagan and J. Goldshmid (eds). Pollutants in Porous Media. Springer Verlag, Berlin, 1984
9. Licensing Requirements for Land Disposal of Radioactive Waste. Final Environmental Impact Statement on 10CFR61. Rept. NUREG - 0945, U.S. Nuclear Regulatory Commission, Washington, D.C. 1982
10. Management of Commercially Generated Radioactive Waste. Final Environmental Impact Statement. Rept. DOE/EIS-0046F, U.S. Dept. of Energy, Wasington, D.C. 1980
11. G.D. DeBuchananne. Geohydraulic Considerations in the Management of Radioactive Waste. Nuclear Technology 24, 356-361 (1974)
12. R.J. Serne and J.F. Relyea. The Status of Radionuclide Sorption-Desorption Studies Performed by the WRIT Program; in The Technology of High-Level Nuclear Waste Disposal, Vol. 1, U.S. Dept. of Energy, 1981

13. L.L. Ames and D. Rai. Radionuclide Interactions with Soil and Rock Media. Rept. EPA 520/6-78-007, U.S. Environmental Protection Agency, Las Vegas, NV, 1978
14. National Low-Level Radioactive Management Program. Managing Low-Level Radioactive Wastes: A Proposed Approach. Rept. DOE/LLW-9, EG&G Idaho, 1983
15. D.G. Jacobs, J.S. Epler and R.R. Rose. Identification of Technical Problems Encountered in the Shallow Land Burial of Low-Level Radioactive Wastes. Rept. ORNL/SUB-80/13619/1, Oak Ridge National Lab, 1980
16. J. Bear, D. Zaslavsky and S. Irmay, Physical Principles of Water Percolation and Seepage. UNESCO, Paris, 1968
17. G.L. DePoorter, W.V. Abeele, B.W. Burton, T.E. Hakonson and B.A. Perkins. Shallow Land Burial Technology Development - Arid. Proc. 4th Annual Participants Information Meeting - DOE - LLWMP, Rept. ORNL/NFW-82/18, 539-566, 1982
18. W.V. Abeele, G.L. DePoorter, T.E. Hakonson and T.W. Nyhan. Shallow Land Burial Technology - Arid. Proc. 5th Annual Participants Information Meeting, LLWMP, CONF-8308106, p. 140, 1983.
19. T.N. Nyhan, W.V. Abeele, G.L. De Poorter, T.E. Hakonson, B.A. Perkins and G.R. Foster. Field Studies of Erosion Control Technologies for Arid Shallow Land Burial Sites at Los Alamos. Proc. 5th Annual Participants Information Meeting, LLWMP, CONF-8308106, p. 193, 1983
20. R.K. Schulz. Study of Unsaturated Zone Hydrology at Maxey Flats. Proc. 5th Annual Participants Information Meeting, LLWMP, CONF-8308106, p. 674, 1983
21. E.C. Davis, B.P. Spalding and S.Y. Lee. Shallow Land Burial Technology - Humid. Proc. 5th Annual Participants Information Meeting, LLWMP, CONF-8308106, p. 121, 1983
22. H.D. Foth and L.M. Turk. Fundamentals of Soil Science, 5th edition. John Wiley & Sons, New York, 1972
23. C. Pescatore and A.J. Machiels. Effects of Water Flow Rates on Leaching; in Geochemical Behavior of Disposed Radioactive Waste, G.S. Barney, J.D. Navratil and W.W. Schulz eds., American Chemical Society, Washington, D.C. 1984
24. S.B. Oblath, J.A. Stone and J.R. Wiley. Special Wasteform Lysimeter Program at the Savannah River Laboratory. Proc. 5th Annual Participants Information Meeting - DOE - LLWMP. CONF-8308106, 441-448, EG&G Idaho, 1983

25. G. R. Free, G. M. Browning, and G. W. Musgrave. Relative Infiltration and Related Physical Characteristics of Certain Soils, U.S. Dept. Agr. Tech. Bull. 729, 1940.
26. L.G. Mezga. The Role of Trench Caps in the Shallow Land Burial of Low-level Wastes. Rept. ORNL-TM-9156, Oak Ridge National Lab., 1984.
27. C. N. Ostrowski, T. J. Nicholson, D. D. Evans and D. H. Alexander, Disposal of High-level Wastes in the Unsaturated Zone: Technical Considerations. Rept. NUREG-1046, U.S. Nuclear Regulatory Commission, Washington, D.C. 1984.
28. M.T. Van Genuchten. Mass Transport in Saturated - Unsaturated Media: One-dimensional Solutions. Reserch Rept. 78-WR-11 Water Resources Program, Princeton Univ., Princeton, NJ, 1978.
29. A.W. Warrick, T.W. Biggar and D.R. Nielsen. Simultaneous Solute and Water Transfer for an Unsaturated Soil. Water Resources Res. 7, 1216-1225, (1971).

APPENDIX A

Water Characteristics, Hydraulic Conductivity and Sorption Models

by F. N. Carneiro de Sousa

What makes the unsaturated flow equation difficult to solve is the fact that the pressure head and the hydraulic conductivity are both a function of the water content; these relations can be incorporated in the model in table form or by means of analytical expressions. In this study the available data for each soil type was fitted to three different analytical relations, which were called Brooks and Corey, Haverkamp, and Van Genuchten models.

The solution of the transport equation needs also a relation to represent the sorption process. The model was developed in such a way that any equilibrium sorption model can be used, and the three most used ones are described in this section. Some alterations have to be done if a kinetic sorption model is to be used.

1. - Water characteristics and Hydraulic Conductivity Models

a - Brooks and Corey

Brooks and Corey (1964) suggested the following relation to represent the soil-water characteristics

$$\frac{\theta - \theta_r}{n - \theta_r} = \left(\frac{\psi_e}{\psi} \right)^\lambda \quad (\text{A.1})$$

where θ is the volumetric water content, n is the porosity, θ_r is the residual water content, ψ is the soil suction, ψ_e is the air-entry value, and λ is the pore-size distribution index.

The associated hydraulic conductivity is given by

$$K = K_s \left(\frac{\theta - \theta_r}{n - \theta_r} \right)^{\frac{2 + 3\lambda}{\lambda}} \quad (\text{A.2})$$

where K is the unsaturated hydraulic conductivity and K_s is the saturated one. This equation was obtained by Brooks and Corey with the use of the Burdine theory (see Van Genuchten model). If the Mualem theory is used the equation becomes

$$K = K_s \left(\frac{\theta - \theta_r}{n - \theta_r} \right)^{\frac{4 + 5\lambda}{\lambda}} \quad (\text{A.3})$$

This set of equations is one of the most used to describe the hydraulic properties of the soil.

b - Haverkamp

Haverkamp (Haverkamp et al., 1977) proposed the following relation for the soil-water characteristics based on laboratory infiltration experiments:

$$\theta = \frac{\alpha (n - \theta_r)}{\alpha + |h|^\beta} + \theta_r \quad (\text{A.4})$$

where n is the porosity, θ_r is the residual water content, h is the pressure head, and α and β are empirical constants.

As is discussed by McKeon (McKeon et al., 1983), this relation provides for the proper behavior of the soil-water characteristics, since as h approaches zero, the water content approaches saturation, and as h assumes large negative values, the water content approaches the residual value.

The associated hydraulic conductivity relation is given by

$$K = K_s \left(\frac{A}{A + |h|^\beta} \right) \quad (\text{A.5})$$

where K_s is the saturated hydraulic conductivity and A and β are empirical constants.

c - Van Genuchten

Van Genuchten (1978) presents a relation for the soil-water characteristics which is a development of the Haverkamp relation; it is given by

$$\theta = (n - \theta_r) \left(\frac{1}{1 + |\alpha h|^\beta} \right)^\lambda + \theta_r \quad (\text{A.6})$$

where α and β are empirical constants and $\lambda = 1 - 1/\beta$. This equation provides the same limits and smoothness as those obtained with the Haverkamp model.

The hydraulic conductivity/water content relation presented by Van Genuchten (1980) is an integral form of the Childs and Collis-George (1950) equation, which is an attempt to calculate the unsaturated hydraulic conductivity using a pore-size distribution obtained from the soil-water characteristics curve. Several investigators modified the equation, and Mualem (1976) presented a simple analytical model given by

$$K_r(\theta) = \frac{\left\{ S_e^\beta \sum_{i=1}^m \frac{2(n-i)+1}{\psi_i^2} \right\}}{\left\{ \sum_{i=1}^m \frac{2(m-i)+1}{\psi_i^2} \right\}} \quad (\text{A.7})$$

where m represents the total number of intervals into which the water content is divided (water characteristics curve), n is the number of intervals up to a prescribed value of θ , β is a constant related to the pore-size distribution, $S_e = (\theta - \theta_r) / (n - \theta_r)$, and $K_r = K/K_s$. If $\beta = 0$, Collis-George equation is obtained; if $\beta = 4/3$, it becomes Millington and Quirk (1959) equation; if $\beta = 1$ Kunze (Kunze et al., 1968) is obtained. Mualem (1976) presented an alternative formulation given by

$$K_r = (S_e)^{1/2} \left[\int_0^{S_e} \frac{dS_e}{dh} \bigg/ \int_0^1 \frac{dS_e}{dh} \right]^2 \quad (\text{A.8})$$

A similar equation is given by Burdine (1958)

$$K_r = S_e^2 \left[\int_0^{S_e} \frac{1}{h^2} dx \bigg/ \int_0^1 \frac{1}{h^2} dx \right] \quad (\text{A.9})$$

The equation presented by Van Genuchten (1980) is an integral form of the Millington and Quirk equation, and is given by

$$K = K_s S_e^{1/2} \left[1 - (1 - S_e^{1/\lambda})^\lambda \right]^2 \quad (\text{A.10})$$

where $S_e = (\theta - \theta_r) / (n - \theta_r)$, and λ and β and α (from eq. A. 6) are empirical constants obtained from the shape of the water characteristics curve. The advantage of this model is the ability to fit data in the near saturation range.

2-Equilibrium Sorption Isotherms

a-Linear Adsorption

The linear adsorption isotherm is the most common relation used to simulate the sorption of radionuclides by the soil particles. It is given by

$$S = K_d C \quad (\text{A.11})$$

where S is the amount of solution absorbed by the soil matrix, C is the concentration of solute in the soil solution and K_d is the distribution coefficient. The velocity of the tracer (V_t) is related to the water velocity (V_e) by

$$V_t = V_w / R \quad (\text{A.12})$$

where R is the retardation factor which is given by

$$R = 1 + \frac{\rho K_d}{\theta} \quad (\text{A.13})$$

where ρ is the bulk density.

The disadvantage of this relation is that it assumes equilibrium conditions, and it does not describe a maximum quantity of adsorption. On the other hand, its use makes the transport equation linear, facilitating the numerical simulation. A similar relation is presented by Lapidus and Amundson (1952),

$$S = K_1 C + K_2 \quad (\text{A.14})$$

where K_1 and K_2 are constants.

b - Freundlich Isotherm

The Freundlich (1926) isotherm is given by

$$S = K C^n \quad (\text{A.15})$$

where S is the amount of solute adsorbed per unit weight of soil, C is the equilibrium solute solution concentration, and K and n are constants. If n is equal to zero, it becomes the linear isotherm. The disadvantages are that equilibrium conditions are assumed, it does not specify a maximum quantity of adsorption, and its use makes the transport equation non-linear, which implies in an iterative solution.

c-Langmuir Isotherm

The Langmuir isotherm (1918) was originally developed to describe the adsorption of gas molecules onto the surface of solids; it was after extended to represent the adsorption of aqueous solutes onto solid sorbates. It is given by

$$S = \frac{K b C}{1 + K C} \quad (\text{A.16})$$

where S is the amount of solute adsorbed for unit mass of solid, C is the equilibrium solute concentration, K is a constant related to the energy of adsorption, and b is the maximum amount which can be adsorbed by the solid. It becomes the linear isotherm as C approaches zero. The disadvantage is that it assumes equilibrium conditions, and the transport equation becomes non-linear when it is used.

Other equilibrium sorption isotherms as well as kinetic sorption models are given by Travier and Etnier (1981).

APPENDIX B

MODEL IMPLEMENTATION

In this appendix a description is given of the one-dimensional unsaturated flow and transport mode. The program consists of a main program and 12 subroutines. The main program is responsible for the organization of the program, basically, it performs the scheme shown in Fig. 37.

Subroutine INPU1 is used to initialize the values of all variables needed for the solution of the water flow equation; it defines the geometry and the initial and boundary conditions of the case under study; it also introduces the physical and chemical properties of the soils. Subroutine INPU2 is used to introduce the values of the variables needed to obtain the solution of the transport equation; it includes the initial and boundary conditions as well as the soil properties that were not already introduced by INPU1.

Subroutine SET performs a coordinate transformation; it changes the global coordinates of the nodes of each element to a local coordinate system, which simplifies the evaluation of the element matrices.

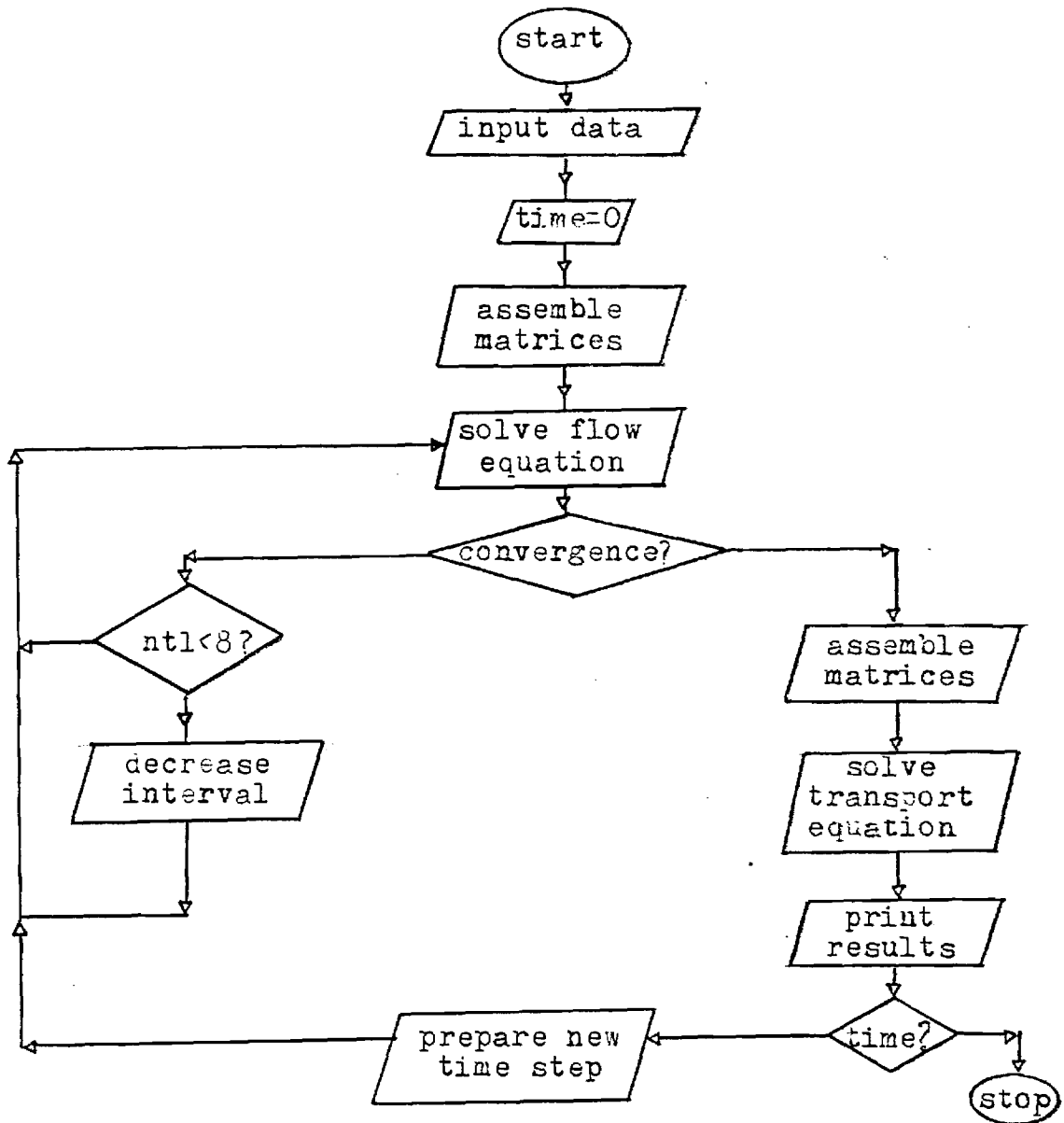


Fig. 37 Model Flow Diagram

Subroutine ELEM generates the local element matrices by calculating each coefficient of the matrices necessary to solve the matrix flow equation. Subroutine ELEM 1 does the same calculations for the transport equation. The soil properties needed for the evaluation of the matrix coefficients are calculated in subroutine HCWC, which is called by subroutine ELEM.

Once the global matrices are assembled, a set of partial differential equations is obtained; these equations are solved by applying a finite difference scheme, and this is done in subroutine CALC1. This subroutine is also responsible for the introduction of the boundary conditions. The output of this subroutine is a system of ordinary equations which is solved by subroutine SOLVE. The method used to solve these equations is the Thomas algorithm, which is a special form of the Gaussian elimination method.

When the solution is obtained for the flow equation, the convergence criteria is checked by subroutine ERROR. If convergence is not attained, the iterative process continues; if convergence is attained, the variables needed for the solution of the transport equation are evaluated by subroutine PROP and the transport equation is then solved. Subroutine OUT presents the values of the hydraulic head, water content, and solute concentration at each time interval.

Table B.1 presents the major variables used in the numerical implementation of the program; Table B2 presents the input cards needed to solve the flow equation, and Table B.3 presents the listing of the actual program.

TABLE B.1 - PROGRAM VARIABLES

AG(30.3)	- Global matrix
AI(3)	- Residual Water Content of each soil
AL1	- Distance between the two last nodes of the soil column.
ALF(3)	- Compressibility of the soil
BI(3)	- Value of α in eq. A.4 and A.5, and value of β in eq. A.1
BUD(3)	- Bulk density of the soils.
CI(3)	- Pore-size distribution index.
CL	- Value of the constant concentration at the last node of the column when a constant boundary condition is used.
CO(20)	- Variable concentration at the top of the column when a variable boundary condition is used.
CON(30)	- Concentration at time t .
CONI(30)	- Initial concentration profile.
COO	- Constant concentration at surface when a constant boundary condition is used.
DEV(30)	- Value of σ at each node.
DEVO(30)	- Value of σ_0 at each node.
DI(3)	- Value of A in EQ. A.5
DICO(30)	- Distribution coefficient of each soil
DIFU(3)	- Diffusion coefficient of each soil
DISP(3)	- Dispersivity of each soil.
EI(3)	- Value of ϵ in eq. A.5
ERR1	- Value of ϵ_1 in eq. VII. 31.
ERR2	- Value of ϵ_2 in eq. VII.31.
FLUX(30)	- Value of the water flux at each node.
GAM(3)	- Zero-order rate constant of each soil.

TABLE B.1 cont.

HCl	- Hydraulic conductivity of the first node
HCL	- Hydraulic conductivity of the last node.
HCOS(3)	- Saturated hydraulic conductivity of each soil.
HEDI1	- Value of the pressure head at first node of each element at time
HEDI2	- Value of the pressure head at second node of each element at time
HEDIL(30)	- Value of the pressure head at each node at time t.
HEDIN(30)	- Value of the pressure head at each node at time .
HEDIX(30)	- Value of the pressure head at each node at time .
HEDO	- Value of the initial pressure head if it is constant through the soil column.
HL	- constant pressure head at the last node if a constant boundary condition is used.
HO	- Constant pressure head at surface if a constant boundary condition is used.
I1	- Determines which sorption model is used. = 1 Linear adsorption isotherm.
I2	- Determines which soil-water characteristics model is used. = 1 Brooks and Corey = 2 Van genuchten = 3 Haverkamp
I3	- Determines which hydraulic conductivity model is used. = 1 Brooks and Corey = 2 Van genuchten = 3 Haverkamp
I4	- If it is equal to one $Q_0(I) = \text{constant}$.
ICON(30,2)	- Relates each node number to its element.
IE	- Constant used to indicate if convergence is attained.
IK	- Constant used to indicate which soil type applies to each element.
IKK	- Constant used to indicate which value of the constant flux at surface is being used

TABLE B.1 cont.

ISA	- Constant used to indicate if the initial concentration is constant over the whole soil profile.
ISP	= 1 equally spaced nodes.
ISS	= 1 Constant initial pressure head.
IST	= 1 Homogeneous soil
ISU	= 1 Transport model is used
ISX	= 1 Mass lumping is used.
JI(3)	- Contains the node number at which each soil type ends.
K1	= 1 Constant concentration at surface.
K2	= 1 Constant flux of concentration at surface at each specified time.
K3	= 1 Free draining profile.
K4	= 1 Constant concentration at last node.
K21	= 1 Constant flux of concentration at surface.
KB1	= 1 Constant flux at surface.
KB2	= 1 Constant flux at last node.
KB3	= 1 Constant pressure head at surface.
KB4	= 1 Constant pressure head at last node.
KB5	= 1 Variable flux at last node.
NELEM	- Number of elements used.
NEWN(2)	- Contains the nodes numbers for each element.
NL	- Number of iterations at each time step.
NNODE	- Number of nodes.
NST	- Maximum number of iterations allowed at each time step.
NT	- Counts number of time steps.
NTM	- Maximum number of time steps allowed.

TABLE B.1 cont.

PF(30)	- Global matrix.
PORO(3)	- Porosity of each soil type.
QL	- Constant flux at last node.
QO(20)	- Values of constant flux at different times at surface.
SCAP1	- Soil water capacity of first node of an element.
SCAP2	- Soil water capacity at second node of an element.
SS(3)	- Specific storage of each soil.
TETIX(30)	- Water content at each node at time .
TETOX(30)	- Water content at each node at time t.
TI	- Time since start of simulation.
TIM	- Value of the time interval at time t.
TIMAX	- Maximum time interval allowed.
TIME	- Total time of simulation.
TIMEX(20)	- Time at which constant flux ends at the surface.
TIMIN	- Minimum time interval allowed.
TIVAL	- Time interval at time t+ t
TORT(3)	- Tortuosity factor of each soil.
XL	- Length of the soil profile.
XLAM	- Decay rate fo the radionuclide under study.
XMG(30,3)	- Global matrix.
W	= 0 explicit algorithm is used. = 1/2 Crank-Nicholson algorithm is used. = 1 Implicit algorithm is used.
Z(30)	- global coordinates of the nodes.

TABLE B.2 - INPUT DATA FOR FLOW EQUATION

CARDS	COLUMNS	FORMAT	VARIABLE
1	1-8	F8.3	XL
	9-16	F8.3	TIME
	17-24	F8.5	TTIVAL
	25-32	F8.3	TIMAX
	33-40	F8.5	TIMIN
	41-48	F8.3	
	49-53	I5	NELEM
	54-58	I5	NTM
	59-63	I5	NST
	2	1	I5
3	1	I5	ISS
4	1	F8.3	HEDO
5	1	I5	IST
6-8	1-8	F8.3	AI(3)
	9-16	F8.3	BI(3)
	17-24	F8.3	CI(3)
	25-32	F8.3	DI(3)
	33-40	F8.3	DI(3)
	41-48	F8.3	HCOS(3)
	49-56	F8.3	PORO(3)
	57-64	E8.3	SS(3)
	65-69	I5	JI(3)
	9	1-5	I5
6-13		F8.3	ERR1
14-21		F8.3	ERR2
22-26		I5	I1
27-31		I5	I2
32-36		I5	I3
36-40		I5	I4
10		1-5	I5
	6-10	I5	KB2
	11-18	F8.3	QL
	19-23	I5	KB3
	24-28	I5	KB4
	29-35	F8.3	HO
	36-42	F8.3	HL
	43-47	I5	KB5
11	1	F8.3	QOO
12	1	I5	ISX

```

PROGRAM OEDIT(IN,OUT,TAPE5=IN,TAPE6=OUT)
DIMENSION Z(30),ICON(30,2),HEDIN(30),AI(3),BI(3),CI(3),DI(3),
1 EI(3),HCO3(3),PORO(3),SS(3),TIMEY(20),QO(20),XSG(30,3),
2 XMG(30,3),XPG(30),ZE(2),NEWN(2),JI(3),XM(2,2),XS(2,2),
3 XP(2),TMG(30,3),FPG(30,3),HEDIX(30),HEDIL(30),PF(30),
4 TETIX(30),HEDIS(30),HEDIP(30)
*
----READ INPUT VALUES----
REWIND 6
CALL INPU1(XL,TIME,TIVAL,TIMAX,TIMIN,NELEM,W,NNODE,Z,HEDIN,
1 AI,BI,CI,DI,EI,HCO3,PORO,SS,ISU,I1,I2,I3,ERR1,ERR2,KB1,KB2,
2 KB3,KB4,KB5,QO,QL,HO,HL,ISX,TIMEY,NTM,NST,JI,ICON)
*
----DETERMINE IF TRANSPORT EQUATION IS USED----
*
IF(ISU.LT.1)GO TO 2
*
CALL INPU2(
* 2 CONTINUE.
NL=1
NT=1
NNN=1
DO 3 I=1,NNODE
HEDIP(I)=HEDIN(I)
HEDIS(I)=HEDIN(I)
3 HEDIL(I)=HEDIN(I)
TIM=TIVAL
IKK=1
IK=1
TI=0
TI=TI+TIVAL
6 DO 10 I=1,NNODE
DO 10 J=1,3
XSG(I,J)=0
XMG(I,J)=0
10 XPG(I)=0
*
----DETERMINE LOCAL MATRICES----
DO 20 I=1,NELEM
HEDI1=HEDIN(I)
HEDI2=HEDIN(I+1)
DO 15 J=1,2
15 NEWN(J)=ICON(I,J)
*
WRITE(6,1102)NEWN
*1102 FORMAT(/2I5,(NEW NODE/))
CALL SET(NEWN,ZE,Z,NELEM,ISP,XL)
CALL ELEM(HEDI1,HEDI2,PORO,SS,ISX,I2,I3,HCO3,AI,BI,CI,DI,EI,
1 JI,NEWN,IK,ZE,XM,XS,XP,NNODE,HC1,HCL,AL1)
*
----ASSEMBLE GLOBAL MATRICES----
20 CALL ASSEM(NEWN,XM,XMG,XS,XSG,XP,XPG)
*
----INTRODUCE BOUNDARY CONDITIONS----
CALL CALC1(TIVAL,HEDIS,XMG,XSG,XPG,NNODE,W,KB1,KB2,KB3,KB4,
1 KB5,QO,QL,HO,HL,TIMEY,TI,HC1,HCL,AL1,IKK,TMG)
CALL SOLVE(TMG,XPG,HEDIX,FPG,NNODE)
*
----CHECK FOR CONVERGENCE----
CALL ERROR(HEDIX,HEDIL,IE,ERR1,ERR2,NNODE)
*
WRITE(6,111)(HEDIX(I),HEDIL(I),I=1,NNODE)
* 111 FORMAT(3X,F8.3,3X,F8.3)
IF(NNN.GT.1)GO TO 21
TI=TIVAL
21 IF(IE.EQ.0)GO TO 50
IF(NL.LE.NST)GO TO 25
TI=TI-.5*TIVAL
TIVAL=0.5*TIVAL
IF(TIVAL.LT.TIMIN)GO TO 100
DO 22 I=1,NNODE
HEDIN(I)=HEDIS(I)+(TIVAL/(2*TIM))*(HEDIS(I)-HEDIP(I))

```

```

22 HEDIL(1)=HEDIX(1)
NL=1
GO TO 6
25 DO 30 I=1,NNODE
HEDIN(I)=0.5*(HEDIX(I)+HEDIS(I))
30 HEDIL(I)=HEDIX(I)
NL=NL+1
GO TO 6
* ----CONVERGENCE IS ATTAINED----
50 IF(NNN.GT.1)GO TO 55
TI=TIVAL
55 DO 57 I=1,NNODE
H=ABS(HEDIX(I))
HH=29.484
IF(H.GT.HH)GO TO 56
TETIX(I)=.4581-.02732*LOG(H)
GO TO 57
56 TETIX(I)=.6829-.09524*LOG(H)
57 CONTINUE
CALL OUT(TI,Z,HEDIX,NT,NL,NNODE,TETIX)
NNN=NNN+1
DO 60 I=1,NNODE
HEDIN(I)=HEDIX(I)+(TIVAL/(2*TIM))*(HEDIX(I)-HEDIS(I))
HEDIP(I)=HEDIS(I)
HEDIS(I)=HEDIX(I)
60 HEDIL(I)=HEDIN(I)
IF(NL.GT.3)GO TO 70
TIVAL=1.5*TIVAL
IF(TIVAL.LE.TIMAX)GO TO 70
TIVAL=TIMAX
70 NT=NT+1
TI=TI+TIVAL
IF(TI.GT.TIME)GO TO 100
IF(NT.GT.NTM)GO TO 100
NL=1
TIM=TIVAL
GO TO 6
100 WRITE(6,1001)TI,NT
1001 FORMAT(3X,"PROGRAM TERMINATED WITH TI=",1X,F8.5,2X,"AND NT=",
1 2X,I5)
STOP
END
SUBROUTINE INPUT(XL,TIME,TIVAL,TIMAX,TIMIN,NELEM,W,NNODE,Z,
1 HEDIN,AI,BI,CI,DI,EI,HCOS,PORO,SS,ISU,I1,I2,I3,ERR1,ERR2,
2 KB1,KB2,KB3,KB4,KB5,GO,QL,HO,HL,ISX,TIMEX,NTM,NST,JI,ICON)
DIMENSION Z(30),HCOS(3),PORO(3),SS(3),TIMEX(20),GO(20),JI(3),
1 ICON(30,2),HEDIN(30),AI(3),BI(3),CI(3),DI(3),EI(3)
WRITE(6,1000)
READ(5,1010)XL,TIME,TIVAL,TIMAX,TIMIN,W,NELEM,NTM,NST
WRITE(6,1020)XL,TIME,TIVAL,TIMAX,TIMIN,W,NELEM,NTM,NST
NNODE=NELEM+1
* ----DETERMINE GLOBAL COORDINATES OF THE NODES----
READ(5,1030)ISP
DO 1 I=1,NNODE
1 Z(I)=0
IF(ISP.LT.1)GO TO 5
DO 2 I=1,NNODE
Z(I)=(I-1)*XL/NELEM
2 WRITE(6,1040)I,Z(I)
GO TO 10
5 DO 7 I=1,NNODE
READ(5,1050)Z(I)
7 WRITE(6,1040)I,Z(I)

```

```

10      DO 12 I=1,NLEFT
        DO 12 J=1,2
12      ICON(I,J)=I+J-1
*      ----OBTAIN INITIAL PRESSURE HEADS----
        READ(5,1030)ISS
        IF(188.LT.1)GO TO 17
        READ(5,1050)HEDC
        WRITE(6,1070)HEDC
*      DO 15 I=1,NNODE
        DO 15 I=1,12
        XX=.15+.000833*(I-1)*5/1
        XXX=(.6829-XX)/.09524
        HEDIN(I)=-EXP(XXX)
15      WRITE(6,1040)I,HEDIN(I)
        DO 16 J=13,26
        HEDIN(I)=HEDC
16      WRITE(6,1040)I,HEDIN(I)
* 15      HEDIN(I)=HEDC
        GO TO 20
17      DO 18 I=1,NNODE
        READ(5,1050)HEDIN(I)
18      WRITE(6,1040)I,HEDIN(I)
20      READ(5,1030)IST
        IF(IST.LT.1)GO TO 25
        READ(5,1090)AII,BII,CII,DII,EII,HCOSI,POROI,SSI,JII
        WRITE(6,1100)AII,BII,CII,DII,EII,HCOSI,POROI,SSI,JII
        DO 22 I=1,3
        AI(I)=AII
        BI(I)=BII
        CI(I)=CII
        DI(I)=DII
        EI(I)=EII
        HCOS(I)=HCOSI
        PORO(I)=POROI
        JI(I)=JII
22      SS(I)=SSI
        GO TO 30
25      DO 28 I=1,3
        READ(5,1090)AI(I),BI(I),CI(I),DI(I),EI(I),HCOS(I),PORO(I),
1      SS(I),JI(I)
28      WRITE(6,1100)AI(I),BI(I),CI(I),DI(I),EI(I),HCOS(I),PORO(I),
1      SS(I),JI(I)
30      CONTINUE
*      ----DETERMINE IF TRANSPORT MODEL IS USED----
        READ(5,1105)ISU,ERR1,ERR2,I1,I2,I3,I4
*      ----OBTAIN BOUNDARY CONDITIONS----
        READ(5,1110)KB1,KB2,QL,KB3,KB4,H0,HL,KB5
        IF(KB3.LT.1)GO TO 31
        HEDIN(1)=H0
31      IF(KB4.LT.1)GO TO 315
        HEDIN(NNODE)=HL
*      HEDIN(NNODE)=HL
*      IF(I4.LT.1)GO TO 32
315      READ(5,1050)Q00
        DO 316 I=1,20
        TIMEX(I)=TIME
316      Q0(I)=0.
*      Q0(1)=0.
*      TIMEX(1)=TIME/2.
*      Q0(2)=Q00
*      TIMEX(2)=TIME
        GO TO 40
32      DO 35 I=1,20

```

```

      READ(5,1120) T1,T2,XL,Z,NELEM
35      WRITE(6,1130) TIMEX(I),GO(I)
*      -----DETERMINE IF MASS LUMPING IS USED-----
40      READ(5,1030) ISX
*      -----
1000     FORMAT(/,7X,"UNSATURATED FLOW AND TRANSPORT",/)
1010     FORMAT(2F8.3,F8.5,F8.3,F8.5,F8.3,3I5)
1020     FORMAT(3X,"XL=",F8.3,3X,"TIME=",F8.3,3X,"TIVAL=",E8.3,3X,
1       "TIMAX=",F8.3,/,3X,"TIMIN=",E8.3,3X,"W=",F8.3,3X,"NELEM=",
2       I5,3X,"NTM=",I5,3X,"NST=",I5)
1030     FORMAT(I5)
1040     FORMAT(4X,I4,6X,F8.3)
1050     FORMAT(F8.3)
1070     FORMAT(/,4X,"HEDG=",F8.3)
1090     FORMAT(7F8.3,E8.3,I5)

1100     FORMAT(3X,7(3X,F8.3),3X,E8.3,3X,I5)
1105     FORMAT(I5,2F8.3,4I5)
1110     FORMAT(2I5,F8.3,2I5,2F8.3,I5)
1120     FORMAT(2F8.3)
1130     FORMAT(3X,F8.3,3X,F8.3)
      RETURN
      END
      SUBROUTINE SET(NEWN,ZE,Z,NELEM,ISP,XL)
      DIMENSION Z(30),ZE(2),NEWN(2)
      IF(ISP.LT.1)GO TO 1
      ZE(1)=0
      ZE(2)=XL/NELEM
      GO TO 5
1       J=NEWN(1)
      JJ=NEWN(2)
      ZE(1)=0
      ZE(2)=Z(JJ)-Z(J)
5       RETURN
      END
      SUBROUTINE ELEM(HEDI1,HEDI2,PORG,SS,ISX,I2,I3,HCO1,AI,BI,
1       CI,DI,EI,JI,NEWN,IK,ZE,XM,XS,XP,NNODE,HC1,HCL,AL1)
      DIMENSION PORG(3),SS(3),HCO1(3),AI(3),BI(3),CI(3),DI(3),
1       EI(3),JI(3),NEWN(2),ZE(2),XM(2,2),XS(2,2),XP(2)
      IAS=NEWN(1)
      IASS=JI(1K)
      IF(IAS.LT.IASS)GO TO 5
      IK=IK+1
5       AL=ZE(2)-ZE(1)
      CALL HOWD(HCO1,HCO2,TETI1,TETI2,SCAP1,SCAP2,HEDI1,HEDI2,
1       I2,I3,IK,PORG,HCO1,AI,EI,CI,DI,EI,IAS)
      IF(ISX.EQ.1)GO TO 10
1       XM(1,1)=(AL/12)*(3*(TETI1*SS(IK)/PORG(IK)+SCAP1)+(TETI2*SS(IK)
1       /PORG(IK)+SCAP2))
1       XM(1,2)=(AL/12)*(TETI1*SS(IK)/PORG(IK)+SCAP1+TETI2*SS(IK)/
1       PORO(IK)+SCAP2)
1       XM(2,1)=XM(1,2)
1       XM(2,2)=(AL/12)*(3*(TETI2*SS(IK)/PORG(IK)+SCAP2)+(TETI1*SS(IK)
1       /PORG(IK)+SCAP1))
      GO TO 15
10      XM(1,1)=(AL/6)*(2*(TETI1*SS(IK)/PORG(IK)+SCAP1)+(TETI2*SS(IK)
1       /PORG(IK)+SCAP2))
1       XM(1,2)=0
1       XM(2,1)=0
1       XM(2,2)=(AL/6)*(2*(TETI2*SS(IK)/PORG(IK)+SCAP2)+(TETI1*SS(IK)
1       /PORG(IK)+SCAP1))
15      XS(1,1)=(1/(2*AL))*(HCO1+HCO2)
      XS(1,2)=-XS(1,1)

```

```

XS(2,1)=XS(1,2)
XS(2,2)=XS(1,1)
XP(1)=0.5*(HCO1-HCO2)
XP(2)=XP(1)
IF(1AS.GT.1)GO TO 30
HC1=HCO1
* 30 DO 22 I=1,2
* DO 22 J=1,2
* 22 WRITE(6,112)XM(I,J),XS(I,J),XP(I)
*112 FORMAT(3X,3(E9.3,3X))
* WRITE(6,111)HC1
*111 FORMAT(/,3X,"HC1 =",F8.3)
30 IASL=NEWN(2)
IF(IASL.LT.NNODE)GO TO 40
AL1=AL
HCL=HCO2
40 RETURN
END
SUBROUTINE HCWC(HCO1,HCO2,TET11,TET12,SCAP1,SCAP2,HEDI1,
1 HEDI2,I2,I3,IK,PORO,HCOS,AI,BI,CI,DI,EI,IAS)
DIMENSION PORO(3),HCOS(3),AI(3),BI(3),CI(3),DI(3),EI(3)
* 1 TETIX(30)
* ----DETERMINE WHICH WATER CONTENT MODEL APPLIES----
* ----BROOKS AND COREY MODEL----
HED11=ABS(HEDI1)
HED22=ABS(HEDI2)
IF(I2.GT.1)GO TO 10
XP=CI(IK)
TET11=AI(IK)+((PORO(IK)-AI(IK))*(BI(IK)/HED11)**XP)
TET12=AI(IK)+((PORO(IK)-AI(IK))*(BI(IK)/HED22)**XP)
XPPP=1/XP
XPP=(XP+1)/XP
SCAP1=(XP/(BI(IK)*(PORO(IK)-AI(IK))**XPPP*(TET11-AI(IK))**XPP))
SCAP2=(XP/(BI(IK)*(PORO(IK)-AI(IK))**XPPP*(TET12-AI(IK))**XPP))
GO TO 50
* ----VAN GENUCHTEN MODEL----
10 IF(I2.GT.2)GO TO 20
XP=CI(IK)
XPP=1-1/XP
XP1=XP-1
XPP1=XPP+1
TET11=(PORO(IK)-AI(IK))*((1/(1+(BI(IK)*HED11)**XP))**XPP)+AI(IK)
TET12=(PORO(IK)-AI(IK))*((1/(1+(BI(IK)*HED11)**XP))**XPP)+AI(IK)
SCAP1=XPP*(PORO(IK)-AI(IK))*((1/(1+(BI(IK)*HED11)**XP))**XPP1)*
1 XP*(BI(IK)**XP)*(HED11**XP1)
SCAP2=XPP*(PORO(IK)-AI(IK))*((1/(1+(BI(IK)*HED22)**XP))**XPP1)*
1 XP*(BI(IK)**XP)*(HED22**XP1)
GO TO 50
* ----HAVERKAMP MODEL----
20 IF(I2.GT.3)GO TO 30
XP=CI(IK)
XPP=XP-1
TET11=BI(IK)*(PORO(IK)-AI(IK))/(BI(IK)+HED11**XP)+AI(IK)
TET12=BI(IK)*(PORO(IK)-AI(IK))/(BI(IK)+HED22**XP)+AI(IK)
SCAP1=BI(IK)*XP*(PORO(IK)-AI(IK))*(1/(BI(IK)+HED11**XP)**2)*
1 HED11**XPP
SCAP2=XP*BI(IK)*(PORO(IK)-AI(IK))*(1/(BI(IK)+HED22**XP)**2)*
1 HED22**XPP
* ----DETERMINE WHICH HYDRAULIC CONDUCTIVITY MODEL APPLIES----
* ----WARRICK MODEL----
30 IF(I2.GT.4)GO TO 50
XP=-29.484
XPP=-14.495

```

```

      TET11=.6829-.09524*LOG(HED11)
      HCO1=1934000/(HED11)**3.4095
      SCAP1=-.09524/HED11
      GO TO 34
32    TET11=.4581-.02732*LOG(HED11)
      HCO1=516.8/(HED11)**0.97814
      SCAP1=-.02732/HED11
34    IF(HEDI2.GT.XP)GO TO 36
      TET12=.6829-.09524*LOG(HED22)
      HCO2=1934000/(HED22)**3.4095
      SCAP2=-.09524/HEDI2
      GO TO 100
36    TET12=.4581-.02732*LOG(HED22)
      HCO2=516.8/(HED22)**.97814
      SCAP2=-.02732/HEDI2
      GO TO 100
*    ----BROOKS AND COREY MODEL----
50    IF(I3.GT.1)GO TO 60
      XP=(2+3*CI(IK))/CI(IK)
      HCO1=HCOS(IK)*((TET11-AI(IK))/(PORO(IK)-AI(IK)))**XP
      HCO2=HCOS(IK)*((TET12-AI(IK))/(PORO(IK)-AI(IK)))**XP
      GO TO 100
*    ----VAN GENUCHTEN MODEL----
60    IF(I3.GT.2)GO TO 70
      XP=1-1/CI(IK)
      XPP=1/XP
      HCO1=HCOS(IK)*((TET11-AI(IK))/(PORO(IK)-AI(IK)))**0.5*(1-(1-((
1    TET11-AI(IK))/(PORO(IK)-AI(IK)))**XPP)**XP)**2
      HCO2=HCOS(IK)*((TET12-AI(IK))/(PORO(IK)-AI(IK)))**0.5*(1-(1-((
1    TET12-AI(IK))/(PORO(IK)-AI(IK)))**XPP)**XP)**2
      GO TO 100
*    ----HAVERKAMP MODEL----
70    IF(I3.GT.3)GO TO 100
      XP=EI(IK)
      HCO1=HCOS(IK)*(DI(IK)/(DI(IK)+HED11**XP))
      HCO2=HCOS(IK)*(DI(IK)/(DI(IK)+HED22**XP))
100   IF(HEDI1.LE.0)GO TO 150
      TET11=PORO(IK)
      SCAP1=0
      HCO1=HCOS(IK)
150   IF(HEDI2.LE.0)GO TO 200
      TET12=PORO(IK)
      SCAP2=0
      HCO2=HCOS(IK)
* 200   TETIX(IAS)=TET11
*       IF(IAS.LT.25)GO TO 300
*       IAS=IAS+1
*       TETIX(IAS)=TET12
* 200   WRITE(6,101)TET11,TET12,HCO1,HCO2,SCAP1,SCAP2
*101   FORMAT(3X,6(E9.3,2X))
200   RETURN
      END
      SUBROUTINE ASSEM(NEWN,XM,XMG,XS,XSG,XP,XPG)
      DIMENSION NEWN(2),XM(2,2),XMG(30,3),XS(2,2),XSG(30,3),
1     XP(2),XPG(30)
      IUBW=2
      DO 11 I=1,2
      DO 10 J=1,2
      II=NEWN(J)
      JJ=NEWN(J)
      KK=IUBW+JJ-II

```

```

      XMG(I,IKK)=XPG(I,IKK)+XMG(I,J)
10     XSG(I,IKK)=XSG(I,I,IKK)+XSG(I,J)
11     XPG(I)=XPG(I)+XPG(I)
* 10     WRITE(6,15)(XMG(I,IKK),XSG(I,IKK),XPG(I),J=1,NNODE)
* 15     FORMAT(3X,3(EB,3,3X))
      RETURN
      END
      SUBROUTINE CALC1(TIVAL,HEDIS,XMG,XSG,XPG,NNODE,W,KB1,KB2,KB3,
1     KB4,KB5,QQ,QL,HQ,HL,TIMEX,TI,HC1,HCL,AL1,IKK,TMG)
      DIMENSION HEDIS(30),XMG(30,3),XSG(30,3),XPG(30),TMG(30,3),
1     FPG(30,3),TIMEX(20),QQ(20)
      DO 1 I=1,NNODE
      DO 1 J=1,3
      TMG(I,J)=0
1     FPG(I,J)=0
*     ----DETERMINE IF NEUMANN VARIABLE FLUX APPLIES----
      IF(KB5.LT.1)GO TO 5
      AAL=HCL/AL1
      GO TO 7
5     AAL=0
7     DO 10 I=1,NNODE
      DO 10 J=1,3
      TMG(I,J)=XMG(I,J)/TIVAL+W*XSG(I,J)
10     FPG(I,J)=XMG(I,J)/TIVAL+(W-1)*XSG(I,J)
      TMG(NNODE,1)=TMG(NNODE,1)-W*AAL
      TMG(NNODE,2)=TMG(NNODE,2)+W*AAL
      FPG(NNODE,1)=FPG(NNODE,1)-(W-1)*AAL
      FPG(NNODE,2)=FPG(NNODE,2)+(W-1)*AAL
      DO 15 I=1,NNODE
      DO 15 J=1,3
15     XMG(I,J)=0
      DO 20 J=2,3
      L=J-1
20     XMG(I,1)=XMG(I,1)+FPG(I,J)*HEDIS(L)
      II=NNODE-1
      DO 25 I=2,II
      DO 25 J=1,3
      K=I+J-2
25     XMG(I,1)=XMG(I,1)+FPG(I,J)*HEDIS(K)
      DO 30 J=1,2
      L=NNODE-2+J
30     XMG(NNODE,1)=XMG(NNODE,1)+FPG(NNODE,J)*HEDIS(L)
*     ----DETERMINE IF CONSTANT FLUX APPLIES----
      TTT=TIMEX(IKK)
      IF(TI.LT.TTT)GO TO 35
      IKK=IKK+1
35     QQ1=QQ(IKK)-HC1
      QQ2=HCL-QL
      IF(KB1.EQ.1)GO TO 40
      QQ(IKK)=0
40     IF(KB2.EQ.1)GO TO 45
      QL=00
45     XPG(1)=XPG(1)+XMG(1,1)+QQ1
      L=NNODE-1
      DO 50 I=2,L
50     XPG(I)=XPG(I)+XMG(I,1)
      XPG(NNODE)=XPG(NNODE)+XMG(NNODE,1)+QQ2
*     ----DETERMINE IF CONSTANT HYDRAULIC HEAD APPLIES----
      IF(KB3.LT.1)GO TO 60
      TMG(1,2)=1
      TMG(1,3)=0
      XPG(2)=XPG(2)-HQ*TMG(2,1)
      XPG(1)=HQ

```

```

      TMG(2,3)=0
60    IF(KB4,LT,1)GO TO 70
      NN=NNODE-1
      XFG(NNODE)=HL
      XFG(NN)=XFG(NN)-HL*TMG(NN,3)
      TMG(NNODE,1)=0
      TMG(NNODE,2)=1
      TMG(NN,3)=0
70    CONTINUE
*     DO 100 I=1,NNODE
*     DO 100 J=1,3
* 100  WRITE(6,110)FPG(I,J),TMG(I,J),XFG(I)
* 110  FORMAT(3X,3(E9,3,3X))
      RETURN
      END
      SUBROUTINE SOLVE(TM, XFG, HEDIX, FPG, NNODE)
      DIMENSION TM(30,3), XFG(30), HEDIX(30), FPG(30,3)
      DO 5 I=1,NNODE
      DO 5 J=1,3
5     FPG(I,J)=0
      FPG(I,1)=TM(1,2)
      FPG(I,2)=TM(1,3)/FPG(I,1)
      FPG(I,3)=XFG(I)/FPG(I,1)
      DO 10 I=2,NNODE
      II=I-1
      FPG(I,1)=TM(I,2)-TM(I,1)*FPG(II,2)
      FPG(I,2)=TM(I,3)/FPG(I,1)
10     FPG(I,3)=(XFG(I)-TM(I,1)*FPG(II,3))/FPG(I,1)
      HEDIX(NNODE)=FPG(NNODE,3)
      NI=NNODE-1
      DO 20 I=1,NI
      II=NNODE-I
      III=II+1
20     HEDIX(II)=FPG(II,3)-FPG(II,2)*HEDIX(III)
*     DO 50 I=1,NNODE
*     DO 50 J=1,3
* 50    WRITE(6,110)FPG(I,J),HEDIX(I)
* 110   FORMAT(3X,2(E9,3,3X))
      RETURN
      END
      SUBROUTINE ERROR(HEDIX, HEDIL, IE, ERR1, ERR2, NNODE)
      DIMENSION HEDIX(30), HEDIL(30)
      DO 5 I=1,NNODE
      TTT=ABS(HEDIX(I)-HEDIL(I))
      TTTT=ERR2*HEDIX(I)
      TT=ERR1+ABS(TTTT)
      IF(TTT.GT.TT)GO TO 10
5     CONTINUE
      IE=0
      GO TO 15
10    IE=1
15    RETURN
      END
      SUBROUTINE OUT(TI, Z, HEDIX, NT, NL, NNODE, TETIX)
      DIMENSION Z(30), HEDIX(30), TETIX(30)
*     DO 11 I=1,NNODE
*     H=-HEDIX(I)
*     HH=29.484
*     WRITE(6,111)
* 111   FORMAT("00")
*     IF(H.GT.HH)GO TO 6
*     TETIX(I)=.4591-.02732*LOG(H)
*     GO TO 11

```

```

* 6      TETLAX(17),.00277,UNOZAKLELXAT
* 11     CONTINUE
        WRITE(6,20)TI,NL,NT
        WRITE(6,150)
        WRITE(6,200)(I,Z(I),HEDIX(I),TETIX(I),I=1,NNODE)
20      FORMAT(/,10X,"TIME= ",1X,F8.5,4X,"NL= ",15,4X,"NT= ",15)
150     FORMAT(/,4X,"NNODE",8X,"COORDINATE",7X,"PRESSURE HEAD",
1       7X,"WATER CONTENT")
200     FORMAT(4X,14,9X,F8.3,10X,F8.3,10X,F8.3)
        RETURN
        END

```

--EOR--

```

125.    .40    .0100    .1    .00001    1.0    25    015    10
1
1
-159.19
1.
.0      .00.    .0.    .0.    .0.    .00.    .4    .400E-0726
0      .50    .001    0    4    1    0
0      0      0.    1    1    -14.495 -159.19 0
0.00
00

```

--EOR--

UNSATURATED FLOW AND TRANSPORT

```

XL= 125.000    TIME=    .400    TIVAL=.100E-01    TIMAX=    .100
TIMIN=.100E-04    W=    1.000    NELEM=    25    NTM=    15    NST=    10
1      .000
2      5.000
3      10.000
4      15.000
5      20.000
6      25.000
7      30.000
8      35.000
9      40.000
10     45.000
11     50.000
12     55.000
13     60.000
14     65.000
15     70.000
16     75.000
17     80.000
18     85.000
19     90.000
20     95.000
21     100.000
22     105.000
23     110.000
24     115.000
25     120.000
26     125.000

```

```

HEDO=-159.190
1      -269.169
2      -257.651
3      -246.626
4      -236.074
5      -225.972
6      -216.308

```